Contributions of keratins to epithelial cell architecture and signaling

Dissertation

zur

Erlangung des Doktorgrades (Dr. rer. nat.)

der Mathematisch-Naturwissenschaftlichen Fakultät

der Rheinischen Friedrich-Wilhelms-Universität Bonn

vorgelegt von

Cornelia Kröger

aus

Dormagen

Bonn, September 2010

Angefertigt mit Genehmigung der Mathematisch-Naturwissenschaftlichen Fakultät der Rheinischen Friedrich-Wilhelms-Universität Bonn

1. Gutachter: **Prof. Dr. Thomas Magin**
2. Gutachter: **Prof. Dr. Michael Hoch**

Tag der Promotion: 28.01.2011

Erscheinungsjahr: 2011

Die vorliegende Arbeit wurde in der Zeit von Januar 2006 bis September 2010 am Institut für Biochemie und Molekularbiologie der Universität Bonn, Nussallee 11, 53115 Bonn unter Leitung von Prof. Dr. Thomas Magin durchgeführt.

Index

List of Figures

List of Tables

Abbreviations

4EBP1	4E-binding protein 1
AGM	aorta–gonad mesonephros
AJ	adherens junction
Ala	alanine
AMPK	AMP kinase
Ang	angiopoietin
BiP	binding immunoglobulin protein
BMP-4	bone morphogenetic protein 4
BPAG	bullous pemphigoid antigen
Casp	caspase
CD	consensus domain
Cdc25	cell division cycle 25
Cdc42	cell division control protein 42 homolog
cDNA	complementary deoxyribonucleic acid
CFTR	cystic fibrosis transmembrane conductance regulator
CK	cytokeratin
C-TGC	canal-associated trophoblast giant cell
Cx	connexin
DNA	deoxyribonucleic acid
DP	desmoplakin
E	embryo
EBS	Epidermolysis bullosa simplex
E-Cadherin	epithelial cadherin
ECM	extra cellular matrix
eIF2α	eukaryotic initiation factor 2 α
EMT	epithelial-mesenchymal transition
EPC	ectoplacental cone
ER	endoplasmic reticulum
ERAD	endoplasmic reticulum associated degradation
ERK1/2	extracellular signal-regulated kinase 1 and 2
FACS	fluorescence-activated cell sorting
FAK	focal adhesion kinase
FGFR2	fibroblast growth factor receptor 1
Flk1	fetal liver kinase 1

Flt1	Fms-related tyrosine kinase 1
Foxf1	Forkhead box protein F1
FTCD	formiminotransferase cyclodeaminase
Fzd5	Frizzeld 5
GFP	green fluorescent protein
GLUT	glucose transporter
Gly	glycine
grp78	78 kDa glucose-regulated protein
GTP	guanine triphosphate
HEK293	human embryonic kidney 293 cells
Hif1α	hypoxia inducible factor 1 α
HR	hair keratin
Hsp	heat shock protein
ICM	inner cell mass
IF	intermediate filament
IRS	inner root sheet
JNK	Jun NH_2-terminal kinase
K	keratin
KAP	keratin-associated protein
KO	knockout
KOMP	knockout mouse project
Krt	keratin gene
MAPK	mitogen-activated protein kinase
MDB	*Mallory-Denk* body
MF	microfilament
MHCI	major histocompatibility complex 1
miRNA	micro ribonucleic acid
MMP	matrix metalloproteinase
MT	microtubule
mTor	mammalian target of rapamycin
mTORC1	mammalian target of rapamycin complex 1
NIH	National Institutes of Health
NK	natural killer cell
ORF	open reading frame
PDI	protein disulphide isomerase
PERK	PKR-like ER-localized eIF2α kinase
pers. com.	personal communication

PG	plakoglobin
PGK	phosphoglycerate kinase
PKC	protein kinase C
PKP	plakophilin
PL	placental lactogen
PLF	proliferin
PLP	prolactin-like protein
PPARγ	peroxisome proliferator-activated receptor γ
Prlpa	prolactin-like protein A
PRP	proliferin-related protein
P-TGC	parietal trophoblast giant cell
PTM	post translational modification
S6K	ribosomal protein S6 kinase
Sec3	secretory protein 3
Ser	serine
SERCA	sarco(endo)plasmic reticulum Ca^{2+}-ATPase
SNARE	soluble *N*-ethylmaleimide-sensitive factor attachment protein receptors
Spa-TGC	spiral artery-associated trophoblast giant cell
SPCA1	Ca^{2+}/Mn^{2+}-ATPase
S-TGC	sinusoidal trophoblast giant cell
SynT	syncytiotrophoblast
Tfeb	transcription factor eb
TGC	trophoblast giant cell
Thr	threonine
Tie2	tyrosine kinase with Ig and EGF homology domains 2
TJ	tight junction
TM	transmembrane
TSC	trophoblast stem cell
ULF	unit length filament
UPR	unfolded protein response
VE-cadherin	vascular enothelial cadherin
VEGF	vascular endothelial growth factor
VEGFR	vascular endothelial growth factor receptor
WT	wildtype
ZO	zona occludens

%	percent
°C	degree Celsius
µg	mikrogram
µl	mikroliter
µm	mikrometer
µM	mikromolar
bp	base pair
g	gram
g	standard gravity
h	hour
kDa	kilo Dalton
l	liter
M	molar
mA	milliampere
Mb	mega base pair
mg	milligram
min	minute
ml	milliliter
mm	millimeter
mM	millimolar
nm	nanometer
o/n	overnight
OD	optical density
rpm	revolutions per minute
s	seconds
U	Unit

BSA	bovine serum albumine
DAPI	4,6-diamidino-2-phenylindole
DMSO	dimethylsulfoxide
DTT	dithiotreitol
EDTA	ethylenediaminetetraacetic acid
EGTA	ethyleneglycoltetraacetic acid
ES	embryonic stem cell
EtOH	ethanol
FBS	fetal bovine serum
FCS	fetal calf serum

PBS	phosphate buffered saline
PFA	paraformaldehyde
RNase	ribonuclease
SDS	sodium dodecyl sulfate
TBS	Tris buffered saline
TEMED	tetramethylethylenediamine

1. Introduction

- Nothing makes sense except in the light of evolution. -

(Dobzhansky)

Intermediate filaments (IFs) are one of the most diverse and complex protein families in the metazoan cell structure (Erber et al., 1998). In deuterostomia, IFs have evolved into five subfamilies consisting of nuclear and cytosolic IFs specific for distinct cell types and differentiation statuses. However, already in nematodes 12 genes are differentially expressed in specific cell types in the cytoplasm and the nucleus (Carberry et al., 2009), whereas in insects IFs remain restricted to two nuclear proteins (McKeon et al., 1983).

In all mammalian epithelial cells the IF cytoskeleton is formed by the keratin proteins, whose most ancient homologs can be found in invertebrates, as in the tunicate *Styela* (Wang et al., 2000). In contrast to other cytoplasmic and nuclear IFs, keratins advanced within vertebrate evolution into a large and highly conserved gene family consisting of more than 50 keratin genes in mammals. Their expression is highly regulated and reflects the functional diversity of the mammalian epithelia (Fuchs and Marchuk, 1983; Hesse et al., 2004).

One of the major challenges in modern biology is to unravel the functional significance of multiprotein families. The present thesis aims to address this issue by focusing on the functional analysis of the keratin multiprotein family, with a comprehensive approach based on loss-of-function studies in mice, and extends to cell culture models that allow gain- and loss-of-function studies and in depth biochemical analysis.

1.1 Keratins: A large multigene family

The keratin gene clusters

The keratin gene family is divided in 29 type I and 27 type II genes, which are located in two separate contiguous gene clusters in mammals. In mice these clusters are found on chromosome 11D and 15F, respectively (Hesse et al., 2004).

Keratin type I cluster

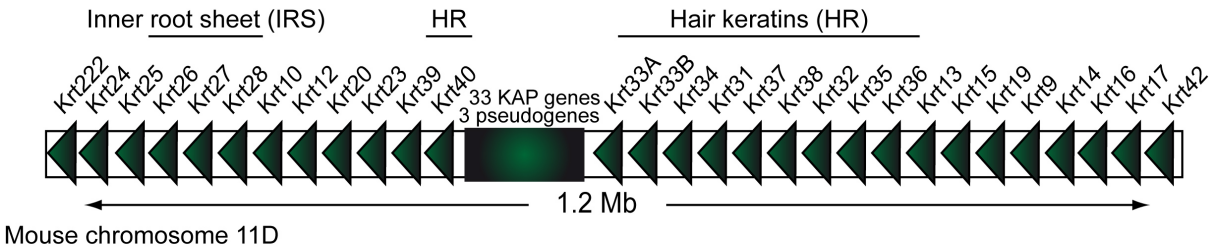

Mouse chromosome 11D

Keratin type II cluster

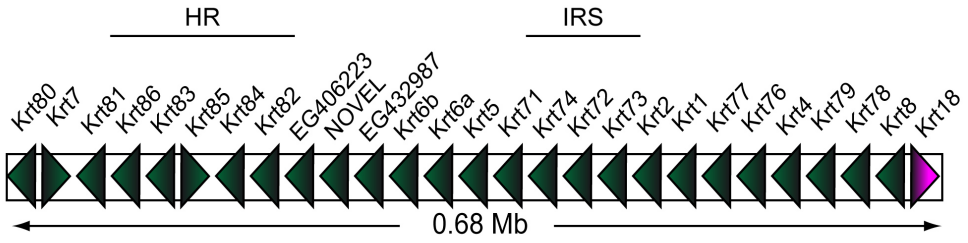

Mouse chromosome 15F

Figure 1.1.1: **Keratins are located in two contiguous clusters in the mouse genome.** Schematic representation of the keratin type I and type II cluster. Arrowheads indicate the orientation of the keratin genes. The pink arrowhead identifies the only type I keratin (*Krt18*) at the end of the type II cluster.

The type I keratin cluster encompasses 1.2 Mb containing 16 cytokeratins (K9-K28) and 11 hair keratins (K31-K40). This cluster also contains a group of genes encoding the high and ultrahigh sulfur keratin-associated proteins (KAPs), which are major components of the hair fiber, and play crucial roles in forming a strong hair shaft through a cross-linked network with hair keratin IFs (Rogers et al., 2006). The type II cluster has a size of 0.68 Mb and contains 20 cytokeratins (K1-K8, K71-74, K80), six hair keratins (K81-K86) and an additional type I keratin at the very end of the cluster, namely K18 (Figure 1.1.1) (Schweizer et al., 2006). Keratin 8 and 18 are thought to be the oldest keratins and are the first ones to be expressed during embryogenesis. They originated from a common ancestor and evolved through concerted gene duplication and gene conversion of type I and type II genes into the type I and type II gene clusters (Blumenberg, 1988; Fuchs and Marchuk, 1983; Hesse et al., 2001). A consequence of gene duplication is the relatively small size of keratin genes with 5-8 kb, including regulatory elements, which are directly adjacent or even within the coding sequences (Neznanov et al., 1997; Willoughby et al., 2000). In the keratin cluster targeted in this work no additional open reading frames (ORF), including regions coding for miRNAs could be detected by bioinformatical analysis with the Sanger database, release miRBase 15, August 2010 (http://www.mirbase.org/index.shtml). A selective advantage for the conserved cluster organization throughout mammalian evolution could be facilitated gene silencing by chromatin condensation, resulting in the inhibition of keratin expression in non

epithelial cells, with only minor exceptions in muscle cells (Bader et al., 1988; Jahn et al., 1987; Kuruc and Franke, 1988; O'Neill et al., 2002; Ursitti et al., 2004).

Keratin filament structure and domain homology

All IF proteins, including keratins, share the same basic tripartite structural organization, which consists of a central α-helical rod domain flanked by non α-helical amino- and carboxy-terminals, head and tail domains, respectively (Figure 1.1.2). Analogs with similar protein structure were even found in bacteria (Ausmees et al., 2003; Bagchi et al., 2008).
The central rod domain comprises four coiled-coil segments, i.e. coils 1A, 1B, 2A and 2B, of highly conserved amino acids connected by three linkers termed L1, L12 and L2.

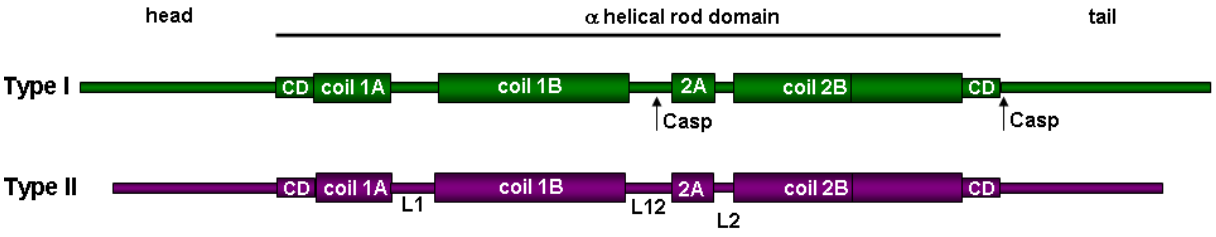

Figure 1.1.2: **Schematic representation of the conserved basic keratin type I and type II structures.** Colored boxes represent the α-helical rod domains Coil 1A, Coil 1B, Coil 2A and Coil2B, which are separated by the linker segments, L1, L12 and L2 of type I and type II keratins, respectively. CD, marks the highly conserved consensus motif of the rod domain boundaries and Casp, caspase-sensitive cleavage sites in type I keratins. Adapted from TM Magin.

Each α–helical coil is organized in heptad repeats of apolar and polar amino acids, which drive the association of like molecules into the coiled coil formation (Fuchs and Weber, 1994; Herrmann et al., 2009; Parry et al., 2007).
In contrast to other IFs which can form hetero- as well as homodimers (Herrmann et al., 2009), the basic subunit of a keratin filament is an obligatory heterodimer consisting of a type I and a type II keratin (Hatzfeld and Weber, 1990). However, the exact mechanisms of assembly preference and specificity of keratin heterodimers in a context with more than two different keratin pairs, typical for all epithelial tissues, besides hepatocytes, has not been resolved.
Keratin heterodimers associate along their lateral surfaces, with an antiparallel orientation, to form apolar tetramers. An average of eight tetramers can then assemble laterally and longitudinally into unit-length filaments (ULFs), which further condense into the 10-12 nm thick keratin filaments (Herrmann and Aebi, 1998). It was shown *in vitro* that any type I and type II keratin can assemble (Hatzfeld and Franke, 1985). In this assembly process the head and tail domains are crucial for filament assembly (Bader et al., 1991; Fuchs and Weber,

1994; Hatzfeld and Weber, 1990). They maybe exposed at the polymer surface and most accessible for post-translational modifications (PTMs), including phosphorylation, glycosylation (Ku et al., 2010), transglutamination, sumoylation (pers. com. with B. Omary) and ubiquitination which influence assembly properties and protein-protein interactions (Coulombe and Omary, 2002; Loffek et al., 2010).

The rod domain is highly conserved among all keratins, as depicted exemplarily in Figure 1.1.3 for a selection of type II keratin proteins. In contrast, the head and the tail domain harbor most of the sequence heterogeneity (Figure 1.1.3). Keratin heads expressed in simple epithelia (K7, K8) for instance are rich in Ser-Thr residues and epidermal keratins (K5, K1) are rich in Gly-Gly-X. These features are suggested to be reflected by tissue-specific and cell-specific functions and regulations (Coulombe and Omary, 2002; Herrmann et al., 2003).

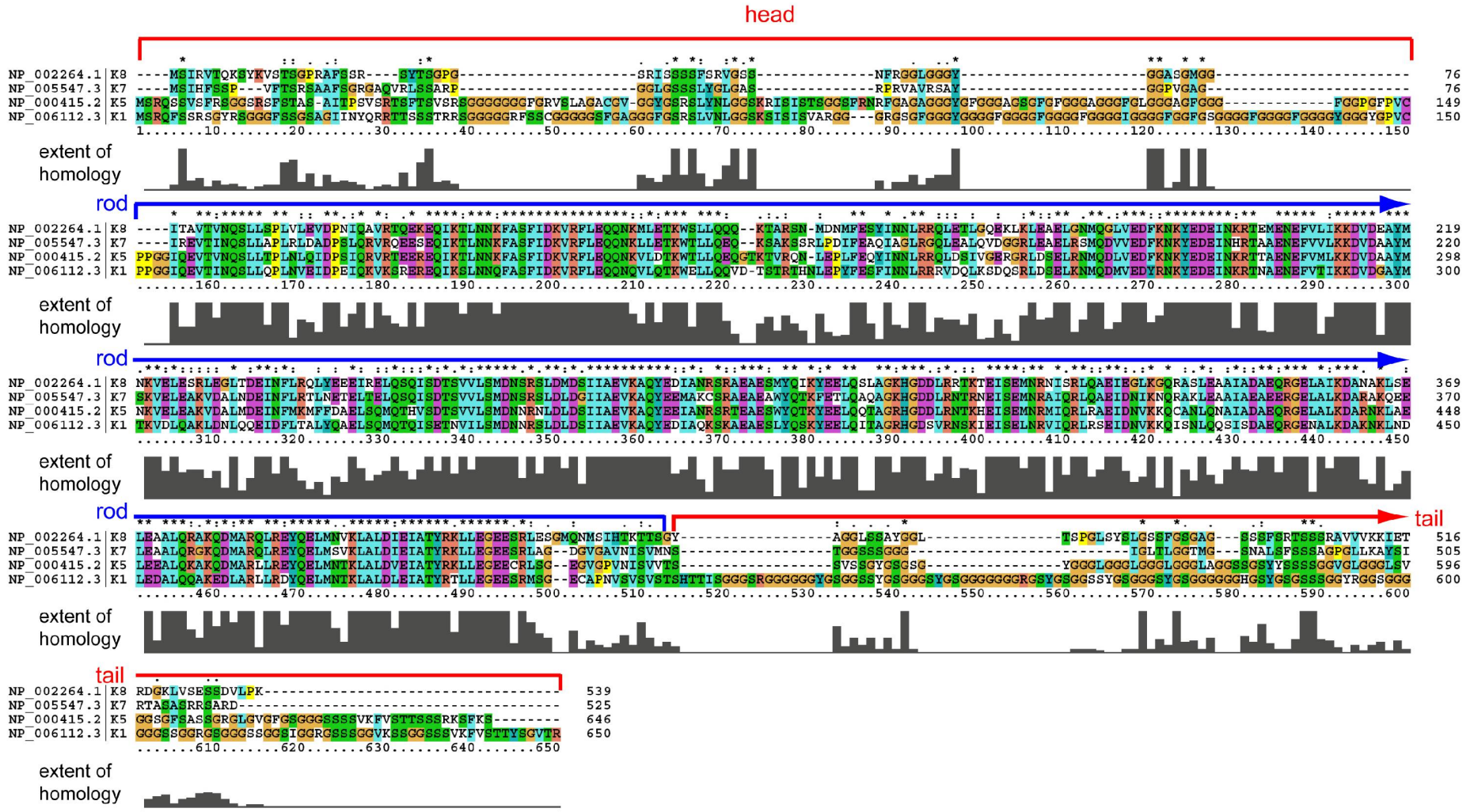

Figure 1.1.3: **Sequence homology between type II mouse keratins**. The type II keratins of early embryonic mouse development, K7 and K8 are aligned against the main type II keratins of basal epidermis, K5 and differentiated stratified epithelia, K1. The conserved rod domain, marked in blue, is highly conserved and up to 80% homologue in all the different keratins. The head and tail domains which share little sequence identity are marked in red. The exact amount of sequence homology is depicted by the size of the grey bars beneath the sequence alignment. Color code: blue: apolar amino acids; green: polar amino acids; purple: acidic amino acids; red: basic amino acids; orange: glycine; yellow: proline; cDNA accession numbers are provided. Alignment performed with ClustalX 2.0.12 (Larkin et al., 2007).

Keratin organization within polarized epithelial cells

Epithelial cells contain three principal filament systems: actin microfilaments (MF), microtubules (MT), and keratin filaments. Together they form a dynamic cytoskeleton that mechanically orchestrates cellular space (Fuchs and Cleveland, 1998; Lazarides, 1980). The cytoplasmic keratin filament may be linked indirectly to the nuclear IF network, composed of lamins, via plectin and interacting inner and outer nuclear membrane proteins, such as nesprin-3 and SUN proteins (Starr, 2007) (Figure 1.2.1 A).

Cytoskeletal filaments of epithelial cells are furthermore linked to the plasma membrane (PM) via adhesion complexes that integrate the cell into the epithelial tissue layer by either establishing lateral cell-cell contacts or by attaching the basal cell surface to the underlying extracellular matrix (ECM). The apical surface of the epithelium is exposed to the environment (for example, in skin) or to a lumen (for instance, the intestinal lumen) (Figure 1.2.1).

The most apical cell junctions are the tight junctions (TJs) which function as a selective permeability barrier towards the apical lumen. Their core consists of the transmembrane (TM) proteins claudin and occludin; and they are linked to the actin cytoskeleton through the zona occludens (ZO) adaptor proteins.

Directly subjacent to the TJ are the adherens junctions (AJs), cell-cell junctions which link actin filaments to the PM. In epithelia they are composed of E-cadherins and are linked to the actin cytoskeleton through adaptor proteins such as catenins and vinculin. Focal adhesions finally, link the actin cytoskeleton to the ECM. They are formed by integrins that are linked to actin by adaptor proteins such as talin, filamin and vinculin.

The adhesion complexes anchoring the keratin filaments to the PM are the desmosomes which form cell-cell contacts and the hemidesmosomes providing cell-matrix adhesion. Desmosomes are formed by desmosomal cadherins called desmocollin and desmoglein and are linked to keratins through desmoplakin (DP) via the adaptor proteins of the armadillo family, plakophillin (PKP) and plakoglobin (PG) (Figure 1.2.1 B). An additional component of the desmosomes is plectin which was observed to localize to desmosomes via desmoplakin (Eger et al., 1997). Hemidesmosomes attach to the ECM via α6β4-integrins and BPAG2 (bullous pemphigoid antigen-2) and are linked to keratins through plectin and BPAG1e (the epithelial form of bullous pemphigoid antigen-1) (Figure 1.2.1 C) (Green et al., 2010; Green and Jones, 1996; Jefferson et al., 2004).

With regard to other cell-cell junctions, gap junctions connect the cytoplasm of neighboring cells and allow ions and small molecules to pass freely in between (Kjenseth et al., 2010).

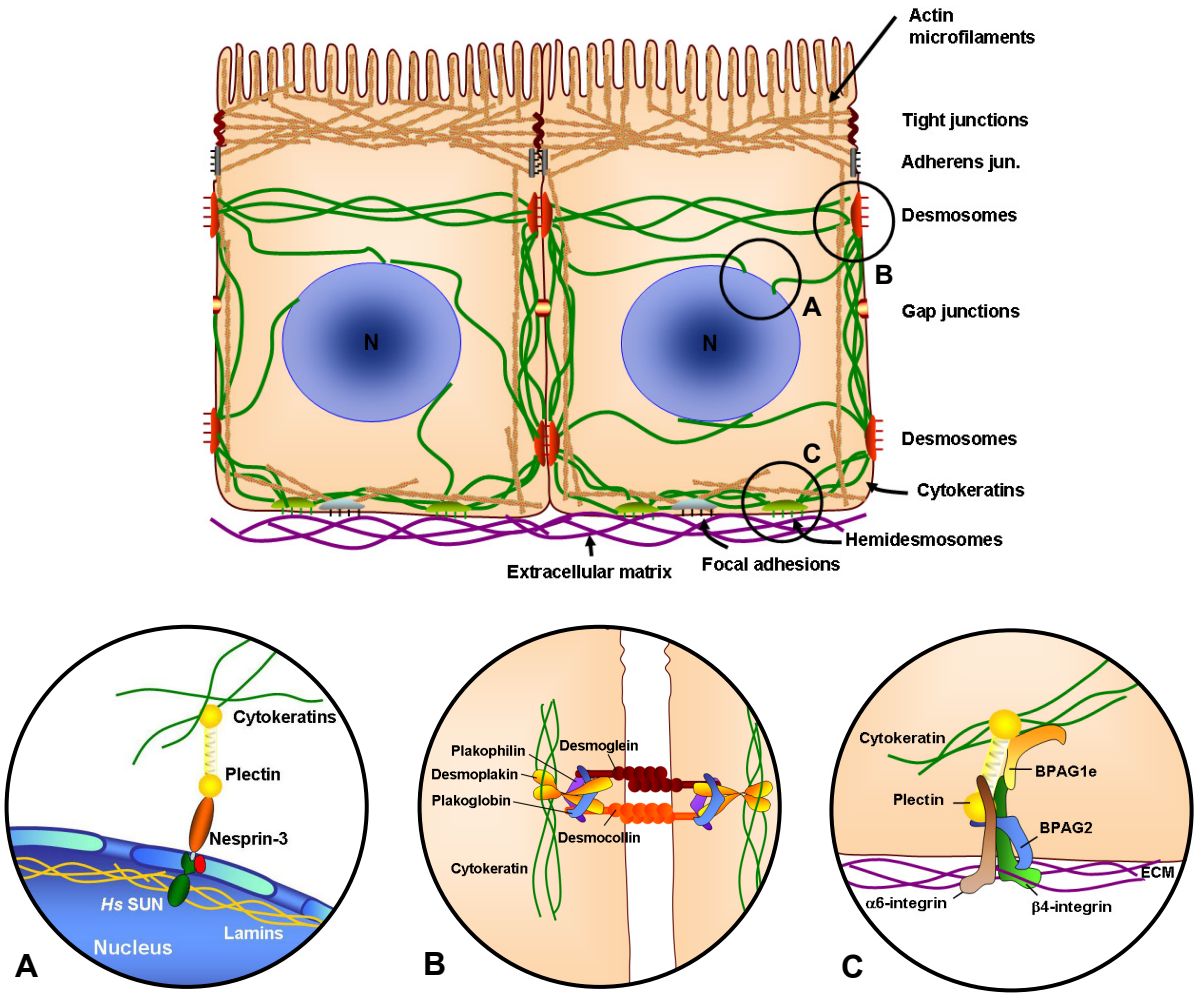

Figure 1.2.1: **Schematic model of a polarized epithelial cell.** Keratins depicted in green form a complex structural network in epithelial cells, next to the actin cytoskeleton (brown). They attach to the nucleus via adapter proteins, and are anchored to the PM via desmosomes (in red) and hemidesmosomes (light green), stabilizing cell-cell and cell-matrix adhesions, respectively. The actin filament network correspondingly interacts with AJs (grey) and focal adhesions (light blue). **(A)** Keratins are connected via plectin and the linker protein nesprin-3 through a nuclear envelope bridge of SUN protein with lamins, the nuclear intermediate filaments. **(B)** Desmosomes are cell-cell adhesion complexes linking keratins via DP to a complex of armadillo proteins (PKP and PG) and desmosomal cadherins (desmoglein and desmocollin) to the PM. **(C)** Hemidesmosomes attach cells to the extracellular matrix via α6β4 integrin signaling and interact with keratins, through an adapter complex of plectin, BRAG1e and BRAG2.

One of the central players in the integration of various cytoskeletal and all adhesion proteins is the cytoskeletal linker plectin. Plectin plays not only a central part in linking keratins to cell junctions and the nuclear membrane, as mentioned above, but also connects keratins with the other cytoskeletal filament systems, MF and MT. Furthermore, it is proposed to act as a signaling platform, providing the crucial link between cytoskeletal dynamics and signaling machineries (Osmanagic-Myers et al., 2006; Wiche, 1998).

The tight integration into the cellular space and the apolar structure of keratin filaments would argue for a sole mechanical function of keratins, however similar to plectin keratins were shown to be essential for a variety of signaling processes in the cell, which will be discussed in the next chapter.

1.2 Keratin functions

Structural and regulating functions

Epidermolysis bullosa simplex (EBS), typified by superficial *bullous* lesions through frictional skin trauma, is caused by genetic mutations in K5 and K14. This suggests that keratins have a major function in providing mechanical stability (Coulombe et al., 2009; Magin et al., 2004). However, in contrast to early views, keratins do not form a rigid, steel frame in the cell, but are a dynamic network constantly disassembling and restructuring (Windoffer and Leube, 1999; Windoffer et al., 2004).

Essential for the regulation of keratin dynamics, by modulating their solubility, conformation and organization are phosphorylation and dephosphorylation as well as glycosylation. The phosphorylation and glycosylation sites in keratins are clustered in the head and tail domains primary at serine and threonine sites. These are targets for many kinases like mitogen-activated protein kinases (MAPK) and protein kinases C (PKC) (Ku et al., 2010; Omary et al., 2006). Conversely, keratins can act as modulators of kinase signaling pathways. For example, in conjunction with heat shock proteins, like Hsp70 they regulate rephosphorylation and localization of atypical PKC (Mashukova et al., 2009). Furthermore, cell architecture and behavior is dependent on keratins in concert with kinases and other interacting proteins, like the cytolinker plectin. In this fashion, keratins influence migration and cell adhesion in a PKC-mediated integrin/FAK dependent manner (Bordeleau et al., 2010; Osmanagic-Myers et al., 2006; Wallis et al., 2000).

By mediating positioning and function of essential cellular organelles keratins define the inner cellular space (Toivola et al., 2005). They influence mitochondria localization and size (Tao et al., 2009), alter Golgi distribution and reassembly (Kumemura et al., 2004) and influence vesicle transport. Along these lines, it was shown, that through an interaction of a mutated K5 head domain with the MT motor protein dynein, melanosome localization in keratinocytes of EBS patients with mottled pigmentation was altered (Betz et al., 2006; Uttam et al., 1996).

Furthermore, keratins were suggested to be involved in coordinating cell polarization by localizing γ-tubulin complexes to the apical domain of cells. Their absence results in the mislocalization of apical TM proteins like ion transporters, cystic fibrosis transmembrane receptors (CFTR) and also soluble *N*-ethylmaleimide-sensitive factor attachment protein

receptors (SNARE) proteins like Syntaxin 3 (Ameen et al., 2001; Oriolo et al., 2007; Toivola et al., 2004).

A 'domino phenotype' emanating from organelle reorganization and protein mistargeting is the proposed increased susceptibility of keratin depleted epithelial cells to apoptosis. However, the exact mechanism could not be determined so far and contradictory results exist. These results indicate that deletion of individual keratins promotes cell death through increased cytochrome c release from mitochondria and elevated surface density of Fas receptors (Gilbert et al., 2001; Ku et al., 2003; Tao et al., 2009). Furthermore, the simple keratins, K8 and K18 protect cells from cell stress by promoting Jun NH_2-terminal kinase (JNK), ERK1/2 and Raf1 signaling cascades (Caulin et al., 2000; Gilbert et al., 2004; He et al., 2002; Ku et al., 2004).

More recent data suggest that type I keratins orchestrate the modulation of apoptotic signals and protection against metabolic stress as well as regulation of the cell cycle and of protein translation through 14-3-3 proteins. In this context, keratins were proposed to function as scaffold for signaling processes and as phosphorylation dependent 'binding sinks' of kinases and 14-3-3 proteins (Kim et al., 2006; Ku et al., 2004; Magin et al., 2007; Reichelt and Magin, 2002).

However, no exact mechanism on how keratins perform all these various functions could be determined so far, due to the complex expression patterns of the keratin multigene family. Existing data provide only indirect modes of keratin action. So the questions still remain, how do keratins function, and why is such diversity essential?

1.3 Keratin functions in early embryonic development

Keratin type II transcripts in murine embryonic development are found as early as E1.5 in the 2-cell stage (Lu et al., 2005), the first filaments form in the emerging epithelial at E3.5 mainly in the trophectoderm, where their assembly starts at nascent desmosomes (Jackson et al., 1980; Lu et al., 2005; Paulin et al., 1980) and to a lesser extent desmosome independent in the ICM. In early post-implantation embryos keratins are predominantly expressed in the extraembryonic epithelial tissues of the trophoblast cell lineages and the yolk sac tissue. In subsequent days keratin expression is maintained in all simple epithelia and the single layered surface ectoderm. At this early developmental stage already 4 different keratins are expressed, namely K7, K8, K18 and K19 and remain to be the sole keratins up to E9.5 when the expression of the basal keratins K5 and K14 starts in the ectoderm overlaying posterior somites and in the periderm (Table 1.3.1) (Byrne et al., 1994; Lu et al., 2005).

Tissue	K7	K8	K18	K19
E3.5	**+**	**+**	**+**	**+**
E6.5				
- trophoblast	**+**	**+**	**+**	**+**
- visceral endoderm	**-**	**+**	**+**	**-**
E9.5				
- yolk sac	**-**	**+**	**+**	**+**
- trophoblast	**+**	**+**	**+**	**+**
- amnion	**-**	**+**	**+**	**+**
- embryo primitive gut	**+**	**+**	**+**	**+**
- embryo surface ectoderm	**(+)**	**+**	**+**	**+**
- embryo notochord	**(+)**	**+**	**+**	**+**

Table1.3.1 **Expression of simple epithelial keratin proteins during early mouse development (modified from Lu et al., 2005).**

Epithelia in early embryonic development

The first epithelium of the blastocyst, which expresses a typical keratin filament network, is the trophectoderm which coats the blastocoel and the inner cell mass. Overlying the inner cell mass (ICM) is the polar trophectoderm, which gives rise to the trophoblast stem cells (TSCs) and differentiates into the placenta. The ICM develops into the yolk sac and the epiblast. The epiblast provides the future umbilical cord, the allantois and the embryo proper (Figure 1.3.1) (El-Hashash et al., 2010).

The yolk sac

The development of the yolk sac starts with the formation of the visceral endoderm at E5.5 which arises from the ICM and orchestrates the signaling processes during gastrulation (Rossant and Tam, 2009). In the process of mesoderm formation the first mesodermal cells migrate to the extraembryonic region of the embryo. The visceral endoderm and the extraembryonic mesoderm together form the yolk sac, the keratin expressing bilaminar membrane that surrounds the developing embryo (Baron, 2005).

The yolk sac provides the embryo with nutrients and oxygen and simultaneously functions as a barrier towards the uterine environment which is maintained with TJs as well as gap junctions and desmosomes interlinking the endoderm cells (Jollie, 1990; King, 1982).

Beginning at E7.5, the mesoderm layer differentiates into endothelial and primitive erythroid cells, which form the so called blood islands in the yolk sac. These primitive nucleated erythroid colony-forming cells provide the first embryonic blood before they are replaced by

the enucleated definitive erythroid cells as soon as the liver takes over as hematopoietic organ at E10.5. Therefore, the yolk sac functions as the first haematopoietic stem cell niche, which is gradually replaced by the placenta, the aorta–gonad mesonephros (AGM), the fetal liver and finally by the bone marrow and the thymus (Orkin and Zon, 2008).

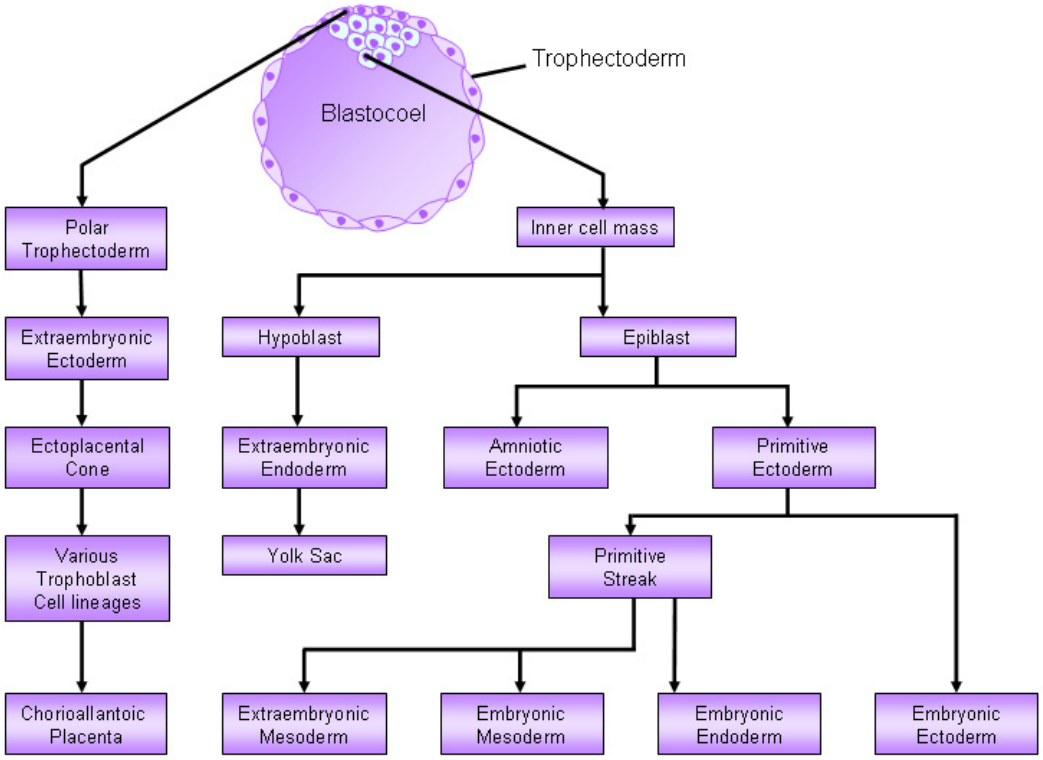

Figure 1.3.1: **Lineage relationships in the developing mouse embryo.** The polar trophectoderm overlies the ICM and gives rise to the TSCs, which develop into the keratin expressing epithelial part of the chorioallantoic placenta. From the inner cell mass the hypoblast, the future yolk sac and the epiblast arise. The epiblast provides the mesodermal part of the placenta the allantois (amniotic ectoderm) and also gives rise to the embryo proper (primitive ectoderm) (modified from El-Hashash et al., 2010).

The placenta

Survival and growth of the embryo are critically dependent on the placenta. At around E9.5 the placenta starts to support the function of the yolk sac by forming the interface between maternal and fetal circulation, facilitating gas, nutrient and waste exchange (Cross et al., 2006). It is comprised of the epithelial trophectoderm cells which invade and attach to the uterine wall and induce decidualization by altering specific gene expression amongst others for vascular remodeling and angiogenesis as well as maternal immune suppression by secreting various paracrine and autocrine hormones (Bany and Cross, 2006). Placental vascularization provides the platform for the maternal-fetal exchange. A disturbance in any of

these signaling processes results in a range of pregnancy complications starting from mild intrauterine growth restriction up to miscarriage (Cross et al., 2002).

Placental development and function

Plancental development starts upon implantation of the embryo into the uterine wall at around E4.5 with the expansion and differentiation of the trophectoderm cells. The first embryonic cells to interact with the maternal tissue are the polyploid trophoblast giant cells (TGCs), which arise from the outer trophectoderm layer of the blastocyst through endoreduplication. The trophectoderm cells overlying the ICM continue to proliferate and give rise to the diploid extraembryonic ectoderm and the ectoplacental cone (EPC) (Copp, 1979). From the outer regions of the EPC secondary giant cells develop to surround the entire conceptus.

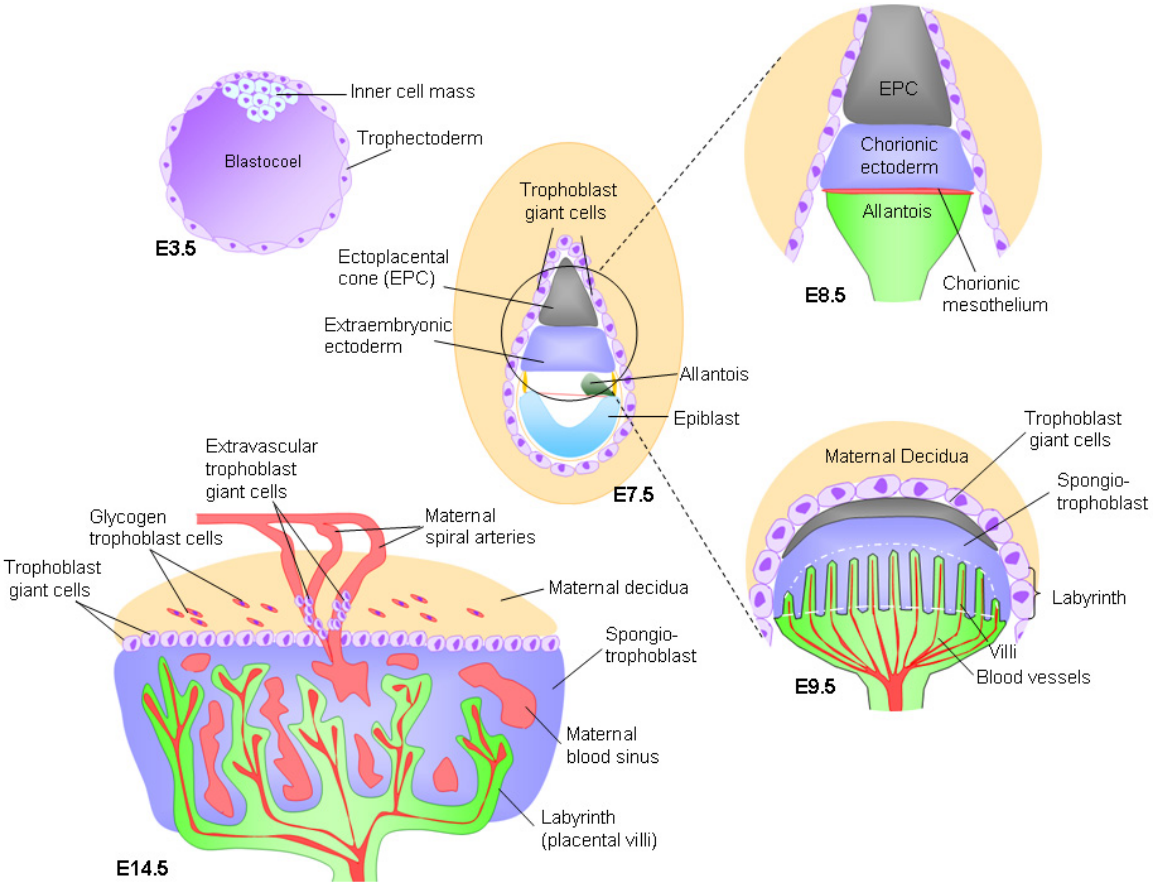

Figure 1.3.2: **Schematic representation of placental development.** The origins of the extraembryonic lineages begin at embryonic day E3.5 with the formation of the blastocyst. At around E8.0, chorioallantoic attachment occurs, followed by branching morphogenesis of the labyrinth (structure contained in dashed white lines) to form dense villi, within which nutrients are exchanged (E9.5). The mature placenta (E14.5) consists of three layers: the labyrinth, the spongiotrophoblast, and the maternal decidua (modified from Watson and Cross, 2005).

The extraembryonic ectoderm expands to form the chorionic ectoderm, which is lined by a thin layer of mesothelial cells. At E8.5, in a process called the chorioallantoic fusion, the allantois attaches to the chorion. The allantoic mesoderm develops into the fetal vascular compartment of the placenta and arises from the posterior end of the epiblast. Hours after attachment the allantois starts to invaginate into the chorion at pre-marked folds. The chorion in turn starts to undergo extensive villous branching, to form the placental labyrinth (Figure 1.3.2) (Rossant and Cross, 2001). The maternal blood flow is controlled by extravascular trophoblast cells. They infiltrate the maternal spiral arteries and prevent premature blood flow into the placenta by replacing the maternal endothelial cells. The maternal blood enters controlled into the labyrinth where it circumfluents directly the fetal trophoblastic villi in so called blood sinuses (Adamson et al., 2002). Coincident with the onset of morphogenetic branching, the epithelial chorionic trophoblast cells begin to differentiate into the highly specialized trophoblast cell lineages. The spongiotrophoblast cells structurally support the labyrinth by forming a compact cell layer between the labyrinth and the outer giant cells (Rossant and Cross, 2001). During later gestation, glycogen trophoblast cells begin to differentiate within the spongiotrophoblast layer, and subsequently diffusely invade the uterine wall (Figure 1.3.2) (Adamson et al., 2002).

In the labyrinth, the exchange between maternal blood sinuses and the fetal vasculature has to cross three layers of trophoblast cells (tri-chorial) and one layer of fetal endothelial cells. The trilaminar trophoblast includes two layers of syncytiotrophoblast, SynT-I and -II, the latter of which is in contact with fetal endothelial cells and a single layer of mononuclear sinusoidal trophoblast giant cells (S-TGCs) that line the maternal blood sinusoids (Figure 1.3.3) (Simmons et al., 2007; Simmons et al., 2008; Watson and Cross, 2005).

The two multinucleated syncytiotrophoblast layers, a result of trophoblast cell-cell fusion (Dupressoir et al., 2009), are very thin and are tightly adherent to one another through TJs; they are situated on basement membranes overlying the fetal capillary endothelium (Coan et al., 2005; Hernandez-Verdun, 1974; Simmons et al., 2008). The syncytiotrophoblast functions mainly in gas and waste exchange, as well as nutrient transport; inter-cellular transport is facilitated through expression of specialized gap junctions and glucose transporters (GLUT1) between the syncytiotrophoblast layers (Gabriel et al., 1998). S-TGCs are loosely attached to the underlying syncytial layers via desmosomal adhesions and contain fenestrations to allow the SynT-I cells direct access to maternal blood (Coan et al., 2005; Simmons et al., 2008). The S-TGCs express hormones such as placental lactogen II and are likely to have a primary endocrine function (Figure 1.3.3) (Hu and Cross, 2010; Simmons et al., 2007).

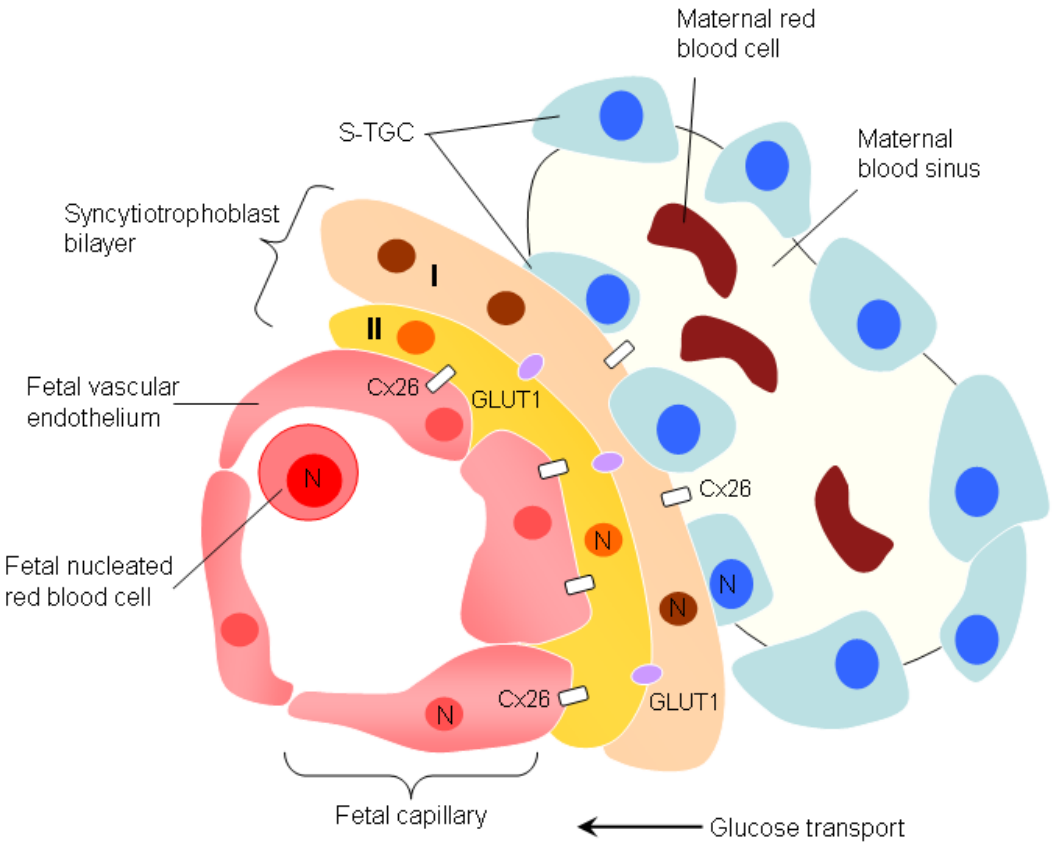

Figure 1.3.3: **Maternal-fetal nutrient exchange across the trilaminar trophoblast layer.** The trilaminar trophoblast layer consists of two syncytiotrophoblast layers (layer I and II) enclosing the fetal endothelial cells and a mononucleated layer of S-TGCs that line the maternal blood sinuses. Gap junctions, consisting of Cx26 and GLUT1 transporters were shown to facilitate the nutrient transport in the placental labyrinth from the maternal blood into the fetal capillaries N, nucleus; Cx26, connexin 26. (modified from Watson and Cross, 2005).

Besides the S-TGC three other TGC subtypes have been indentified in the placenta; the parietal TGC (P-TGC) that line the implantation site and are in direct contact with decidual and immune cells in the uterus, the maternal blood canal-associated TGCs (C-TGC) and the above mentioned extravascular trophoblast cells or spiral artery-associated TGCs (SpA-TGC). The different TGC lineages can be distinguished by their anatomical location and gene expression (Simmons et al., 2007). All TGC subtypes share the characteristics that they are large, have polyploid (usually single) nuclei, and are secretory in nature with their content of Golgi and endoplasmic reticulum increasing during differentiation (Bevilacqua and Abrahamsohn, 1988).

The mural trophectoderm-derived TGCs mediate attachment of blastocyst to the uterine epithelium, induce uterine decidualization and invade into the uterine stroma. The mechanisms of trophoblast invasion are best studied in P-TGCs but SpA-TGCs and glycogen trophoblast cells also invade into the uterus (Adamson et al., 2002). TGCs secrete a variety of proteinases, such as matrix metalloproteinases (MMP-2, -3, - 9, -13) that are

thought to digest the ECM as well as phagocytose maternal cells and matrix materials (Das et al., 1997; Teesalu et al., 1999). After implantation, TGCs produce hormones and cytokines for maintenance of the feto-maternal interface which target various maternal physiological systems to maintain maternal adaptations to pregnancy (Figure 1.3.4) (Bany and Cross, 2006; Hu and Cross, 2010).

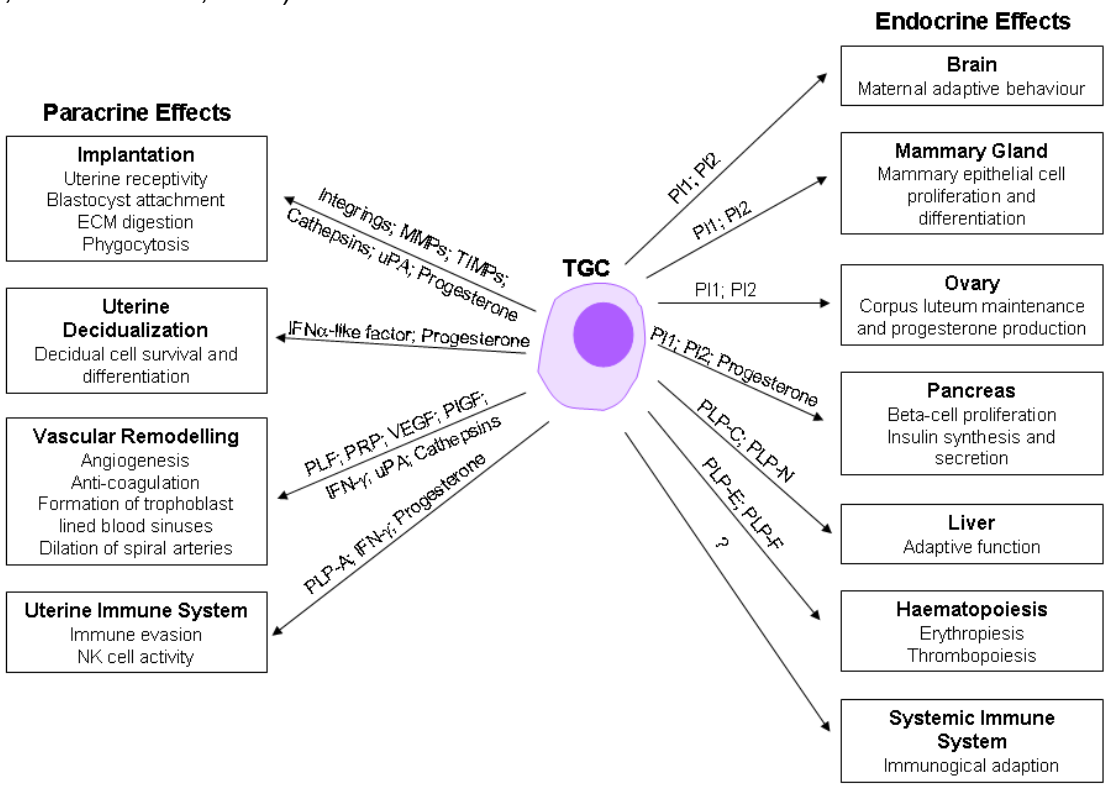

Figure 1.3.4: **Summary of the paracrine and endocrine functions of TGCs.** TGCs secrete a variety of hormones that alter their direct environment and enable intrauterine growth, however they also affect the mother systemically for the adaption to the pregnancy (modified from Hu and Cross, 2010).

The most prominent family of endocrine hormones secreted from the TGCs is the prolactin/placental lactogen (PL) / prolactin-like protein (PLP) gene family, especially PI1 and PI2, which have a systemic effect on the mother and the embryo (Hu and Cross, 2010; Linzer and Fisher, 1999). However, TGCs also act paracrine by secreting vascular remodelling cytokines of the PLP family, namely proliferin (PLF) and proliferin-related protein (PRP) (Jackson et al., 1994) as well as vascular endothelial growth factor (VEGF) (Voss et al., 2000) that induces decidual vasculature. In this fashion, they also stimulate angiogenic signals in the decidua like angiopoietin1 and 2 (Ang1 and Ang2) and furthermore secrete hormones which suppress the immune system of the mother (Bany and Cross, 2006). One of these hormones is Prlpa, which inhibits maternal natural killer cells (NKs) (Ma and Linzer, 2000).

The development of the placenta is dependent on an intensive crosstalk between the epithelial trophoblast lineage and the endothelial cells of the allantois. Different receptor KO

studies, including FGFR2 and Fzd5 (Ishikawa et al., 2001; Xu et al., 1998), as well as various transcription factors JunB, PPARγ and Tfeb (Barak et al., 1999; Barak et al., 2008; Schorpp-Kistner et al., 1999; Steingrimsson et al., 1998) display severe developmental defects. Various kinases were also reported to influence placental and yolk sac development when deleted, such as p38 MAPK (Mudgett et al., 2000). However, signaling factors expressed in the allantoic endothelium are equally responsible for the proper maturation of the placenta. Mutations in the Notch signaling pathway, for instance, block chorioallantoic branching and prevent proper invagination of the allantois into the placenta (Duarte et al., 2004; Gale et al., 2004; Limbourg et al., 2005). This is also the case for Ang1, Ang2, the vascular remodelers and their receptor Tie2 (Dumont et al., 1994; Maisonpierre et al., 1997; Sato et al., 1995; Suri et al., 1996). Defects in yolk sac and placental vascularization were also reported for the VEGFR receptors, Flk1, and Flt1 (Breier et al., 1995; Fong et al., 1995; Shalaby et al., 1995). Given that keratins are expressed in all embryonic epithelial cells, one might expect phenotypes with altered embryonic and extra-embryonic development.

1.4 Analysis of keratin function

Analyzing keratin function has been targeted from many angles, using in vitro assays, cell culture and gain and loss of function studies in transgenic mice, as well as genetic analysis of patient material. *In vitro* assays are mainly used to identify keratin filament structure and assembly properties. Constitutive studies are performed in cell culture models assessing properties of *in vitro* cultured cells transfected with mutant or fluorescent-tagged keratins to identify function and interaction with keratin associated proteins (Herrmann et al., 2003; Herrmann et al., 2009). However, no immortal keratin free epithelial cell line has so far been generated, which would allow long term functional assays in a natural physiological setting without compensatory affects.

Most rewarding results in analyzing keratin function were obtained in keratin mouse models, foremost in understanding the keratin mutation based genetic disease EBS (Coulombe et al., 2009; Coulombe and Omary, 2002). The analysis of these model systems suggests that keratins have a major impact on cell architecture, cell size and proliferation depending on cell context but do not act as major regulators of epithelial differentiation (Magin et al., 2004; Magin et al., 2007).

Keratin mouse models: From single knockout (KO) studies to the complete cluster deletion

The first keratin to be inactivated by gene targeting and homologous recombination was K8 (Baribault et al., 1993). Since then 15 additional keratin KO mice were generated (Table 1.4.1), besides various transgenic mice with keratin overexpressions and mutations. Their phenotypes range from major defects causing embryonic lethality or skin fragility to subtle and late onset of liver alterations (Coulombe and Omary, 2002; Omary et al., 2009).

Deletions of K5 or K14, both expressed in basal keratinocytes, show severe blistering in the skin and the oral mucosa and die shortly after birth. The phenotype is more prominent in K5 KO mice and resembles very severe forms of EBS (Lloyd et al., 1995; Peters et al., 2001). In contrast the deletions of K1 or K10, present in stratifying and cornifying epithelia, do not show any severe skin abnormalities. Upregulation of K5 and K14 argues for their compensatory abilities in these settings (Reichelt et al., 2001), however, only to a certain degree, as K1 KO mice also die shortly after birth (W. Roth and T. Magin personal communication). This is consistent with the notion that keratin type II KOs are generally more severe, than their type I counterparts; indicating, that type I keratins can be easier compensated for, by other type I family members.

Cluster	Keratin	Phenotype	References
Type II	K1	Neonatal death, no compensation	pers. com. Roth & Magin
	K4	Compensation by K6; basal hyperplasia, lack of maturation, hyperkeratosis, atypical nuclei, perinuclear clearing, and cell degeneration in K4 positive tissues	(Ness et al., 1998)
	K5	Neonatal death, K14 aggregates-gain of toxic function, induction of immune response	(Peters et al., 2001; Roth et al., 2009)
	K6a	Total compensation by K6b, lysis of nail bed epithelia,	(Wojcik et al., 2000; Wojcik et al., 2001; Wong et al., 2000)
	K8	Phenotype strain dependent, compensation by K7, liver haemorrhage with embryo lethality (C57Bl/6), colorectal hyperplasia; colitis and mild hepatitis (FVB/n)	(Baribault et al., 1994; Baribault et al., 1993)

	Type II Cluster	Embryo lethality at E9.5, defects in desmosomal junctions, reduced translation through GLUT mislocalization and defective vascularization	(Vijayaraj et al., 2010; Vijayaraj et al., 2009)
Type I	K10	Compensation by K14, skin hyperproliferation, altered sebocytes differentiation	(Reichelt et al., 2004; Reichelt et al., 2001; Reichelt and Magin, 2002)
	K12	Mild corneal epithelia erosion	(Kao et al., 1996)
	K14	Compensation by K15	(Lloyd et al., 1995)
	K16	Not yet reported	NIH KOMP
	K17	Compensation by K16/ K14, lysis of nail bed epithelia, reduced translation through defective 14-3-3 signaling	(Kim et al., 2006; Wong et al., 2005)
	K18	K8 aggregates, gain of toxic function in old mice, spontaneous MDB formation, mild hepatitis, increased hepatocyte fragility	(Ku and Omary, 2006; Magin et al., 1998)
	K19	Compensation by K18/ K20, mild myopathy in adult mice	(Hesse et al., 2000; Stone et al., 2007; Tamai et al., 2000)
	K18, K19	K7 and K8 aggregates, gain of toxic function, embryonic lethality at E9.5 due to TGC fragility	(Hesse et al., 2000)
Type II and type I	K8, K19	Residential expression of K7/ K18, embryonic lethality at E9.5, placental degeneration	(Tamai et al., 2000)

Table 1.4.1 **Compilation of mouse keratin null mutations.** To analyze keratin function a number of transgenic mouse models were generated, from single KO studies to the complete cluster KO.

The deletion of the embryonic and simple K8 causes in C56Bl/6 mice up to 90% embryonic lethality due to placental failure at E12.5. In contrast, neither K18 nor K19 deletions display any obvious phenotypes during embryonic development and in young mice. During embryonic development, both K18 and K19 are expressed, and single deletions of either one can be compensated by the remaining type I keratin. However, in adult K18 deficient mice mild hepatitis and increased hepatocytes fragility can arise, due to spontaneous *Mallory-Denk* body (MDB) formation from accumulating K8 aggregates. In liver cells K8 and K18 are the only keratins expressed, no additional keratin can compensate for the loss of K18. The K8 aggregates are possibly more efficiently targeted by the ubiquitin degradation machinery

in young mice, resulting in the accumulation and the formation of MDB in older mice (Ku and Omary, 2000; Ku and Omary, 2006; Loffek et al., 2010; Magin et al., 1998). Furthermore, recent evidence also demonstrates a phenotype in K19 KO mice, where mild myopathies were observed (Stone et al., 2007). A double KO of both embryonic type I keratins, K18 and K19, results in a complete deletion of all keratin filaments in early embryonic development (Hesse et al., 2000) (similar to the K8, K19 KO (Tamai et al., 2000)) and causes embryonic death at E9.5. Data from *C. elegans* suggested that an equilibrium of intermediate filaments and a cytoplasmic soluble pool is needed for proper embryo development and the knockout of the degradation machinery Sumo consequently resulted in excessive filaments and embryo lethality (Kaminsky et al., 2009). In this fashion, aggregates of K8 and K7 remaining in the K18, K19 double KO, led to a gain of toxic function, reminiscent of the deletion of the chaperone Hsp40 which resulted in a similar keratin aggregate phenotype (Watson et al., 2007). This pathology resulted in an impaired placenta, followed by extensive haemorrhages, similar to keratinocyte fragility in EBS.

Given the potential toxicity of K7/K8 aggregates in the K18/19 double-deficient embryos (Hesse et al., 2000); the precise function of keratins in development is still unclear and requires deletion of all 4 genes. The deletion of all keratins provides for the first time the possibility to study keratin function without aggregation artifacts with cytotoxic side affects or possible resident keratin genes which could compensate.

2. Aim

The most intriguing feature of keratin filaments is an epithelial cell and differentiation state dependent expression of specific keratin pairs. For example, in skin tissues, basal keratinocytes express K5 and K14, in their differentiation process towards the stratum corneum these are replaced by K1 and K10. In wound healing and inflammation additional keratins K6, K16 and K17 are activated (Moll et al., 1982). Simple epithelia on the other hand express a completely different set of keratins, mainly K7, K8, K18, K19, K20 and K23, which mix in stratified epithelia with basal keratins. This incites the phenomenon that a single cell can express up to 10 different keratin proteins (Omary et al., 2009).

Some major questions arise: 1) Why do all those different keratins exist and what defines their expression patterns and their specific functions? 2) What are filament pair specific functions?

To analyze keratin function systematically and to target the problem of compensatory upregulation/ stabilization a large scale genome deletion was attempted in order to knockout the complete keratin type II cluster (Vijayaraj et al., 2009). Hence, by deleting the type II cluster (containing the type I keratin 18), one abolishes formation of keratin filaments as well as avoids aggregates of the early type I keratins thereby circumventing possible dominant negative effects (Vijayaraj, 2008). This new mouse model provides for the first time the unique possibility to study embryonic development in a keratin free background.

The major part of this thesis aims to analyze the function of keratins in embryonic and extraembryonic tissue development and summarizes the data so far acquired in the examination of the keratin type II cluster KO mice.
This thesis discusses how keratin IF proteins regulate embryo growth upstream of the mammalian target of rapamycin (mTOR) pathway through GLUT1 receptor localization and how they contribute to yolk sac vasculogenesis through altered BMP-4 signaling. Furthermore, it reveals that keratins regulate the maternal-fetal vascularization through the correct localization of TGCs and the secretion of TGC hormones; their absence predisposing to pregnancy loss due to decidual hyperoxia.

In addition to the *in vivo* model, a more accessible system was needed to analyze keratin function at a molecular level. Therefore, in order to perform systematic biochemical assays,

gain and loss of function assay and replacement approaches to identify the molecular mechanisms of keratin actions, a cell culture model was generated.

In combination with the in vivo model to verify the cell culture data, the CK minus cell line will prove to be a powerful tool to analyze all the formerly proposed functions of keratins in cell architecture, cell attachment and migration, apoptosis, cell proliferation and growth, and finally organelle distribution and vesicle transport. The last part of this thesis provides the first insights into keratin KO dependent alterations in cell architecture in this new cell line.

3. Materials and Methods

Materials and Methods used in chapters 4.1-4.3 are described in the respective articles and manuscripts.

3.1 Materials

3.1.1 Chemicals

Unless otherwise stated, chemicals were purchased from Serva (Heidelberg, Germany), Sigma (Deisenhofen, Germany), Roche (Basel, Switzerland), Fermentas (St.Leon-Rot, Germany), Merck (Darmstadt, Germany), Fluka (Deisenhofen, Germany), Invitrogen Life Technologies (Karlsruhe, Germany), or Applichem (Darmstadt, Germany). All cell culture solutions, buffers or antibiotics were from Sigma (Deisenhofen, Germany) or Invitrogen/Life technologies & GibcoBRL (Karlsruhe, Germany). Restriction enzymes, protein and DNA markers were from Fermentas (St.Leon-Rot, Germany).

3.1.2 Ready-to-use solutions/reagents

Acetic acid
Acrylamide solution (37.5:1) Acrylamide/Bisacrylamide for protein-SDS gel
Dimethylsulfoxide (DMSO)
Ethanol
Ethidiumbromide, 10 mg/ml
Isopropanol
Lipofectamin™ 2000 (Invitrogen, 11668-019)
Methanol
ProLong® Gold antifade reagent (Molecular Probes, P36930)
TEMED for protein-SDS gel
TRIzol for isolation of RNA
Tween-20
Triton-X100

3.1.3 Kits

Amaxa Nucleofector Kit prim. Endothelial Cells (Lonza, VPI-1001)
QIAEX II Gel Extraction Kit (Qiagen, 20021)
Qiagen Plasmid Maxi kit (Qiagen, 12163)

3.1.4 Solutions

DNA analysis

Name	Final concentration	Constituents and their amounts
Sodium acetate	3 M	40.82 g Sodium acetate in 100 ml water. pH was adjusted to 5.2 with acetic acid and stored at room temperature.
DNA loading Buffer (10x)	30% 100 mM 0.25% 0.25% 0.25 2%	Ficoll Type 400 3.72 g EDTA 125 mg bromphenolblue 125 mg xylenecyanol Orange G 20% SDS
Lysis buffer	100 mM 5 mM 0.2% 200 mM	10 ml of 1 M Tris-HCl 1 ml of 0.5 M EDTA 1 ml SDS-solution, 20 % 4 ml 5 M NaCl The above ingredients were added to 84 ml of Dnase/Rnase free water and stored as 10 ml aliquots at -20°C.
Proteinase K solution	20 mg/ml	1 g Proteinase K (Applichem, A38300025) was added to 50 ml Dnase/Rnase free water, aliquoted and stored at -80°C.
RNase Solution	20 mg/ml	500 mg RNase was dissolved in 25 ml sterile water and heated for 15 min at 95°C. Aliquoted and stored at -80°C.
TAE (50x)	2 M 5.71% 50 mM	242 g Tris-base 57.1 ml acetic acid 14.61 g EDTA Dissolved in 1 l water and pH adjusted to 8.1-8.3.
TBE (10 x) 900 mM	900 mM 25 mM 25 mM	109 g Tris-base 55.6 g boric acid 0.93 g EDTA Dissolved in 1 l water and pH adjusted to 8.3.
TE buffer	10 mM 1 mM	121 mg Tris 37.2 mg EDTA Dissolved in 100 ml sterile water, pH adjusted to 8.0 and sterilized by autoclaving. Stored at RT.

10x Phosphate buffered saline (PBS)	137 mM 2.7 mM 10 mM 2 mM	40 g NaCl 1 g KCl 89 g $Na_2HPO_4 \bullet 2H_2O$ 12 g KH_2PO_4 Salts were dissolved in 4.5 l water, pH was adjusted to 7.4 with HCl, and volume was adjusted to 5 l with water and autoclaved. Stored at RT.
Magnesium chloride	1 M	101.65 g $MgCl_2$ in 500 ml water.

Bacterial Cultures

Name	Final concentration	Constituents and their amounts
Ampicillin solution	200 µg/ml	100 g ampicillin in 50 ml of water. Sterile filtered. End concentration used was 200 mg/ml.
LB Agar	 2%	1 l LB Medium 32 g LB Agar in 1 l water Sterilized by autoclaving. Antibiotics were added at 55°C and plates were poured.
LB Medium	25 g	LB medium was dissolved in 1 l water and sterilized by autoclaving.
Buffer 1	50 mM 12.7 mM 100 µg/ml	6.06 g Tris-base 3.72 g EDTA Dissolved in 1 l water and pH adjusted to 8.0. 100 mg/ml RNaseA add fresh
Buffer 2	200 mM 1%	8 g NaOH 50 ml 20% EDTA Dissolved in 1 l water.
Buffer 3	3.6 M	294.5 g potassium acetat Dissolved in 500 ml water and pH adjusted to 5.5 with acetic acid, then volume was made up to 1 l.

Keratinocyte cell culture

Name	Final concentration	Constituents and their amounts
FBS Gold (PAA)		To remove calcium ions, serum was pre-treated with 8 g/50 ml Chelex 100 (Bio-Rad, 142-2842) overnight on a rotating wheel at 4°C. Procedure was 1x repeated followed by sterile filtration (0.1 µm filter).

FAD Medium		FAD medium (DMEM/Ham's F12) with 50 µM Ca^{2+} (FAD low Ca^{2+}, manufactured by Biochrom, FZ 9995)
FAD + Medium		Was prepared by combining the following:
		460 ml FAD medium
	10%	50 ml FBS (Chelex treated)
	1x	5 ml GlutaMax (100x) (Invitrogen)
	0.18 mM	2 ml 45 mM adenine (Sigma) in 0.05 N HCl
	0.5 µg/ml	250 µl 1 mg/ml hydrocortison in EtOH (Sigma)
	5 µg/ml	500 µl 5 mg/ml insulin (Sigma) in 5 mM HCl
	10 ng/ml	500 µl 10 µg/ml EGF (Sigma) in FAD
	100 pM	5 µl 1 µM cholera toxin (Sigma) in sterile water
	0.5x	2.5 ml 100x penicillin/streptomycin (Invitrogen)
Feeder Medium		Was prepared by combining the following:
	500 ml	DMEM high glucose (Invitrogen)
	50 ml	FCS
	5 ml	sodium pyruvate (100x) (Invitrogen)
Freezing medium	10%	5 ml DMSO
Keratinocytes	90%	45 ml FBS (Chelex treated)
		Aliquoted and stored at -20°C.
2x Freezing medium	20% DMSO	10 ml DMSO
Feeder	20% FBS	10 ml FBS
		Filled with DMEM to 50 ml, aliquoted and stored at -20°C.
Keratinocyte trypsin		468 ml cell culture grade PBS
	0.025 %	27 ml ES-EDTA-Solution (1.85 g/l in cell culture grade water)
	0.025%	5 ml trypsin, 2.5%
		Solution was stored at -20°C and once thawed, it was stored at 4°C.
Collagen I	50 µg/ml	3.75 mg/ml Collagen I (rat tail, Invitrogen) in 0.02 N acetic acid
Hygromycin B		
Feeder	50 µg/ml	50 mg/ml hygromycin solution (Invitrogen)
Keratinocytes	20 µg/ml	
Mitomycin C (Stock)	0.4 mg/ml	2 mg mitomycin powder resuspended in 5 ml PBS

Immunofluorescence analysis

Name	Final concentration	Constituents and their amounts
Blocking solution	1%	1 g BSA fraction V
	1x	10 ml 10x TBS
		Volume was made up to 100 ml with water. Solution was aliquoted and stored at -20°C.
10x PBS	137 mM	40 g NaCl
	2.7 mM	1 g KCl
	10 mM	89 g $Na_2HPO_4 \bullet 2H_2O$
	2 mM	12 g KH_2PO_4
		Salts were dissolved in 4.5 l water, pH was adjusted to 7.4 with HCl, and volume was adjusted to 5 l with water and autoclaved. Stored at RT.
4% formaline solution	4%	4 g paraformaldehyde (PFA)
	1x	10 ml 10x PBS
		Dissolved in 100 ml sterile water, pH adjusted to 7.5. Always prepared fresh.
TBS-Triton	0,5%	0.5 ml Triton X
	1x	10 ml 10x TBS
		Volume made up to 100 ml with DD water.
10x Tris buffered saline (TBS)	0.1 M	12.1 g Tris
	1.5 M	87.6 g NaCl
		Contents were dissolved in 750 ml water, pH was adjusted to 7.5 and the volume was made up to 1 l. Solution was sterilized by autoclaving and stored at room temperature.

Protein biochemistry

Name	Final concentration	Constituents and their amounts
5x Laemmli Sample buffer	50 mM	sodium phosphate pH 6.8
	5%	SDS
	40 mM	DTT
	5 mM	EDTA
	5 mM	EGTA
	20%	glycerol
	0.01%	bromphenolblue
		Solution was stored at -20°C and freeze/thawed not more than 5 times.
APS 10%	10%	1 g ammonium persulfate in 10 ml water. Stored at 4°C for not longer than 1 month.

Stacking gel buffer (Upper Tris)	0.5 M 0.4%	15.1 g Tris-base 1 g SDS Volume made up to 250 ml after adjusting pH to 6.8, sterile filtered and stored at 4°C.
Separating gel buffer (Lower Tris)	1.5 M 0.4%	181.7 g Tris 4 g SDS Volume made up to 1 l after adjusting to pH 8.8, sterile filtered and stored at 4°C.
SDS-running buffer (1x Laemmli buffer)	23 mM 190 mM 0.1%	2.78 g Tris Base 14.26 g glycine 5 ml 20% SDS stock The contents were mixed in 1 l water and pH was adjusted to 8.8. Stored at room temperature.
Coomassie staining solution	0.4% 5% 40%	1.0 g Coomassie Brilliant Blue G-250 25 ml acetic acid 200 ml methanol Volume was adjusted to 500 ml with distilled water, filtered through a Whatman filter paper and stored at room temperature. Solution was used more than once.
Coomassie destaining solution	10% 30%	50 ml acetic acid 150 ml methanol Solution made up to 500 ml with water.
Ponceau S staining solution	0.5% 3%	0.5 g Ponceau S 3 ml acetic acid Contents were dissolved in 100 ml distilled water and filtered; Solution was stored in dark at room temperature.
Transfer buffer (1x Towbin buffer)	25 mM 192 mM 0.1% 10%	3.028 g Tris 14.41 g Glycine 1 g SDS 100 ml methanol The contents were dissolved in 1 l water, and pH was adjusted to 8.3. Solution was stored at room temperature.
10x Tris buffered saline (TBS)	0.1 M 1.5 M	12.1 g Tris 87.6 g NaCl Contents were dissolved in 750 ml water, pH was adjusted to 7.5 and the volume was made up to 1 l. Solution was sterilized by autoclaving and stored at room temperature.
Western washing buffer	1x 0.1%	100 ml 10x TBS 1 ml Tween 20 Volume was made up to 1 l with water.

Blocking solution	5% 1x 0.1%	5 g skimmed milk (Sucofin) 10 ml 10x TBS 0.1 ml Tween 20 Volume was made up to 100 ml with water. Always prepared fresh.
Alternative blocking solution	5% 1x 0.1%	5 g BSA fraction V 10 ml 10x TBS 0.1 ml Tween 20 Volume was made up to 100 ml with water. Always prepared fresh.
ECL	1.25 mM 6.7 mM	50 mg Luminol in 200 ml 0.1 M Tris-HCl; pH 8,6 (Solution A) 11 mg para-hydroxycoumarinsäure in 10 ml DMSO (Solution B) Before use, 1 ml Solution A was mixed with 100 µl Solution B and 0.3 µl of H_2O_2
Protease inhibitor	1x	Complete protease inhibitor cocktail tablets. 7 x stock solution was prepared by dissolving one tablet in 1.5 ml water, aliquoted and stored up to 6 months at -20°C.
Phosphatase inhibitor	1x	Phosphatase Inhibitor Cocktail Tablets. 10 x stock solutions was prepared by dissolving one tablet in 1 ml water, aliquoted and stored up to 6 months at -20°C.

3.1.5 Plasmids

Name [size in base pairs]	Description	Reference
pcDNA3.1/Hygro (+) [5597 bp]	Mammalian expression vector	Invitrogen
pPGK-Cre-bpa [4850 bp]	Eukaryotic expression vector	Willecke lab
pcCre Hygro [6691 bp]	Mammalian Cre expression vector	Magin lab

3.1.6 Bacterial strains

Description	Characteristics and applications	Reference
E. coli XL1-blue MRF	Genotype: recA1 endA1 gyrA96 thi-1 hsdR17 supE44 relA1 lac [F´ proAB lacIqZΔM15 Tn10 (Tetr)] ; Amplification of plasmid	(Bullock and Wright, 1987)

3.1.7 Mouse lines

Genotype	Short description	Source
C57BL/6N	Wild type mice with black color for breeding and back crossing.	Charles River, Germany
KTyII +/-	Transgenic mice heterozygous for the keratin type II cluster deletion.	Generated by P. Vijayaraj (Vijayaraj et al., 2009)
KTyII fl/fl	Transgenic mice with floxed keratin type II cluster.	Generated by P. Vijayaraj (Vijayaraj, 2008)

3.1.8 Eukaryotic cell lines

Description	Characteristics and applications	Source
NIH 3T3 Swiss	Murine fibroblast cell line	ATCC- CRL-1658

3.1.9 Antibodies

Primary antibodies

Name	Antigen	Source	Subclass	Dilution/ application	Source
GoH3	α6-integrin	Rat	Monoclonal IgG1	1:10; [IF]	A. Sonnenberg (Progen)
AC-15	β-actin	Mouse	Monoclonal IgG1	1:1000; [WB]	Sigma
GTU-88	y-Tubulin	Mouse	Monoclonal IgG1	1:250; [IF]	Sigma
DP1	Desmoplakin	Guinea Pig	Polyclonal	1:1000; [WB]	Progen
II-5F	Desmoplakin 2	Mouse	Monoclonal IgG1	1:100; [IF]	Garrod
ECCD-2	E-Cadherin	Rat	Monoclonal IgG2a	1:100; [IF]	Sigma
DECMA-1	E-Cadherin	Rat	Monoclonal IgG1	1:100; [IF]	Sigma
1/GS28	GS28	Mouse	Monoclonal IgG2a	1:200; [IF]	BD Transduction Laboratories
pk5-kopf	K5	Guinea Pig	Polyclonal	1:;100 [IF]	Magin lab
a-K5	K5	Rabbit	Polyclonal	1:50; [IF] 1:50,000; [WB]	Davids Biotechnologies
K6	K6	Mouse	Monoclonal IgG1	1:500; [WB]	Progen
TROMA1	K8	Rat	Monoclonal IgG1	Neat; [IF] 1:50; [WB]	B. Omary

1864/07 #1	K14	Rabbit	Polyclonal	1:50; [IF] 1:300,000; [WB]	PSL Heidelberg
KH Anti-mK16	K16	Rabbit	Polyclonal	1:20,000; [WB]	Progen
CK17.1	K17	Guinea Pig	Polyclonal	1:50,000; [WB]	Lutz Langbein
EP 1628Y	K18	Rabbit	Monoclonal IgG	1:5000; [WB]	Epitomics
Pka19	K19	Guinea Pig	Polyclonal	1:5000; [WB]	Magin lab
B 5-1-2	α-tubulin	Mouse	Monoclonal IgG1	1:5000; [WB]	Sigma
YOL1/34	Tubulin	Rat	Monoclonal IgG2a	1:50; [IF]	Abcam
DL-11	PDI	Rabbit	Polyclonal	1:200; [IF]	Sigma
HD 1 (=121) mAb-121	Plectin	Mouse	Monoclonal IgG1	1:50; [IF] 1:1000; [WB]	Katsushi Owaribe, Japan
VIM-CT	Vimentin	Rabbit	Polyclonal	1:10.000; [WB]	Magin lab
a-vinculin	Vinculin	Mouse	Monoclonal IgG1	1:50; [IF] 1:1000; [WB]	Sigma

Secondary/ conjugated antibodies, conjugated toxins

Name	**Anti species**	**Species**	**Dilution/ application**	**Source**
Alexa 488	Rat	Goat	1:800; [IF]	Dianova
Alexa 594	Rat	Goat	1:800; [IF]	Dianova
Cy2	Mouse	Donkey	1:400; [IF]	Dianova
Cy3	Guinea Pig	Donkey	1:800; [IF]	Dianova
DyLight 488	Rabbit	Donkey	1:800; [IF]	Dianova
DyLight 546	Rabbit	Donkey	1:800; [IF]	Dianova
HRP	Guinea Pig	Goat	1:20,000; [WB]	Dianova
HRP	Mouse	Goat	1:20,000; [WB]	Dianova
HRP	Rabbit	Goat	1:20,000; [WB]	Dianova
HRP	Rat	Goat	1:20,000; [WB]	Dianova
Phalloidin A555			1:6; [IF]	Invitrogen

3.1.10 General lab materials

All sterile cell culture plastic-ware were purchased from Falcon, Sarstedt, TPP (Renner), Nunc and Becton Dickinson if not stated otherwise.

Pipette tips and tubes were purchased from Sarstedt.

Coverslips 13 mm

Fuji Medical X-Ray film (Fuji)

High density photo paper (Mitsubishi)

Microscope slides 76 x 26 mm (Engelbrecht)

Protran nitrocellulose hybridization transfer membrane, 0.2 µm, 30 cm x 3 m roll (Schleicher & Schuell)

Sterile filters 0.45 µm, 0.2 µm, 0.1 µm (Schleicher & Schuell)

Whatman 3 mm paper GB 002 (Schleicher & Schuell #426693)

Whatman filter paper (Schleicher & Schuell)

3.1.11 Equipment and materials used

Instrument/ Software	Model/ Version	Company
Agarose gel electrophoresis system	B2; B1A	Angewandte Gentechnologie
AIDA software	Aida 2.11	Raytest
Axiovison	Axiovision 4.61	Carl Zeiss
Blotting chamber fast blot	B49	Biometra
Centrifuges	5417R, 5810R, 5417C	Eppendorf
CO_2 incubator		Heraeus Instruments
Film developer	Curix 60	Agfa
Fluorescence microscope	AxioPhot II	Zeiss
Incubators for bacterial cultures	Function line	Heraeus Instruments
Inverted microscope equipped with ApoTome	Axiovert 200M	Zeiss
Laser scanning microscope	LSM 710	Zeiss
pH-Meter	761 Calimatic	Knick
Photoshop software	Adope Photoshop 7.0	Adobe
PowerPoint/ Add-on: Science slides	PowerPoint 2003 2005 Fall Edition Full	Microsoft Office VisiScience Corporation 2005
UV-spectrophotometer	Genesys 10UV	Thermoelectron corporation
Water purifier Milli-Q Plus	Nanopure	Barnstead

3.2 Methods

3.2.1 Bacterial cloning

To generate a Cre recombinase protein expression plasmid with Hygromycin resistance, Cre cDNA was subloned from PGK Cre into pcDNA3.1/Hygro (+) (Invitrogen), using the restriction enzymes XhoI (40 U/µl) and XbaI (40 U/µl) from *Fermentas* (Fig. 2.3.1.1).

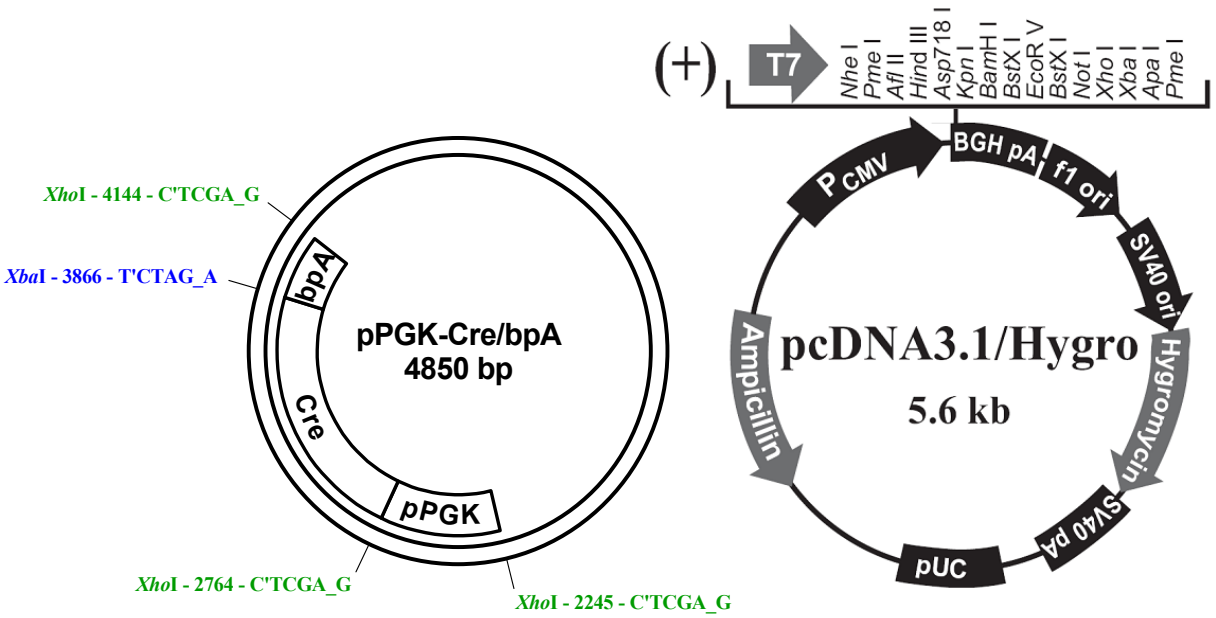

Figure 3.2.1.1 **pPGK Cre/bpA and pcDNA3.1/Hygro (+) expression plasmid (Invitrogen).**

After restriction, DNA fragments were separated on a 1% agarose TAE gel and the required DNA sequences were extracted according to the manufacturer's instructions with the QIAEX II® Gel Extraction Kit (Qiagen). Subsequently, cDNA and vector were ligated in a 3:1 molar ratio at 16°C overnight using T4 DNA ligase (0.2-0.4 Weiss units/µl, Fermentas). The reaction was transformed into XL1 Blue chemo-competent bacteria. For this step, cells and DNA were chilled on ice and LB-media pre-heated to 37°C. DNA was added to the bacteria and incubated for 30 min on ice. Subsequently, bacteria were heat shocked at 42°C for 90 s, followed by immediate incubation on ice for 90 s. The cells were allowed to recover in 400 µl of pre-warmed LB medium at 37°C for 1h. Finally, the bacteria were spread on ampicillin resistant plates and the cultures were incubated at 37°C overnight (o/n). The following day, single colonies were picked from plates and inoculated into 3 ml LB-media containing 200 µg/ml ampicillin; in parallel a master plate was set up. Small scale liquid cultures were incubated o/n at 225 rpm at 37°C. The following day 2 ml of the liquid culture were used for DNA extraction.

Bacteria were pelleted by centrifugation at 8000 *g* for 5 min. The supernatant was discarded. Pellets were resuspended in 400 µl Buffer 1 and lysed for 5 min by mixing with 400 µl Buffer 2, the reaction was neutralized with 400 µl Buffer 3. Protein and cell debris were removed by centrifugation at 20,000 g for 10 min in a table top centrifuge. Supernatant was transferred into a fresh tube and precipitated with 840 µl isopropanol and pelleted by centrifugation at 20,000 *g* for 10 min. DNA was washed with 500 µl 70% ethanol, pelleted with centrifugation at 20,000 *g* and washed once more with 500 µl 100% ethanol, pelleted with centrifugation at 20,000 *g* and air-dried. Finally the DNA was resuspended in 30 µl TE-buffer. Clones were confirmed with restriction analysis and amplified from the master plate via Maxi-Prep.

For Maxi-Preps 250 ml of LB containing 200 µg/ml ampicillin were inoculated and grown overnight at 225 rpm at 37°C. The following day plasmids were extracted from cultures using the Qiagen Plasmid Maxi Kit (Qiagen) according to the manufacturers' directions. After plasmid extraction, DNA concentrations were determined by measuring OD at 260 nm and 280 nm with a conversion factor of 1 OD_{260} = 50 µg/ml DNA; DNA quality was controlled via gel electrophoresis.

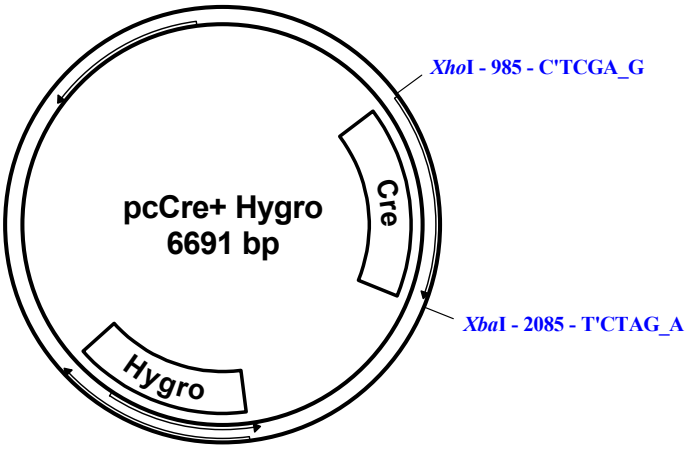

Figure 3.2.1.2 **Final pcCre Hygro vector.**

3.2.2 Isolation of murine keratinocytes

Keratinocytes were derived from C57Bl6 KTyII fl/- and KTyII fl/+ mice and cultivated under conditions that permit spontaneous immortalization as described in Turksen (ed.) (Epidermal Cells, Methods in Molecular Biology 585, Chapter 5), here described in detail. For the isolation of keratinocytes newborn mice were used, not older than three days post natal. The CK minus and plus cell lines were generated from one day old embryos. The embryos were sacrificed by decapitation and the bodies were cooled in a 50 ml Falcon on ice for 1 h. The rest of the isolation was performed under the laminar flow hood. In the next step the embryos were washed and disinfected: 1 min 50% beta iodine / 50% 1x PBS; rinsed briefly in 1x PBS; 1 min 70% EtOH; rinsed briefly in 1x PBS and transferred to a sterile 100 mm dish. Tails and limbs were cut off and used for genotyping. A lengthwise incision was made along the side of

the embryo, from neck to tail; the mouse body was unwrapped from the back to the front using forceps and the dull part of scissors to take the skin off in one piece. The skin was transferred to a 30 mm dish with the epidermal side up and was filled with 1 ml of trypsin solution (0.025% trypsin / 0.02% EDTA / PBS) so that the skin floated on the trypsin solution. However, it was assured that only the dermal side of the skin would be in contact with Trypsin solution. The skin was incubated overnight (o/n) at 4°C. On the next day, the skin was transferred with as little trypsin as possible to a fresh 100 mm dish with the dermal side up. The dermis was peeled off the epidermis using forceps and was discarded. Subsequently, the epidermis was minced into small pieces using a scalpel. When the minced epidermis was drying out, a drop of trypsin was added. The epidermis was transferred with a scalpel into a sterile 2 ml tube; the scalpel and the 100 mm dish were rinsed with 500 µl of trypsin to transfer all cells completely. The cells were trypsinized shaking for 15 min at 37 °C and stopped with 1 ml complete FAD medium. Cells were centrifuged at 1000 *g* for 5 min, resuspended in 1.5 ml complete FAD media by pipetting up and down with a blue tip and then plated on Collagen I (Rat tail, Becton Dickinson) coated 6-well plates (coated for 1 h at room temperature and then washed with 1x PBS) with an inactivated 3T3 Swiss NIH feeder layer.

Feeder cells were cultivated in DMEM medium and when confluent treated with 100 µl mitomycin in 10 ml medium for 2 h at 37°C, 5% CO_2. They were washed extensively with PBS at least 5 times before trypsinization; feeder were resuspended in FAD Media and transferred to the 6-well plates, usually seeding a confluent 10 cm dish per complete 6-well plate (~ 400,000 cells per well).

The primary keratinocytes were incubated at 32°C, 5% CO_2 in a cell culture incubator. Colonies became visible in the second or third week. Dead inactivated feeders were replaced with mitomycin treated fresh feeders.

When keratinocytes were confluent they were split 1:2 on collagen coated dishes. After passage 4-5 they were split at lower densities up to 1:3. Murine keratinocytes were very sensitive, especially during the first passages after isolation. After passage four they were passaged without feeders and after 5-6 passages cells started to immortalize spontaneously.

3.2.3 Culture of murine keratinocytes and 3T3 NIH feeder cells

CK minus cells were grown in FAD^+ media supplemented with 10% serum, 5% CO_2 at 32°C. Cells were grown on collagen I (rat tail) coated cell culture dishes and up to passage four with additional with feeder cells.

For subculturing, medium was aspirated off and cells were washed shortly with PBS. If keratinocytes were cultured on feeder cells, they were briefly incubated with 0.025% EDTA for 5 min to detach the feeder cells, which were subsequently washed off with PBS and

aspirated. To trypsinize keratinocytes, fresh trypsin (0.025%) / EDTA (0.02%) / PBS solution was added. Cells were incubated for about 15 min at 37°C until they detached. Fresh medium was added and cells were pipetted up and down several times to neutralize the trypsin/EDTA and to disperse the cells. Cells were pelleted by low speed centrifugation (1,000 *g*) for 5 min, the fluid was aspirated off, and cells were resuspended in fresh media and promptly replated. As keratinocytes need cell contact, not less than 1.2 x10^6 cells were seeded per T75 flask. The media was changed every 2-3 days.
To freeze keratinocyte cells, pellets were resuspended in Freeze solution: 90% FCS Gold (Chelex treated), 10% DMSO and aliquoted at 1-2 x10^6 cells in cryo tubes.
To thaw cells, vials were placed in a container of 37°C water and rapidly brought to 37°C. The thawed cells were transferred to a centrifuge tube containing 9 ml prewarmed medium. Cells were pelleted as above, resuspended in fresh medium and plated into a T25 flask.

Feeder cells were cultivated in high glucose DMEM medium supplied with 10% serum, 5% CO_2 at 37°C. For subculturing, medium was aspirated and cells washed shortly with PBS and trypsinized with 0.25% Trypsin / EDTA (Gibco) for about 2 min at 37°C until cells detached. Fresh medium was added and the cells were pipetted up and down several times to neutralize the trypsin/EDTA and disperse the cells. Cells were pelleted by low speed centrifugation (1,200 *g*) for 3 min, the fluid was aspirated off, and they were resuspended in fresh media and promptly replated. Before use as feeder cells in keratinocyte culturing, cells were Mitomycin C treated as described in the previous chapter. Feeder cells can be split up to 1:10 every 3 days. To freeze feeder cells the cell pellets were resuspended in 2x Freeze solution: 20% DMSO, 10% FCS in DMEM medium and aliquoted at 2 x10^6 cells in cryo tubes.

3.2.4 Generation of a keratin-deficient keratinocyte cell line

To obtain a stable cell line depleted of all keratins hygromycin resistant feeder cells had to be generated. For this purpose 3T3 NIH cells were transfected with pcDNA3.1/Hygro (+) (Invitrogen) using Lipofectamin™ 2000 (Invitrogen) in a 100 mm dish according to manufactures protocol. 12 h after transfection 3T3 NIH cells were selected for hygromycin resistance using 50 µg/ml of hygromycin solution (Invitrogen), as established in a killing curve. After 2 weeks resistant feeders could be expanded and stored.
C57Bl6 KTyII fl/- keratinocytes were transfected using the Amaxa Nucleofector Kit for primary endothelial cells according to the manufactures protocol program T27, however with a few alterations; for each transfection 1 x10^6 cells were used and 4 µg super-coil plasmid DNA with a concentration of 1 µg/µl. 24 h after transfection, parallel to selection with 20 µg/ml of hygromycin solution, 2 x10^6 inactivated feeder cells were added (~50% confluency).

After 2 weeks single colonies could be picked with metal clone rings and were trypsinized into 24-well plates with feeder cells. Confluent wells were split without feeder cells into two 24-wells before they were both transferred into 30 mm dishes. Clones were tested for keratins with immunofluorescences for K5 and vimentin to exclude eventual feeder cell contaminations. Keratin clones were expended and frozen for storage.

3.2.5 Immunofluorescence

Coverslips were placed into the cell culture dishes prior to collagen coating. Coverslips were harvested with fine forceps, washed briefly in PBS and were directly emerged into the fixative. Depending on the antigen, different fixatives were used. As standard method cells were fixed for 5 min in -20°C methanol, 30 s in –20°C acetone and then dried for 30 min. Soluble antigens and filamentous actin were fixed for 10 min in 4% formaline, made freshly from PFA, at RT, washed 3x in TBS and then permeabilized for 3 min in 0.1% Triton/TBS. After additional three washes in TBS, coverslips were further processed. For keratin/phalloidin double immunofluorescences cells were permeabilized after fixation 30 s in –20°C acetone. All antibodies were diluted in PBS containing 1% BSA. The primary antibody was applied with optimal dilution (listed in 2.1.5 Antibodies) and incubated for 1 h at room temperature. After washing three times in TBS, appropriate secondary antibody dilutions (listed in 2.1.5 Antibodies) were applied and incubated for 1 h. The nuclei were counterstained using 1:1000 diluted 4,6-diamidino-2-phenylindole (DAPI) along with the secondary antibody. After washing 3 times in PBS for 5 min, coverslips were mounted with Prolong Gold (Invitrogen). Image analysis and processing were performed using the AxioVision 4.61 (Carl Zeiss) and Adobe Photoshop 7.0 software.

3.2.6 Protein biochemistry: SDS- and Western blot

Prior to electrophoresis, samples were prepared by adding 200 µl of boiling Laemmli Buffer containing 1x protease inhibitor and 1x phosphatase inhibitor into one 6-well plate, the lysate was transferred into an Eppendorf tube and was heated for 15 min at 95°C, sample was pelleted by centrifugation at 20,000 *g* for 10 min and then loaded on a gel.

Protein lysates were separated on a SDS-polyacrylamide gel. SDS- gels were poured with either an 8% or 10% acrylamide resolving gel in Lower Tris Buffer depending on the molecular weight of the protein of interest (for 10 ml: 8% gel: 4.8 ml H_2O, 2.5 ml Lower Tris, 2.7 ml 30% acrylamide, 100 µl APS, 10 µl TEMED; 10% gel: 4.2 ml H_2O, 2.5 ml Lower Tris, 3.3 ml 30% acrylamide, 100 µl APS, 10 µl TEMED). The stacking gel was 5% acrylamide in Upper Tris Buffer (for 4.5 ml: 2.6 ml H_2O, 1 ml Upper Tris, 440 µl 30% acrylamide, 40 µl APS, 6 µl TEMED). Gels were run in 1x Laemmli running buffer at constant 10 mA per gel for

approximately 1.5 h. Onto each gel 5 µl of the Ruler^{TM} protein standard from Fermentas were loaded. Gels were then either used for Western blotting or stained with Coomassie Blue overnight and destained in Destain until the background was removed.

SDS-PAGE gels were transferred to nitrocellulose using semi-dry blotting for all 10% gels and a wet blot apparatus for all 8% gels. Membrane (after brief incubation in H_2O), gel and filter paper were presoaked in transfer buffer. The gel and membrane were sandwiched between the filter paper, and each layer smoothed to remove air bubbles. The transfer was performed for the semi-dry blotter at 300mA for 1-2 h and at 100 mA o/n at 4°C for the wet blot. The transfer was checked by staining the membrane with Ponceau S.

For Western blots, membranes were either treated according to manufatures' protocol (Cell signaling) or treated by default as following. Membranes were blocked with TBS / 0.1% Tween20 containing 5% skim milk for 1 h at RT (shaking). The primary antibodies were incubated at 4°C o/n, or 1 h at RT in 5% milk in TBS / 0.1% Tween20 at optimal dilution (listed in 2.1.5 Antibodies). After the primary antibody incubation, blots were washed in TBS / 0.1% Tween20 three times. Horse-radish peroxidase conjugated secondary antibodies (dilutions listed in 2.1.5 Antibodies) were added to the blot in 15% milk in TBS / 0.1% Tween20 and incubated at RT for 1 h. Blots were washed in TBS / 0.1% Tween20 three times and once in TBS. After washing, membranes were developed with ECL for 5 min and then exposed to X-ray films between 10 s and 30 min, depending on the antigen, before developing.

4. Results

4.1 Keratins regulate protein biosynthesis through localization of GLUT1 and -3 upstream of AMP kinase and Raptor

This work was published in a scientific journal.

Journal:
Journal of Cell Biology

Published:
2009 Oct 19;187(2):175-84.

Authors:
Preethi Vijayaraj, Cornelia Kröger, Ursula Reuter, Reinhard Windoffer, Rudolf E. Leube, and Thomas M. Magin

Contribution:
Histology, immunofluorescence, FACS analysis, pathway analysis via Western blot, rescue experiments, image formatting, paper writing

Published

This article has original data in the JCB DataViewer
http://jcb-dataviewer.rupress.org/jcb/browse/1801

JCB: REPORT

Keratins regulate protein biosynthesis through localization of GLUT1 and -3 upstream of AMP kinase and Raptor

Preethi Vijayaraj,[1,2,4] Cornelia Kröger,[1,2] Ursula Reuter,[1,2] Reinhard Windoffer,[3] Rudolf E. Leube,[3] and Thomas M. Magin[1,2]

[1]Abteilung für Zellbiochemie, Institut für Biochemie und Molekularbiologie and [2]Bonner Forum Biomedizin, Universität Bonn, 53115 Bonn, Germany
[3]Institut für Molekulare und Zelluläre Anatomie, Rheinisch-Westfälische Technische Hochschule Aachen Universität, 52074 Aachen, Germany
[4]Center for Vascular Biology Research, Department of Medicine, Beth Israel Deaconess Medical Center, Harvard Medical School, Boston, MA 02215

Keratin intermediate filament proteins form cytoskeletal scaffolds in epithelia, the disruption of which affects cytoarchitecture, cell growth, survival, and organelle transport. However, owing to redundancy, the global function of keratins has not been defined in full. Using a targeted gene deletion strategy, we generated transgenic mice lacking the entire keratin multiprotein family. In this study, we report that without keratins, embryonic epithelia suffer no cytolysis and maintain apical polarity but display mislocalized desmosomes. All keratin-null embryos die from severe growth retardation at embryonic day 9.5. We find that GLUT1 and -3 are mislocalized from the apical plasma membrane in embryonic epithelia, which subsequently activates the energy sensor adenosine monophosphate kinase (AMPK). Analysis of the mammalian target of rapamycin (mTOR) pathway reveals that AMPK induction activates Raptor, repressing protein biosynthesis through mTORC1's downstream targets S6 kinase and 4E-binding protein 1. Our findings demonstrate a novel keratin function upstream of mTOR signaling via GLUT localization and have implications for pathomechanisms and therapy approaches for keratin disorders and the analysis of other gene families.

Introduction

Embryonic development is a fine-tuned interplay of rapid cell growth and differentiation. It is governed by signaling processes that are coordinated in a spatiotemporal manner through interactions with cytoskeletal and scaffold proteins such as keratins in epithelia. However, the function of keratins in spatiotemporal scaffolding and signaling control is unclear. K7, -8, -18, and -19 represent the first keratins during mouse development and begin to form a primary cytoskeleton at nascent desmosomes in the trophectoderm (Jackson et al., 1980). From then on, these keratins are present in all embryonic and extraembryonic epithelia. Owing to their redundancy, it has not been possible to assign and discriminate their mechanical and signaling functions during embryo development and in tissue homeostasis (Hesse et al., 2000; Tamai et al., 2000; Jaquemar et al., 2003). The former is highlighted by previous gene knockout (KO) studies, which have arrived at contradictory results (Baribault et al., 1993; Magin et al., 1998; Hesse et al., 2000; Tamai et al., 2000; Jaquemar et al., 2003). Deletion of K8 caused an embryonic lethal phenotype at embryonic day (E) 12.5, which is associated with placental malfunctions caused by maternal TNF-induced apoptosis (Baribault et al., 1993; Jaquemar et al., 2003). Deletion of K18 permitted normal development because of the presence of K19, illustrating functional redundancy, at least for these two keratins (Magin et al., 1998). The combined deletion of K18/K19 and of K8/K19, which eliminated redundancy, caused fragility of giant trophoblast cells followed by extensive hemorrhages, which led to death at ∼E10 (Hesse et al., 2000; Tamai et al., 2000). This was

P. Vijayaraj and C. Kröger contributed equally to this paper.

Correspondence to Thomas M. Magin: t.magin@uni-bonn.de

Abbreviations used in this paper: 4E-BP1, 4E-binding protein 1; AMPK, AMP kinase; E-cadherin, epithelial cadherin; ES, embryonic stem; KO, knockout; MICER, Mutagenic Insertion and Chromosome Engineering Resource; mTOR, mammalian target of rapamycin; S6K, S6 kinase; WT, wild type.

The Rockefeller University Press $30.00
J. Cell Biol. Vol. 187 No. 2 175–184
www.jcb.org/cgi/doi/10.1083/jcb.200906094

Supplemental Material can be found at:
http://jcb rupress.org/cgi/content/full/jcb.200906094/DC1
Original image data can be found at:
http://jcb-dataviewer rupress.org/jcb/browse/1801

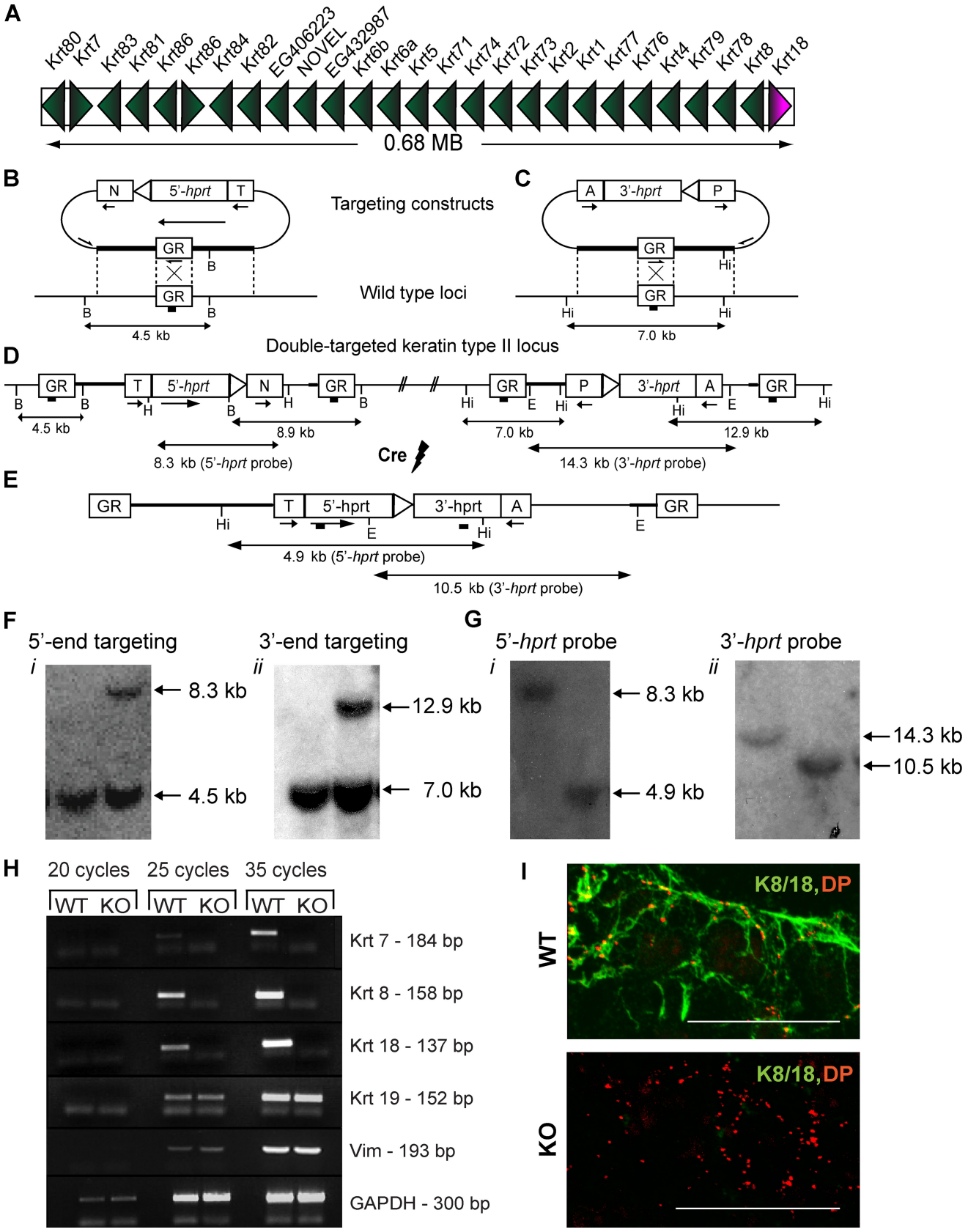

Figure 1. **Constitutive deletion of *Ktyll*$^{-/-}$ keratin gene locus.** (A) Schematic representation of the keratin type II cluster. Green arrowheads identify type II keratin genes oriented in the direction of the tip. The pink arrowhead identifies the only type I keratin (*Krt18*) at the end of type II cluster. (B) 5′-targeting vector (MHPN117k13; Adams et al., 2004). (C) 3′-targeting vector (MHPP322c09; Adams et al., 2004). Gaps [GR] are introduced into the region of homology before targeting. (D) During homologous recombination, the gap is repaired. PCR primers to identify homologous recombinants spanned the gap

interpreted to indicate a primary mechanical function of keratins, which is analogous to that seen in skin epidermis (Fuchs and Cleveland, 1998; Hesse et al., 2000; Tamai et al., 2000; Kim and Coulombe, 2007; Magin et al., 2007).

To systematically analyze keratin functions during embryo development, we exploited the genomic organization of keratin genes. The mouse type I and II keratin families are clustered on two contigs, which are located on chromosomes 11 and 15, respectively (Hesse et al., 2001, 2004; Schweizer et al., 2006). In this study, we describe mice lacking the type II gene cluster. Given that the assembly of keratin filaments from heterodimers requires one member from each family and that keratins are rapidly degraded in the absence of a dimerization partner, mice lacking the type II gene cluster should be devoid of the entire keratin multiprotein family.

Results and discussion

To test current hypotheses on keratin function in mouse development, we used the Cre-loxP system (Ramírez-Solis et al., 1995) to flox the type II keratin gene cluster spanning 0.68 Mb of the genome in mouse embryonic stem (ES) cells (Fig. 1 A; Hesse et al., 2004). Targeting constructs from the Mutagenic Insertion and Chromosome Engineering Resource (MICER; Adams et al., 2004) were engineered with gaps to aid in insertional targeting (Fig. 1, B and C; and Fig. S1 A). Southern blotting confirmed correct targeting at a frequency of 8% (Fig. 1, F and G; and Fig. S1 A). Empty 3′ and 5′ *hprt* vectors labeled for in situ hybridization against spread chromosomes from double-targeted ES cell clones identified double-targeted clones in cis (Fig. S1 B). The floxed gene cluster contained all type II keratins and the type I keratin Krt18, which with K8 forms the first keratin pair during embryonic development (Fig. 1 A; Lu et al., 2005), but no other known genes, including microRNA genes.

Cre-mediated deletion of the keratin type II cluster (Fig. 1, D and E) did not affect ES cell pluripotency, and mice with a constitutive deletion of the keratin type II cluster ($KtyII^{-/-}$) were generated. Deletion of all 27 keratin genes was confirmed by RT-PCR and immunofluorescence microscopy (Fig. 1, H and I; and Fig. 2). Consistent with the proteolytic sensitivity of type I keratins in the absence of their type II keratin binding partners, the sole embryonic type I keratin K19 was expressed at the mRNA but not at the protein level (Fig. 1 H and Fig. S1 D; Magin et al., 2007). Therefore, our mice lack all 54 mammalian keratins (Fig. 1 H). The type III intermediate filament protein vimentin, which is frequently up-regulated during epithelial-mesenchymal transition after loss of keratin expression (Thiery, 2002; Yang and Weinberg, 2008), was not up-regulated at the transcript or protein level, indicating that deletion of the $KtyII^{-/-}$ cluster did not grossly perturb epithelial cell morphology or function (Fig. S2). In support, the expression of the constitutive chaperone Hsc70, which can bind keratins (Liao et al., 1997; Betz et al., 2006), was unaltered. The stress-inducible Hsp70 was not detectable (see Fig. 4 A). Furthermore, activity of MAPK, as examined by Western blotting of candidate target proteins, appeared largely unchanged (see Fig. 4 C).

All $KtyII^{-/-}$ mice died at ∼E9.5 (Fig. S1 E). Because keratins maintain tissue integrity by interacting with desmosomes to provide intercellular adhesion, we investigated the gross appearance and histology of E9.5 embryos. Unlike previous single or double keratin KO mice, which suffered from cytolysis and hemorrhages (Baribault et al., 1993; Hesse et al., 2000; Tamai et al., 2000), $KtyII^{-/-}$ embryos had intact embryonic and extraembryonic epithelia (Fig. 3, A–F). These findings suggest that keratins have no essential mechanical function until this stage of mouse development and that the phenotype of previous keratin KOs may result from dominant-negative effects. Yet, the desmosomes in $KtyII^{-/-}$ embryos were smaller and partially mislocalized (Figs. 1 I and 2, A and B), which is consistent with the involvement of keratins in desmosome assembly (Godsel et al., 2005). During epidermal differentiation, desmoplakin was reported to regulate microtubule organization through ninein (Lechler and Fuchs, 2005). Staining for ninein revealed a prominent localization along the plasma membrane of yolk sac tissue (not depicted) and at centrosomes in embryonic epithelia (Fig. 2 C). Ninein-positive centrosomes retained their apical position in $KtyII^{-/-}$ embryos (Fig. 2 C′), which is in agreement with unaltered γ-tubulin staining (not depicted). This is in contrast to a previous study (Ameen et al., 2001), indicating other and possibly compensatory mechanisms involved in centrosome positioning. The localization of the adherens junction protein epithelial cadherin (E-cadherin) and the tight junction–associated proteins ZO-1 and occludin were highly similar in both genotypes of embryos, indicating that actin-associated adhesion complexes and the actin cytoskeleton (not depicted) maintain epithelial integrity and polarity (Fig. 2, D–F).

$KtyII^{-/-}$ embryos exhibited a striking growth retardation, which started at ∼E8.5 and was fully apparent 1 d later (Fig. 3, G–J). Before the onset of placenta formation at E9.5, the embryo is fully dependent on the yolk sac for nutrient supply. The mammalian target of rapamycin (mTOR) C1 complex regulates protein synthesis by integrating growth factor signals and nutrients. Stimulation of the mTORC1 complex up-regulates protein synthesis by phosphorylation of its downstream targets ribosomal protein S6 kinase (S6K) and eukaryotic initiation factor 4E-binding protein 1 (4E-BP1; Wullschleger et al., 2006). We hypothesized that the embryonic mortality was caused by defective energy metabolism in the yolk sac.

and the proximal vector sequences (Table S1). (E) Cre-mediated recombination between *loxP* sites in cis leading to deletion of the keratin cluster. Southern probes are indicated as bold bars in B–E. (F) Southern blot analysis of ES cell clones targeted at the 5′ (i) and the 3′ end (ii) with a probe that distinguishes BsrGI (B) and HincII (Hi) fragments in the WT and targeted allele, respectively. (G) Southern blot analysis of ES cells after Cre-mediated recombination using unique probes spanning the 5′ and 3′ *hprt*. Probes distinguish double-targeted 8.3-kb and recombined 4.9-kb HinDIII (H) fragments using the 5′ *hprt* probe (i) and double-targeted 14.3-kb and recombined 10.5-kb EcoRI (E) fragments using the 3′ *hprt* probe (ii). (H) mRNA expression of keratins and vimentin (Vim) in E9.5 WT and mutant embryos. Glyceraldehyde 3-phosphate dehydrogenase (GAPDH) was used as a normalization control. (I) Immunofluorescence of K8/ K18 desmoplakin (DP) on sections of E9.5 WT and KO embryos. Bars, 10 μm.

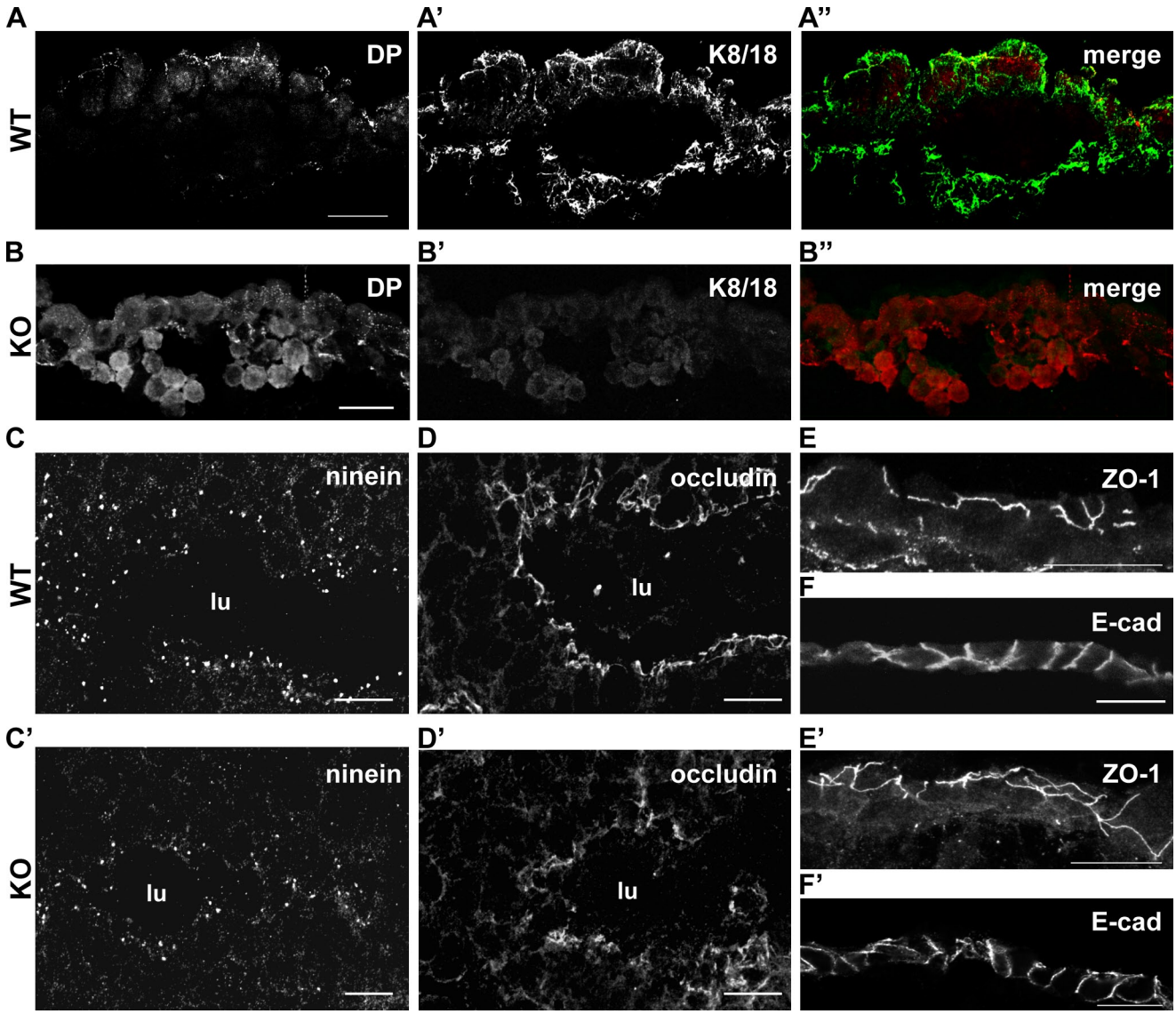

Figure 2. ***Ktyll*$^{-/-}$ embryos show reduced and mislocalized desmoplakin, whereas adherens junctions and cell polarity are unaltered.** (A and B) Double immunolabeling of keratin and desmoplakin (DP) on yolk sac indicates altered distribution and size of desmosomes in the presence (A) and absence (B) of keratins in yolk sac tissue. (C) Ninein part of the microtubule-organizing center complex at the centrosomes is located apically in WT (C) and KO embryonic intestine (C'). (D) Note the apical localization of occludin, a transmembrane protein of tight junctions. (E) Antibody staining of the tight junction marker ZO-1 in the yolk sac revealed no changes in WT (E) compared with *KtyII*$^{-/-}$ (E') E9.5 embryos. (D and E) ZO-1 and occludin are located at the apical plasma membrane of the yolk sac and the intestine, respectively, indicating normal cell polarity. (F) Intact adherens junctions in mutants (F') and their WT littermates (F), as demonstrated by staining for E-cadherin (E-cad) in yolk sac tissues of E9.5 embryos. lu, lumen. Bars: (A–B" and E–F') 10 µm; (C–D') 2 µm.

In a metabolic labeling experiment, analysis of ^{35}S-labeled Met/Cys incorporation showed that protein biosynthesis was reduced by ∼48% in the yolk sac and by ∼45% in the embryonic tissue of *KtyII*$^{-/-}$ embryos (Fig. 3 K). Moreover, phosphorylation of the mTORC1 targets S6K and 4E-BP1 was reduced (Fig. 4 D), and eIF2-α phosphorylation was increased (Fig. 4 B). mTORC1 activity is regulated by several mechanisms, among them sequestration through 14-3-3 proteins. Previously, the skin keratin K17 was found to positively regulate protein biosynthesis and keratinocyte growth through 14-3-3–σ-mediated mTOR sequestration, suggesting a distinct role of certain keratins in wound repair (Kim et al., 2006). Although we detected sufficient 14-3-3 protein by Western blotting, the small size of embryos prevented a more detailed analysis. Given that limited glucose supply is known to severely restrict embryo growth and to increase apoptosis (Schmidt et al., 2009) and that mTORC1 is nutrient sensitive (Shaw and Cantley, 2006), we were prompted to investigate upstream regulators of mTORC1 that might depend on keratins.

Limited nutrition represses growth and protein biosynthesis, and early mouse embryos predominantly rely on glycolysis (Pantaleon and Kaye, 1998). Therefore, we analyzed the AMP kinase (AMPK), the cellular energy sensor which is phosphorylated when AMP levels are elevated (Hardie, 2007). Phosphorylated (P) AMPK inhibits the mTORC1 complex through its binding partner Raptor (Gwinn et al., 2008). Using phosphospecific antibodies, we found increases of 20% in

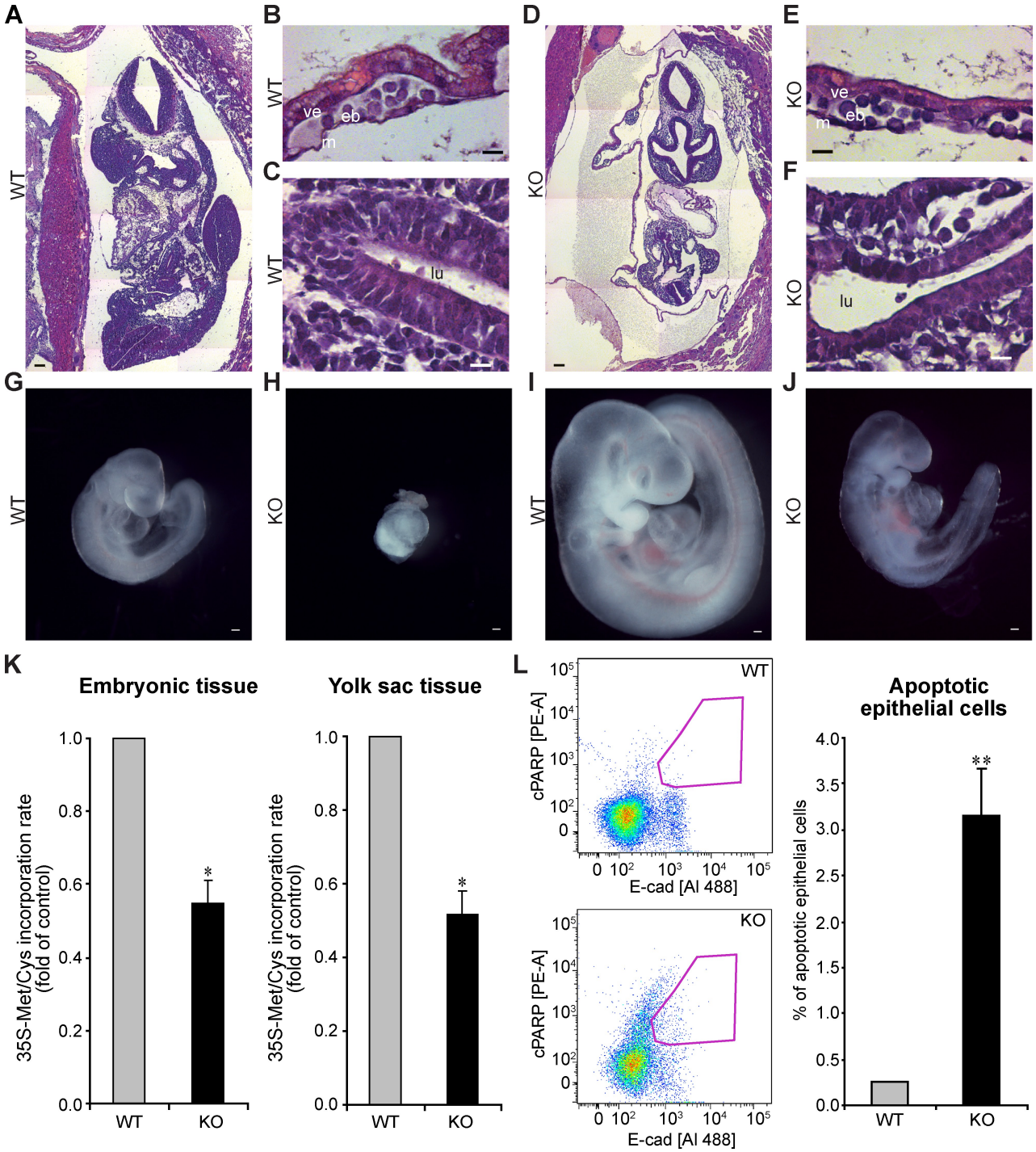

Figure 3. ***Ktyll*$^{-/-}$ embryos exhibit severe growth retardation and apoptosis, resulting from reduced protein biosynthesis, but maintain tissue integrity.** (A–F) Semithin sections through WT (A–C) and mutant (D–F) embryos were stained with H&E. Note the tissue integrity in overview sections through complete E9.5 embryo in the WT (A) and the KO (D) mice. Higher magnifications of the visceral yolk sac (B and E) and embryonic intestine (C and F) from WT and KO embryos at E9.5 confirmed tissue integrity. (G–J) Whole mount photographs of WT (G and I) and mutant (H and J) embryos dissected from the yolk sac at E8.5 (G and H) and E9.5 (I and J). *Ktyll*$^{-/-}$ embryos were growth retarded by ~50%. (K) Metabolic labeling of dissected WT and *Ktyll*$^{-/-}$ embryos and corresponding yolk sac tissues with ^{35}S-labeled Met/Cys. (L) FACS analysis of apoptotic cells in WT and KO embryos. Apoptosis was analyzed with cleaved poly(ADP-ribose) polymerase (cPARP) staining, and epithelial cells were detected with E-cadherin (E-cad) labeling. Subsequently, the percentage of apoptotic epithelia cells was determined to be 10-fold increased in KO compared with WT embryos. *, $P < 0.05$; **, $P < 0.005$ (two-tailed *t* test). Error bars represent SEM. eb, embryonic blood; lu, lumen; m, mesothelium; ve, visceral endoderm. Bars: (A, D, and G–J), 100 µm; (B, C, E, and F), 10 µm.

P-AMPK and 30% in P-Raptor (Fig. 4, E and F). Furthermore, we detected no change in phosphorylation of Akt, which is a positive regulator of mTOR signaling (Fig. 4 E). These findings confirmed our hypothesis that nutrient shortage, which can signal through AMPK, reduced protein synthesis in *KtyII*$^{-/-}$ embryos.

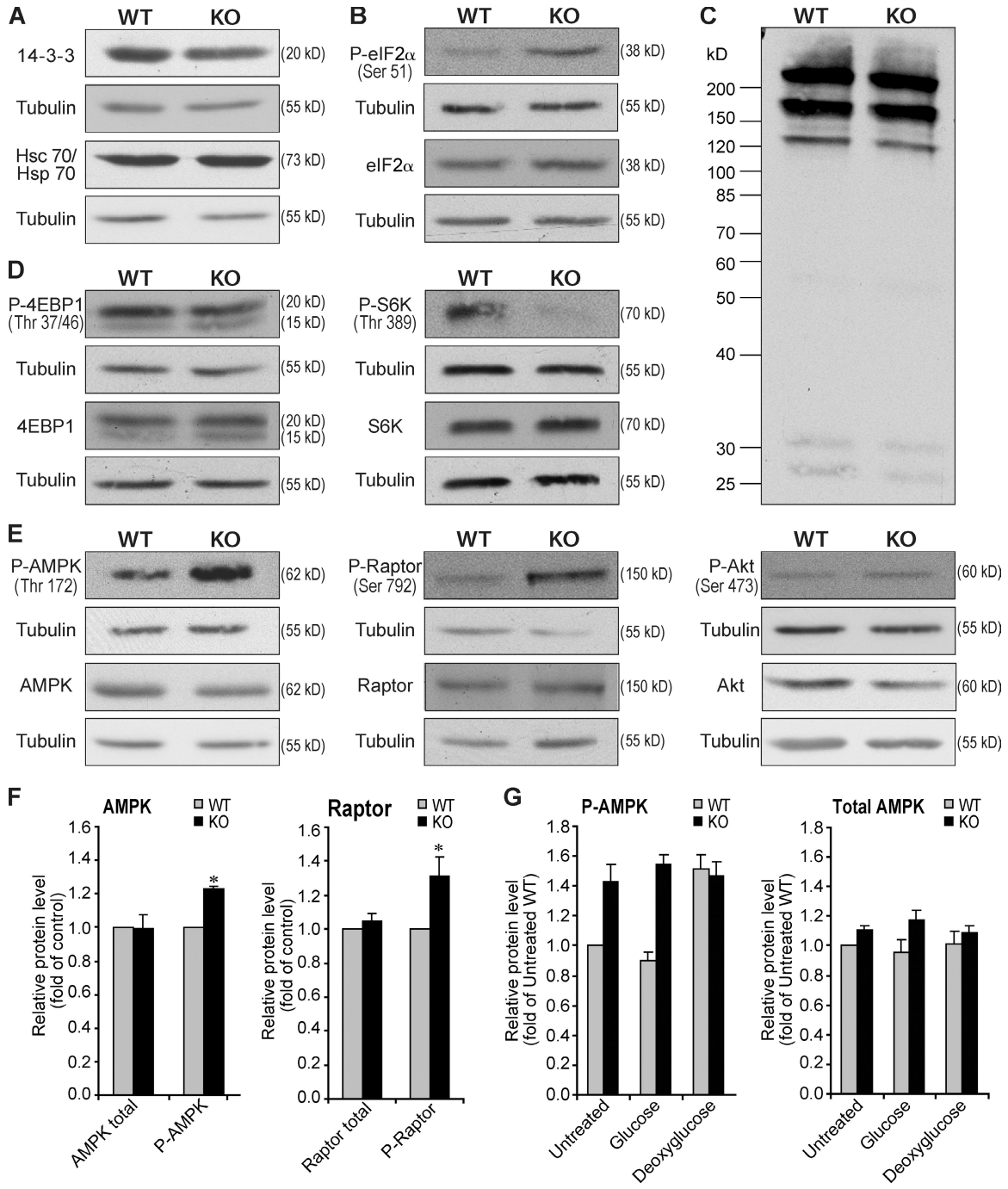

Figure 4. **Depletion of keratins activates AMPK and Raptor as the result of impaired glucose transport.** (A and C) 14-3-3, chaperones Hsc70/Hsp70 (A), and P (Thr)-MAPK/Cdk substrate levels (C) were found to be similar, comparing protein lysates of keratin WT and *KtyII*$^{-/-}$ E9.5 embryos by immunoblotting. (B and D) Detection of total and phosphorylated (P) proteins in protein lysates of keratin WT and *KtyII*$^{-/-}$ E9.5 embryos by immunoblotting of three independent pools of embryo lysates. (E and F) E9.5 lysates were analyzed by Western blotting for changes in P-AMPK and Raptor in both genotypes. Total protein and phosphoprotein levels of AMPK and Raptor were quantified by densitometry and normalized to tubulin ($n = 3$; F). (G) E9.5 embryos were incubated at 37°C for 10 min in M2^{-} medium containing 5.5 mM glucose or 5.5 mM deoxyglucose or left untreated. E9.5 lysates were Western blotted for changes in the phosphoprotein levels of AMPK in *KtyII*$^{-/-}$ and WT littermates. Total phosphoprotein levels of AMPK were quantified by densitometry and normalized to tubulin ($n = 3$). *, $P < 0.05$ (two-tailed *t* test). Error bars represent SEM.

Next, we performed a biochemical rescue experiment in which glucose was added to isolated *KtyII*$^{-/-}$ and wild-type (WT) embryos in ex vivo culture; the metabolic inhibitor deoxyglucose served as a negative control. In WT embryos, P-AMPK levels were decreased by 10% in 5 mM glucose and increased by 52% in deoxyglucose medium (Fig. 4 G). However, *KtyII*$^{-/-}$ embryos failed to respond to either treatment, indicating an unsuccessful rescue. Their P-AMPK levels were similar to those of deoxyglucose-treated WT embryos, and their total AMPK levels were unchanged (Fig. 4 G). These findings strongly suggest that keratins participate in the regulation of cellular glucose uptake.

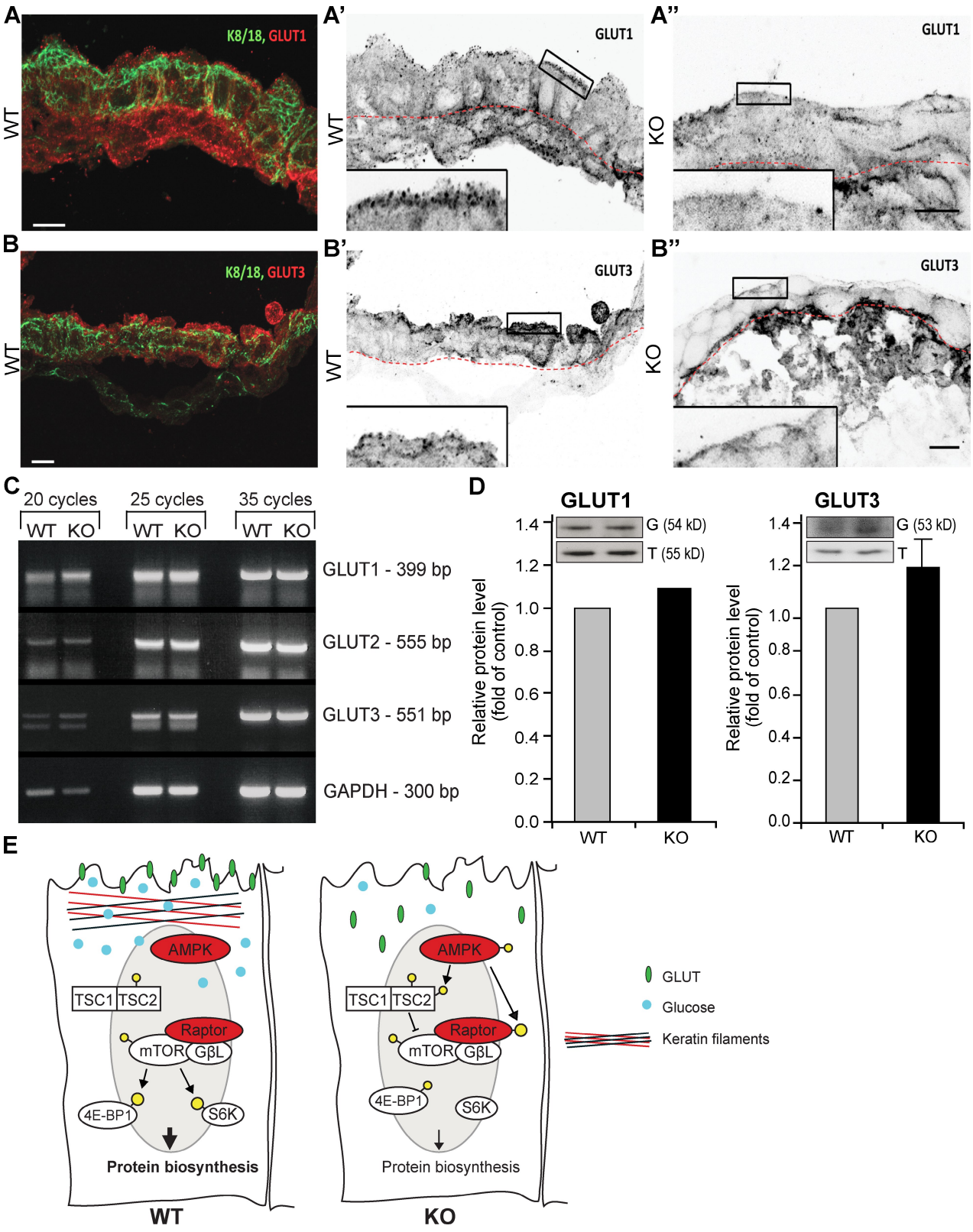

Figure 5. **Keratins regulate AMPK activity through localization of GLUT1 and -3.** (A and B) Double immunofluorescence of keratins and GLUT1 and -3 (A and B) in WT yolk sac tissue. (A′, A″, B′, and B″) Yolk sacs of E9.5 WT and *Ktyll*$^{-/-}$ embryos were analyzed for GLUT1 (A′ and A″) and -3 (B′ and B″) localization. Insets show enlargement of the region encompassing the plasma membrane. (C) mRNA expression of GLUT transporters in E9.5 WT and mutants. Glyceraldehyde 3-phosphate dehydrogenase (GAPDH) was used as a normalization control. (D) Total GLUT1 and -3 protein levels in protein lysates of E9.5 keratin WT and *Ktyll*$^{-/-}$ embryos. Error bars represent SEM. G, GLUT; T, tubulin. (E) Model for function of apical keratins in GLUT localization. Our model suggests that full activation of mTORC1 depends on the correct localization of GLUT1 and -3 by subapical keratins in the mouse embryo. Bars, 10 µm.

Glucose transport is mainly performed by energy-independent facilitative transporters of the GLUT family, which are expressed during blastocyst formation when embryos switch from pyruvate to glucose as the major energy source (Barbehenn et al., 1974). In early embryos, GLUT1 and -3 are the main transporters that regulate glucose distribution, and their KO causes severe growth retardation with increased apoptosis during embryo development (Wang et al., 2006; Ganguly et al., 2007; Schmidt et al., 2009). FACS sorting of trypsinized *KtyII*$^{-/-}$ embryos confirmed a 10-fold increase in apoptotic cells, indicating a nutrition defect (Fig. 3 L). To analyze this further, double immunofluorescence analysis with GLUT1 and -3 and K8/K18 antibodies were performed. This showed that GLUT1 and -3 were predominantly localized to the apical plasma membrane of the yolk sac. In WT yolk sacs, K8/K18 keratins were confined in the subapical region (Figs. 1 I and 5, A and B). Of note, subapical intermediate filament organization is evolutionarily conserved down to *Caenorhabditis elegans*, where it is required for gut epithelial organization (Hüsken et al., 2008). In *KtyII*$^{-/-}$ embryos, GLUT1 and -3 levels at the apical plasma membrane of the yolk sac were markedly reduced, causing redistribution of the transporters throughout endodermal cells (Fig. 5, A′, A″, B′, and B″). In line with AMPK activation, their total transcript and protein levels were unaltered (GLUT1) or slightly elevated (GLUT3; Fig. 5, C and D). Our data lead to a model in which full activation of mTORC1 depends on the correct localization of GLUT1 and -3 by subapical keratins in the mouse embryo (Fig. 5 E).

These findings reveal a novel regulatory mechanism by which keratins coordinate cell growth and protein synthesis at the level of GLUT transporters. The highly regulated expression and subcellular organization of keratins strongly suggest their involvement in growth regulation and protein targeting beyond embryo development, as demonstrated for K17 in skin wound healing and K8 in colonic epithelia (Toivola et al., 2004; Kim et al., 2006). Although the molecular mechanisms are not yet known, it is well established that the correct localization of cell adhesion proteins depends on keratins and vimentin (Godsel et al., 2005; Toivola et al., 2005; Nieminen et al., 2006). Possibly, keratins and vimentin orchestrate the local interaction of 14-3-3 proteins with their multiple binding partners during organelle transport, cell polarity, and signaling. Furthermore, our data have far-ranging implications for the analysis of other large mammalian gene families as they suggest that some of the previous single and double keratin KOs may represent gain-of-toxic-function phenotypes (Hesse et al., 2000; Tamai et al., 2000; Jaquemar et al., 2003; Magin et al., 2004). This implicates that the pathomechanisms underlying skin keratin disorders not only result from mechanical fragility but from disturbed regulation of cell growth and signaling, opening new therapeutic opportunities (Kim et al., 2006; Kerns et al., 2007; Roth et al., 2009).

Materials and methods

Targeting the 5′ end of the keratin type II cluster

The *5′ hprt* vector clone MHPN117k13 (Adams et al., 2004) was used to target the *5′* end of the type II keratin cluster. This contained an insert of 6.0 kb spanning 101,202,450–101,208,417 bp on chromosome 15. A gap of 1.5 kb was generated with unique restriction sites, NheI and Bsp119I, to yield 2.0- and 2.4-kb arms of homology (Figs. 1 A and S1 A). NotI linkers were introduced at the cut sites to obtain a NotI restriction site. The plasmid was linearized with NotI before targeting and transfected (200 µg) into AB2.2 cells (gift from A. Bradley, Wellcome Trust Sanger Institute, Cambridge, England, UK) at 3 µF and 800 V. G418 selection was initiated 24 h after targeting at 350 µg/ml. Neomycin-resistant colonies were screened for homologous recombination; the plasmid without the gap served as a positive control. PCR primers spanned the gap region and vector backbone (Table S1). Eight clones that were PCR positive for the homologous recombination event were further confirmed by Southern blotting with a probe specific to the gap region (Table S1). Five were positive for the homologous recombination at the *5′* end of the keratin type II cluster. Clone 2 was used to target the 3′ end of the keratin type II cluster.

Targeting the 3′ end of the keratin type II cluster

The insert from the MICER *5′ hprt* clone MHPN322c09 (Adams et al., 2004) was excised from the vector at the AscI sites flanking the insert, cloned into an empty 3′ *hprt* vector, and named MHPP322c09. This contained a 6.9-kb insert spanning 101,876,016–101,882,964 bp on chromosome 15. A gap of 1.4 kb was generated with SacI restriction sites to yield 3.0- and 2.4-kb arms of homology (Fig. 1 B and Fig. S1 A). SacI was used to linearize the plasmid to target into the aforementioned clone 2. ES cells were targeted as described in the previous section and selected in 3 µg/ml puromycin 24 h after electroporation. 8 of 96 picked clones showed homologous recombination, as determined by PCR with primers spanning the gap region and vector backbone (Table S1). These clones were confirmed by Southern blot analysis with a 487-bp probe designed within the gap region (Table S1). All PCR-positive clones were correctly recombined at the 3′ end of the keratin type II cluster, as confirmed by Southern blot analysis.

Identification of double-targeted cis ES clones by fluorescence in situ hybridization

Metaphase chromosome spreads on slides were performed as previously described (Henegariu et al., 2001). Empty 3′ and *5′ hprt* vectors were labeled with biotin and digoxigenin, respectively, by nick translation and used for chromosomal in situ hybridization against spread chromosomes from double-targeted ES cell clones according to a standard protocol (Wrehlke et al., 1999). Red and green signals (or a yellow overlap) on a single chromosome confirmed the double targeting in cis (Fig. S1 B). One of the three double-targeted clones tested by fluorescence in situ hybridization was confirmed to have the targeted constructs in cis. This clone was subjected to Cre expression.

Cre-mediated deletion of the keratin type II cluster

The double-targeted clone in cis was transiently transfected with 200 µg of CrePac vector (Taniguchi et al., 1998) using the identical conditions described in Targeting the *5′* end of the keratin type II cluster. Selection with 1× hypoxanthine and thymine was initiated 24 h after transfection for 10 d. 96 colonies were screened for deletion of the keratin cluster with primers specific to the 3′ and *5′ hprt* regions. This was further confirmed by Southern blot analysis with probes specific to the 3′ and *5′ hprt* regions. Two independent clones positive for the deleted cluster were used to generate male chimeras by blastocyst injections (gift from R. Maniu, Universität Bonn, Bonn, Germany). Male chimeras were outbred to C57BL/6 WT females to generate mice heterozygous for the keratin type II deletion. Heterozygous progeny were inbred to generate *KtyII*$^{-/-}$ mice.

RT-PCR and Western blotting

Total RNA was isolated from E9.5 embryos and yolk sacs with RNeasy Micro kits (QIAGEN). Reverse transcription was performed with RevertAid First Strand cDNA Synthesis kits (Fermentas). The primers and PCR conditions have been described previously (Tonack et al., 2004; Lu et al., 2005). For vimentin cDNA synthesis, 2 µg of total RNA was reverse transcribed in a volume of 20 µl. PCR with Platinum Taq polymerase (Invitrogen) was performed in 25-µl reactions containing 0.1 µl of template cDNA, according to the manufacturer's protocol. PCR reactions were performed as follows: 35 cycles at 94°C for 30 s, 65°C for 30 s, and 72°C for 20 s. The sequences of the primer pairs are outlined in Table S1.

Western blotting was performed as follows. Total protein was extracted in SDS-PAGE sample buffer (50 mM Na phosphate, pH 6.8, 5% SDS, 40 mM DTT, 5 mM EDTA, 5 mM EGTA, and 15% glycerol). The samples were heated for 5 min at 95°C, sonicated three times for 30 s and, in between intervals, kept for 30 s at 95°C; the procedure was repeated, and

after an additional 10 min at 95°C, the insoluble material was removed by centrifugation. Total protein was determined by the protein quantification kit (Bio-Rad Laboratories), and extracts were loaded equally. Separation of total protein extracts was performed by standard procedures (8 and 10% SDS-PAGE). Proteins were electrotransferred to 0.1-µm nitrocellulose membranes (GE Healthcare) by wet blotting in Towbin buffer (25 mM Tris-HCl, pH 8.8, 192 mM glycin, 0.1% SDS, and 10% methanol). Membranes were stained with 0.5% Ponceau S. Secondary antibodies were used with Super Signal (Thermo Fisher Scientific) as a substrate (Reichelt and Magin, 2002). Antibodies and dilutions are listed in Table S2.

Histology and immunofluorescence analysis

Mouse concepti at different gestational ages were prepared. For light microscopy and immunofluorescence, tissues were snap frozen in isopentane precooled at −80°C and cryosectioned (10 µm). Immunofluorescence analysis was performed as follows: tissues were snap frozen in isopentane precooled at −80°C and stored at the same temperature. Frozen sections (8–12 µm thick) were fixed in acetone at −20°C for 10 min and dried for a few hours before further processing. All antibodies were diluted in TBS containing 1% BSA, as stated in Table S2. Primary mouse monoclonal antibodies were detected with subclass-specific secondary antibodies to minimize background. Slides were mounted in ProLong Gold antifade reagent (Invitrogen; Reichelt and Magin, 2002). Antibodies and dilutions are listed in Table S2. For routine histology, tissues were fixed overnight at 4°C in 4% formalin, sequentially incubated at 4°C overnight in 15% and 30% sucrose, embedded in paraffin, and sectioned (5 µm). Sections were placed on Superfrost Plus slides (Menzel-Gläser) and dried. After deparaffination, sections were stained with hematoxylin and eosin (H&E; Reichelt and Magin, 2002).

Immunofluorescence microscopy and data processing

The images of the H&E-stained paraffin sections were acquired using a fluorescence microscope (Axioplan 2; Carl Zeiss, Inc.) with a Plan-Neofluar 10× 0.30 NA objective and a Plan-Apochromat 63× 1.4 NA oil immersion objective at RT using a camera (AxioCam MR; Carl Zeiss, Inc.). Image analysis and processing were performed using AxioVision 4.6 (Carl Zeiss, Inc.) and Photoshop 6.0 (Adobe) software. Whole mount images were taken using a stereoscopic zoom microscope (model 1500; Nikon) with an HR Plan-Apochromat 1–3× zoom objective at RT using a camera (DS-U2/L2; Nikon). Image analysis and processing were performed with Photoshop software. Immunofluorescent samples were analyzed with a fluorescence laser-scanning confocal microscope (LSM 710; Carl Zeiss, Inc.). For immunofluorescence microscopy and data processing, image stacks were collected with confocal microscope (TCS SP5; Leica) or a laser-scanning microscope (LSM 710) with a Plan-Apochromat 63× 1.4 NA oil immersion objective at RT, and projection views of stacks were produced with the aid of Amira software (Visage Imaging). LUT (lookup table; brightness and gamma) was adjusted using Photoshop. In some instances, single focal planes are shown.

Flow cytometry

E9.5 embryos were trypsinized, and single-cell suspensions were fixed in 2% PFA/PBS for 10 min at 4°C, washed with PBS, and permeabilized with 0.25% Triton X-100/PBS for 5 min at 4°C. The cells were washed and then stained for 30 min at 4°C with E-cadherin (Invitrogen) in 0.5% BSA/TBS and, after washing, were labeled with goat anti–rat Alexa Fluor 488 (Dianova) for 15 min at 4°C. Cells were washed again and stained for 30 min at RT with cleaved poly(ADP-ribose) polymerase–phycoerythrin (BD) in 0.5% BSA/TBS. Cells were sorted on a flow fluorocytometer (FACSCanto II or LSRII; BD), and data were analyzed using FlowJo software (Tree Star, Inc.).

Antibodies

We used antibodies against biotinylated antiavidin (Vector Laboratories), antidigoxigenin (Boehringer Ingelheim), K8/K18 (Progen), K19 (Troma-3; American Type Culture Collection), desmoplakin (gift from D. Garrod, University of Manchester, Manchester, England, UK), vimentin (T.M. Magin laboratory), ZO-1 (Zytomed Systems GmbH), occludin (Invitrogen), E-cadherin (Invitrogen), ninein (gift from J.B. Rattner, University of Calgary, Calgary, Alberta, Canada), 4E-BP1, P–4E-BP1 (Thr37/46), p70 S6K, P–p70 S6K (Thr389), eIF2-α, P–eIF2-α (Ser51), AMPK, P–AMPK-α (Thr172), Raptor, P-Raptor (Ser792), Akt, P-Akt (Ser473), P (Thr)-MAPK/Cdk substrates (all from Cell Signaling Technology), GLUT1 (Millipore), GLUT3 (Alpha Diagnostic International, Inc.), Hsc70/Hsp70 (Stressgen), 14-3-3–β (Santa Cruz Biotechnology, Inc.), and secondary antibodies (Dianova). Dilutions are listed in Table S2.

Metabolic labeling

E9.5 embryos and yolk sacs were dissected from the uterus, and the head was retained for genotyping. Embryos and yolk sac were incubated separately in Met-free Dulbecco's modified Eagle's medium (Invitrogen) containing 25 mM Hepes buffer, 10% dialyzed fetal calf serum, 1% nonessential amino acids, 1× Na pyruvate, and 1% Glutamax (all Invitrogen) at 37°C for 15 min to remove endogenous Met. The medium was discarded, and tissues were labeled with 100 µl of ^{35}S-labeled Met/Cys (1,000 Ci/mmol; 0.1 mCi/ml) in Met-free Dulbecco's modified Eagle's medium for 1 h at 37°C. The medium was aspirated, and tissues were washed in ice-cold PBS. Proteins were precipitated with 10% trichloroacetic acid, and incorporated radioactivity was measured by liquid scintillation. The rate of ^{35}S-labeled Met/Cys incorporation per minute per milligram of protein was calculated using the Bradford reagent (Bradford, 1976).

Glucose assay

E9.5 embryos and yolk sacs were dissected from the uterus. Embryos and yolk sac together were incubated in M2$^-$ medium (94.59 mM NaCl, 4.78 mM KCl, 1.19 mM KH_2PO_4, 1.19 $MgSO_4$, 1.71 mM $CaCl_2$, 4.0 mM $NaHCO_3$, 21 mM Hepes, and 4 g/liter albumin bovine fraction V; all from Sigma-Aldrich) without glucose or its metabolites, with 5.5 mM glucose (Sigma-Aldrich), or with 5.5 mM deoxyglucose (Sigma-Aldrich) for 10 min at 37°C. Subsequently, embryos were lysed in boiling Laemmli buffer and analyzed by Western blotting for total and P-AMPK levels.

Online supplemental material

Fig. S1 shows additional characterizations of the genetic engineering at the keratin type II gene locus. Fig. S2 demonstrates that the deletion of keratins does not induce vimentin. Tables S1 and S2 provide the details of the primers and the antibodies, respectively, used in this study. Online supplemental material is available at http://www.jcb.org/cgi/content/full/jcb.200906094/DC1.

We thank Prof. A. Bradley for providing the AB2.2 ES cell line, snlp feeder cell line, and MICER clones for targeting and Mrs. R. Maniu for the blastocyst injections. We gratefully thank Prof. J.B. Rattner for his gift of ninein antiserum and E. Endl, A. Dolf, and P. Wurst from the Flow Cytometry Core Facility at the Institute for Molecular Medicine and Experimental Immunology, University of Bonn. We thank our former colleague Dr. M. Hesse for stimulating ideas and input in the experimental design. We are grateful to our colleagues M. Hatzfeld and M. Hoch for critical input. Also, we thank colleagues who provided antibodies.

This project was funded by Deutsche Forschungsgemeinschaft (German Research Council MA 1316/7) grant SFB832, Bonfor (Cytoskeletal Research Group), and the Bonner Forum Biomedizin.

Submitted: 15 June 2009
Accepted: 2 September 2009

References

Adams, D.J., P.J. Biggs, T. Cox, R. Davies, L. van der Weyden, J. Jonkers, J. Smith, B. Plumb, R. Taylor, I. Nishijima, et al. 2004. Mutagenic insertion and chromosome engineering resource (MICER). *Nat. Genet.* 36:867–871. doi:10.1038/ng1388

Ameen, N.A., Y. Figueroa, and P.J. Salas. 2001. Anomalous apical plasma membrane phenotype in CK8-deficient mice indicates a novel role for intermediate filaments in the polarization of simple epithelia. *J. Cell Sci.* 114:563–575.

Barbehenn, E.K., R.G. Wales, and O.H. Lowry. 1974. The explanation for the blockade of glycolysis in early mouse embryos. *Proc. Natl. Acad. Sci. USA*. 71:1056–1060. doi:10.1073/pnas.71.4.1056

Baribault, H., J. Price, K. Miyai, and R.G. Oshima. 1993. Mid-gestational lethality in mice lacking keratin 8. *Genes Dev.* 7:1191–1202. doi:10.1101/gad.7.7a.1191

Betz, R.C., L. Planko, S. Eigelshoven, S. Hanneken, S.M. Pasternack, H. Bussow, K. Van Den Bogaert, J. Wenzel, M. Braun-Falco, A. Rutten, et al. 2006. Loss-of-function mutations in the keratin 5 gene lead to Dowling-Degos disease. *Am. J. Hum. Genet.* 78:510–519. doi:10.1086/500850

Bradford, M.M. 1976. A rapid and sensitive method for the quantitation of microgram quantities of protein utilizing the principle of protein-dye binding. *Anal. Biochem.* 72:248–254. doi:10.1016/0003-2697(76)90527-3

Fuchs, E., and D.W. Cleveland. 1998. A structural scaffolding of intermediate filaments in health and disease. *Science*. 279:514–519. doi:10.1126/science.279.5350.514

Ganguly, A., R.A. McKnight, S. Raychaudhuri, B.C. Shin, Z. Ma, K. Moley, and S.U. Devaskar. 2007. Glucose transporter isoform-3 mutations cause early pregnancy loss and fetal growth restriction. *Am. J. Physiol. Endocrinol. Metab.* 292:E1241–E1255. doi:10.1152/ajpendo.00344.2006

Godsel, L.M., S.N. Hsieh, E.V. Amargo, A.E. Bass, L.T. Pascoe-McGillicuddy, A.C. Huen, M.E. Thorne, C.A. Gaudry, J.K. Park, K. Myung, et al. 2005. Desmoplakin assembly dynamics in four dimensions: multiple phases differentially regulated by intermediate filaments and actin. *J. Cell Biol.* 171:1045–1059. doi:10.1083/jcb.200510038

Gwinn, D M., D.B. Shackelford, D.F. Egan, M.M. Mihaylova, A. Mery, D.S. Vasquez, B.E. Turk, and R.J. Shaw. 2008. AMPK phosphorylation of raptor mediates a metabolic checkpoint. *Mol. Cell*. 30:214–226. doi:10.1016/j.molcel.2008.03.003

Hardie, D.G. 2007. AMP-activated/SNF1 protein kinases: conserved guardians of cellular energy. *Nat. Rev. Mol. Cell Biol.* 8:774–785. doi:10.1038/nrm2249

Henegariu, O., N.A. Heerema, L. Lowe Wright, P. Bray-Ward, D.C. Ward, and G.H. Vance. 2001. Improvements in cytogenetic slide preparation: controlled chromosome spreading, chemical aging and gradual denaturing. *Cytometry*. 43:101–109. doi:10.1002/1097-0320(20010201)43:2<101::AID-CYTO1024>3.0.CO;2-8

Hesse, M., T. Franz, Y. Tamai, M.M. Taketo, and T.M. Magin. 2000. Targeted deletion of keratins 18 and 19 leads to trophoblast fragility and early embryonic lethality. *EMBO J.* 19:5060–5070. doi:10.1093/emboj/19.19.5060

Hesse, M., T.M. Magin, and K. Weber. 2001. Genes for intermediate filament proteins and the draft sequence of the human genome: novel keratin genes and a surprisingly high number of pseudogenes related to keratin genes 8 and 18. *J. Cell Sci.* 114:2569–2575.

Hesse, M., A. Zimek, K. Weber, and T.M. Magin. 2004. Comprehensive analysis of keratin gene clusters in humans and rodents. *Eur. J. Cell Biol.* 83:19–26. doi:10.1078/0171-9335-00354

Hüsken, K., T. Wiesenfahrt, C. Abraham, R. Windoffer, O. Bossinger, and R.E. Leube. 2008. Maintenance of the intestinal tube in *Caenorhabditis elegans*: the role of the intermediate filament protein IFC-2. *Differentiation*. 76:881–896. doi:10.1111/j.1432-0436.2008.00264.x

Jackson, B.W., C. Grund, E. Schmid, K. Bürki, W.W. Franke, and K. Illmensee. 1980. Formation of cytoskeletal elements during mouse embryogenesis. Intermediate filaments of the cytokeratin type and desmosomes in preimplantation embryos. *Differentiation*. 17:161–179. doi:10.1111/j.1432-0436.1980.tb01093.x

Jaquemar, D., S. Kupriyanov, M. Wankell, J. Avis, K. Benirschke, H. Baribault, and R.G. Oshima. 2003. Keratin 8 protection of placental barrier function. *J. Cell Biol.* 161:749–756. doi:10.1083/jcb.200210004

Kerns, M.L., D. DePianto, A.T. Dinkova-Kostova, P. Talalay, and P.A. Coulombe. 2007. Reprogramming of keratin biosynthesis by sulforaphane restores skin integrity in epidermolysis bullosa simplex. *Proc. Natl. Acad. Sci. USA*. 104:14460–14465. doi:10.1073/pnas.0706486104

Kim, S., and P.A. Coulombe. 2007. Intermediate filament scaffolds fulfill mechanical, organizational, and signaling functions in the cytoplasm. *Genes Dev.* 21:1581–1597. doi:10.1101/gad.1552107

Kim, S., P. Wong, and P.A. Coulombe. 2006. A keratin cytoskeletal protein regulates protein synthesis and epithelial cell growth. *Nature*. 441:362–365. doi:10.1038/nature04659

Lechler, T., and E. Fuchs. 2005. Asymmetric cell divisions promote stratification and differentiation of mammalian skin. *Nature*. 437:275–280. doi:10.1038/nature03922

Liao, J., D. Price, and M.B. Omary. 1997. Association of glucose-regulated protein (grp78) with human keratin 8. *FEBS Lett.* 417:316–320. doi:10.1016/S0014-5793(97)01315-X

Lu, H., M. Hesse, B. Peters, and T.M. Magin. 2005. Type II keratins precede type I keratins during early embryonic development. *Eur. J. Cell Biol.* 84:709–718. doi:10.1016/j.ejcb.2005.04.001

Magin, T.M., R. Schröder, S. Leitgeb, F. Wanninger, K. Zatloukal, C. Grund, and D.W. Melton. 1998. Lessons from keratin 18 knockout mice: formation of novel keratin filaments, secondary loss of keratin 7 and accumulation of liver-specific keratin 8-positive aggregates. *J. Cell Biol.* 140:1441–1451. doi:10.1083/jcb.140.6.1441

Magin, T M., J. Reichelt, and M. Hatzfeld. 2004. Emerging functions: diseases and animal models reshape our view of the cytoskeleton. *Exp. Cell Res.* 301:91–102. doi:10.1016/j.yexcr.2004.08.018

Magin, T.M., P. Vijayaraj, and R.E. Leube. 2007. Structural and regulatory functions of keratins. *Exp. Cell Res.* 313:2021–2032. doi:10.1016/j.yexcr.2007.03.005

Nieminen, M., T. Henttinen, M. Merinen, F. Marttila-Ichihara, J.E. Eriksson, and S. Jalkanen. 2006. Vimentin function in lymphocyte adhesion and transcellular migration. *Nat. Cell Biol.* 8:156–162. doi:10.1038/ncb1355

Pantaleon, M., and P.L. Kaye. 1998. Glucose transporters in preimplantation development. *Rev. Reprod.* 3:77–81. doi:10.1530/ror.0.0030077

Ramírez-Solis, R., P. Liu, and A. Bradley. 1995. Chromosome engineering in mice. *Nature*. 378:720–724. doi:10.1038/378720a0

Reichelt, J., and T.M. Magin. 2002. Hyperproliferation, induction of c-Myc and 14-3-3sigma, but no cell fragility in keratin-10-null mice. *J. Cell Sci.* 115:2639–2650.

Roth, W., U. Reuter, C. Wohlenberg, L. Bruckner-Tuderman, and T.M. Magin. 2009. Cytokines as genetic modifiers in K5-/- mice and in human epidermolysis bullosa simplex. *Hum. Mutat.* 30:832–841. doi:10.1002/humu.20981

Schmidt, S., A. Hommel, V. Gawlik, R. Augustin, N. Junicke, S. Florian, M. Richter, D.J. Walther, D. Montag, H.G. Joost, and A. Schürmann. 2009. Essential role of glucose transporter GLUT3 for post-implantation embryonic development. *J. Endocrinol.* 200:23–33. doi:10.1677/JOE-08-0262

Schweizer, J., P.E. Bowden, P.A. Coulombe, L. Langbein, E.B. Lane, T M. Magin, L. Maltais, M.B. Omary, D.A. Parry, M.A. Rogers, and M.W. Wright. 2006. New consensus nomenclature for mammalian keratins. *J. Cell Biol.* 174:169–174. doi:10.1083/jcb.200603161

Shaw, R.J., and L.C. Cantley. 2006. Ras, PI(3)K and mTOR signalling controls tumour cell growth. *Nature*. 441:424–430. doi:10.1038/nature04869

Tamai, Y., T. Ishikawa, M.R. Bösl, M. Mori, M. Nozaki, H. Baribault, R.G. Oshima, and M.M. Taketo. 2000. Cytokeratins 8 and 19 in the mouse placental development. *J. Cell Biol.* 151:563–572. doi:10.1083/jcb.151.3.563

Taniguchi, M., M. Sanbo, S. Watanabe, I. Naruse, M. Mishina, and T. Yagi. 1998. Efficient production of Cre-mediated site-directed recombinants through the utilization of the puromycin resistance gene, pac: a transient gene-integration marker for ES cells. *Nucleic Acids Res.* 26:679–680. doi:10.1093/nar/26.2.679

Thiery, J.P. 2002. Epithelial-mesenchymal transitions in tumour progression. *Nat. Rev. Cancer*. 2:442–454. doi:10.1038/nrc822

Toivola, D.M., S. Krishnan, H.J. Binder, S.K. Singh, and M.B. Omary. 2004. Keratins modulate colonocyte electrolyte transport via protein mistargeting. *J. Cell Biol.* 164:911–921. doi:10.1083/jcb.200308103

Toivola, D M., G.Z. Tao, A. Habtezion, J. Liao, and M.B. Omary. 2005. Cellular integrity plus: organelle-related and protein-targeting functions of intermediate filaments. *Trends Cell Biol.* 15:608–617. doi:10.1016/j.tcb.2005.09.004

Tonack, S., B. Fischer, and A. Navarrete Santos. 2004. Expression of the insulin-responsive glucose transporter isoform 4 in blastocysts of C57/BL6 mice. *Anat. Embryol. (Berl.)*. 208:225–230.

Wang, D., J.M. Pascual, H. Yang, K. Engelstad, X. Mao, J. Cheng, J. Yoo, J.L. Noebels, and D.C. De Vivo. 2006. A mouse model for Glut-1 haploinsufficiency. *Hum. Mol. Genet.* 15:1169–1179. doi:10.1093/hmg/ddl032

Wrehlke, C., W.R. Wiedemeyer, H.P. Schmitt-Wrede, A. Mincheva, P. Lichter, and F. Wunderlich. 1999. Genomic organization of mouse gene zfp162. *DNA Cell Biol.* 18:419–428. doi:10.1089/104454999315303

Wullschleger, S., R. Loewith, and M.N. Hall. 2006. TOR signaling in growth and metabolism. *Cell*. 124:471–484. doi:10.1016/j.cell.2006.01.016

Yang, J., and R.A. Weinberg. 2008. Epithelial-mesenchymal transition: at the crossroads of development and tumor metastasis. *Dev. Cell*. 14:818–829. doi:10.1016/j.devcel.2008.05.009

Published

Vijayaraj et al., http://www.jcb.org/cgi/content/full/jcb.200906094/DC1

A

Targeting construct (MICER clone)	Region on chromosome 15 targeted	Insert Size (kb)	Gap size (kb)	Size of small arm of homology (kb)	Size of large arm of homology (kb)	Targeting frequency
MHPN117k13 (Flipped prior to targeting)	101202450 - 101208417	6.0	1.5	2.1	2.4	8%
MHPN332c09 (insert released and subcloned into 3'-hprt vector)	101876016 - 101882964	6.9	1.4	2.5	2.4	8%

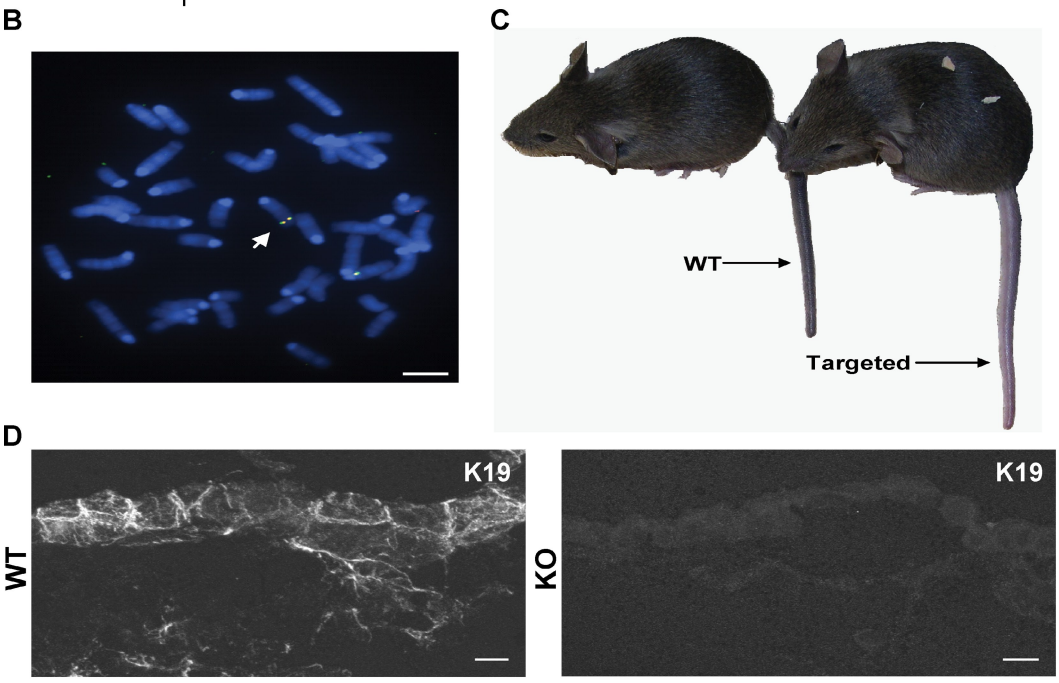

E

Age	Genotype: Wild type	Heterozygous	Homozygous mutant
8.5 dpc	20	55	22
9.5 dpc	477	943	321 (27/321 Nonviable)
10.5 dpc	10	20	8 (8/8 Nonviable)
Postnatal	32	73	0

Figure S1. **Genetic engineering at the keratin type II gene locus.** (A) Targeting efficiency at the keratin type II locus using insertional vectors, excluding the gap when calculating total size of homology. The targeting efficiency of both constructs was 8%. (B) Fluorescence in situ hybridization to identify double-targeted ES cell clones in cis. Empty 3′ and 5′ *hprt* vectors were labeled with biotin and digoxigenin, respectively, and used for chromosomal in situ hybridization against spread chromosomes from double-targeted ES cells clones. Red and green signals (or yellow overlap) on a single chromosome confirmed cis-targeted clones (arrow). (C) Tail color conferred by agouti gene (Wang et al. 2006. *Hum. Mol. Genet.* 15:1169–1179). Mice heterozygous for the deleted keratin type II cluster consistently had lighter tails than their WT littermates. (D) Immunofluorescence shows complete loss of K19 protein expression. (E) Genotype analysis of progeny from keratin type II heterozygous intercrosses. Postnatal mice were scored at P0 d postcoitum (dpc). Bars: (B) 5 µm; (D) 10 µm.

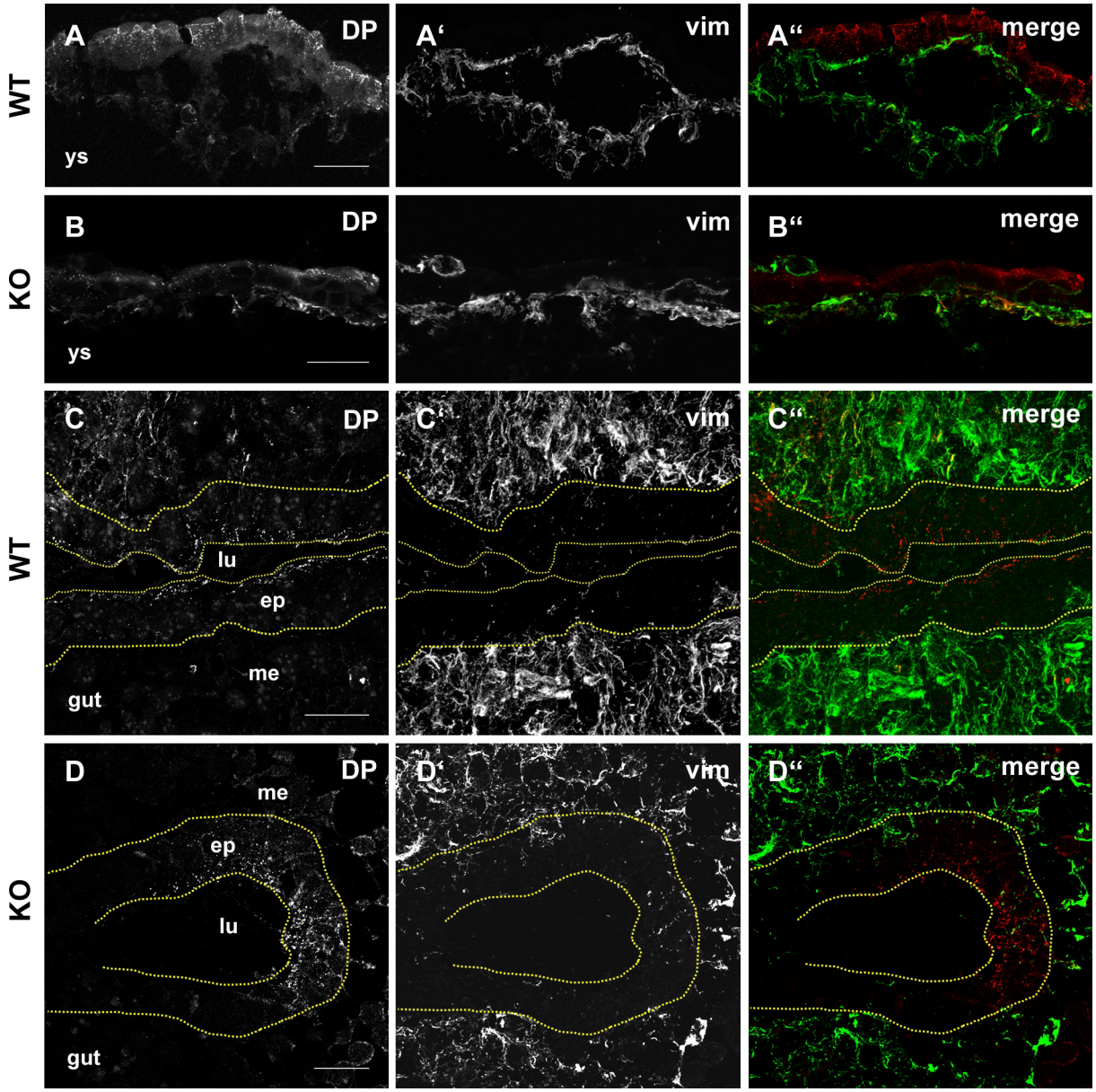

Figure S2. **Deletion of keratins does not induce vimentin.** (A–D) Note the lack of vimentin (vim) expression in embryonic epithelia devoid of keratins. Epithelia are identified by desmoplakin (DP) immunofluorescence. WT (A and C) versus *Ktyll*$^{-/-}$ (B and D) is shown. Note the yolk sac (ys; A and B) and gut (C and D). Dotted lines denote simple epithelia (ep) of the embryonic gut tissue. me, mesoderm; lu, lumen. Bars, 10 µm.

Table S1. **List of primers designed for various steps during genetic engineering at the keratin type II gene locus**

Primer sequence	Product size and remarks
Forward 5′-GATAACCGTATTACCGCCTTTG-3′ Reverse 5′-CGCCCTCTTGTCTATATCAACC-3′	2,562 bp; targeting of 5′ end of keratin type II cluster by PCR
Forward 5′-CCCAAGGTTAGCCAATAATAACC-3′ Reverse 5′-AGCACTTATCTGACCAAATCCAG-3′	397 bp; probes of 5′ end of keratin type II cluster–targeted clones (BsrG1 fragment)
Forward 5′-AGGGAAGAAAGCGAAAGGAG-3′ Reverse 5′-GCAGTTCCAGACCTGATGGT-3′	2,708 bp; targeting of 3′ end of keratin type II cluster by PCR
Forward 5′-GCCGATGTCGTGTGATATTG-3′ Reverse 5′-TGCAGCTGGAGACACGTAAC-3′	487 bp; probes for 3′ end of keratin type II cluster–targeted clones (EcoRI fragment)
Forward 5′-GTGGGACTCTGTAGGGACCA-3′ Reverse 5′-TGAACCCAGGAGGTTGAGAC-3′	826 bp; *hprt* primers to identify Cre-mediated deletion in ES cells and in mice
Forward 5′-TGGGACAGGAAGAGAGGTGATC-3′ Reverse 5′-ACCAAAACCAAATCCACTGCCG-3′	1.8 kb; primers to identify WT *KtyII* cluster allele, which recognizes Krt5
Forward 5′-CATTCTGCACGCTTCAAAAG-3′ Reverse 5′-GATTCAGCCCCAGTCCATTA-3′	616 bp; 5′ *hprt* probes to identify targeted and recombined loci
Forward 5′-AGGGCAAAGGATGTGTTACG-3′ Reverse 5′-CCTGACCAAGGAAAGCAAAG-3′	656 bp; 3′ *hprt* probes to identify targeted and recombined loci
Forward 5′-GCACGATGAAGAGATCCAGG-3′ Reverse 5′-AGCCTCAGAGAGGTCAGCAA-3′	193 bp; primers used for vimentin RT-PCR

Table S2. **List of antibodies, including species and dilutions**

Antibodies	Species	Dilution
K8/K18	poly gp	1:200
Desmoplakin (11-5F)	momo	1:100
GLUT1 (IF)	poly rb	1:500
GLUT3 (IF)	poly rb	1:100
K19 (Troma-3)	ratmo	1:5,000
Vimentin	poly rb	1:4,000
ZO-1	poly rb	1:200
Occludin	poly rb	neat
Ninein	poly rb	1:500
E-cadherin (ECCD-2; IF)	r mo	1:300
Cy2 or Cy3 (IF)	goat	1:800
E-cadherin (ECCD-2; FACS)	r mo	1:500
cPARP-PE (Asp214)	momo	1:5
Alexa Fluor 488 (FACS)	goat	1:400
Tubulin (B 5-1-2)	momo	1:5,000
4E-BP1 (11G12C11)	rb mo	1:10,000
P–4E-BP1(236B4)	rb mo	1:1,000
S6K (49D7)	rb mo	1:1,000
P-S6K (1A5)	momo	1:1,000
eIF2-α	poly rb	1:2,000
P–eIF2-α	poly rb	1:1,000
AMPK	poly rb	1:1,000
P–AMPK-α (40H9)	rb mo	1:500
Raptor (24C12)	rb mo	1:2,000
P-Raptor	poly rb	1:2,000
P-MAPK	momo	1:1,000
Akt	poly rb	1:5,000
P-Akt	poly rb	1:1,000
GLUT1 (WB)	poly rb	1:1,000
GLUT3 (WB)	poly rb	1:500
14-3-3–β	poly rb	1:500
Hsc70/Hsp70 (SPA-820)	momo	1:1,000
HRP (WB)	goat	1: 20,000

cPARP-PE, cleaved poly(ADP-ribose) polymerase–phycoerythrin; IF, immunofluorescence; WB, Western blot.

4.2 Keratins regulate yolk sac haematopoiesis and vasculogenesis through reduced BMP-4 signaling

This work was published in a scientific journal.

Journal:
European Journal of Cell Biology

Published:
2010 Apr;89(4):299-306.

Authors:
Preethi Vijayaraj, Cornelia Kröger, Ursula Reuter, Dieter Hartmann and Thomas M. Magin

Contribution:
Immunofluorescence of junctional proteins, FACS analysis, image formatting

European Journal of Cell Biology 89 (2010) 299–306

Contents lists available at ScienceDirect

European Journal of Cell Biology

journal homepage: www.elsevier.de/ejcb

Keratins regulate yolk sac hematopoiesis and vasculogenesis through reduced BMP-4 signaling

Preethi Vijayaraj [a,c], Cornelia Kroeger [a], Ursula Reuter [a], Dieter Hartmann [b], Thomas M. Magin [a,*]

[a] Institute of Physiological Chemistry, Division of Cell Biochemistry, Bonner Forum Biomedizin and LIMES-Institute, Rheinische Friedrich-Wilhelms-Universität, Nussallee 11, 53115 Bonn, Germany
[b] Institute of Anatomy, Rheinische Friedrich-Wilhelms-Universität, Nussallee 10, 53115 Bonn, Germany
[c] Department of Medicine, Center for Vascular Biology Research, Beth Israel Deaconess Medical Center, Harvard Medical School, Boston, MA, USA

ARTICLE INFO

Article history:
Received 8 July 2009
Received in revised form
8 October 2009
Accepted 19 October 2009

Keywords:
Keratins
Knockout mice
Chromosome engineering
*Bmp*4
p38-MAPK
Yolk sac
Hematopoiesis
Vasculogenesis

ABSTRACT

Keratin intermediate filament proteins form the major cytoskeleton in all embryonic and adult epithelia. Increasing evidence suggests that keratins, besides their primary cytoskeletal function, can act as scaffolds which locally regulate cell growth and survival in epithelial cells. Many of these functions, however, are not understood in full, owing to keratin redundancy. We have recently created mice which lack all keratins and found that keratins act upstream of mTOR signaling to regulate protein biosynthesis via GLUT localization. Here, we report that keratins are necessary to maintain adhesion between endodermal and mesodermal cell layers of the yolk sac. As a consequence, keratin $^{/}$ embryos suffer from reduced yolk sac hematopoiesis and vasculogenesis. Pathway analysis revealed a reduction of the hedgehog target Foxf1 in yolk sac mesoderm of keratin $^{/}$ embryos, and subsequent reduction of BMP 4 and P p38 MAPK. These defects may be caused by the overall reduction in protein biosynthesis and diminished adhesion. Our data show for the first time that keratins are necessary for the differentiation of a non epithelial cell lineage through a combination of mechanical and signaling mechanisms.

Introduction

Epithelia line the surface of tissues and protect against mechanical stress, dehydration and depend on communication with neighboring cells to generate a highly patterned tissue. Understanding the genetic program that governs the self renewal, polarized architecture and functional diversity of epithelial cells remains a considerable challenge and has implications for many disorders including neoplasia (Fuchs, 2007; Kim and Coulombe, 2007; Magin et al., 2007; Sancho et al., 2004; Yeaman et al., 1999).

Among the multigene families that are particularly suited to participate in the control of distinct epithelial functions are those encoding keratins. Keratins form the intermediate filament cytoskeleton of all epithelia and comprise 54 genes, subdivided into the type I and type II gene families, each numbering ~25 members in the human and the mouse (Hesse et al., 2001, 2004; Schweizer et al., 2006). Owing to their abundance, properties, and organization in epithelial cells, keratin intermediate filaments have been assumed to primarily provide mechanical support. In apparent agreement, mutations in epidermal keratin genes cause a variety of skin fragility conditions that have been confirmed in knockout mice (Fuchs and Cleveland, 1998; Irvine and McLean, 1999; Magin et al., 2004; Omary et al., 2004). More recent data suggest that in addition to providing mechanical support, keratins exert cell type and context dependent functions that include regulation of the cell cycle and of protein translation through 14 3 3 proteins, modulation of apoptotic signals, organelle transport and protection against metabolic stress (Betz et al., 2006; Kim et al., 2006; Magin et al., 2007; Margolis et al., 2006). To investigate keratin function in the absence of redundancy, we have recently generated transgenic mice lacking the entire keratin multiprotein family. We found that without keratins, embryonic epithelia suffer no cytolysis and maintain apical polarity, but display mislocalized desmosomes. The major phenotype causing severe growth retardation and death at ~E9.5 with full penetrance, resulted from a decrease in global protein biosynth esis. This was due to a mislocalization of the glucose transporters GLUT1 and GLUT3 at the apical membrane of the yolk sac, which in turn had an inhibitory effect on the mTOR pathway, via AMPK signaling (Vijayaraj et al., 2009). Furthermore, we found that keratin depleted embryos appeared paler and had a reduced vasculature.

Formation of the first vasculature of the developing vertebrate embryo results from an inductive interaction between two

* Corresponding author. Tel.: +49 228 73 4444; fax: +49 228 73 4558.
E-mail address: t.magin@uni-bonn.de (T.M. Magin).

0171-9335/$ - see front matter © 2010 Elsevier GmbH. All rights reserved.
doi:10.1016/j.ejcb.2009.10.016

keratin expressing cell layers of the yolk sac, visceral endoderm (VE) (Anson Cartwright et al., 2000) and mesoderm which give rise to blood islands around E7 7.5 (Palis et al., 1995). Secretion of the morphogen Indian hedgehog (Baron, 2003) from the VE forms part of the signal that triggers the expression of Foxf1 and Bmp4 in the adjacent mesoderm cells, which subsequently programs hemangioblasts to start primitive hematopoiesis (Astorga and Carlsson, 2007; Baron, 2003). In *Ihh*$^{-/-}$ mice, yolk sac vasculature is poorly developed (Byrd et al., 2002), whereas the absence of BMP 4 or Foxf1 impaired cell adhesion between mesoderm and endoderm layers, which ultimately resulted in reduced vasculo genesis in the yolk sac (Mahlapuu et al., 2001; Winnier et al., 1995). Inactivation of sonic hedgehog is associated with defective vascular development (Brown et al., 2000; Pepicelli et al., 1998), whereas its overexpression causes hypervascularization (Rowitch et al., 1999). This raises the question how these morphogens and their gradients which are essential for vasculogenesis are controlled.

In course of the characterization of keratin deficient embryos, we recognized additional defects beyond reduced protein bio synthesis. Here, we report absence of keratins affects primary hematopoiesis and vasculogenesis. We find reduced adhesion between yolk sac VE and mesoderm with subsequent down regulation of hedgehog and BMP 4, both of which are crucial for extraembryonic hematopoiesis. Our data implicate that keratins are necessary for the differentiation of a non epithelial cell lineage through a combination of mechanical and signaling mechanisms.

Materials and methods

Histology, immunofluorescence analysis and in situ hybridization

Mouse concepti at different gestational ages were prepared. Immunofluorescence analysis was performed as follows: tissues were snap frozen in isopentane (pre cooled at −80 °C) and stored at the same temperature. Frozen sections (8 12 μm thick) were fixed in acetone at 20 °C for 10 min and dried for a few hours before further processing. All antibodies were diluted in Tris buffered saline (TBS) containing 1% bovine serum albumin (BSA). Primary mouse monoclonal antibodies were detected with subclass specific secondary antibodies to minimize background. Slides were mounted in ProLong Gold antifade reagent (Invitro gen) (Reichelt and Magin, 2002). For routine histology, tissues were fixed overnight at 4 °C in 4% formalin, sequentially incubated at 4 °C overnight in 15% and 30% sucrose, embedded in paraffin, and sectioned (5 μm). Sections were placed on superfrost plus slides (Menzel Gläser) and dried. After deparaffi nation, sections were either stained with hematoxylin and eosin (Reichelt and Magin, 2002) or used for immunohistochemistry. For cleaved caspase 3 staining, paraffin sections were treated according to the manufacturer's protocol (Cell Signaling) with antigen retrieval done in EDTA buffer (1 mM EDTA, pH 8.0). For phospho histone H3 staining, antigens were retrieved with citrate buffer (18 mM citric acid monohydrate, 82 mM sodium citrate, pH 6.0), the antibody (Upstate) was diluted in TBS containing 1% BSA. Histochemistry was performed with Super Sensitive Link Label IHC Detection system (Bio Genex) and visualized with diamino benzidine. For mRNA in situ hybridization experiments, concepti were processed as above and sectioned. Sections (10 μm) were hybridized with digoxigenin labeled riboprobes for the various placental lineage markers (Anson Cartwright et al., 2000), for *Foxf1* (Mahlapuu et al., 2001) and *Bmp4* (Jones et al., 1991). The probes were detected with alkaline phosphatase conjugated anti DIG antibody and BCIP/NBT as chromogenic substrate (Simmons et al., 2008).

Western blotting

Western blotting was performed as follows: Total protein was extracted in SDS PAGE sample buffer. The samples were heated for 5 min at 95 °C, sonicated 3 times for 30 s and in between intervals kept for 30 s at 95 °C; the procedure was repeated and after additional 10 min at 95 °C the insoluble material was removed by centrifugation. Total protein was determined by the BioRad protein quantification kit and equal amounts of protein were loaded. Separation of total protein extracts was carried out by standard procedures (8% and 10% SDS PAGE). Proteins were electrotransferred to 0.1 μm nitrocellulose membranes (What man) by wet blotting in Towbin buffer (25 mM Tris HCl, pH 8.8, 192 mM glycine, 0.1% SDS, 10% methanol). Membranes were stained with 0.5% Ponceau S. The immunostaining with anti p38 and anti P p38 was performed as described by the manufacturer (Cell Signaling). Secondary antibodies (Dianova) were diluted 1:30,000 and detected with Super Signal (Pierce) (Reichelt and Magin, 2002).

Flow cytometry

E9.5 embryos were trypsinized and single cell suspensions were fixed in 2% formaldehyde in phosphate buffered saline (PBS) for 10 min at 4 °C, washed with PBS and permeabilized with 0.25% Triton/PBS for 5 min at 4 °C. The cells were washed and then stained for 30 min at 4 °C with anti E cadherin (Invitrogen) in 0.5% BSA/TBS and after washing were labeled with goat anti rat Alexa 488 (Dianova) for 15 min at 4 °C. Cells were sorted on a FACSCanto or LSRII flow fluorocytometer (BD Biosciences) and data were analyzed using the FlowJo software (Tree Star).

Antibodies

We used antibodies against p38 and P p38 (Cell Signaling), TER 119 (BD Pharmigen), endomucin (gift from Prof. D. Vestwe ber, Vascular Cell Biology, MPI Molecular Biomedicine, Münster, Germany), anti phospho histone H3 (Ser10) (Upstate), cleaved caspase 3 (Cell Signaling), β1 integrin (gift from Prof. D. Vestweber), VE cadherin (eBioscience) and DIG (Roche).

Results

Homozygous keratin mutants retain epithelial integrity until mid gestation

To investigate development in the absence of keratins (named *KtyII*$^{-/-}$ thereafter), the major epithelial cytoskeletal proteins, morphology and histological sections were examined. *KtyII*$^{-/-}$ embryos displayed growth retardation from ∼E8.5 onwards and appeared pale (Fig. 1A F). As *KtyII*$^{-/-}$ embryos were growth retarded, we examined whether cell proliferation (Margolis et al., 2006), cell size or apoptosis (Oshima, 2002) were affected. Staining for P histone H3 revealed no altered mitotic index in any of the keratin expressing epithelia analyzed (Fig. 1I), indicating that the growth retardation was not a consequence of altered proliferation. To determine cell size, epithelial cells were enriched by FACS from trypsinized embryos. This revealed no major difference (Fig. 1K). A positive correlation existed between the size of the embryo and the number of apoptotic cells, with smaller *KtyII*$^{-/-}$ embryos showing a higher number of apoptotic

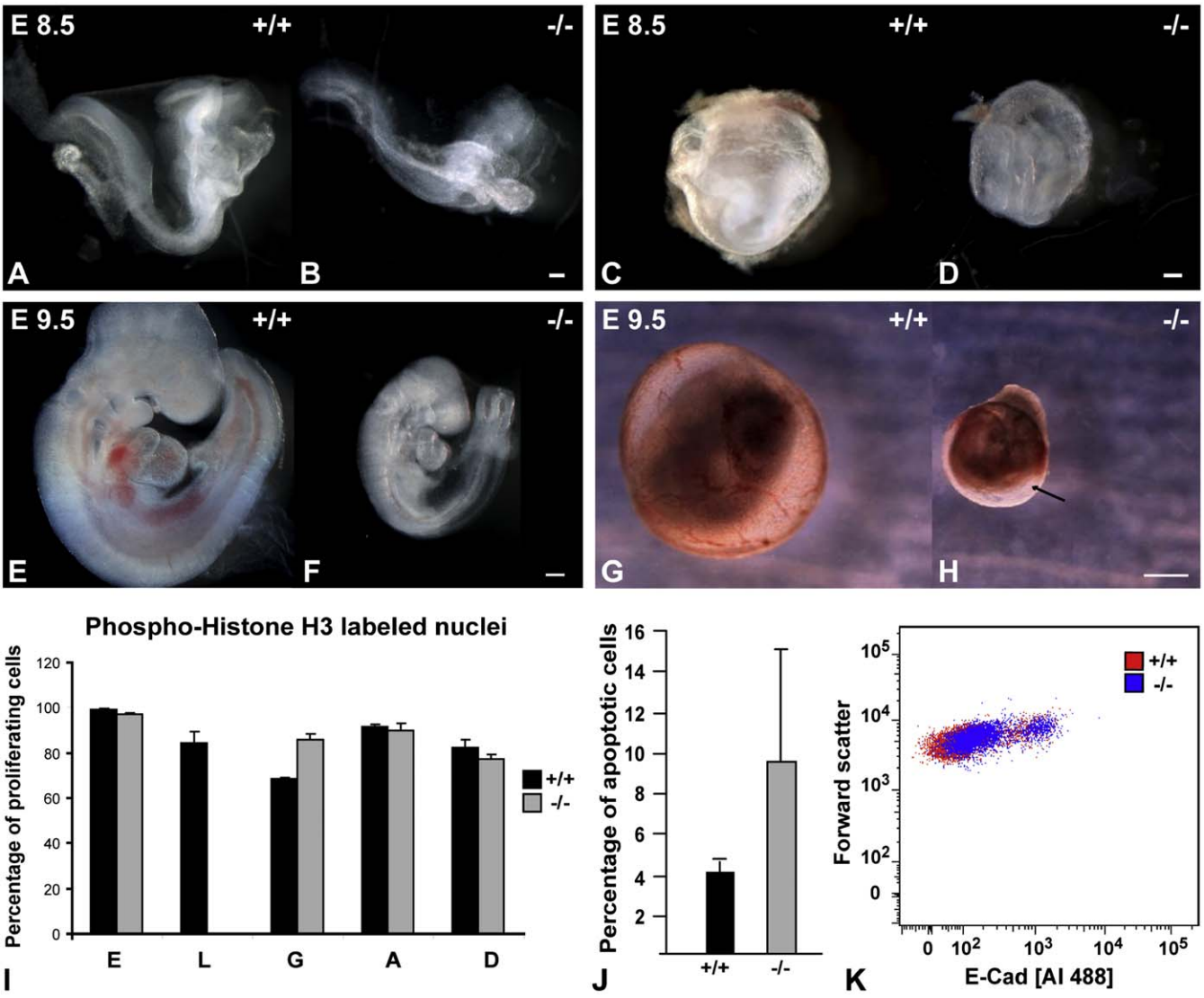

Fig. 1. Reduced size and increased paleness of *KtyII*$^{/}$ embryos. (A-H) Whole-mount wild-type (+/+) and mutant (-/-) embryos dissected from and within the yolk sac at E8.5 (A-D) and E9.5 (E-H). Reduced vasculature is seen in the mutants when compared to their wild-type littermates. Some regions within the yolk sac are completely devoid of vasculature (arrow in H). Scale bars: 100 μm. (I) Mitotic index (calculated as the percentage of total cells with anti-phospho-histone H3-labeled nuclei from three independent experiments). No value for labeled nuclei in the mutant labyrinth (L) was scored due to the absence of this layer in the mutant. E, embryo; G, trophoblast giant cell layer; A, allantois; D, decidua. (J) Percentage of apoptotic cells in wild-type and mutant embryo sections. (K) Size of wild-type and mutant embryo cells determined via FACS analysis as the forward scatter correlates with cell volume. Epithelial cells were labeled with anti-E-cadherin.

cells and vice versa as determined by cleaved caspase 3 staining (Fig. 1J). Most importantly, apoptosis was not restricted to epithelial cells, arguing against a direct role of keratins in regulating apoptosis, but suggesting a secondary effect, which we could show via FACS analysis (Vijayaraj et al., 2009). Given the additional defects in placental development in late E9.5 *KtyII*$^{-/-}$ embryos (Kröger et al., unpublished data), a nutritional deficiency is likely to contribute to greater susceptibility to apoptosis (Gabriel et al., 1998).

Absence of keratins affects hematopoiesis and vasculogenesis through reduced BMP 4 signaling

Based on the timing of growth retardation and paleness indicating paucity of filled blood vessels, we hypothesized that embryo mortality might be due to yolk sac failure, as the yolk sac provides nutrition for the embryo until E9.0 before the establish ment of a functional placenta (Bourget et al., 1995; Freeman and Lloyd, 1983). Yolk sac hematopoiesis in the mouse starts at E7.5 with the formation of mesoderm derived 'blood islands', that proliferate, merge and form the yolk sac vascular network and the vitelline vessel which connects with the embryonic vessels. The yolk sacs of E9.5 *KtyII*$^{-/-}$ embryos were paler and more translucent with blood vessels not readily discernible unlike that of their wild type (WT) littermates (Fig. 1C D, G H). In mutants, numer ous small pools of cells were present without organized vessel formation (Fig. 2B, arrows) and some areas of the yolk sac completely lacked blood islands (Fig. 2B). In contrast, the large vitelline vessel and numerous smaller vessels were clearly seen in WT yolk sacs (Fig. 2A). To analyze the underlying defect in *KtyII*$^{-/-}$ embryos, histology and immunofluorescence analysis were carried out on E9.5 yolk sacs. This revealed two distinct defects. First, the regular contact sites between visceral endoderm and mesoderm, both of which normally express keratins K8, K18 and K19 (Vijayaraj et al., 2009), were severed, causing a separation of the mesodermal/vascular cell layer in the *KtyII*$^{-/-}$ mutants, featuring numerous large spaces that were only sparsely

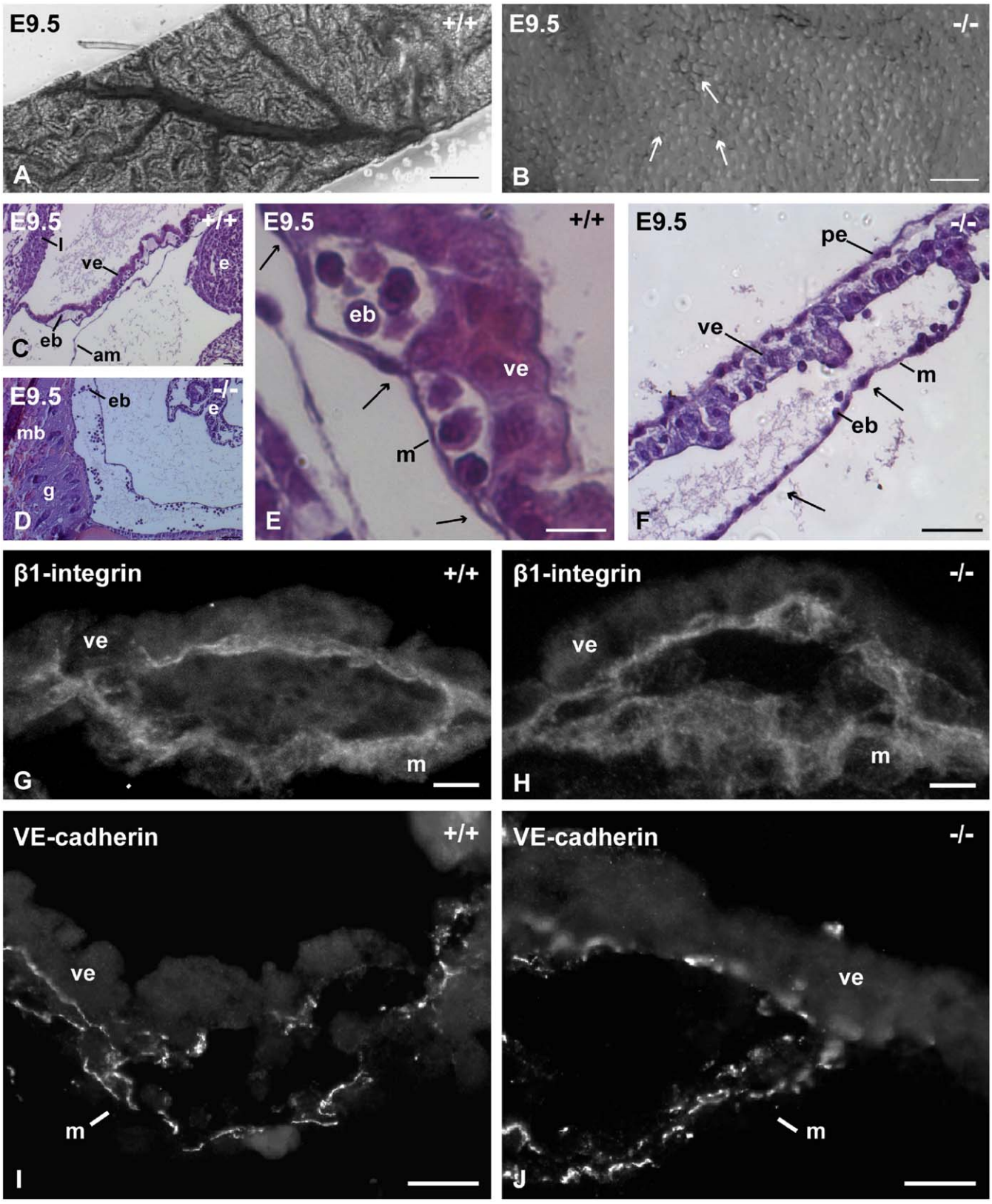

Fig. 2. Keratin deficiency causes a primary yolk sac defect. (A, B) Semi-thin sections through the yolk sac of wild-type and mutant embryos, respectively. The sections from the wild-type yolk sac revealed main and secondary branches of vasculature, whereas the mutants showed discontinuous vasculature (arrows in B) and under-developed secondary branches. (C-F) Hematoxylin and eosin-stained sections through the visceral yolk sac at E9.5. Regular attachments between visceral endoderm and mesoderm layers are depicted by arrows in the wild type. Such attachments are rare in the mutant indicating a lack of regular vascular structures carrying lesser amount of fetal blood cells (arrows in F point to severed attachment sites). (G-J) Immunofluorescence staining for β1-integrin (G, H) and VE-cadherin (I, J) in the yolk sac tissue of wild-type (G, I) and mutant (H, J) embryos did not show any differences. ve, visceral endoderm; m, mesoderm; eb, embryonic blood; mb, maternal blood; g, trophoblast giant cells; am, amniotic membrane, pe, parietal endoderm. Scale bars: 100 μm (A-F); 20 μm (G-J).

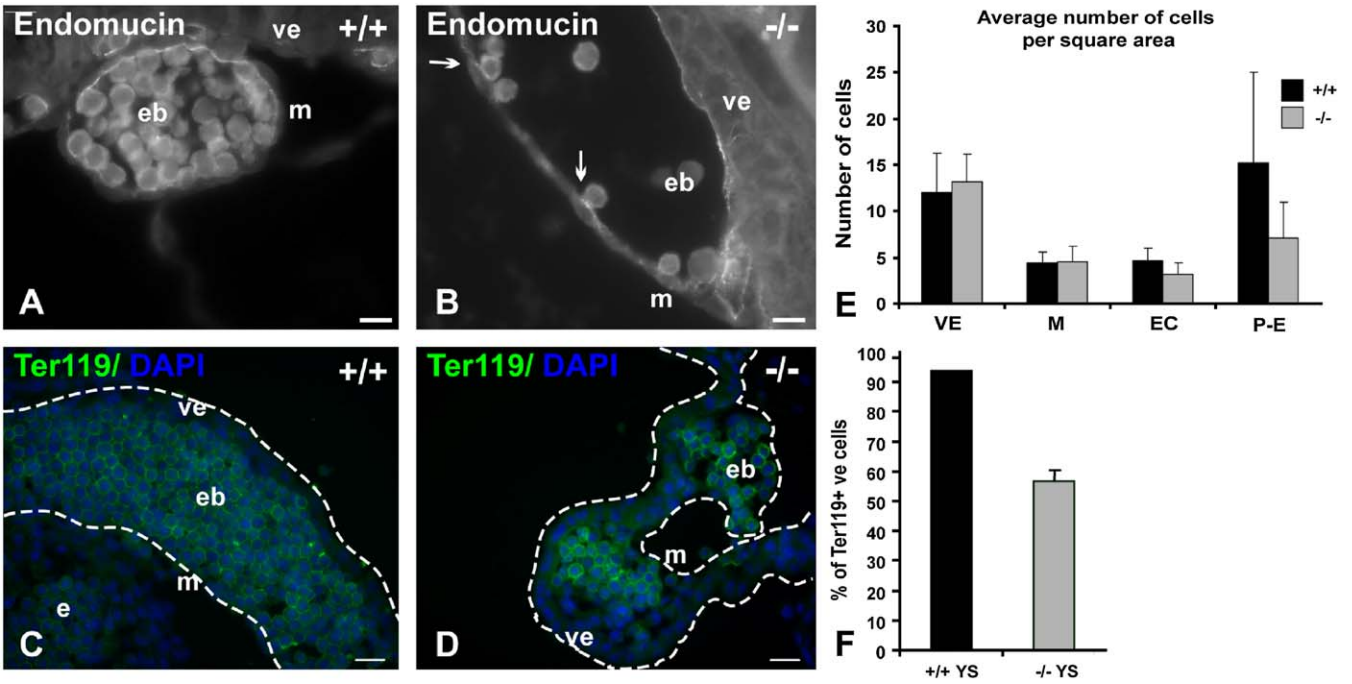

Fig. 3. Altered primitive hematopoiesis in keratin-deficient embryos. (A, B) Staining of yolk sac blood islands with an endothelial-specific antibody against endomucin. Endothelial cells continuously line the wild-type blood island (A), whereas the mutant displays a reduced number and henceforth a discontinuous layer of endothelial cells (B). (C, D) Immunofluorescence analysis using an antibody specific for late erythroid differentiation lineage TER-119 revealed a defective maturation of primitive erythroblasts in about 40% of the cells in *KtyII*$^{/}$ embryos (D) when compared to the wild type (C). ve, visceral endoderm; m, mesoderm; eb, embryonic blood; Scale bars: 10 μm. The percentage of TER-119-positive cells is scored in (F). (E) The average number of different cell types within a yolk sac island from 20 independent microscopic fields were counted and scored; VE, visceral endoderm; M, mesoderm; EC, endothelial cells; P-E primary erythroblasts.

populated with hematopoietic cells (Fig. 2D, F). Second, the apparently altered interaction between the VE and the underlying mesoderm not only affected vascular reorganization but also differentiation of hemangioblasts. Staining for erythroid cells at late differentiation stages (early proerythroblast to mature erythrocyte) with anti Ter119, which recognizes a cell surface antigen in erythroid lineage cells (Kina et al., 2000), demonstrated that hematopoiesis was reduced by 50% in the *KtyII*$^{-/-}$ mutants and only about 60% of the primitive erythroid progenitors had matured to primary erythroblasts (Fig. 3C D, F). Furthermore, the number of endothelial cells which line the blood islands in the *KtyII*$^{-/-}$ mutants were reduced by ∼35%, as revealed by immunolabeling using an endothelial specific antibody directed against endomucin (Fig. 3A B, E). The above defects demonstrate for the first time that keratins are required in a small subset of endodermal cells to maintain contacts to the underlying mesoderm, and that loss of these contacts causes severe defects in the subsequent hematopoiesis. However, staining for the junctional proteins β1 integrin and VE cadherin did not show any obvious aberrations in the *KtyII*$^{-/-}$ mutants (Fig. 2G J).

To examine how severed endoderm mesoderm attachment caused by the absence of keratins affected hematopoiesis and vascular development, known pathways were analyzed. Hedge hog proteins are secreted by the VE and induce the activation of the forkhead transcription factor *Foxf1* in the mesoderm where it activates *Bmp 4* expression. In response to BMP 4, a subset of mesodermal cells give rise to primitive erythroblasts and endothelial cells arising from hemangioblasts (Vogeli et al., 2006), thereby initiating primitive hematopoiesis and the assem bly of the first primitive vessels in the yolk sac (Astorga and Carlsson, 2007). Given the increased distance between yolk sac VE and mesoderm cell layers resulting from the strongly reduced contacts in the mutants, we reasoned that mesodermal cells might receive less Indian hedgehog signal. By in situ hybridiza tion, we found that activation of the hedgehog target *Foxf1* and of downstream *BMP 4* was significantly reduced in *KtyII*$^{-/-}$ yolk sacs compared to WT littermates (Fig. 4A D). This suggests that defective hematopoiesis and vasculogenesis are a consequence of an altered morphogen gradient (Fig. 4F, G). To further substantiate the reduction of the *Bmp4* pathway, we analyzed p38 MAP kinase, known to act downstream of BMP 4 in a SMAD independent manner. Consistently, P p38 MAP kinase was reduced by 50% in the *KtyII*$^{-/-}$ mutants (Fig. 4E), in line with a signaling defect in the absence of contacts between the VE and the mesoderm.

Discussion

Keratins are required for yolk sac hematopoiesis and vasculogenesis

The recent generation of mice which lack the entire keratin multiprotein family has revealed a novel role of keratins in the control of protein biosynthesis through AMPK and mTOR (Vijayaraj et al., 2009). Knockout of all keratins caused severe growth retardation of mouse embryos.

The phenotype resulting from the lack of all keratins is in stark contrast to those observed in single or double keratin gene knockouts during mouse development (Baribault et al., 1993; Hesse et al., 2000; Jaquemar et al., 2003; Magin et al., 1998; Tamai et al., 2000). While absence of K18 was fully compensated by K19, the other knockouts caused severe placental anomalies, caused either by trophoblast fragility or by maternal TNF α, contributing to apoptosis in placental tissues. A common denominator of all above knockouts, except K18 which lacks an embryonic pheno type, is the continued expression of other, unpaired keratins. We suggest that these may induce a stress response absent in the *KtyII*$^{-/-}$ embryos.

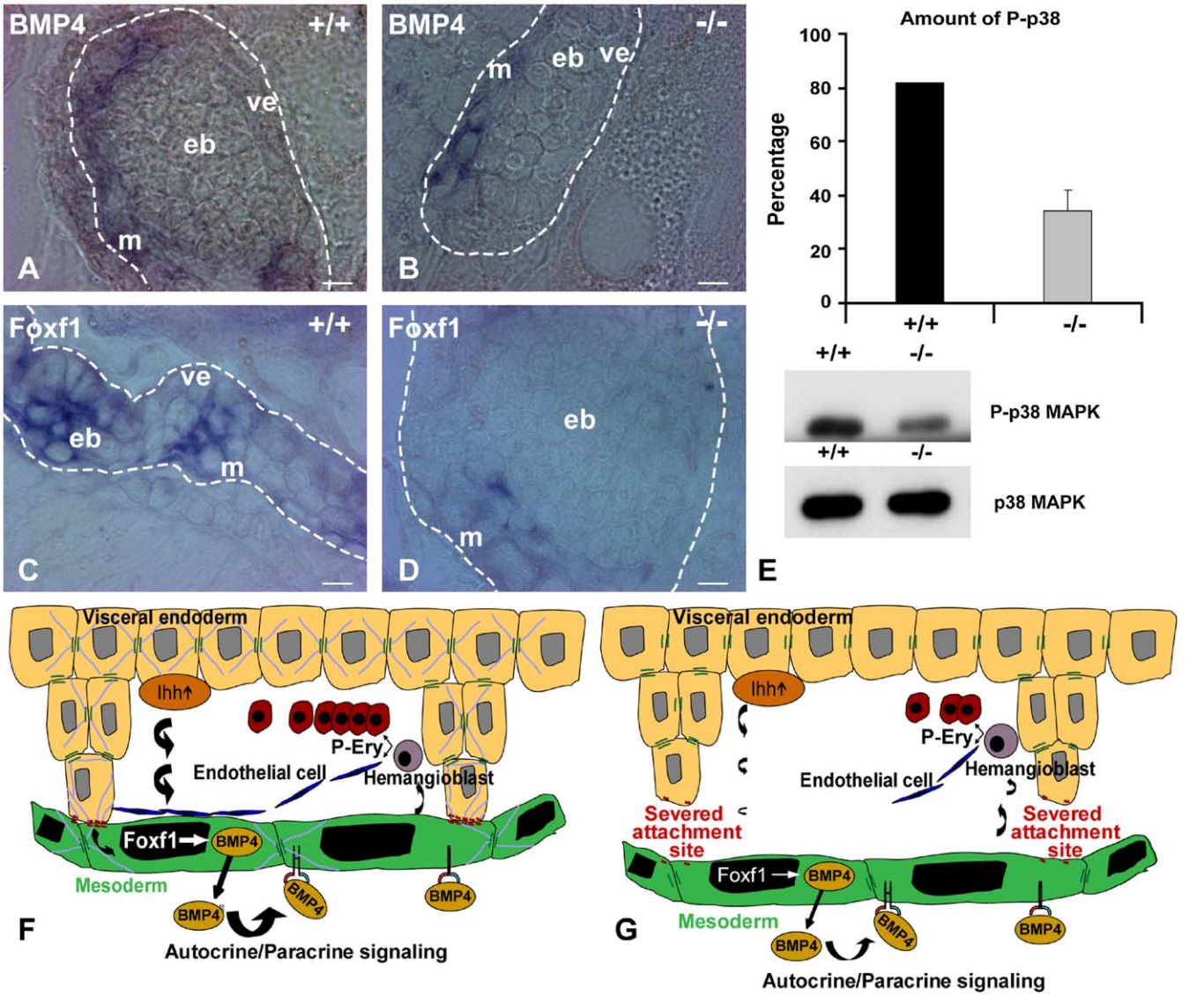

Fig. 4. Altered hedgehog/BMP4 crosstalk in *KtyII*$^{-/-}$ mutants. (A-D) In situ hybridization for *Bmp*4 and *Foxf1* transcripts. Staining is in the visceral endoderm of the *KtyII*$^{-/-}$ embryos. ve, visceral endoderm; m, mesoderm; eb, embryonic blood. Scale bars: 10 μm. (E) Immunoblot analysis of activated and basal p38 MAP kinase in wild-type and mutant embryos at E9.5, indicating reduced activated p38 MAP kinase as a consequence of reduced *Bmp4* expression in *KtyII*$^{-/-}$ embryos. (F, G) A model to illustrate endoderm–mesoderm attachment sites within a blood island – a prerequisite for initiation of hematopoiesis and vasculogenesis in wild-type (F) and *KtyII*$^{-/-}$ (G) embryos. Severed attachment sites in the mutant lead to enlarged spaces between the two layers, subsequently reducing the activation of *Foxf1* and *Bmp*4 expression.

Here, we identified another defect which sheds light on additional keratin functions. We found that adhesion between yolk sac endoderm and mesoderm in *KtyII*$^{-/-}$ was decreased, interfering with blood island formation, vasculogenesis and hematopoiesis. By analyzing surface antigen expression of Ter119 and endomucin, we found a 40% reduction in the maturation of primitive erythroblasts and a 35% reduction in the number of endothelial cells in the mutants when compared to WT embryos, indicating an alteration of cell lineage specification. Differentiation of the hematopoietic lineage requires cues from the mesoderm downstream from VE signals. Reduced interaction between VE and mesoderm, accompanied by similar defects in vasculogenesis and hematopoiesis has been previously reported in knockouts of genes regulating cell adhesion, cell communication and cell signaling. Mice deficient in αv integrins died in utero and also displayed distended yolk sac vasculature with altered VE and mesoderm interaction (Bader et al., 1998). Moreover, mice lacking the fibronectin receptor α5β1 showed embryonic lethality with pronounced defects in yolk sac mesoderm, displaying defective cell matrix adhesion (Yang et al., 1993). Deletion of tight junction associated ZO 1 affected interaction between yolk sac endoderm and mesoderm and reduced angiogenesis, possibly through mislocalization of the tight junction associated protein JAM A (Katsuno et al., 2008). In connexin45 mutant embryos, the reduced adhesion between yolk sac endoderm and mesoderm affected the formation of vascular trees, possibly through reduced TGF β signaling (Kruger et al., 2000). Moreover, several components of the TGF β signaling pathway, which cause defects in hematopoiesis and vasculogenesis, display impaired interaction between VE and mesoderm (Chang et al., 1999; Dickson et al., 1995; Oshima et al., 1996). Recently, it was shown that hedgehog mediates the induction of BMP 4 by Foxf1 (Astorga and Carlsson, 2007). Moreover, in support of our previous findings that keratins act upstream of the mTOR pathway (Vijayaraj et al., 2009), reduced Foxf1 expression could result from decreased protein biosynthesis.

Here, we show that absence of keratins leads to a lower expression of Foxf1, BMP 4, and reduced p38 MAPK activity. These defects affected the differentiation of a non epithelial cell lineage. How can these changes be explained in the light of known keratin functions? We hypothesize that keratins act as distinct scaffolds acting in diverse functions. Keratins are linked to hemidesmosomes at the cell substrate junctions via α6β4 integrins. A function in integrin trafficking and stability is known for the type III IF protein vimentin. PKCε dependent phosphorylation of the vimentin head domain controls the release of integrins from a vesicular and cytoskeletal compartment to the plasma membrane (Ivaska et al., 2005). Furthermore, vimentin regulates the distribution of ICAM 1 and VCAM 1 on endothelial cells and of β1 integrin, critical in the homing of peripheral blood mononuclear cells (Nieminen et al., 2006). Finally, plakophilin 2 and PKCα dependent trafficking of desmoplakin is controlled by transient interaction with a subset of keratins (Bass Zubek et al., 2008).

Our *KtyII*$^{-/-}$ mouse model provides a starting point to address isotype specific keratin functions in embryonic and adult tissues, using conditional deletion combined with replacement by single keratin pairs. Collectively, these approaches will permit the mechanistic analysis of keratin function in cell architecture, adhesion and during tissue differentiation in the absence of dominant negative effects. Most importantly, they will reveal keratin functions in settings in which angiogenesis is crucial, including tumorigenesis and metastasis.

Acknowledgements

We thank our colleagues M. Hatzfeld, M. Hoch and R. Leube for critical input. We thank Prof. Vestweber for donating antibodies and Elmar Endl, Andreas Dolf, and Peter Wurst from the Flow Cytometry Core Facility at the Institute for Molecular Medicine and Experimental Immunology, University of Bonn. This project was funded by the Deutsche Forschungsgemeinschaft (German Research Council), and in parts by Bonfor (Research group cytoskeleton), Thyssen Stiftung and Bonner Forum Biomedizin.

References

Anson-Cartwright, L., Dawson, K., Holmyard, D., Fisher, S.J., Lazzarini, R.A., Cross, J.C., 2000. The glial cells missing-1 protein is essential for branching morphogenesis in the chorioallantoic placenta. Nat. Genet. 25, 311–314.

Astorga, J., Carlsson, P., 2007. Hedgehog induction of murine vasculogenesis is mediated by Foxf1 and Bmp4. Development 134, 3753–3761.

Bader, B.L., Rayburn, H., Crowley, D., Hynes, R.O., 1998. Extensive vasculogenesis, angiogenesis, and organogenesis precede lethality in mice lacking all alpha v integrins. Cell 95, 507–519.

Baribault, H., Price, J., Miyai, K., Oshima, R.G., 1993. Mid-gestational lethality in mice lacking keratin 8. Genes Dev. 7, 1191–1202.

Baron, M.H., 2003. Embryonic origins of mammalian hematopoiesis. Exp. Hematol. 31, 1160–1169.

Bass-Zubek, A.E., Hobbs, R.P., Amargo, E.V., Garcia, N.J., Hsieh, S.N., Chen, X., Wahl 3rd, J.K., Denning, M.F., Green, K.J., 2008. Plakophilin 2: a critical scaffold for PKC alpha that regulates intercellular junction assembly. J. Cell Biol. 181, 605–613.

Betz, R.C., Planko, L., Eigelshoven, S., Hanneken, S., Pasternack, S.M., Bussow, H., Van Den Bogaert, K., Wenzel, J., Braun-Falco, M., Rutten, A., Rogers, M.A., Ruzicka, T., Nöthen, M.M., Magin, T.M., Kruse, R., 2006. Loss-of-function mutations in the keratin 5 gene lead to Dowling-Degos disease. Am. J. Hum. Genet. 78, 510–519.

Bourget, P., Roulot, C., Fernandez, H., 1995. Models for placental transfer studies of drugs. Clin. Pharmacokinet. 28, 161–180.

Brown, L.A., Rodaway, A.R., Schilling, T.F., Jowett, T., Ingham, P.W., Patient, R.K., Sharrocks, A.D., 2000. Insights into early vasculogenesis revealed by expression of the ETS-domain transcription factor Fli-1 in wild-type and mutant zebrafish embryos. Mech. Dev. 90, 237–252.

Byrd, N., Becker, S., Maye, P., Narasimhaiah, R., St-Jacques, B., Zhang, X., McMahon, J., McMahon, A., Grabel, L., 2002. Hedgehog is required for murine yolk sac angiogenesis. Development 129, 361–372.

Chang, H., Huylebroeck, D., Verschueren, K., Guo, Q., Matzuk, M.M., Zwijsen, A., 1999. Smad5 knockout mice die at mid-gestation due to multiple embryonic and extraembryonic defects. Development 126, 1631–1642.

Dickson, M.C., Martin, J.S., Cousins, F.M., Kulkarni, A.B., Karlsson, S., Akhurst, R.J., 1995. Defective haematopoiesis and vasculogenesis in transforming growth factor-beta 1 knock out mice. Development 121, 1845–1854.

Freeman, S.J., Lloyd, J.B., 1983. Evidence that protein ingested by the rat visceral yolk sac yields amino acids for synthesis of embryonic protein. J. Embryol. Exp. Morphol. 73, 307–315.

Fuchs, E., 2007. Scratching the surface of skin development. Nature 445, 834–842.

Fuchs, E., Cleveland, D.W., 1998. A structural scaffolding of intermediate filaments in health and disease. Science 279, 514–519.

Gabriel, H.D., Jung, D., Butzler, C., Temme, A., Traub, O., Winterhager, E., Willecke, K., 1998. Transplacental uptake of glucose is decreased in embryonic lethal connexin26-deficient mice. J. Cell Biol. 140, 1453–1461.

Hesse, M., Franz, T., Tamai, Y., Taketo, M.M., Magin, T.M., 2000. Targeted deletion of keratins 18 and 19 leads to trophoblast fragility and early embryonic lethality. EMBO J. 19, 5060–5070.

Hesse, M., Magin, T.M., Weber, K., 2001. Genes for intermediate filament proteins and the draft sequence of the human genome: novel keratin genes and a surprisingly high number of pseudogenes related to keratin genes 8 and 18. J. Cell Sci. 114, 2569–2575.

Hesse, M., Zimek, A., Weber, K., Magin, T.M., 2004. Comprehensive analysis of keratin gene clusters in humans and rodents. Eur. J. Cell Biol. 83, 19–26.

Irvine, A.D., McLean, W.H., 1999. Human keratin diseases: the increasing spectrum of disease and subtlety of the phenotype-genotype correlation. Br. J. Dermatol. 140, 815–828.

Ivaska, J., Vuoriluoto, K., Huovinen, T., Izawa, I., Inagaki, M., Parker, P.J., 2005. PKCepsilon-mediated phosphorylation of vimentin controls integrin recycling and motility. EMBO J. 24, 3834–3845.

Jaquemar, D., Kupriyanov, S., Wankell, M., Avis, J., Benirschke, K., Baribault, H., Oshima, R.G., 2003. Keratin 8 protection of placental barrier function. J. Cell Biol. 161, 749–756.

Jones, C.M., Lyons, K.M., Hogan, B.L., 1991. Involvement of bone morphogenetic protein-4 (BMP-4) and Vgr-1 in morphogenesis and neurogenesis in the mouse. Development 111, 531–542.

Katsuno, T., Umeda, K., Matsui, T., Hata, M., Tamura, A., Itoh, M., Takeuchi, K., Fujimori, T., Nabeshima, Y., Noda, T., Tsukita, S., Tsukita, S., 2008. Deficiency of zonula occludens-1 causes embryonic lethal phenotype associated with defected yolk sac angiogenesis and apoptosis of embryonic cells. Mol. Biol. Cell 19, 2465–2475.

Kim, S., Coulombe, P.A., 2007. Intermediate filament scaffolds fulfill mechanical, organizational, and signaling functions in the cytoplasm. Genes Dev. 21, 1581–1597.

Kim, S., Wong, P., Coulombe, P.A., 2006. A keratin cytoskeletal protein regulates protein synthesis and epithelial cell growth. Nature 441, 362–365.

Kina, T., Ikuta, K., Takayama, E., Wada, K., Majumdar, A.S., Weissman, I.L., Katsura, Y., 2000. The monoclonal antibody TER-119 recognizes a molecule associated with glycophorin A and specifically marks the late stages of murine erythroid lineage. Br. J. Haematol. 109, 280–287.

Kruger, O., Plum, A., Kim, J.S., Winterhager, E., Maxeiner, S., Hallas, G., Kirchhoff, S., Traub, O., Lamers, W.H., Willecke, K., 2000. Defective vascular development in connexin 45-deficient mice. Development 127, 4179–4193.

Magin, T.M., Schroder, R., Leitgeb, S., Wanninger, F., Zatloukal, K., Grund, C., Melton, D.W., 1998. Lessons from keratin 18 knockout mice: formation of novel keratin filaments, secondary loss of keratin 7 and accumulation of liver-specific keratin 8-positive aggregates. J. Cell Biol. 140, 1441–1451.

Magin, T.M., Reichelt, J., Hatzfeld, M., 2004. Emerging functions: diseases and animal models reshape our view of the cytoskeleton. Exp. Cell Res. 301, 91–102.

Magin, T.M., Vijayaraj, P., Leube, R.E., 2007. Structural and regulatory functions of keratins. Exp. Cell Res. 313, 2021–2032.

Mahlapuu, M., Ormestad, M., Enerback, S., Carlsson, P., 2001. The forkhead transcription factor Foxf1 is required for differentiation of extra-embryonic and lateral plate mesoderm. Development 128, 155–166.

Margolis, S.S., Perry, J.A., Forester, C.M., Nutt, L.K., Guo, Y., Jardim, M.J., Thomenius, M.J., Freel, C.D., Darbandi, R., Ahn, J.H., Arroyo, J.D., Wang, X.F., Shenolikar, S., Nairn, A.C., Dunphy, W.G., Hahn, W.C., Virshup, D.M., Kornbluth, S., 2006. Role for the PP2A/B56delta phosphatase in regulating 14-3-3 release from Cdc25 to control mitosis. Cell 127, 759–773.

Nieminen, M., Henttinen, T., Merinen, M., Marttila-Ichihara, F., Eriksson, J.E., Jalkanen, S., 2006. Vimentin function in lymphocyte adhesion and transcellular migration. Nat. Cell Biol. 8, 156–162.

Omary, M.B., Coulombe, P.A., McLean, W.H., 2004. Intermediate filament proteins and their associated diseases. N. Engl. J. Med. 351, 2087–2100.

Oshima, M., Oshima, H., Taketo, M.M., 1996. TGF-beta receptor type II deficiency results in defects of yolk sac hematopoiesis and vasculogenesis. Dev. Biol. 179, 297–302.

Oshima, R.G., 2002. Apoptosis and keratin intermediate filaments. Cell Death Differ. 9, 486–492.

Palis, J., McGrath, K.E., Kingsley, P.D., 1995. Initiation of hematopoiesis and vasculogenesis in murine yolk sac explants. Blood 86, 156–163.

Pepicelli, C.V., Lewis, P.M., McMahon, A.P., 1998. Sonic hedgehog regulates branching morphogenesis in the mammalian lung. Curr. Biol. 8, 1083–1086.

Reichelt, J., Magin, T.M., 2002. Hyperproliferation, induction of c-Myc and 14-3-3sigma, but no cell fragility in keratin-10-null mice. J. Cell Sci. 115, 2639–2650.

Rowitch, D.H., St-Jacques, B., Lee, S.M., Flax, J.D., Snyder, E.Y., McMahon, A.P., 1999. Sonic hedgehog regulates proliferation and inhibits differentiation of CNS precursor cells. J. Neurosci. 19, 8954–8965.

Sancho, E., Batlle, E., Clevers, H., 2004. Signaling pathways in intestinal development and cancer. Annu. Rev. Cell Dev. Biol. 20, 695–723.

Schweizer, J., Bowden, P.E., Coulombe, P.A., Langbein, L., Lane, E.B., Magin, T.M., Maltais, L., Omary, M.B., Parry, D.A., Rogers, M.A., Wright, M.W., 2006. New consensus nomenclature for mammalian keratins. J. Cell Biol. 174, 169–174.

Simmons, D.G., Natale, D.R., Begay, V., Hughes, M., Leutz, A., Cross, J.C., 2008. Early patterning of the chorion leads to the trilaminar trophoblast cell structure in the placental labyrinth. Development 135, 2083–2091.

Tamai, Y., Ishikawa, T., Bosl, M.R., Mori, M., Nozaki, M., Baribault, H., Oshima, R.G., Taketo, M.M., 2000. Cytokeratins 8 and 19 in the mouse placental development. J. Cell Biol. 151, 563–572.

Vijayaraj, P., Kröger, C., Reuter, U., Windoffer, R., Leube, R.E., Magin, T.M., 2009. Keratins regulate protein biosynthesis through localization of GLUT1 and -3 upstream of AMP kinase and Raptor. J. Cell Biol. 187, 175–184.

Vogeli, K.M., Jin, S.W., Martin, G.R., Stainier, D.Y., 2006. A common progenitor for haematopoietic and endothelial lineages in the zebrafish gastrula. Nature 443, 337–339.

Winnier, G., Blessing, M., Labosky, P.A., Hogan, B.L., 1995. Bone morphogenetic protein-4 is required for mesoderm formation and patterning in the mouse. Genes Dev. 9, 2105–2116.

Yang, J.T., Rayburn, H., Hynes, R.O., 1993. Embryonic mesodermal defects in alpha 5 integrin-deficient mice. Development 119, 1093–1105.

Yeaman, C., Grindstaff, K.K., Nelson, W.J., 1999. New perspectives on mechanisms involved in generating epithelial cell polarity. Physiol. Rev. 79, 73–98.

4.3 Placental vasculogenesis is regulated by keratin-mediated hyperoxia in murine decidual tissues

This work is currently submitted in a scientific journal.

Journal:
American Journal of Pathology

Authors:
Cornelia Kröger, Preethi Vijayaraj, Reinhard Windoffer, David Simmons, Ursula Reuter, Rudolf E. Leube, and Thomas M. Magin

Contribution:
Histology, immunofluorescence, pathway analysis via Western blot, image formatting, paper writing

Placental vasculogenesis is regulated by keratin-mediated hyperoxia in murine decidual tissues

Cornelia Kröger[1,2], Preethi Vijayaraj[1,5], Reinhard Windoffer[3], David Simmons[4], Ursula Reuter[1] , Rudolf Leube[3] and Thomas M. Magin[1,2,*]

[1]Institute of Biochemistry and Molecular Biology, Div. of Cell Biochemistry, University of Bonn, 53115 Bonn, Germany.

[2]Institute of Biology II and Translational Center for Regenerative Medicine, University of Leipzig, 04109 Leipzig, Germany.

[3]Institute of Molecular and Cellular Anatomy, RWTH Aachen University, 52074 Aachen, Germany.

[4]School of Biomedical Sciences, The University of Queensland, St Lucia 4072, Australia.

[5]Department of Medicine, Centre for Vascular Biology Research, Beth Israel Deaconess Medical Centre, Harvard Medical School, Boston, MA, USA.

This project was funded by the Deutsche Forschungsgemeinschaft (German Research Council), and in parts by Bonfor (Research group cytoskeleton), Thyssen Stiftung and Bonner Forum Biomedizin.

Text pages:13
Tables:2
Figures:6
Supplementary Tables:1
Supplementary Figures:3

*Corresponding author: Prof. Thomas M. Magin, phone 0049-341-97-39662, fax 0049 341 97 39609, e-mail: thomas.magin@trm.uni-leipzig.de

Abstract

The mammalian placenta represents the interface between maternal and embryonic tissues and provides nutrients and gas exchange during embryo growth. Recently, keratin intermediate filament proteins were found to regulate embryo growth upstream of the mTOR pathway and contribute to yolk sac vasculogenesis through altered BMP-4 signalling. Whether keratins have vital functions in extraembryonic tissues is not well understood.

Here we report that keratins are essential for placental function. We find that in the absence of keratins, hypoxia in the decidual tissue directly adjacent to the placenta is reduced, due to an increased maternal vasculature. Hyperoxia causes impaired vasculogenesis through defective Hif1α and VEGF signalling, resulting in invagination defects of the fetal blood vessels into the chorion. In turn, the reduced labyrinth and its inability of gas exchange between maternal and embryonic blood led to increased hypoxia in keratin-deficient embryos. We propose that trophoblast giant cell signalling during decidualisation is altered in the absence of keratins, leading to increased vascularization of the maternal decidua. Our findings suggest that keratin mutations predispose to early pregnancy loss in conditions that cause hyperoxia in the decidua.

Introduction

Epithelial cells line the surface of internal organs and tissues. They provide mechanical support and protection from the external environment but are contemporaneously essential for the communication and the exchange of nutrients and oxygen from the environment, as in the gut and lung tissue, respectively.

The intermediate filament system of the epithelial cytoskeleton, formed by members of the keratin multiprotein family, is particularly suited to fulfil these functions. Keratins have been confirmed to provide mechanical stability, as diverse skin mutations account for [1-4], but in addition have been shown to exert important signalling functions in epithelial cells. Previous mutation and knockout (KO) studies revealed their involvement in the regulation of cell cycle, in protein translation through 14-3-3 proteins and the mTOR complex, modulation of apoptotic signals, organelle transport and protection against metabolic stress [5-9]. The functional analysis of individual keratins has been obscured by compensatory expression of other keratins expressed in the same epithelia. The recently reported deletion of all keratins in mice provided unexpected and novel insights into keratin function during mouse development [10]. It revealed that keratins play an essential role in embryogenesis, as mutant embryos died at E9.5 in midgestation due to severe growth retardation, caused by a drastic decrease in protein biosynthesis. This was due to a mislocalization of the GLUT1 and GLUT3 transporters from the apical plasma membrane, which resulted in the inhibition of the mTOR pathway through AMP kinase [10]. In contrast to previous gene KO studies, in which the deletion of K8 or the combined deletion of K18/K19 and of K8/K19 caused fragility of trophoblast giant cells, followed by extensive haemorrhages [11, 12], we found that tissue integrity and apical cell polarity of the embryonic epithelia were largely maintained in keratin null embryos. The depletion of keratins rather caused an attachment defect of endodermal and mesodermal tissue in the yolk sac, resulting in decreased haematopoiesis and vasculogenesis through reduced Foxf1 signalling and its downstream targets BMP4 and P-p38 MAPK in the yolk sac mesoderm [9].

The function of keratins in the placenta has not been fully elucidated. In a subset of K8-deficient embryos, increased sensitivity to TNF-mediated apoptosis was observed in a mouse strain-dependent manner [13, 14]. In contrast, other studies reported trophoblast fragility following the combined deletion of K18/19 or K8/K19 [11, 12]. Survival and growth of the embryo are critically dependent on the placenta. The placenta forms the interface between maternal and fetal circulation, facilitating gas, nutrient and waste exchange [15]. It is comprised of the epithelial trophectoderm cells that upon implantation of the embryo into the uterine wall at around E4.5 expand and differentiate. The first embryonic cells to interact with the maternal tissue are the trophoblast giant cells (TGCs) which invade and attach to the uterine wall and induce decidualisation by altering specific gene expression amongst others for vascular

remodelling and angiogenesis secreting various hormones like prolactin-like-protein a (Prlpa) [16].

The vascularization of the murine placenta starts at E8.5 with the fusion of the mesodermal allantois to the chorion and the invagination of the fetal blood vessels. This process relies on a highly coordinated crosstalk between the epithelial trophoblast and the embryonic endothelium, modulated by transcription factors and signalling receptors on the epithelial [17-29] as well as on the endothelial side [30-39] which are essential for the development of the proper vasculature in the placental labyrinth (Tables 1 and 2).

Furthermore, a localized oxygen gradient has been shown to be critical in human decidualisation and placentation by influencing vascular remodelling in the decidua and differentiation of trophoblast cells [40]. There is increasing evidence that the same holds true for mice [41]. Implantation and ensuing placentation start under hypoxic conditions until the vascular network between maternal and embryonic tissue is properly established and the placenta is flooded with maternal blood. Hypoxia is necessary for normal vascularization [42]. The hypoxia-inducible factors (HIF), HIF1a, HIF2a and HIF1β (ARNT) directly promote VEGF expression [43], as their absence in various KO models showed a reduced vascularization and developmental retardation of the placenta [17, 20, 24]. In humans, increased hypoxia leads to preeclampsia, a syndrome causing substantial maternal and fetal mortality in pregnancies. Hallmarks of preeclampsia are reduced trophoblast invasion, reduced vasculature of the placenta and increased serum levels of sFlt1 [44, 45]. Conversely, untimely elevated oxygen levels in decidual and placental tissues cause regression of placental villi, spongiotrophoblast tissue and intrauterine growth restriction (IUGR) through premature maternal blood flow to the placenta [46, 47]. The underlying gene defects, however, are not well known and molecular defects causing these alterations still have to be identified.

Here, we demonstrated a crucial role of keratins for vascular remodelling in the decidua and in the labyrinth through an altered localization of TGC. Subsequently, TGC mislocalization altered proper hormone secretion and induced hypervascularization and increased oxygen levels in the decidua. Our findings suggest that keratin mutations predispose to early pregnancy loss in conditions of maternal hyperoxia.

Materials and methods

Transgenic mice, histology, immunofluorescence microscopy and *in situ* hybridization

Mouse concepti at different gestational ages were prepared. For light microscopy and immunofluorescence analysis, tissues were snap-frozen in isopentane precooled at -80°C and stored at the same temperature. Immunofluorescence analysis was performed as follows: Frozen sections (8-12 µm thick) were fixed in acetone at –20°C for 10 min and dried for a few hours before further processing. All antibodies were diluted in TBS containing 1% BSA and 5% normal goat serum (NGS). Primary mouse monoclonal antibodies were detected with subclass-specific secondary antibodies to minimize background. Slides were mounted in ProLong Gold antifade reagent (Invitrogen) [48]. For routine histology, tissues were fixed overnight at 4°C in 4% formalin, sequentially incubated at 4°C overnight in 15% and 30% sucrose, embedded in paraffin, and sectioned (5 µm). Sections were placed on superfrost-plus slides (Menzel-Gläser) and dried. After deparaffination, sections were either stained with hematoxylin and eosin [48], periodic acid-Schiff [49] or used for immunohistochemistry. For CD31 (Dianova), CD34 (Hycult Biotech), Hif1α (Novus Biologicals) and VEGF (Abcam) staining on paraffin sections, antigens were retrieved with citrate buffer (18 mM citric acid monohydrate, 82 mM sodium citrate, pH 6.0) and the antibody was diluted in TBS containing 1% BSA and 5% NGS. The histochemistry was performed with Super Sensitive Link Label IHC Detection system (Bio Genex) and visualized with DAB (Dabko). For mRNA *in situ* hybridization experiments, concepti were processed as above and sectioned. Sections (10 µm) were hybridized with digoxigenin-labeled riboprobes for the various placental lineage markers [50, 51], K8, Pl1 [52], Tpbp1 [53], Prlpa [54], Gcm1 [55] and SyncytinA [50]. The probes were detected with alkaline phosphatase-conjugated anti-DIG antibody and BCIP/ NBT as chromogenic substrate [50].

Immunofluorescence microscopy and data processing

Images of stained paraffin sections were acquired using a fluorescence microscope (Axioplan 2; Carl Zeiss, Inc.) with a Plan-Neofluar 10× 0.30 NA objective or a Plan-Apochromat 63× 1.4 NA oil immersion objective at RT using an AxioCam MR camera (Carl Zeiss, Inc.). Image analysis and processing were performed using AxioVision 4.6 (Carl Zeiss, Inc.) and Photoshop 6.0 (Adobe) software. LUT (lookup table; brightness and gamma) was adjusted using Photoshop.

Western blotting

Western blotting was performed as described [10]. In short: total proteins were extracted in SDS-PAGE sample buffer under repeated heating (95°C) and sonication cycles. Total protein concentration was determined by the BioRad protein quantification kit and equal amounts of protein were loaded. Separation of total protein extracts was carried out by standard

procedures (8% and 10% SDS-PAGE). The immunostaining was performed as described earlier [10]. Secondary antibodies (Dianova) were diluted 1:20,000 and detected with Super Signal (Pierce) [48].

Hypoxia Assay and sFlt1 ELISA

Mice were injected with 60 mg/kg pimonidazole i.p. (Hypoxyprobe-1, Hypoxyprobe, Inc., Burlington, MA, USA) 2.5 h before they were sacrificed. E9.5 mouse embryos were dissected and prepared for histology as described above. Immunohistochemical analysis labelling with Hypoxyprobe-1 were performed as described by the manufacturer (Hypoxyprobe, Inc., Burlington, MA, USA) using the hybridoma 4.3.11.3 (dilution: Supplementary Table 1).

For the sFLT1 ELISA, non-pregnant and pregnant mice (E9.5) were sacrificed by cervical dislocation and blood was extracted from the heart. Serum was collected and the ELISA assay for sFLT1 was performed according to manufacturer's protocol (R&D Systems).

Antibodies. We used antibodies against K8/K18 (Progen), tubulin (Progen), CD31/ Pecam (Dianova), CD34 (Hycult Biotech), Hif1α (Novus Biologicals), VEGF (Abcam) and Alexa 488 / 594 conjugated secondary antibodies (Dianova). Dilutions are listed in Supplementary Table S1.

Results

Keratins are necessary for placental labyrinth and decidual development, but do not affect cell-fate determination

To investigate to which extent formation of placental epithelia depends on keratins, we first analysed placenta morphology in histological sections of various developmental stages of keratin deficient (KtyII$^{-/-}$) and wild type (WT) embryos with their surrounding placental and decidual tissue. Until E8.5, the placenta of keratin null embryos developed normally forming a normal chorioallantoic attachment (data not shown). By E9.5 however, a drastic difference in size became apparent (Figure 1, B and G). Mutant placentas seemed smaller, enriched in cells (Figure1, G-J) compared to WT controls (Figure1, C-F) and showed significantly impaired vasculature. Hematoxylin and eosin (H&E) staining of these placentas revealed that fetal blood vessels were present, but that they were fewer in number and appeared dilated (Figure 1, J and K) compared to WT placentas (Figure 1, E and F). In addition, embryonic vessels of the KO placenta demonstrated a defect in embryonic haematopoiesis, containing less embryonic erythrocytes in comparison to WT placentas. KtyII$^{-/-}$ embryos also had defects in the vascularization of the decidua, characterized by a discontinuous, decomposed loose structure of the peri-vitelline network (Figure 1G, Figure 2 A', Figure 4 B) and the aggregation of maternal blood lacunae in between the trophoblast layers of the TGCs and the spongiotrophoblast (Figure 3 F). This was due to a defective layer of the TGCs, surrounding the KtyII$^{-/-}$ embryos. TGCs assembled in various areas and showed a thinned out layer in others (Figure 1G, Figure 4B), which led to the leakage and accumulation of maternal blood (Figure 3 F, Figure 4 D', F') in over 90% of the KO embryos, depending on the severity of the phenotype.

To further analyze the misdistribution of TGCs, epithelial differentiation was investigated by using several lineage markers for the major trophoblast cell types (Figure 2). In situ hybridization with differentiation markers revealed that the outermost trophoblast layer, the giant cells, expressed placental lactogen 1 (Pl1) (Figure 2, B and G) and the spongiotrophoblast cells were positive for Tpbpa (also known as 4311, Figure 2, C and H) [52, 53]. This demonstrated that lack of keratins did not alter epithelial differentiation in the placenta per se. However, we noted an altered distribution of the TGC marker Pl1, indicating a mislocalization of TGCs (Figure 2 B' arrow heads). Moreover, the mRNA for the secreted Prlpa, a member of the prolactin family was strongly reduced in KtyII$^{-/-}$ TGCs compared to WT cells. Prlpa regulates the decidual immune response of the NK cells [56, 57] and was further demonstrated to show a decidual expression pattern dependent on TGCs [16]. The embryonic death of KtyII$^{-/-}$ embryos was therefore due to keratin dependent abnormalities in both the spatial distribution of the TGCs and the compromised secretion of hormones [10] resulting in a deficit of maternal circulation.

In situ hybridization on implantation sites of E8.5 and E9.5 embryos with a Gcm1 probe, which demarcates the sites for the initiation of branching morphogenesis along the leading edge of the chorion at the interface with the allantois [51] and for SyncytinA, a marker for the development of the syncytiotrophoblast [50], did not show any alterations in expression levels in KtyII$^{-/-}$ embryos (Supplementary Figure 1).

Vascular defects in KtyII$^{-/-}$ placentas

We recently demonstrated that KtyII$^{-/-}$ embryos at E9.5 could be easily discriminated from WT embryos by their pale yolk sacs. The depletion of keratins caused an attachment defect of endodermal and mesodermal tissue in the yolk sac, resulting in decreased haematopoiesis and vasculogenesis through reduced Foxf1 signalling and its downstream targets BMP4 and P-p38 MAPK in the mesoderm [9].

The distribution of fetal capillaries in the labyrinth was investigated by immunohistochemistry using antibodies that recognize CD34 and CD31/ PECAM-1, adhesion molecules expressed on the surface of vascular endothelial cells [58, 59]. In the WT placenta, the fetal vessels were evenly distributed throughout the placental labyrinth, always in close contact to maternal blood sinuses to enable the fetal-maternal exchange of gas and nutrients (Figure 3 A-E, Supplementary Figure 2 A-E). However, in the KtyII$^{-/-}$ placenta, fetal blood vessels mostly innervated the chorio-allantoic plate and did not show extensive branching into the labyrinth trophoblast as the WT vessels did. They were fewer, appeared dilated and contained less embryonic blood, and in addition, very few maternal blood sinuses were identified near the embryonic vessels (Figure 3 F-J, Supplementary Figure 2 F-J).

KtyII$^{-/-}$ embryos develop decidual hyperoxia with an altered expression of vasculogenesis-promoting factors

In human embryonic development, vascularization of the placenta is dependent upon oxygen tension in the surrounding decidual tissues [40]. Recent murine gene knockout studies of HIF proteins indicated that hypoxia is required for vasculogenesis, angiogenesis, and haematopoiesis in the mouse as well [17, 20, 24, 43].

This prompted us to examine the state of hypoxia in KtyII$^{-/-}$ embryos (Figure 4 A-B'). Surprisingly, hypoxia was reduced in the KO decidua compared to the WT controls (Figure 4 A and A') because of increased maternal vasculature (Figure 4 B and B'). However, Hypoxyprobe-1 detects only a severe decrease in oxygen levels of $\leq$10 mmHg (1.5% oxygen) and hence would not detect concentrations of oxygen consistent with milder hypoxia. Therefore, we assessed the localization of Hif1α, which is one of the earliest induced proteins in hypoxia, as soon as 8% oxygen. We found a strong placental staining in the WT placenta of E9.5 embryos and a weaker staining in the hypoxic areas of the decidua,

as Hif1α is no longer responsive under continuous low oxygen levels and its accumulation levels drop [60] (Figure 4 C and C'). The implantation side of the KO also showed an increase of Hif1α staining in the placental tissues (Figure 4 D and D'). In contrast, the level of Hif1α in the embryo proper seemed to be elevated in the KtyII$^{-/-}$ embryo compared to the WT embryos. This was confirmed by Western blot analysis of protein lysates of the embryo proper and the yolk sac (Figure 5 A and B). Recent studies have shown that Hif1α induces VEGF expression to induce placental vasculogenesis [43] through a direct binding of the Hif1α dimer to the VEGF promoter region [61]. Therefore, we localized and measured VEGF expression in the WT decidua and placenta (Figure 4 E and E') and compared them to keratin deficient specimen (Figure 4 F, F'). We found that there was a decrease of Hif1α and VEGF in KO placental tissues, which is consistent with the poor vascularization of the KO placenta (Figure 4). In the embryo proper, no differences in VEGF expression levels were observed (Figure 5 A and B).

Hypoxia was also shown to induce the expression of GLUT1 transporters in early embryonic development [41]. In line, we found a doubling of the GLUT1 expression by quantitative PCR (data not shown) as indicated in our previous findings [10]. Moreover, a reduction of glycogen storage in the KO trophoblast cell lineage was identified (data not shown). This vascularization defect of the labyrinth induced by a defect in the hypoxic signalling cascade of keratin depleted embryos and the mislocalization of GLUT1 transporters resulted in the lack of nutrition and gas uptake, and hence contributed to the embryonic death at midgestation.

KtyII$^{-/-}$ mice represent a novel model for decidual hyperoxia

Hypoxia induced HIF1α protein accumulation in placentas is associated with shallow invasion of trophoblasts into the spiral arteries and the uterine wall (Supplementary Figure 3), probably resulting in vascular remodelling defects and further hypoxia [44]. In addition, secretion of sFlt1 into the maternal blood stream and proteinuria are phenotypic hallmarks of the severe pregnancy complication, preeclampsia, in humans and mice [45, 62]. Therefore, we measured protein contents in urine of E9.5 pregnant mice (data not shown), as well as sFlt1 levels in non-pregnant vs. pregnant WT and KtyII$^{+/-}$ mice at E9.5. Both assays excluded keratins as a major contributor to preeclampsia, as there neither was an increase in protein levels in urine (data not shown), nor could a difference in sFlt1 levels in WT and mutant mice sera be detected (Figure 5 C).

Discussion

The results reported here provide for the first time evidence that keratins coordinate vascular remodelling in the decidua as well as proper vascularization of the labyrinth in placental development. Their loss led to a disruption of gas exchange and due to reduced oxygen uptake, severe hypoxia and growth retardation of the embryo itself.

We propose that this is due to a mislocalization of the giant cells, visualized by Pl1 staining, a hormone specifically secreted by the giant cells. The primary giant cells are the first embryonic epithelial cells to interact with the maternal tissue and highly express keratins; they are responsible for the implantation of the embryo [16]. KO embryos developed normally until E8.5 when growth retardation defects emerged; therefore we propose a defect in secondary giant cells, which arise from the ectoplacental cone [63]. This became evident from their failure to form a continuous peri-vitelline network, as the decidua of KtyII$^{-/-}$ embryos displayed hypervascularization compared to the WT placenta leading to a very loose meshwork with wide maternal blood lacunae. In humans, high oxygen concentration in the periphery of early placentas, induced by a premature onset of maternal placental circulation, is a key factor for early pregnancy loss. In fact, the intervillous space of the developing placenta is separated from the uterine circulation by plugs of trophoblast cells that occlude the tips of the uteroplacental arteries. In complicated pregnancies, invasion of the endometrium by the extravillous trophoblast is severely restricted compared to the normal situation. Plugging of the spiral arteries is therefore less complete and may predispose to the early onset of the maternal circulation [40, 47]. In mice, the TGCs which function equivalent to human extravillous trophoblasts, invade into the spiral decidual arteries and remodel the maternal blood vessels [63, 64] (Supplementary Figure 3). The mislocalization of the TGCs could account for a defective plugging of maternal vessels caused by keratin deletion, as keratin depleted cells were shown to exhibit severe migration and attachment defects [65].

In addition, TGCs are required for initiating decidualisation and regulate its development by the secretion of paracrine hormones, which have a direct influence on promoting and inhibiting PLF and PRP decidual vasculature, respectively [66]. In this fashion they stimulate angiogenic signals in the decidua like Ang1 and Ang2 and secrete hormones which suppress the immune system of the mother [16]. One of these hormones is Prlpa, expressed in secondary TGCs [67], which suppresses the maternal natural killers cells (NK); here, we demonstrated a reduction in the TGCs, as early as E8.5 in KtyII$^{-/-}$ embryos. An involvement of keratins in the secretion of hormones is in line with their reported function in vesicular trafficking and in receptor and transporter localization at the plasma membrane [10, 68].

Hypoxia is a prerequisite for embryonic implantation and development in mammals [40, 41] and is necessary for a normal development of the vasculature [42]. The increased vascularization of the mutant decidua led to an increase in oxygen level of the placenta and in strong support,

we detected hyperoxia. Furthermore, we found a drastic reduction in Hif1α in the KtyII$^{-/-}$ decidua and placenta compared to WT. HIFs form heterodimers of Hif1β (Arnt) and Hif1α or Hif2α. Knocking out any of these 3 proteins, leads to a small labyrinth due to drastically impaired vasculogenesis of the placenta, similar to the phenotype we reported in our KO embryos [17, 20, 24, 43]. As a consequence, reduction of placental vasculogenesis led to a drastic increase in hypoxic levels of the embryo proper itself.

Hypoxia triggers multiple responses to overcome decreased O_2 availability, including the expression of growth factors required for establishment of a functional circulatory system. HIF proteins can induce VEGF, a growth factor important for angioblast specification and vasculogenesis [43]. Entailing the reduced amount of Hif1α, we saw a drastic reduction in the VEGF expression in KO decidua and placenta, which accounted for the vascularization defects. Furthermore, VEGF is a known survival factor for embryonic stem cells (ES) during prolonged hypoxia as well as for haematopoietic stem cells (HSCs) [69, 70], which are generated amongst others in the placenta [71]. In line with these findings, we reported that keratin deficient placentas did not only exhibit reduced vasculature, but the vessels that were present were dilated and filled with fewer embryonic blood cells, corresponding to haematopoiesis defects in keratin deficient embryos in the yolk sac [9].

The development of the labyrinth is dependent on an intensive crosstalk between the epithelial trophoblast lineage and the endothelial cells of the allantois. Different receptor knockout studies, including FGFR2 and Fzd5 [22, 29], as well as various transcription factors JunB, PPARγ and Tfeb [18, 19, 26, 27] displayed very similar phenotypes to the keratin deficient embryos, which might be linked to keratin expression. JunB, for example, an AP1 transcription factor, can induce K18 expression in differentiating ES cells by binding to an enhancer complex in the first intron [72]. Various kinases were also reported to demonstrate vascularization defects in the placenta and the yolk sac when deleted, such as p38 MAPK [25]. We linked keratin deficiency to a reduction of phospho-specific activation of p38 in yolk sacs earlier [9], which would suggest that keratins influence these signalling functions in the trophoblast cells of the labyrinth as well.

Important signalling factors expressed in the allantoic endothelial side of the labyrinth contribute to the development of the labyrinth. Mutations in the Notch signalling pathway, for instance, block chorioallantoic branching and prevent proper invagination of the allantois into the placenta [33, 35, 36]. This is also the case for Ang1, Ang2, the vascular remodelers and their receptor Tie2 [30, 31, 38, 39]. Defects in yolk sac and placental vascularization defects were also reported for the VEGFR receptors, Flk1, and Flt1. [32, 34, 37].

Increased secretion of sFlt1 into the maternal blood stream is a hallmark of preeclampsia. Keratin KO embryos seemed to express the common symptoms, defective trophoblast invasion, hypoxia of the embryo, growth retardation and defective placental vasculature.

However, we could not detect an increase in sFLt1 in the maternal serum. The notion that we did not discover preeclampsia may result from the fact that KO embryos die before the onset of this condition [62, 73].

In summary, we propose that keratins are crucial for regulating the maternal-fetal vascularization through the correct localization of TGCs and the secretion of TGC hormones. Keratin-dependent failure of trophoblast localization and secretory function elicited multiple decidual defects (see Model in Figure 6). Based on our data, we suggest that mutations in K8 or K18 predispose to pregnancy loss due to decidual hyperoxia.

Acknowledgements

We thank our colleagues M. Hatzfeld and M. Hoch for critical input. Also, we thank those colleagues who generously provided antibodies. This project was funded by the Deutsche Forschungsgemeinschaft (German Research Council), and in parts by Bonfor (Research group cytoskeleton), Thyssen Stiftung and Bonner Forum Biomedizin.

Literature

1. Fuchs E, Cleveland DW: A structural scaffolding of intermediate filaments in health and disease, Science 1998, 279:514-519

2. Irvine AD, McLean WH: Human keratin diseases: the increasing spectrum of disease and subtlety of the phenotype-genotype correlation, Br J Dermatol 1999, 140:815-828

3. Magin TM, Reichelt J, Hatzfeld M: Emerging functions: diseases and animal models reshape our view of the cytoskeleton, Exp Cell Res 2004, 301:91-102

4. Omary MB, Coulombe PA, McLean WH: Intermediate filament proteins and their associated diseases, N Engl J Med 2004, 351:2087-2100

5. Betz RC, Planko L, Eigelshoven S, Hanneken S, Pasternack SM, Bussow H, Van Den Bogaert K, Wenzel J, Braun-Falco M, Rutten A, Rogers MA, Ruzicka T, Nothen MM, Magin TM, Kruse R: Loss-of-function mutations in the keratin 5 gene lead to Dowling-Degos disease, Am J Hum Genet 2006, 78:510-519

6. Kim S, Wong P, Coulombe PA: A keratin cytoskeletal protein regulates protein synthesis and epithelial cell growth, Nature 2006, 441:362-365

7. Magin TM, Vijayaraj P, Leube RE: Structural and regulatory functions of keratins, Exp Cell Res 2007, 313:2021-2032

8. Margolis SS, Perry JA, Forester CM, Nutt LK, Guo Y, Jardim MJ, Thomenius MJ, Freel CD, Darbandi R, Ahn JH, Arroyo JD, Wang XF, Shenolikar S, Nairn AC, Dunphy WG, Hahn WC, Virshup DM, Kornbluth S: Role for the PP2A/B56delta phosphatase in regulating 14-3-3 release from Cdc25 to control mitosis, Cell 2006, 127:759-773

9. Vijayaraj P, Kroeger C, Reuter U, Hartmann D, Magin TM: Keratins regulate yolk sac hematopoiesis and vasculogenesis through reduced BMP-4 signaling, Eur J Cell Biol 2010, 89:299-306

10. Vijayaraj P, Kroger C, Reuter U, Windoffer R, Leube RE, Magin TM: Keratins regulate protein biosynthesis through localization of GLUT1 and -3 upstream of AMP kinase and Raptor, J Cell Biol 2009, 187:175-184

11. Hesse M, Franz T, Tamai Y, Taketo MM, Magin TM: Targeted deletion of keratins 18 and 19 leads to trophoblast fragility and early embryonic lethality, Embo J 2000, 19:5060-5070

12. Tamai Y, Ishikawa T, Bosl MR, Mori M, Nozaki M, Baribault H, Oshima RG, Taketo MM: Cytokeratins 8 and 19 in the mouse placental development, J Cell Biol 2000, 151:563-572

13. Baribault H, Price J, Miyai K, Oshima RG: Mid-gestational lethality in mice lacking keratin 8, Genes Dev 1993, 7:1191-1202

14. Jaquemar D, Kupriyanov S, Wankell M, Avis J, Benirschke K, Baribault H, Oshima RG: Keratin 8 protection of placental barrier function, J Cell Biol 2003, 161:749-756

15. Cross JC, Nakano H, Natale DR, Simmons DG, Watson ED: Branching morphogenesis during development of placental villi, Differentiation 2006, 74:393-401
16. Bany BM, Cross JC: Post-implantation mouse conceptuses produce paracrine signals that regulate the uterine endometrium undergoing decidualization, Dev Biol 2006, 294:445-456
17. Adelman DM, Gertsenstein M, Nagy A, Simon MC, Maltepe E: Placental cell fates are regulated in vivo by HIF-mediated hypoxia responses, Genes Dev 2000, 14:3191-3203
18. Barak Y, Nelson MC, Ong ES, Jones YZ, Ruiz-Lozano P, Chien KR, Koder A, Evans RM: PPAR gamma is required for placental, cardiac, and adipose tissue development, Mol Cell 1999, 4:585-595
19. Barak Y, Sadovsky Y, Shalom-Barak T: PPAR Signaling in Placental Development and Function, PPAR Res 2008, 2008:142082
20. Cowden Dahl KD, Fryer BH, Mack FA, Compernolle V, Maltepe E, Adelman DM, Carmeliet P, Simon MC: Hypoxia-inducible factors 1alpha and 2alpha regulate trophoblast differentiation, Mol Cell Biol 2005, 25:10479-10491
21. Gabriel HD, Jung D, Butzler C, Temme A, Traub O, Winterhager E, Willecke K: Transplacental uptake of glucose is decreased in embryonic lethal connexin26-deficient mice, J Cell Biol 1998, 140:1453-1461
22. Ishikawa T, Tamai Y, Zorn AM, Yoshida H, Seldin MF, Nishikawa S, Taketo MM: Mouse Wnt receptor gene Fzd5 is essential for yolk sac and placental angiogenesis, Development 2001, 128:25-33
23. Katschinski DM, Le L, Schindler SG, Thomas T, Voss AK, Wenger RH: Interaction of the PAS B domain with HSP90 accelerates hypoxia-inducible factor-1alpha stabilization, Cell Physiol Biochem 2004, 14:351-360
24. Kozak W, Wrotek S, Walentynowicz K: Hypoxia-induced sickness behaviour, J Physiol Pharmacol 2006, 57 Suppl 8:35-50
25. Mudgett JS, Ding J, Guh-Siesel L, Chartrain NA, Yang L, Gopal S, Shen MM: Essential role for p38alpha mitogen-activated protein kinase in placental angiogenesis, Proc Natl Acad Sci U S A 2000, 97:10454-10459
26. Schorpp-Kistner M, Wang ZQ, Angel P, Wagner EF: JunB is essential for mammalian placentation, Embo J 1999, 18:934-948
27. Steingrimsson E, Tessarollo L, Reid SW, Jenkins NA, Copeland NG: The bHLH-Zip transcription factor Tfeb is essential for placental vascularization, Development 1998, 125:4607-4616
28. Voss AK, Thomas T, Gruss P: Mice lacking HSP90beta fail to develop a placental labyrinth, Development 2000, 127:1-11

29. Xu X, Weinstein M, Li C, Naski M, Cohen RI, Ornitz DM, Leder P, Deng C: Fibroblast growth factor receptor 2 (FGFR2)-mediated reciprocal regulation loop between FGF8 and FGF10 is essential for limb induction, Development 1998, 125:753-765

30. Suri C, Jones PF, Patan S, Bartunkova S, Maisonpierre PC, Davis S, Sato TN, Yancopoulos GD: Requisite role of angiopoietin-1, a ligand for the TIE2 receptor, during embryonic angiogenesis, Cell 1996, 87:1171-1180

31. Maisonpierre PC, Suri C, Jones PF, Bartunkova S, Wiegand SJ, Radziejewski C, Compton D, McClain J, Aldrich TH, Papadopoulos N, Daly TJ, Davis S, Sato TN, Yancopoulos GD: Angiopoietin-2, a natural antagonist for Tie2 that disrupts in vivo angiogenesis, Science 1997, 277:55-60

32. Breier G, Clauss M, Risau W: Coordinate expression of vascular endothelial growth factor receptor-1 (flt-1) and its ligand suggests a paracrine regulation of murine vascular development, Dev Dyn 1995, 204:228-239

33. Duarte A, Hirashima M, Benedito R, Trindade A, Diniz P, Bekman E, Costa L, Henrique D, Rossant J: Dosage-sensitive requirement for mouse Dll4 in artery development, Genes Dev 2004, 18:2474-2478

34. Fong GH, Rossant J, Gertsenstein M, Breitman ML: Role of the Flt-1 receptor tyrosine kinase in regulating the assembly of vascular endothelium, Nature 1995, 376:66-70

35. Gale NW, Dominguez MG, Noguera I, Pan L, Hughes V, Valenzuela DM, Murphy AJ, Adams NC, Lin HC, Holash J, Thurston G, Yancopoulos GD: Haploinsufficiency of delta-like 4 ligand results in embryonic lethality due to major defects in arterial and vascular development, Proc Natl Acad Sci U S A 2004, 101:15949-15954

36. Limbourg FP, Takeshita K, Radtke F, Bronson RT, Chin MT, Liao JK: Essential role of endothelial Notch1 in angiogenesis, Circulation 2005, 111:1826-1832

37. Shalaby F, Rossant J, Yamaguchi TP, Gertsenstein M, Wu XF, Breitman ML, Schuh AC: Failure of blood-island formation and vasculogenesis in Flk-1-deficient mice, Nature 1995, 376:62-66

38. Dumont DJ, Gradwohl G, Fong GH, Puri MC, Gertsenstein M, Auerbach A, Breitman ML: Dominant-negative and targeted null mutations in the endothelial receptor tyrosine kinase, tek, reveal a critical role in vasculogenesis of the embryo, Genes Dev 1994, 8:1897-1909

39. Sato TN, Tozawa Y, Deutsch U, Wolburg-Buchholz K, Fujiwara Y, Gendron-Maguire M, Gridley T, Wolburg H, Risau W, Qin Y: Distinct roles of the receptor tyrosine kinases Tie-1 and Tie-2 in blood vessel formation, Nature 1995, 376:70-74

40. Hustin J, Schaaps JP: Echographic [corrected] and anatomic studies of the maternotrophoblastic border during the first trimester of pregnancy, Am J Obstet Gynecol 1987, 157:162-168

41. Pringle KG, Kind KL, Thompson JG, Roberts CT: Complex interactions between hypoxia inducible factors, insulin-like growth factor-II and oxygen in early murine trophoblasts, Placenta 2007, 28:1147-1157
42. Dunwoodie SL: The role of hypoxia in development of the Mammalian embryo, Dev Cell 2009, 17:755-773
43. Ramirez-Bergeron DL, Runge A, Adelman DM, Gohil M, Simon MC: HIF-dependent hematopoietic factors regulate the development of the embryonic vasculature, Dev Cell 2006, 11:81-92
44. Caniggia I, Mostachfi H, Winter J, Gassmann M, Lye SJ, Kuliszewski M, Post M: Hypoxia-inducible factor-1 mediates the biological effects of oxygen on human trophoblast differentiation through TGFbeta(3), J Clin Invest 2000, 105:577-587
45. Nagamatsu T, Fujii T, Kusumi M, Zou L, Yamashita T, Osuga Y, Momoeda M, Kozuma S, Taketani Y: Cytotrophoblasts up-regulate soluble fms-like tyrosine kinase-1 expression under reduced oxygen: an implication for the placental vascular development and the pathophysiology of preeclampsia, Endocrinology 2004, 145:4838-4845
46. Jauniaux E, Watson AL, Hempstock J, Bao YP, Skepper JN, Burton GJ: Onset of maternal arterial blood flow and placental oxidative stress. A possible factor in human early pregnancy failure, Am J Pathol 2000, 157:2111-2122
47. Jauniaux E, Hempstock J, Greenwold N, Burton GJ: Trophoblastic oxidative stress in relation to temporal and regional differences in maternal placental blood flow in normal and abnormal early pregnancies, Am J Pathol 2003, 162:115-125
48. Reichelt J, Magin TM: Hyperproliferation, induction of c-Myc and 14-3-3sigma, but no cell fragility in keratin-10-null mice, J Cell Sci 2002, 115:2639-2650
49. Mc MJ: Histological and histochemical uses of periodic acid, Stain Technol 1948, 23:99-108
50. Simmons DG, Natale DR, Begay V, Hughes M, Leutz A, Cross JC: Early patterning of the chorion leads to the trilaminar trophoblast cell structure in the placental labyrinth, Development 2008, 135:2083-2091
51. Anson-Cartwright L, Dawson K, Holmyard D, Fisher SJ, Lazzarini RA, Cross JC: The glial cells missing-1 protein is essential for branching morphogenesis in the chorioallantoic placenta, Nat Genet 2000, 25:311-314
52. Colosi P, Thordarson G, Hellmiss R, Singh K, Forsyth IA, Gluckman P, Wood WI: Cloning and expression of ovine placental lactogen, Mol Endocrinol 1989, 3:1462-1469
53. Lescisin KR, Varmuza S, Rossant J: Isolation and characterization of a novel trophoblast-specific cDNA in the mouse, Genes Dev 1988, 2:1639-1646
54. Lin J, Poole J, Linzer DI: Three new members of the mouse prolactin/growth hormone family are homologous to proteins expressed in the rat, Endocrinology 1997, 138:5541-5549

55. Basyuk E, Cross JC, Corbin J, Nakayama H, Hunter P, Nait-Oumesmar B, Lazzarini RA: Murine Gcm1 gene is expressed in a subset of placental trophoblast cells, Dev Dyn 1999, 214:303-311
56. Ain R, Tash JS, Soares MJ: Prolactin-like protein-A is a functional modulator of natural killer cells at the maternal-fetal interface, Mol Cell Endocrinol 2003, 204:65-74
57. Muller H, Liu B, Croy BA, Head JR, Hunt JS, Dai G, Soares MJ: Uterine natural killer cells are targets for a trophoblast cell-specific cytokine, prolactin-like protein A, Endocrinology 1999, 140:2711-2720
58. Baumhueter S, Singer MS, Henzel W, Hemmerich S, Renz M, Rosen SD, Lasky LA: Binding of L-selectin to the vascular sialomucin CD34, Science 1993, 262:436-438
59. Baldwin HS, Shen HM, Yan HC, DeLisser HM, Chung A, Mickanin C, Trask T, Kirschbaum NE, Newman PJ, Albelda SM, et al.: Platelet endothelial cell adhesion molecule-1 (PECAM-1/CD31): alternatively spliced, functionally distinct isoforms expressed during mammalian cardiovascular development, Development 1994, 120:2539-2553
60. Ginouves A, Ilc K, Macias N, Pouyssegur J, Berra E: PHDs overactivation during chronic hypoxia "desensitizes" HIFalpha and protects cells from necrosis, Proc Natl Acad Sci U S A 2008, 105:4745-4750
61. Levy AP, Levy NS, Wegner S, Goldberg MA: Transcriptional regulation of the rat vascular endothelial growth factor gene by hypoxia, J Biol Chem 1995, 270:13333-13340
62. Kanasaki K, Palmsten K, Sugimoto H, Ahmad S, Hamano Y, Xie L, Parry S, Augustin HG, Gattone VH, Folkman J, Strauss JF, Kalluri R: Deficiency in catechol-O-methyltransferase and 2-methoxyoestradiol is associated with pre-eclampsia, Nature 2008, 453:1117-1121
63. Simmons DG, Fortier AL, Cross JC: Diverse subtypes and developmental origins of trophoblast giant cells in the mouse placenta, Dev Biol 2007, 304:567-578
64. Adamson SL, Lu Y, Whiteley KJ, Holmyard D, Hemberger M, Pfarrer C, Cross JC: Interactions between trophoblast cells and the maternal and fetal circulation in the mouse placenta, Dev Biol 2002, 250:358-373
65. Bordeleau F, Galarneau L, Gilbert S, Loranger A, Marceau N: Keratin 8/18 modulation of protein kinase C-mediated integrin-dependent adhesion and migration of liver epithelial cells, Mol Biol Cell 2010, 21:1698-1713
66. Jackson D, Volpert OV, Bouck N, Linzer DI: Stimulation and inhibition of angiogenesis by placental proliferin and proliferin-related protein, Science 1994, 266:1581-1584
67. Ma GT, Linzer DI: GATA-2 restricts prolactin-like protein A expression to secondary trophoblast giant cells in the mouse, Biol Reprod 2000, 63:570-574
68. Toivola DM, Krishnan S, Binder HJ, Singh SK, Omary MB: Keratins modulate colonocyte electrolyte transport via protein mistargeting, J Cell Biol 2004, 164:911-921

69. Brusselmans K, Bono F, Collen D, Herbert JM, Carmeliet P, Dewerchin M: A novel role for vascular endothelial growth factor as an autocrine survival factor for embryonic stem cells during hypoxia, J Biol Chem 2005, 280:3493-3499

70. Gerber HP, Malik AK, Solar GP, Sherman D, Liang XH, Meng G, Hong K, Marsters JC, Ferrara N: VEGF regulates haematopoietic stem cell survival by an internal autocrine loop mechanism, Nature 2002, 417:954-958

71. Rhodes KE, Gekas C, Wang Y, Lux CT, Francis CS, Chan DN, Conway S, Orkin SH, Yoder MC, Mikkola HK: The emergence of hematopoietic stem cells is initiated in the placental vasculature in the absence of circulation, Cell Stem Cell 2008, 2:252-263

72. Pankov R, Neznanov N, Umezawa A, Oshima RG: AP-1, ETS, and transcriptional silencers regulate retinoic acid-dependent induction of keratin 18 in embryonic cells, Mol Cell Biol 1994, 14:7744-7757

73. Maynard SE, Min JY, Merchan J, Lim KH, Li J, Mondal S, Libermann TA, Morgan JP, Sellke FW, Stillman IE, Epstein FH, Sukhatme VP, Karumanchi SA: Excess placental soluble fms-like tyrosine kinase 1 (sFlt1) may contribute to endothelial dysfunction, hypertension, and proteinuria in preeclampsia, J Clin Invest 2003, 111:649-658

Table 1 **Mouse mutants of epithelial trophoblast cells with similar phenotypes.**

Gene	**Gene Product**	**Expression pattern in placental tissue and yolk sac**	**Mutant phenotype**	**Reference**
Arnt (Hif1β)	bHLH/ PAS transcription factor	Placental trophoblasts, trophoblast giant cells	Growth retardation at E9.5, defective placental and yolk sac vascularization	[17, 24]
Cx 26	Connexin	Yolk sac epithelium, syncytiotrophoblast	Small labyrinth	[21]
FGFR2	Fibroblast growth factor receptor	Trophoblast cells	Small labyrinth layer, reduced vascularization, block of trophoblast cell proliferation	[29]
Fzd5	Wnt receptor	Labyrinth trophoblast, yolk sac	Reduced vascularization of yolk sac and placenta	[22]
Hif1α Hif2α	hypoxia-inducible factors	Placenta, yolk sac	Reduced placental vascularization, differentiation regulation of TGC and spongiotrophoblast	[20]
HSP90	Heat shock protein	Labyrinth trophoblast, yolk sac	Small labyrinth layer, reduced vascularization	[23, 28]
JunB	Transcription factor of the AP-1 family	Trophoblast derivatives	Small labyrinth layer, defective placental and yolk sac vascularization	[26]
p38	Mitogen-activated protein kinase	Diploid trophoblasts, Labyrinth trophoblast	Reduced vascularization of yolk sac and placenta	[25]
PPARγ	Nuclear hormone receptor, ligand activated transcription factor	Diploid trophoblast lineage	Reduced vascularization of placenta, impaired differentiation of syncytiotrophoblast	[18, 19]
Tfeb	Transcription factor of the bHLH zipper family	Labyrinth trophoblast	Reduced placental vascularization with embryonic blood vessels	[27]

Table 2 **Mouse mutants of endothelial cells with similar phenotypes.**

Gene	Gene Product	Expression pattern in placental tissue and yolk sac	Mutant phenotype	Reference
Ang1	Tie2 ligand	Arterial endothelial cells of yolk sac and placenta	Defects in angiogenic vascular remodelling in yolk sac and placenta	[30]
Ang2	Tie2, Ang1 antagonist	Arterial endothelial cells of yolk sac and placenta	Overexpression leads to defects in angiogenic vascular remodelling in yolk sac and placenta	[31]
Dll4	Delta like ligand	Arterial endothelial cells of yolk sac and placenta	Arterial atrophy	[33, 35]
Flk1	Vascular endothelia growth factor receptor 2	Yolk sac mesoderm, labyrinth	Lack of endothelia cells and hematopoietic system	[32, 37]
Flt1	Vascular endothelia growth factor receptor 1	Yolk sac mesoderm, spongiotrophoblast	Disorganized embryonic vasculature	[32, 34]
Notch1	Single-pass transmembrane receptor	Arterial endothelial cells of yolk sac and placenta	Defects in angiogenic vascular remodelling in yolk sac and placenta	[36]
Tie 2/ Tek	Receptor tyrosine kinase	Arterial endothelial cells of yolk sac and placenta	Reduced number of endothelia cell, disorganized embryonic vasculature	[38, 39]

Figures

Figure 1

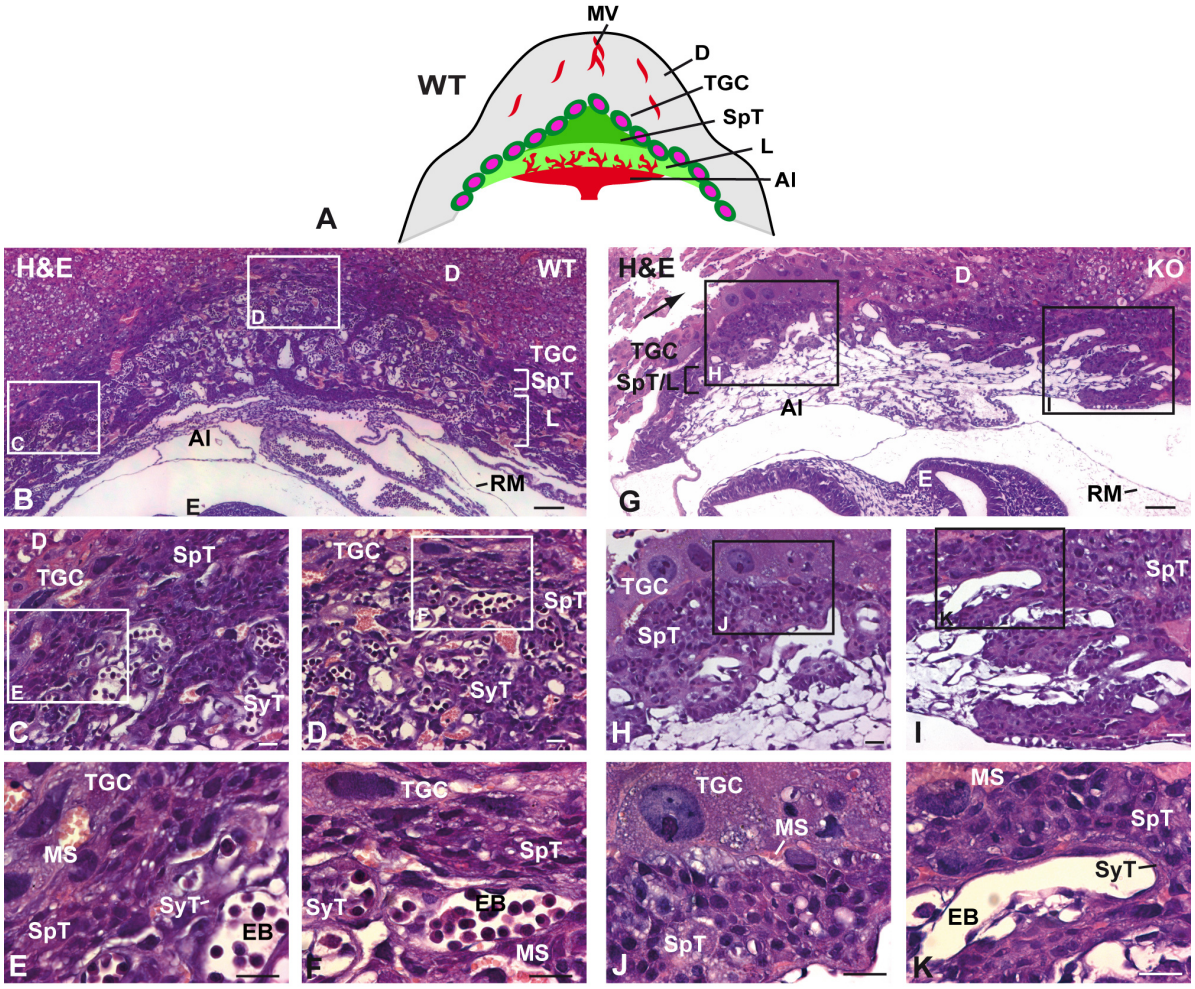

Figure 1 **The placenta of keratin depleted embryos shows severe size reduction of labyrinth and spongiotrophoblast and vascular defects.** (A) Diagram of WT placental architecture. (B-K) Semithin sections through WT (B-F) and mutant (G-K) embryos were stained with H&E. Note the size difference of the labyrinth in keratin deleted placenta (G) compared to the WT control (B). Increased vasculature is seen in the decidua surrounding the mutant embryo (arrow in G). In higher magnifications of the inlays, marked in the overview of WT (C, D, inlays of B) and KO placenta (H, I, inlays of G), WT embryonic blood vessels are packed with embryonic erythrocytes compared to sparsely filled KO blood vessels. Further magnification of WT (E and F, inlays of C and D, respectively) and KO placentas (J and K, inlays of H and I, respectively) demonstrate that WT embryonic blood vessels are in close proximity to maternal blood sinuses in contrast to the keratin deficient labyrinth, which contains very few maternal blood sinuses. MV, maternal blood vessels; D, decidua; TGC, trophoblast giant cells; SpT, spongiotrophoblast; L labyrinth; ML, maternal blood lacuna; Al, allantois; RM, Reichert's membrane; SyT, syncytiotrophoblast; EB, embryonic blood; MS, maternal blood sinus. Bars: (B) 33 µm; (G) 50 µm; (C-F, H-K) 10 µm.

Figure 2

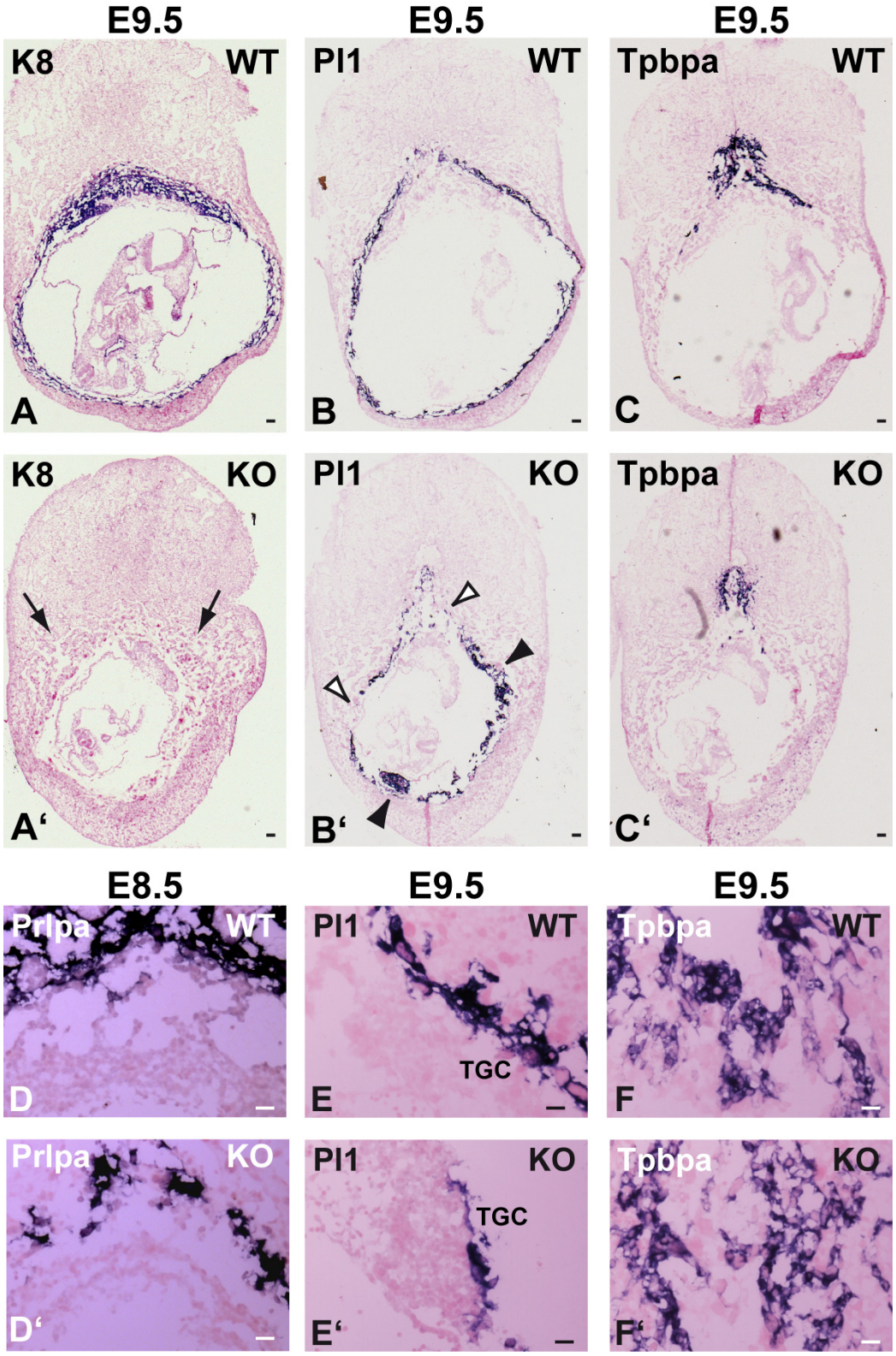
E9.5
K8
WT
A
E9.5
Pl1
WT
B
E9.5
Tpbpa
WT
C
K8
KO
A'
Pl1
KO
B'
Tpbpa
KO
C'
E8.5
Prlpa
WT
D
E9.5
Pl1
WT
TGC
E
E9.5
Tpbpa
WT
F
Prlpa
KO
D'
Pl1
KO
TGC
E'
Tpbpa
KO
F'

Figure 2 **Spatial mislocalization of TGCs, but no differentiation defects in keratin deficient embryos.** In situ hybridizations for the labyrinth trophoblast markers K8, Pl1, Tbpba, Plrpa (A, A'). Keratin 8 staining differentiates between WT (A) and KO (A') embryos. Note the increased vasculature in the KO decidua (arrow in A'). Pl1, a marker for TGCs demonstrates no differentiation defects of TGCs in keratin deficient embryos (B') compared to control TGC (B), however Pl1 staining reveals a discontinuous layer of TGCs in KO embryos, with areas of accumulation (black arrowheads) and areas with a thinned-out TGC lining (white arrowheads). In situ hybridization with the spongiotrophoblast marker Tpbpa did not show any obvious difference in KO (C') compared to WT (C) placentas. (D-F') Higher magnifications of above mentioned markers. (D and D') Staining for Prlpa, a hormone secreted by the TGCs, is notably reduced in the KO TGC (D') compared to WT TGC (D) already at E8.5, which might lead to the increase in decidual vasculature in the KO embryos by E9.5. Pl1 staining in KO placenta demarcates an area with reduced TGCs (E'), compared to a continuous staining in a WT TGC layer (E). At a higher magnification of the Tpbpa marker, there is also no difference between WT (F) and mutant (F') placentas. Bars: (A-C') 100 µm; (D-F') 10 µm.

Figure 3

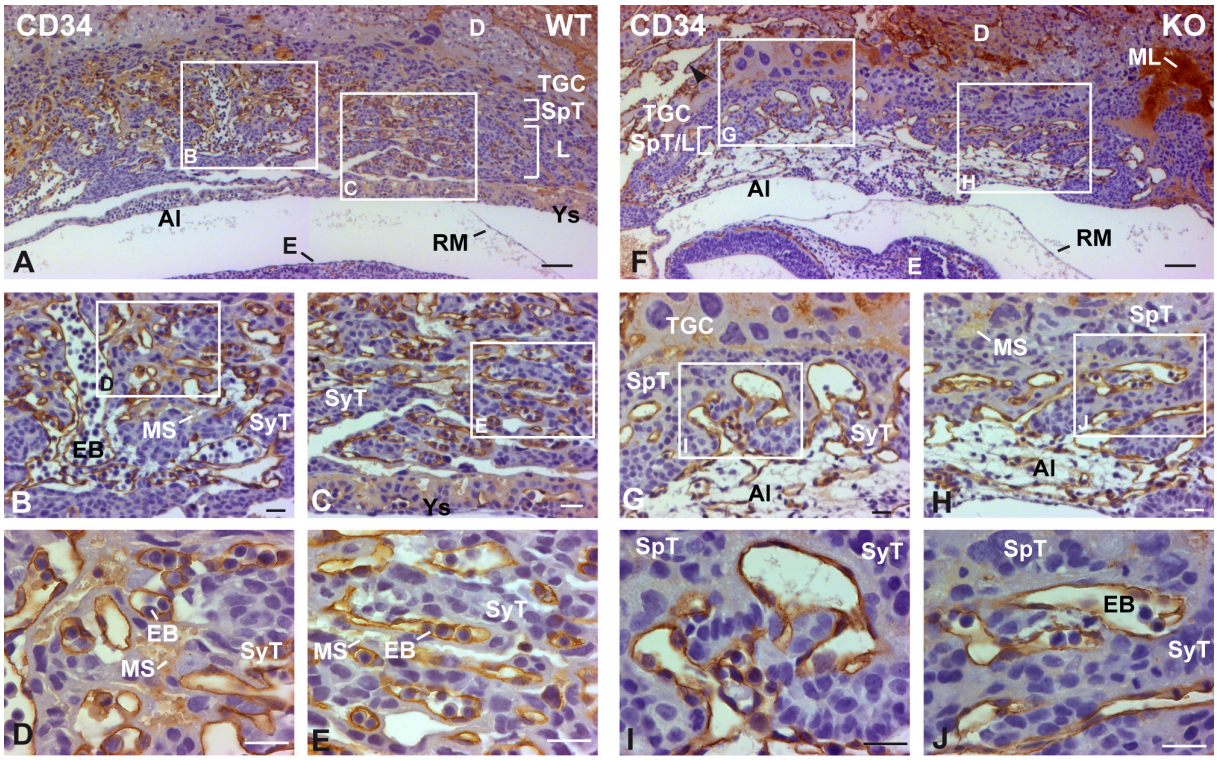

Figure 3 **Keratin deficient embryos show a dysfunctional vasculature in the placental labyrinth area.** Immunohistochemical staining with anti-CD34 antibodies in WT (A-E) and KO (F-J) placentas. The WT labyrinth shows extensive staining with CD34 antibodies (A), displaying an extensive vasculature network. In contrast, embryonic vessels fail to invade the labyrinth properly. Also note the accumulation of TGCs (G) adjacent to the extensive maternal vasculature (black arrow head) and the presence of maternal blood lacunae in the KO placenta (F). In the higher magnifications (B-E, G-J), embryonic WT controls displayed small vessels filled with nucleated embryonic erythrocytes, in close vicinity to maternal blood sinuses (B, C, inlays of A, D and E inlays of B and C, respectively). In contrast, KO vessels seemed dilated with a thickened syncytiotrophoblast layer, containing few nucleated embryonic erythrocytes (G, H, inlays of F, I and J inlays of G and H, respectively). D, decidua; TGC, trophoblast giant cells; SpT, spongiotrophoblast; L labyrinth; ML, maternal blood lacuna; Al, allantois; RM, Reichert's membrane; Ys, yolk sac; E, embryo; SyT, syncytiotrophoblast; EB, embryonic blood; MS, maternal blood sinus. Bars: (A, F) 50 µm; (B-E, G-J) 10 µm.

Figure 4

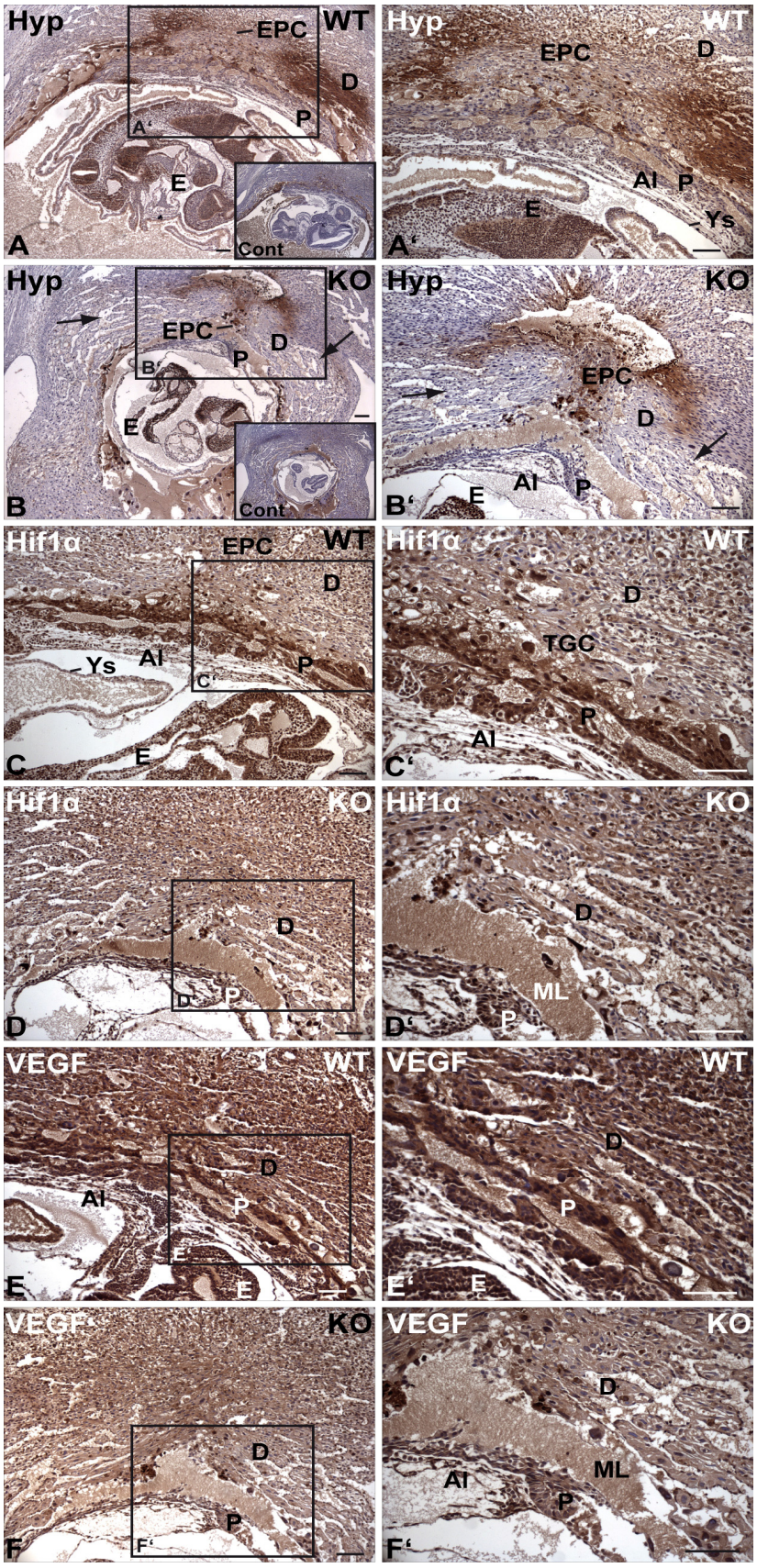
Hyp
WT
EPC
D
P
A'
E
Cont
A
Hyp
WT
EPC
D
Al
P
E
Ys
A'
Hyp
KO
EPC
D
P
B'
E
Cont
B
Hyp
KO
EPC
D
Al
P
E
B'
Hif1α
WT
EPC
D
Ys
Al
P
C'
E
C
Hif1α
WT
D
TGC
P
Al
C'
Huf1α
KO
D
P
D'
D
Hif1α
KO
D
ML
P
D'
VEGF
WT
D
Al
P
E'
E
VEGF
WT
D
P
E'
E
VEGF
KO
D
P
F'
F
VEGF
KO
D
ML
Al
P
F'

Figure 4 **Hyperoxia in decidual tissue surrounding keratin KO embryos leads to reduced induction of the downstream signals Hif1α and VEGF.** Localisation of hypoxic regions in implantation sites of E9.5 WT (A) and KO (B) embryos using Hypoxyprobe-1-specific antibody. Strong hypoxic staining is present in WT decidual tissue enclosing the EPC, more explicit at higher magnification (A', inlay of A) in contrast to mutant decidua, where the hypoxic area around the EPC is reduced due to an increased vasculature of the maternal decidua, marked by black arrows (B', inlay of B). Controls in (A) and (B) are negative controls without antibody staining. Hif1α expression induced by hypoxia manifested predominantly in the placenta of WT (C', inlay of C) and to some extent in KO placentas (D', inlay of D), however not much in the decidua. (E-F') VEGF, as a soluble factor is expressed in decidual and placental tissues of WT (E and E' inlay of E) and KtyII$^{-/}$ embryos, alike (F and F', inlay of F). MV, maternal vessels; D, decidua; TGC, trophoblast giant cells; SpT, spongiotrophoblast; L labyrinth; ML, maternal blood lacuna; Al, allantois; Hyp, hypoxia. Bars: (A-F') 100 µm.

Figure 5

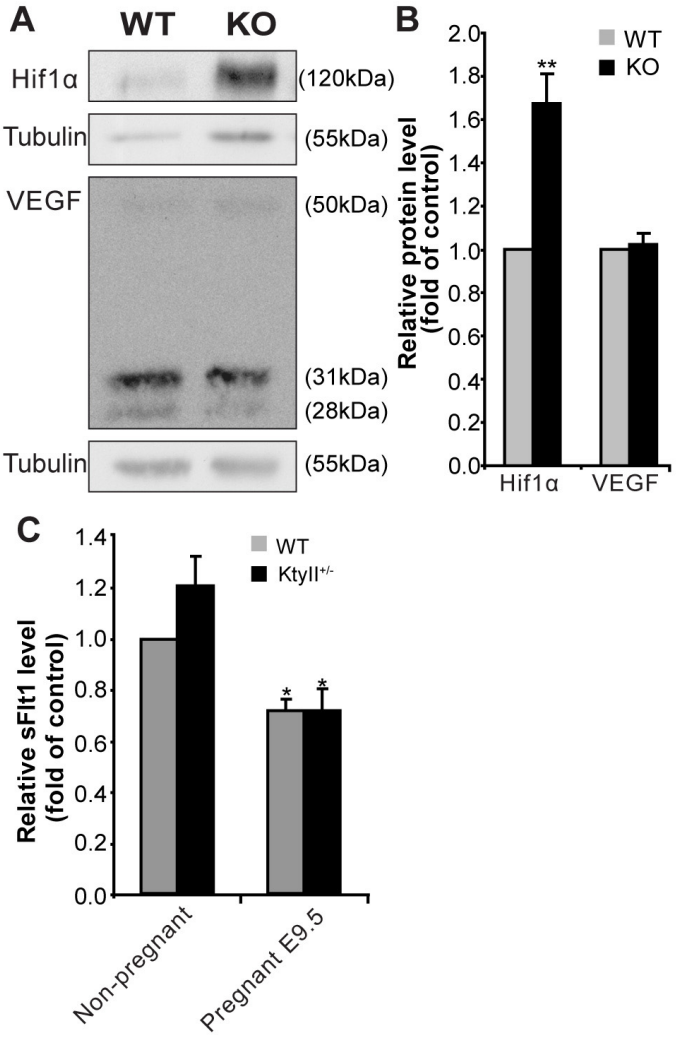

Figure 5 **Increased hypoxia inducible factor in the embryo proper of keratin depleted embryos.** (A and B) Lysates of E9.5 embryo proper and yolk sac were analyzed by Western blotting for changes in Hif1α and VEGF in both genotypes. Total protein levels of Hif1α and VEGF were quantified by densitometry and normalized to tubulin (*n* = 3; B), demonstrating a drastic increase of Hif1α expression in keratin deficient embryos. VEGF levels seemed unaltered. Results are shown as means and SEM, asterisk *, $P < 0.05$ compared to WT controls (two-tailed *t* test). (C) sFLT1 levels in maternal blood serum of untreated vs. pregnant WT and KtyII$^{+/-}$ mice determined by ELISA, did not increase in pregnant KtyII$^{+/-}$ mice, ruling out preeclampsia as a possible cause for the prenatal death of KO embryos. Non-pregnant wild-type, n=8; non-pregnant KtypeII$^{+/-}$, n=13; day E9.5 pregnant wild-type mice, n=9; day E9.5 pregnant KtyII$^{+/-}$, n=8. Results are shown as means and SEM, asterisk *, $P < 0.05$ compared to non pregnant WT controls (two-tailed *t* test).

Figure 6

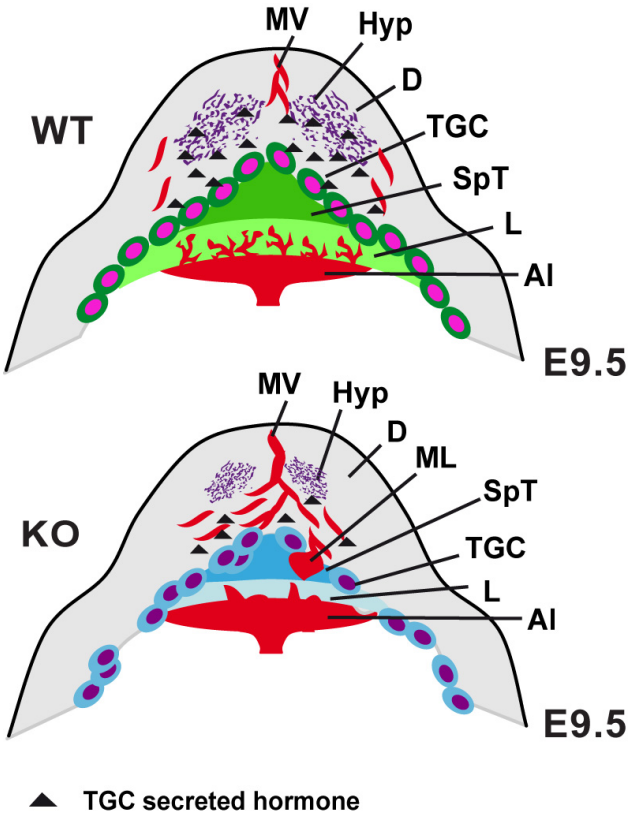

Figure 6 **Model for decidual hyperoxia caused by a keratin deficiency of the TGCs.** TGCs (i) mislocalize and (ii) fail to secrete the right levels of hormones needed for proper decidualisation which in turn results in underdeveloped vascularization of the placental labyrinth (keratin positive cells in green and keratin deficient cells in blue). MV, maternal blood vessels; D, decidua; TGC, trophoblast giant cells; SpT, spongiotrophoblast; L labyrinth; ML, maternal blood lacuna; Al, allantois; Hyp, hypoxia.

Supplementary

Supplementary Figure 1

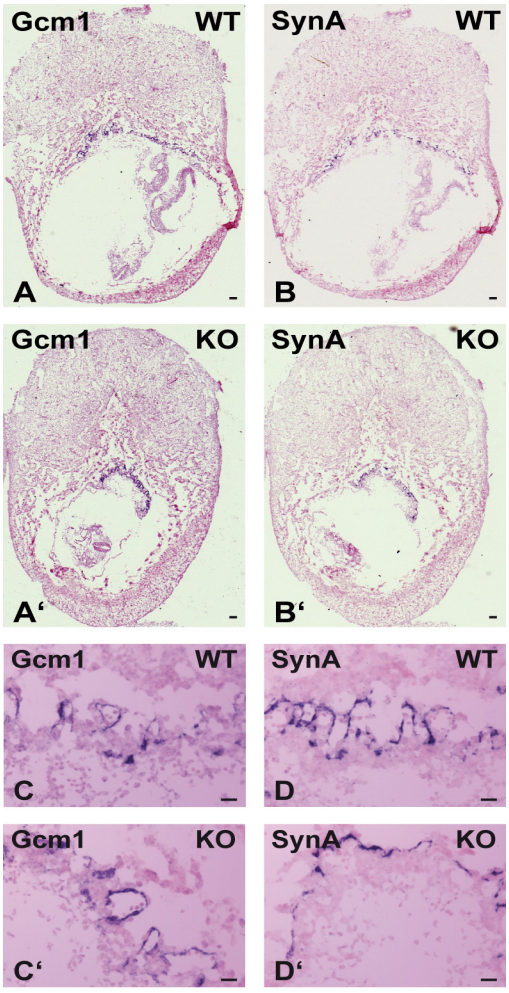

Supplementary Figure 1 **No differentiation defects in keratin deficient embryos.** In situ hybridizations for the labyrinth trophoblast markers Gcm1 and SyncytinA, Gcm1, marks in the chorion the invagination points of the allantois into the labyrinth. The staining shows that Gcm1 expression is unaffected in keratin deficient embryos (A') compared to control embryos (A) In situ hybridization with the syncytiotrophoblast marker SyncytinA (SynA) did not show any obvious difference in KO (B') compared to WT (B) placentas. (C-D') Higher magnifications of above mentioned markers. Gcm1 staining in KO placentas (C'), compared to a WT labyrinth (C) does not demonstrate any differences. At a higher magnification of the SynA marker, there is no obvious differentiation defect in the KO (D') compared to the WT (D) placenta, however SynA staining displays a different localization pattern in the syncytiotrophoblast cells enveloping the dilated embryonic blood vessels in the KO labyrinth compared to the controls (D). Bars: (A-B') 100 µm; (C-D') 10 µm.

Supplementary Figure 2

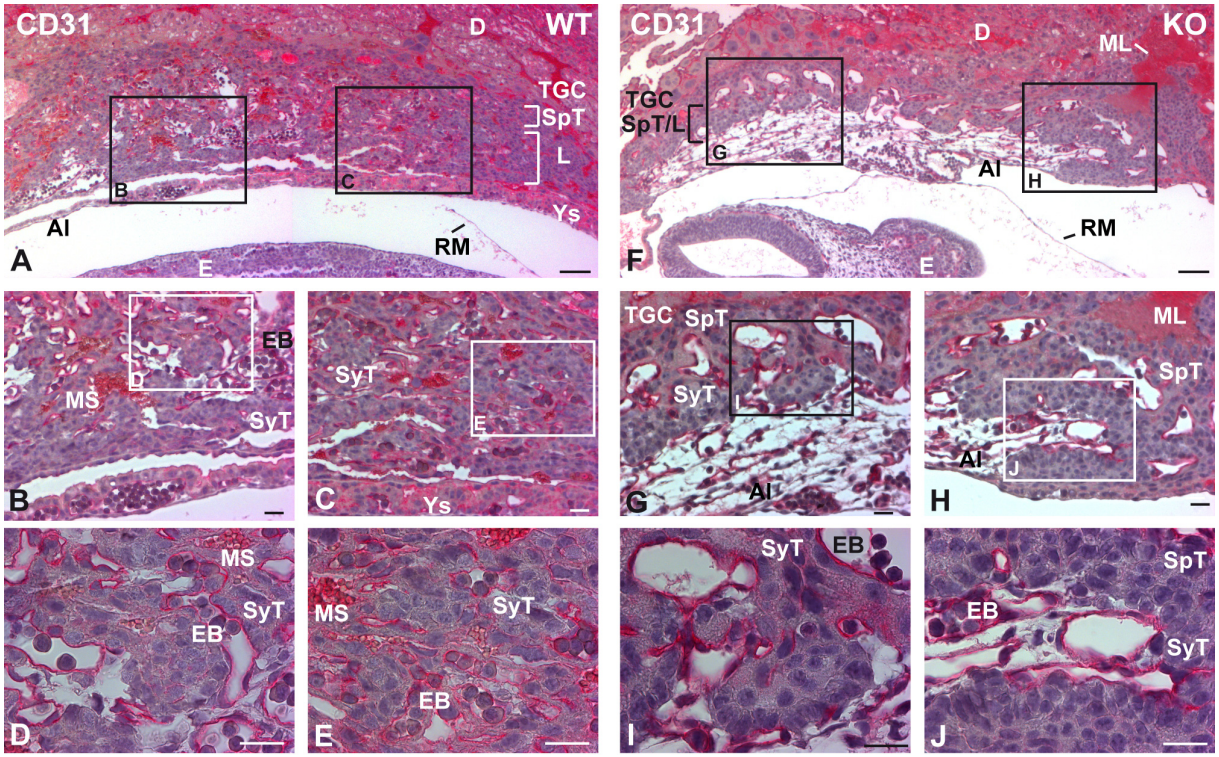

Supplementary Figure 2 **Keratin deficient embryos show a dysfunctional vasculature in the placental labyrinth area.** In Immunohistochemical staining with anti-CD31 antibodies in WT (A-E) and KO (F-J) placentas, the WT labyrinth shows extensive staining with CD31 antibodies (A), displaying an extensive vasculature network. In contrast embryonic vessels fail to invade the labyrinth properly. Also note the accumulation of TGC and the presence of maternal blood lacunae in the KO placenta (F). In the higher magnifications (B-E, G-J), embryonic WT controls displayed small vessels filled with nucleated embryonic erythrocytes, in close vicinity to maternal blood sinuses (B, C, inlays of A, D and E inlays of B and C, respectively). In contrast, KO vessels seemed dilated with a thickened syncytiotrophoblast layer, containing view nucleated embryonic erythrocytes (G, H, inlays of F, I and J inlays of G and H, respectively). D, decidua; TGC, trophoblast giant cells; SpT, spongiotrophoblast; L labyrinth; ML, maternal blood lacuna; Al, allantois; RM, Reichert's membrane; Ys, yolk sac; E, embryo; SyT, syncytiotrophoblast; EB, embryonic blood; MS, maternal blood sinus. Bars: (A, F) 50 µm; (B-E, G-J) 10 µm.

Supplementary Figure 3

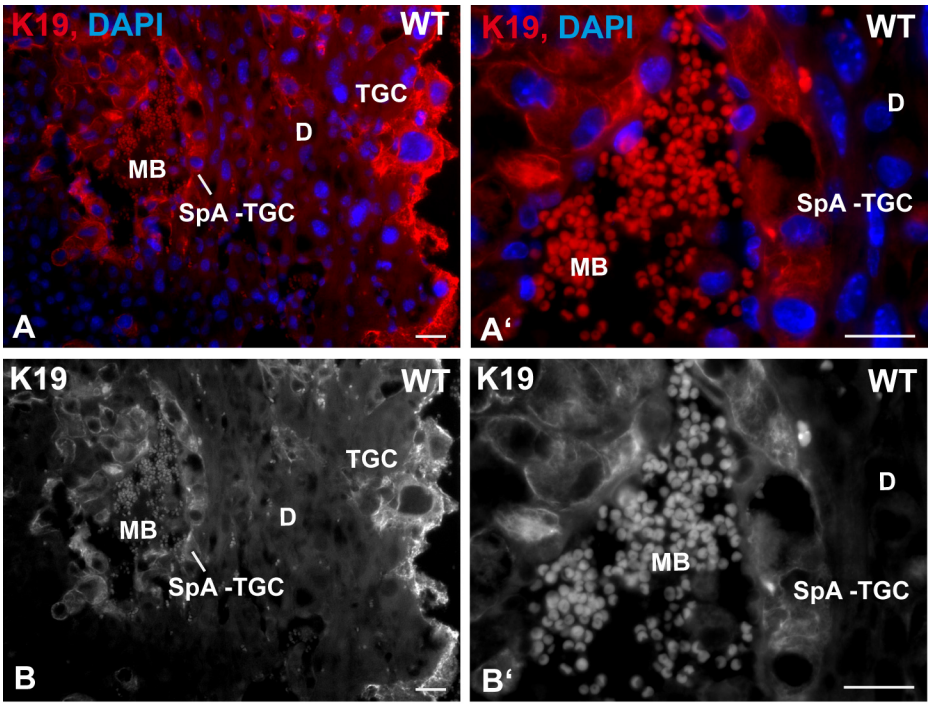

Supplementary Figure 3 **TGCs lining maternal spiral arteries in the WT.** Immunofluorescent analysis of WT decidual tissue staining with K19 depicts TGCs lining the maternal spiral arteries in E9.5 embryos D, decidua; TGC, trophoblast giant cells; SpA-TGC, spiral artery-associated trophoblast giant cells Bars: (A-B') 10 µm.

Supplementary Table 1

Antibodies	Species	Dilution
K8/18	poly gp	IF 1:200
Tubulin (B 5-1-2)	momo	WB 1:5,000
CD34 (MEC 14.7)	momo	1:50
CD31 (SZ31)	mo r	1:20
4.3.11.3	momo	1:25
Hif1α	poly rb	WB 1:500, IF1:100
VEGF (VG-1)	momo	WB 1:500, IF 1:50
Cy2 or Cy3	goat	IF 1:800
HRP	goat	1: 20,000

Supplementary Table 1 **List of antibodies, including species and dilutions.**

4.4 CK minus: An epithelial cell culture model completely devoid of keratins

Keratinocyte cell culture models have been widely employed to study cell differentiation, adhesion and migration properties as well as cytoskeleton-dependent dynamics and signaling processes of the actin and microtubule filament systems. Loss of function experiments, the disassembly of these two filament systems, can easily be achieved with the help of various drugs for instance, latrunculin A and cytochalsin B, as well as nocodazole and colcemide, for actin and mictrotubule networks, respectively.

However, so far no easily accessible drug has been discovered for the IF system. To analyse loss of function of the keratin cytoskeleton, the keratin type II null keratinocyte cell line CK minus was generated for systematic biochemical and functional studies of epithelial cells. For this purpose KtyII$^{+/-}$ mice were mated with KtyII$^{fl/fl}$ mice and keratinocytes were isolated and cultivated from their offspring. Subsequent transfection with Cre recombinant protein resulted in the stable keratin free cell line CK minus; detailed procedures are discussed in chapter 3.2.2-3.2.4.

Deletion of all keratins in CK minus cells was confirmed by immunofluorescence staining, as well as immunoblotting of cell protein lysates for K5 and K14, the most prominent basal keratins (Figure 4.4.1 B and C). It could also be visualized in SDS- analysis which demonstrate the absence of prominent keratin bands in the range of 50 and 60 kDa (Figure 4.4.5 A). In wildtype (WT) keratinocytes (CK plus cells), pairing of the K5 with K14 was visualized by demonstrating complete colocalization in the merged image (Figure 4.4.1 A''). Consistent with the proteolytic sensitivity of type I keratins in the absence of their type II keratin binding partners, no additional keratinocyte specific type I keratins (K16, K17) were detected on protein level by Western blot (Figure 4.4.1 D). The type III IF protein vimentin, which is frequently up-regulated during epithelial-mesenchymal-transition (EMT) after loss of keratin expression (Thiery, 2002; Yang and Weinberg, 2008), was not detected on protein level via immunoblotting (Figure 4.4.1 D), excluding compensation of keratin depletion by other IFs.

Figure 4.4.1 **Generation of keratin free keratinocytes: CK minus.** By eliminating the type II cluster via Cre expression all keratin filaments were deleted in the cells. Immunofluorescence (A-B) and Western blot analysis (C-D) of the newly generated cell line, CK minus (B) compared to CK plus cells (A) demonstrate that not only K5 and K14, are deleted (A-C), but other type I keratins cannot be detected by Western blot, either. Furthermore, there is no compensatory upregulation of vimentin in CK minus cells (D). Bars (A-B'') 10 µm.

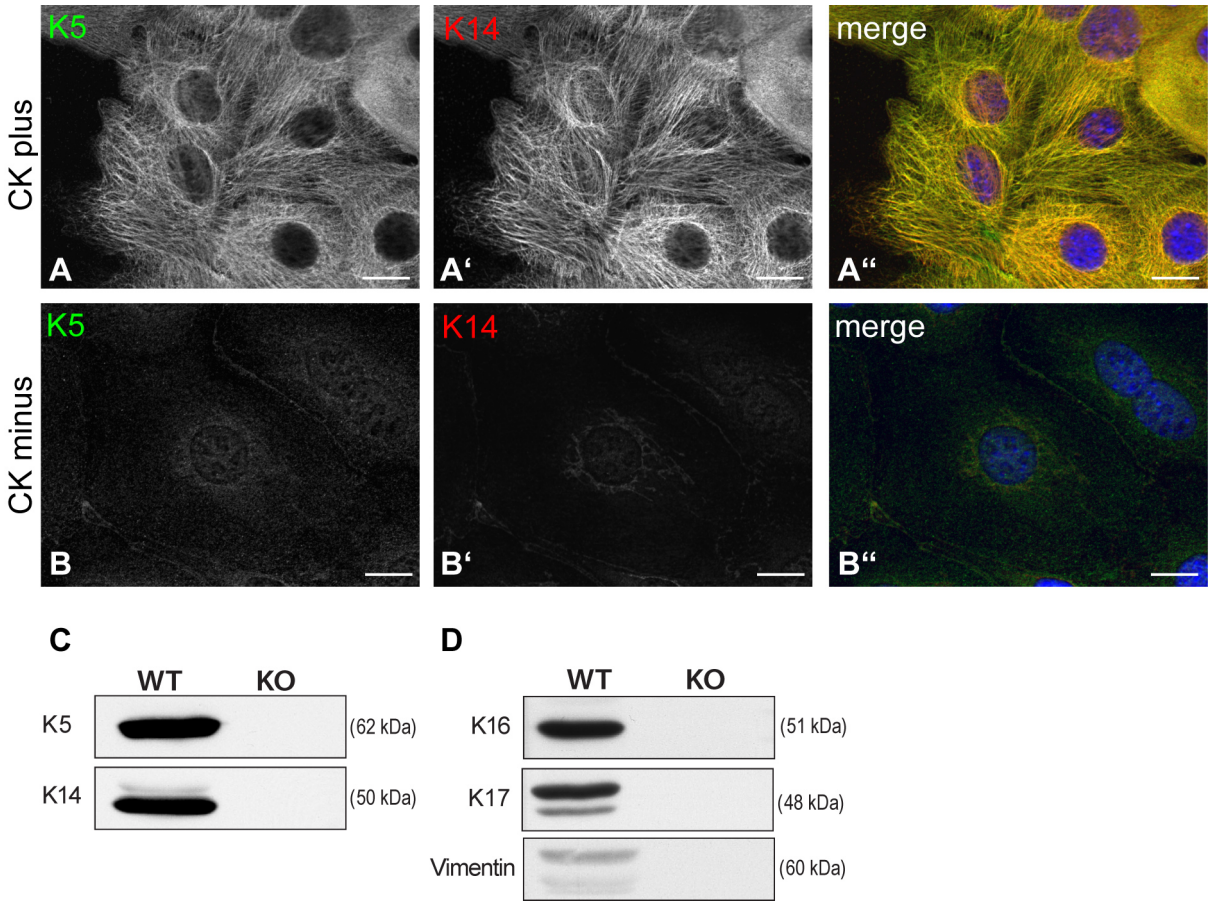

Deletions of K5 or K14, both expressed in basal keratinocytes, show severe blistering in the skin and the oral mucosa and die shortly after birth (Coulombe et al., 2009; Magin et al., 2004). Therefore, a major function of these basal keratins was proposed to be the provision of mechanical stability. To test this hypothesis, we analyzed the gross appearance and morphology of the CK minus cells in comparison to WT cells, under normal culture conditions in low calcium (Figure 4.4.2) and after a calcium switch (Figure 4.4.3). Within several hours of switching the calcium concentration from 0.05 mM to 1.2 mM, keratinocytes formed tight cell-cell contacts resembling physiological conditions in the epidermis (Vaezi et al., 2002; Vasioukhin et al., 2000). At high magnification in low calcium, the morphology of CK minus cells looked very similar to CK plus cells (Figure 4.4.2 B’ and D’). However the gross appearance of the cell sheet was different, it did not display the neat cobble stone pattern of the WT keratinocytes, but was rather irregular. In this fashion, low cell densities of keratin depleted cells, displayed long cytoplasmic protrusions (Figure 4.4.2 C, C’) compared to the prominent lamellipodia in WT cells (Figure 4.4.2 A, A’) and additionally large cytoplasmic exclusions could be noted in the CK minus cell culture (Figure 4.4.2 C).

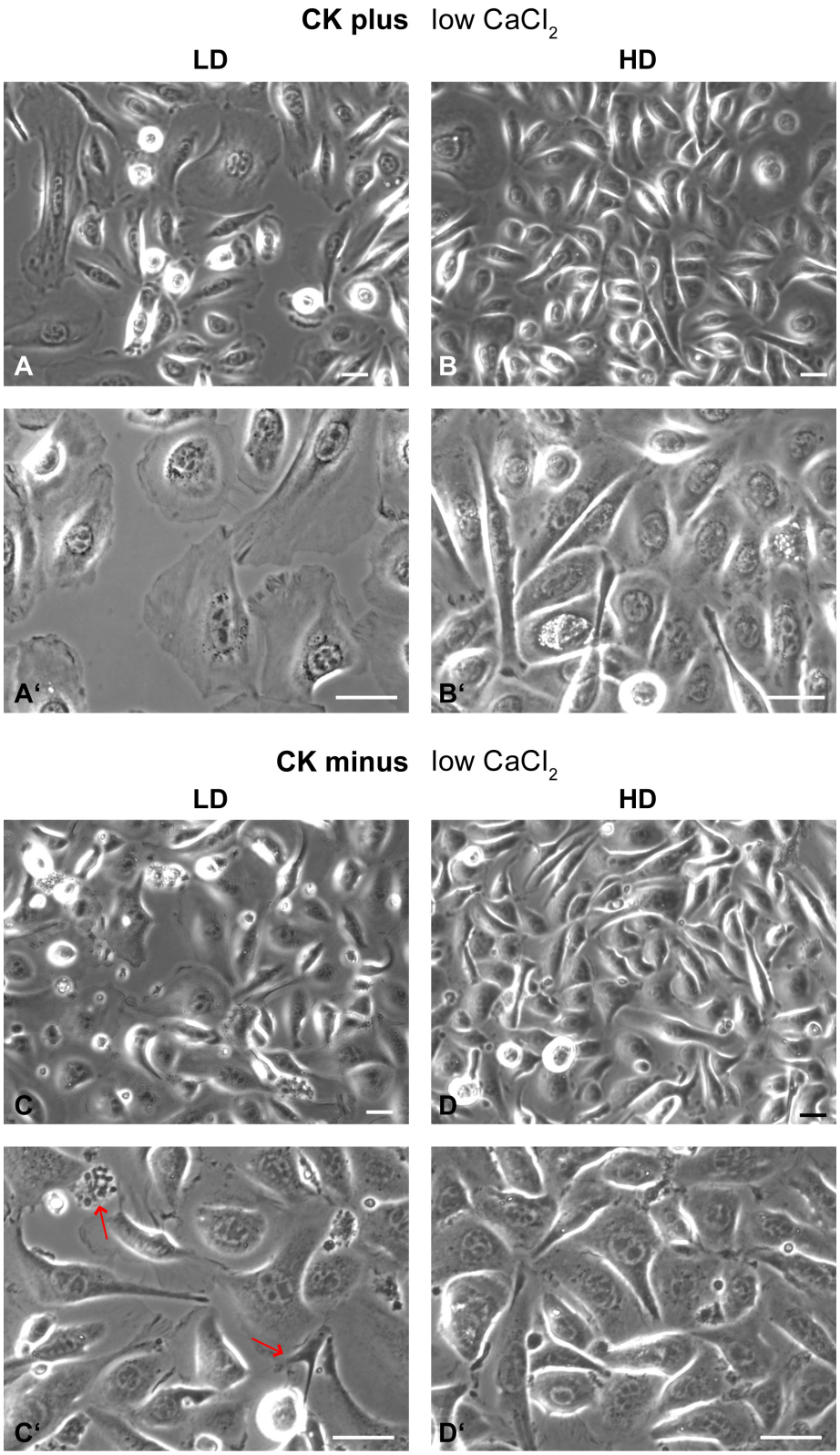

Figure 4.4.2 **Comparison of CK minus vs. CK plus morphology.** Brightfield photomicrographs of the WT keratinocyte cell line CK plus (A-B) and of the keratin KO cell line CK minus (C-D). Cells were cultivated in low calcium medium, where they demonstrated a neat cobble stone pattern under high density (HD) (B, higher magnification B'), under low confluency lammelipodia were detected (A and A'). CK minus cells displayed an irregular cell pattern with more protrusions (D and D') and under low density (LD) cytoplasmic exclusions were noted (red arrows) (C and C'). Bars: (A-D') 10 µm.

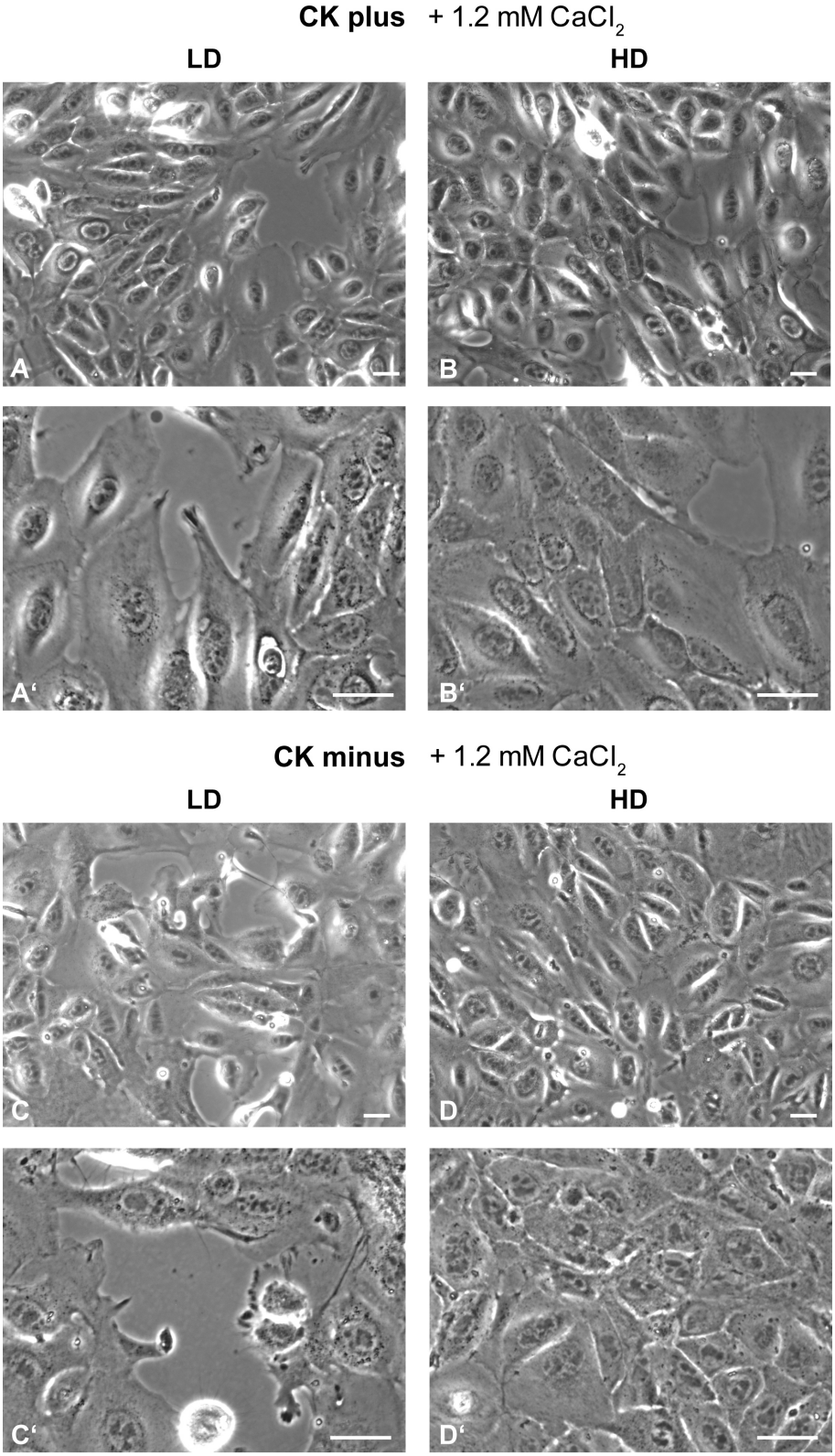

Figure 4.4.3 **Comparison of CK minus vs. CK plus morphology under calcium differentiation.** To analyze cells under physiological conditions, cells were treated for 50 h with 1.2 mM $CaCl_2$. Brightfield photomicrographs of the WT keratinocyte cell line CK plus (A-B) and of the keratin KO cell line CK minus (C-D) demonstrated the formation of cell-cell contacts and the intercellular spaces disappeared in CK plus (under low A, A' and high density B, B') and CK minus cells (low C, C' and high density D, D'). In CK plus cells a dense ring of vesicular like structures was noted around the nucleus (B') which were disperse in CK minus cells (D'). Bars: (A-D') 10 µm.

With the calcium switch these morphological differences between WT (Figure 4.4.3 A, B) and KO (Figure 4.4.3 C, D) cell lines were less explicit. However, what became more apparent under calcium influence was the absence of perinuclear vesicle like structures in the KO cell line, as seen in WT cells (Figure 4.4.3 B'). In CK minus cells, these were irregularly dispersed in the cytoplasm (Figure 4.4.3 D').

The formation of protrusions and lamellipodia, as well as cell-cell junctions is dependent on the organization and function of the other cytoskeletal networks of the cell, the microfilament and the microtubule system (Godsel et al., 2005; Vasioukhin et al., 2000). In particular, local actin polymerization and reorganization were shown to be essential in the dynamic process of intercellular adhesion. The initial step in establishing cell-cell contacts is the appearance of calcium activated filopodial projections. These actin protrusions integrate into newly formed radial bundles of actin filaments in the cell and form the so called adhesion zipper. The zipper is an intermediate on the way to epidermal sheet formation and was visualized with fluorescent dye labeled Phalloidin in WT keratinocytes (Figure 4.4.4 A'). The radial actin fibers anchor to the dynamic flux of actin rings, and the actin network throughout the keratinocyte sheet becomes continuous, with rather gross rearrangements of actin cables, which integrate single cell movements into contractions of the whole cell sheet. In mature cell contacts the filopodia and radial actin bundles disappear and the cortical actin belt forms (Figure 4.4.7 A) (Vaezi et al., 2002). The formation of the cortical actin belt proceeded normally in keratin depleted cells, however in contrast to CK plus cells, filopodia like structures also protruded from KO cells embedded in confluent cell sheets (Figure 4.4.4 B', Figure 4.4.7 B). Furthermore, it was noted that in CK minus cells actin polymerization and bundling was not restricted to the cell periphery, but could take place across the cytoplasm and even perinuclear (Figure 4.4.7 B). Therefore, keratin deletion did not result in major alterations in form and function of the actin cytoskeleton, but resulted in rather subtle differences. The same was true for the microtubule network, keratin absence induced a less organized tubulin network with increased tubule crossing (Figure 4.4.4 D', Figure 4.4.7 D) compared to parallel networks in WT cells (Figure 4.4.4 C', Figure 4.4.7 C), but was otherwise unaffected. This was also reflected in unaltered amounts of total actin and tubulin protein in CK minus compared to CK plus cells (Figure 4.4.4 E).

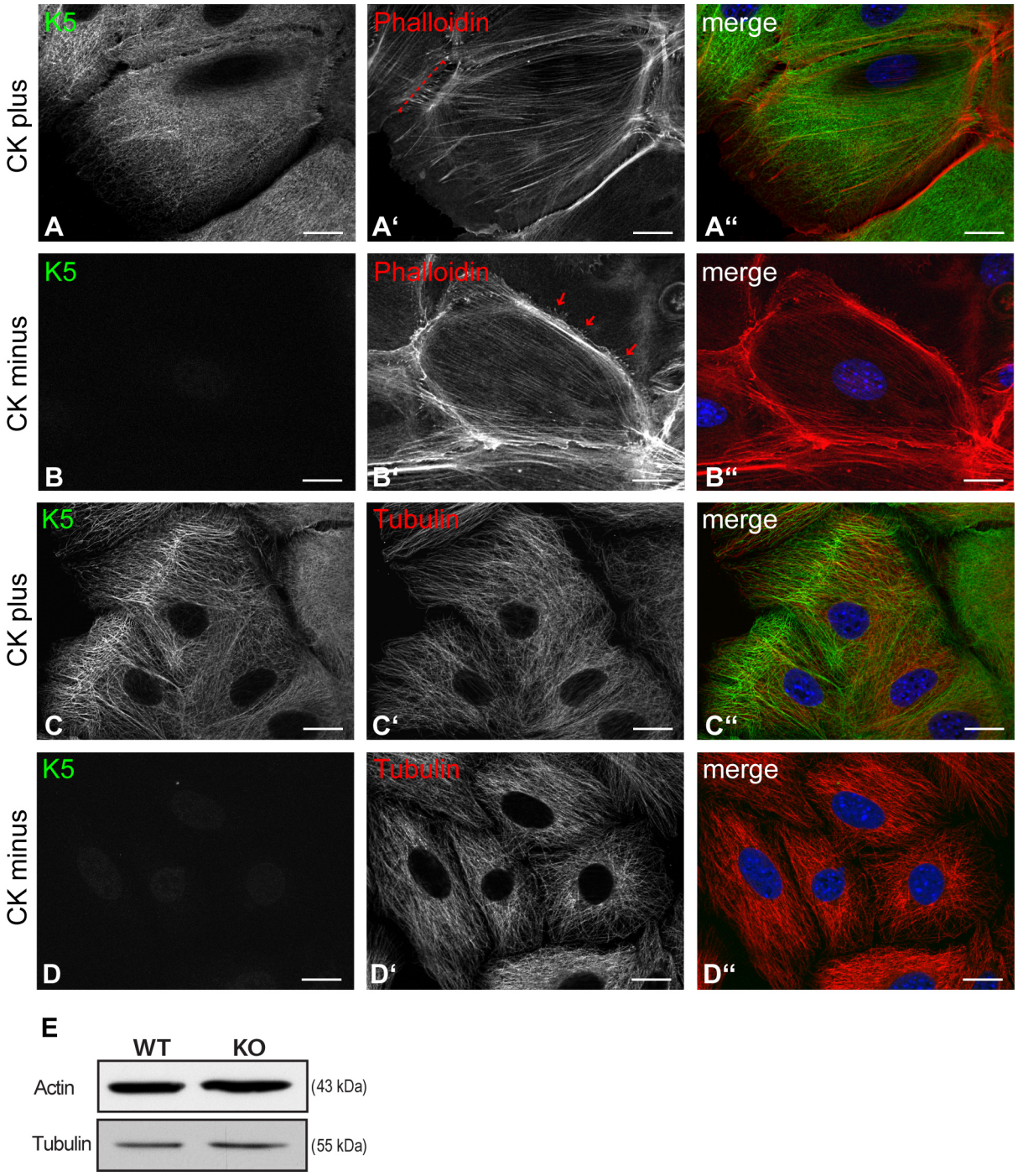

Figure 4.4.4 **Influence of keratin intermediate filaments on the remaining cytoskeletal proteins.** The deletion of keratins resulted in subtle changes in the overall cytoskeleton of actin filaments (A-B) and microtubules (C-D), reflected also in their amounts in CK plus vs. CK minus cells (E). Note the slight misorganization compared to WT cells (B’ and D’); as well as an increased number of filopodia like structures in KO cells embedded in the cell context (red arrows, B’), compared to adhesion zippers (dotted red line, A’) in WT cells which vanished after establishing cell junctions. Bars: (A-D’’) 10 µm.

It is well established that intermediate filaments are linked to desmosomes, intercellular, highly specialized anchoring junctions at the PM which facilitate the formation of a supracellular scaffolding that distributes mechanical forces throughout a tissue (Green and Simpson, 2007). Interruptions of desmosome keratin linkage through drug treatment (Denk et al., 1985), mutation/deletion of the linker protein DP (Godsel et al., 2005; Jonkman et al., 2005; Vasioukhin et al., 2001) or deletions of single keratins (Baribault and Oshima, 1991; Magin et al., 1998) demonstrate that desmosomes per se are able to maintain their characteristic positions along the plasma membrane after disconnection of the keratin filament cytoskeleton. This indicates that maintenance of desmosomal integrity and position is independent of desmosome anchorage to keratin filaments. On the other hand, DP turnover at cell–cell adhesion sites is altered in keratin network-deficient hepatocytes (Loranger et al., 2006; Toivola et al., 2001) and in epithelial cell lines with downregulated keratins (Long et al., 2006, Magin, 2007 #53). This was verified in the keratin depleted mouse model (Vijayaraj et al., 2009). The next step was, to analyze DP localization in the new cell culture model (Figure 4.4.5) and indeed, DP localization at inter cell junctions was disturbed, indicated by smaller and partially mislocalized desmosomes (Figure 4.4.5 C', D' and Figure 4.4.7 B' and D') and resulted in a 30% reduction of total DP in CK minus cells (Figure 4.4.6 B and C). This is consistent with the involvement of keratins in DP assembly (Godsel et al., 2005). The authors showed further, that DP localization at desmosomes is also dependent on microfilaments. Vice versa it was reported that DP deletion in keratinocytes resulted in an inappropriate reorganization of the microfilament network and entailing absence of mature adherens junctions after calcium switch (Vasioukhin et al., 2001). Comparing the previous results with CK minus keratinocytes after calcium switch, the actin filament system resembled to a slight degree the data published by Vasioukhin and Fuchs (Figure 4.4.7 B''), however with the major difference, that adherens junctions, stained with E-cadherin appeared unaltered in CK minus cells (data not shown). Furthermore, Lechler and Fuchs recently reported that during epidermal differentiation and in keratinocyte cell culture after calcium switch, DP regulates microtubule organization (Lechler and Fuchs, 2007). In CK minus cells, however, there was no apparent influence of either keratin deletion or DP misorganization on the MT network compared to WT keratinocytes (Figure 4.4.7 C and D).

Figure 4.4.5 **CK minus cells show reduced and mislocalized desmoplakin.** Cell-cell boundaries display mislocalized desmosomes, visualized by immunofluorescence staining of DP in CK minus (C' and D') vs. CK plus cells (A' and B'). B and D are magnified sections of the cell borders of A and C, respectively. Bars: (A-D'') 10 µm

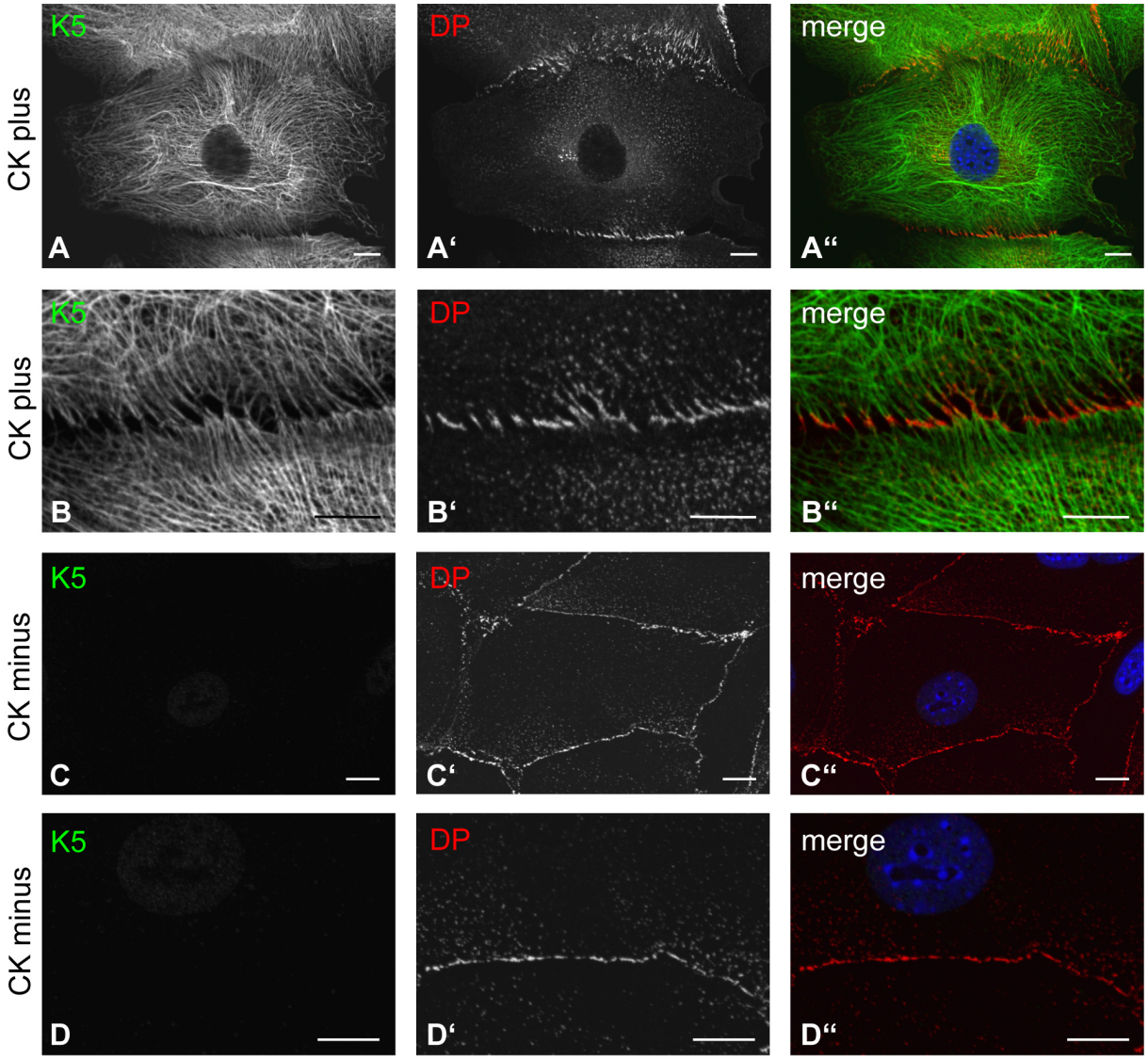

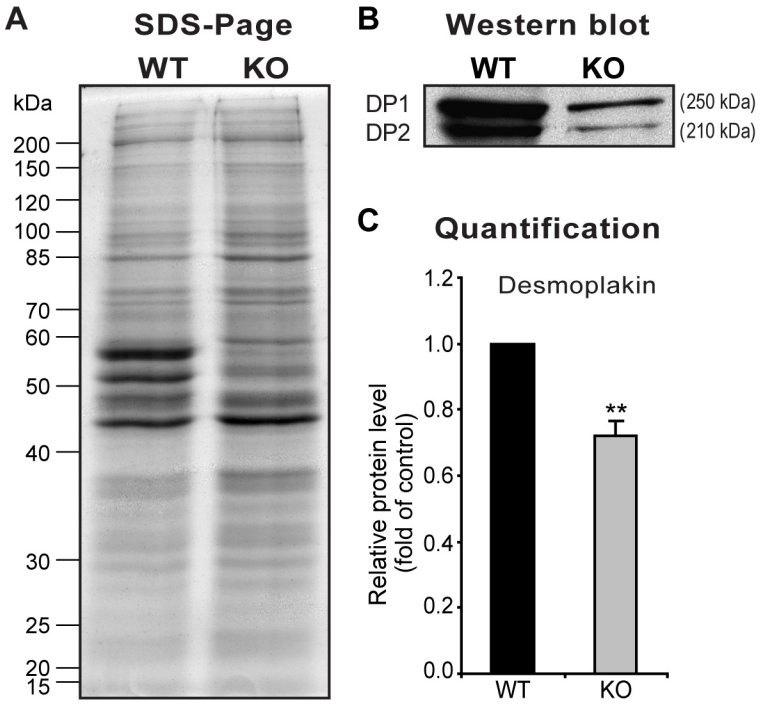

Figure 4.4.6 **Quantification of total desmoplakin in CK plus vs. CK minus cells.** Equal loading was ensured via SDS-PAGE. Note prominent keratin bands between 50 and 60 kDa are absent in CK minus cells (A). Total DP protein levels in cell lysates of CK plus and CK minus cells were determined via Western blot (B) and quantified (C). DP was reduced by 30% in CK minus cells, compared to WT keratinocytes. Results of n=3 are shown as means and SEM, asterisk *, P < 0.005 compared to WT controls (two-tailed *t* test).

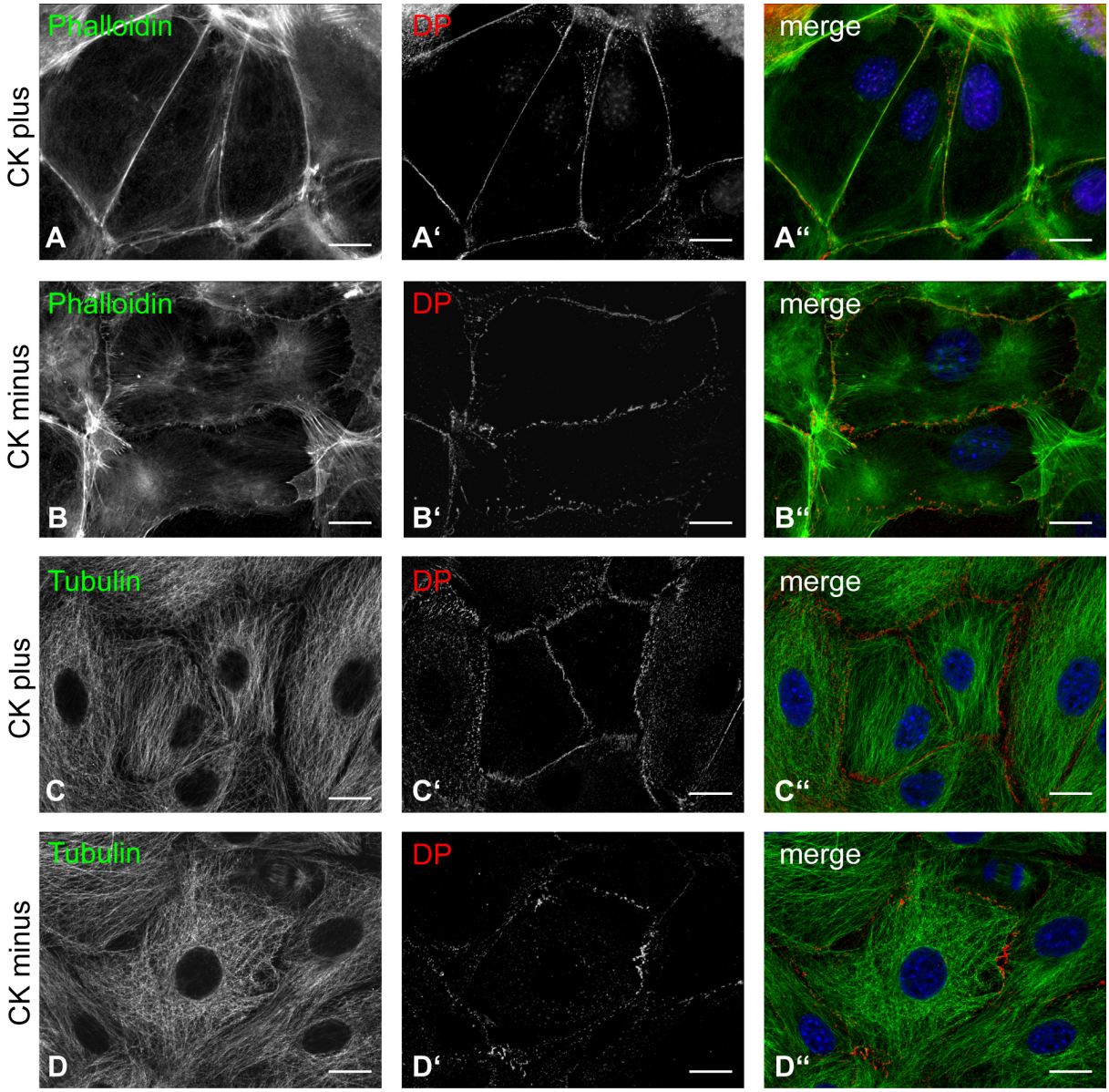

Figure 4.4.7 **Desmoplakin distribution in relation to actin and microtubule filament networks.** Cell-cell boundaries display mislocalized desmosomes, visualized by immunofluorescence staining of DP in CK minus (B’ and D‘) vs. CK plus cells (A’ and C’). Note again the unorganized actin filament (B) and microtubules (D) in the KO cells. Bars: (A-D’’) 10 µm

Hemidesmosomes are adhesive protein complexes that mediate stable attachment of basal epithelial cells to the underlying basement membrane and are linked intracellular to the keratin filament system (de Pereda et al., 2009). To analyze if keratin deletion similar to desmosomes also effects the assembly of hemidesmosomal components, immunostaining against the TM protein α6-integrin and against the linker protein plectin, which links the IFs to the TM complex were performed. In WT keratinocytes plectin co-distributed with the keratin filaments and located to plasma membrane attachment sites of IFs, the hemidesmosomes (Figure 4.4.8 A', A'' and C). Correspondingly, α6-integrin staining visualized the patchy appearance of hemidesmosomes in the perinuclear region in CK plus cells (Figure 4.4.8 B' and C'); and double immunofluorescences of plectin and α6-integrin demonstrated the expected colocalization at hemidesmosomes (Figure 4.4.8 C''). In CK minus cells on the other hand it became apparent that plectin as well as α6-integrin were mislocalized when the IF network is absent (Figure 4.4.8 D). The α6-integrin staining in keratin depleted cells, still strongly resembled WT cells, besides its reduced intensity (Figure 4.4.8 D'). Plectin, however, did not localize properly to hemidesmosomes as exposed by missing colocalization with α6-integrin (Figure 4.4.8 D'') and rather demonstrated increased PM association (Figure 4.4.8 D), due to the missing co-distribution with keratin filaments as seen in WT cells (Figure 4.4.8 C).

Altogether the above phenotypes would suggest that cell motility and adhesion are affected in the CK minus cells, similar to formerly reported EBS phenotypes (Andra et al., 1997; Andra et al., 1998; Jonkman et al., 2005; Magin et al., 2004). Total amounts of vinculin a marker for adherens junctions and focal adhesion were elevated by 40% in CK minus cells (data not shown) which could partially compensate for above phenotypes. On the other hand, immunofluorescence staining of adherens junctions and focal adhesions seemed unaffected as analysed by immunofluorescence staining for E-cadherin and vinculin, respectively (data not shown).

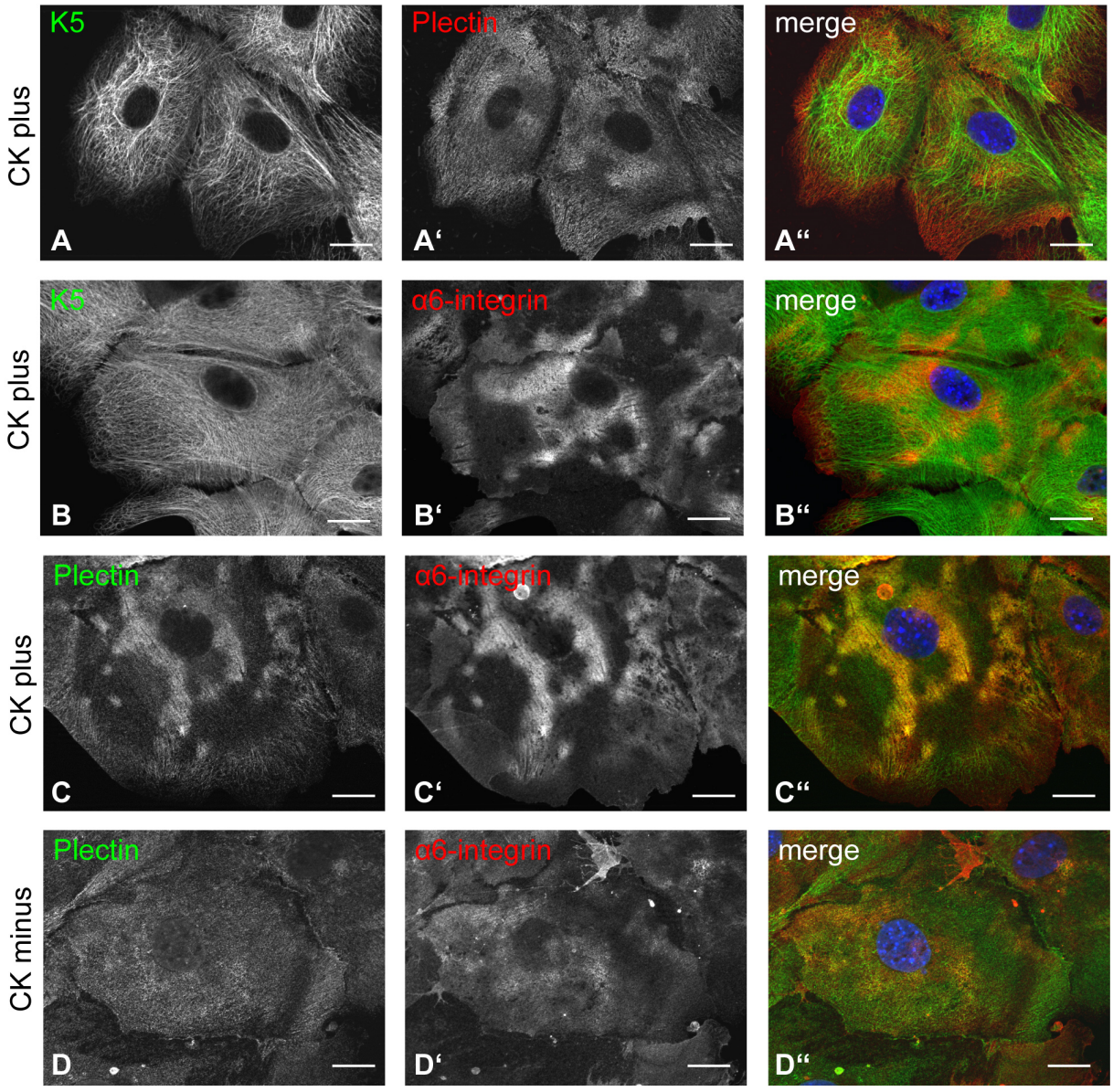

Figure 4.4.8 **CK minus cells show altered composition of hemidesmosomes.** Hemidesmosomes were visualized by plectin and α6-integrin immunofluorescence staining. In CK plus cells, plectin localizes in patches to the basal plasma membrane, the hemidesmosomes (A'), where it colocalizes with α6-integrin (C'') and is also associated with keratin filaments (A''). α6-integrin does not display keratin association in WT keratinocytes (B'') and consequentially seems unaltered in CK minus cells (D'). Plectin, however, is mislocalized in keratin deleted cells (D) and in turn shows reduced colocalization with α6-integrin and therefore reduced presence in hemidesmosomes (D''). Bars: (A-D'') 10 µm

Keratin filaments define the inner cellular space by mediating positioning and function of essential cellular organelles (Toivola et al., 2005). They influence mitochondria localization and size (Tao et al., 2009), alter Golgi distribution and reassembly (Kumemura et al., 2004) and influence vesicle transport. So far no association of intermediate filaments and endoplasmic reticulum (ER) was demonstrated. Furthermore keratin depletion was proposed to alter TM protein localization like ion transporters, CFTR and also SNARE proteins like Syntaxin 3 (Ameen et al., 2001; Oriolo et al., 2007; Toivola et al., 2004). The ER and the Golgi complex are integral to protein translation, modification and sorting of these TM and secretory proteins. To analyze form and positioning of these organelles, Immunofluorescence staining was performed. The ER was marked with protein disulfide isomerase (PDI) a protein present throughout the ER (Vembar and Brodsky, 2008). The Golgi complex was demarcated with the 28-kDa Golgi SNARE (GS28) protein, which was first thought to be a *cis*-Golgi marker, but was later found to be involved in regulating the retrograde transport from early/recycling endosomes to the *trans*-Golgi network (Subramaniam et al., 1996; Tai et al., 2004). Comparing WT keratinocytes with CK minus cells revealed an astounding phenotype (Figure 4.4.9). The architecture of both organelles was drastically altered in keratin free cells. The ER expressed a rather lamellar form with many cisternae compared to a tubular network in CK plus cells (Figure 4.4.9 B' and A', respectively). Along these lines, the Golgi complex formed, compared to the vesicular perinuclear organelles of WT cells, an extensive tubular network in KO cells (Figure 4.4.9 C' and D', respectively). These data provide completely new insights into the function of keratins in organizing cell architecture. However, these are only the first morphological results and the CK minus cells provide for the first time a model to analyze the mechanistic background behind those phenotypes.

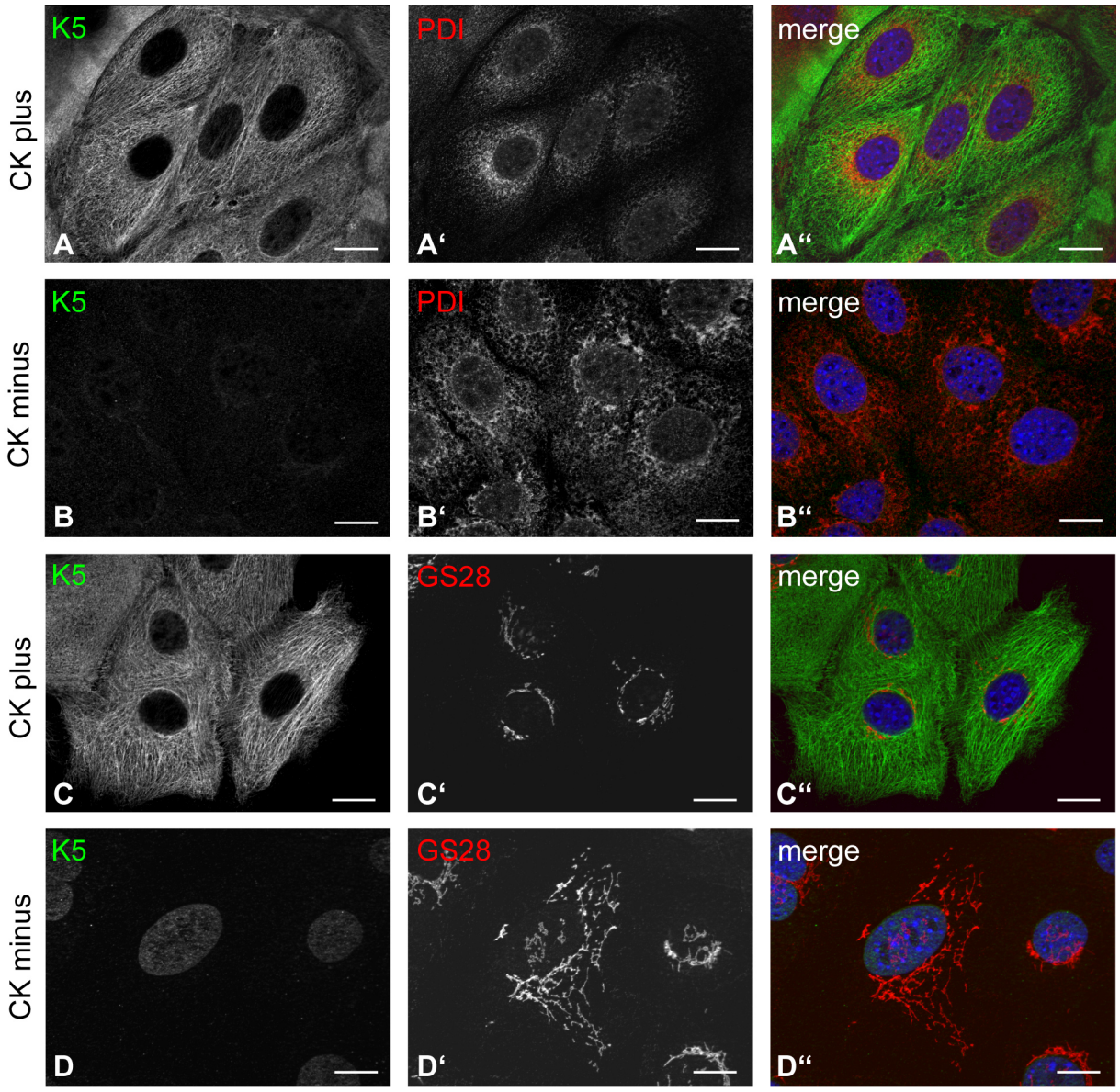

Figure 4.4.9 **Keratin depletion results in modified organelle architecture and size.** The ER and the Golgi complex were stained with organelle specific markers, PDI for ER and GS28 for Golgi complexes in immunofluorescenses. In CK plus cells a fine ER network became apparent (A’), in contrast to keratin deleted CK minus cells, where a very dense network with big ER cisternae was detected (B’). This was comparable to the alterations in the Golgi complex, where in keratin KO cells big tubular like structures were visible (D’) in contrast to the small vesicle like cis-Golgi complexes of WT keratinocytes (C’). Bars: (A-D’’) 10 µm

5. Discussion

Keratin proteins form the IF cytoskeleton in all epithelial cells and are part of a highly conserved gene family consisting of more than 50 keratin genes in mammals. Previous studies of keratin function were performed in mutational studies and several KO studies. To analyze keratin function systematically and to target the problem of compensatory upregulation/stabilization common in multigene family analysis, a large scale genome deletion was performed knocking out the complete keratin type II cluster (Vijayaraj et al., 2009). Hence, by deleting the type II cluster (containing the type I keratin 18), one abolishes formation of keratin filaments as well as avoids aggregates of the early type I keratins thereby circumventing possible dominant negative effects (Vijayaraj, 2008).

It can be argued, that by deleting such a large genomic region, many additional ORF might be eliminated, for example various miRNAs. So far no miRNAs could be determined in the targeted region by bioinformatical analysis with the Sanger database, release miRBase 15, April 2010 (http://www.mirbase.org/index.shtml). In turn, if miRNAs would be depleted, evidence suggests, that the effect would not be dramatic. First, they are frequently present as families of redundant genes, second, the degree of target downregulation imposed by miRNAs often tends to be modest in quantitative terms: measured at the protein level, even an overexpressed miRNA typically downregulates most of its endogenous targets by less than 50% (Inui et al., 2010). However, the existence of functional miRNA genes can only be excluded upon re-expression of keratins. If this fully reconstitutes the observed phenotypes, it would prove dependence on keratins.

Despite intensive research on keratin functions, using transgenic mice and cell culture models the exact mechanism of keratin functions could not be determined so far. The essential questions on how keratins interact with target proteins are still not well understood. Do keratins need to be assembled into a filamentous network or do soluble subunits regulate keratin functions and association with interacting proteins? The fact is, the keratin cytoskeleton is a dynamic network constantly disassembling and restructuring (Magin et al., 2004; Magin et al., 2007; Windoffer et al., 2004). Essential for the regulation of these dynamics, by modulating their solubility, conformation and organization are phosphorylation and dephosphorylation as well as glycosylation, the predominant mechanisms of cellular signaling processes (Ku et al., 2010; Omary et al., 2006). Therefore either scenario, soluble vs. filamentous interactions, could be possible or they could happen in parallel.

Furthermore, with over 50 family members, keratin expression is highly regulated and reflects the functional diversity of its multigene family in the mammalian epithelia (Fuchs and Marchuk, 1983; Hesse et al., 2004). What determines keratin specific expression and function? Are there isotype specific functions or is it rather the interaction with unique target proteins, which determines their unique properties? What defines keratin specific expression and function in specialized differentiated tissues, influencing cell and subsequently tissue architecture?

The aim of this thesis was to address the functional significance of this keratin multiprotein family, using the complete keratin type II cluster KO mice in embryonic development and as an extension a cell culture model, which was derived from these mice. In combination these two models provide the tools to answer the questions about keratin specificity, interacting proteins and their mode of action in regulating signaling pathways and cell, as well as tissue architecture.

Keratin function in embryonic development

Analysis of the keratin type II cluster KO mice, demonstrated that keratin filaments are essential for embryonic development. Comparable to the double KO studies of embryonic keratins reported before (Hesse et al., 2000; Tamai et al., 2000), keratin deficient embryos died at E9.5. The KO embryos displayed drastic growth retardation (Vijayaraj et al., 2009, Fig. 3 G-J) due to a 40% reduction in protein biosynthesis (Vijayaraj et al., 2009, Fig 3 K). This confirmed previous cell culture data (Kim and Coulombe, 2007) and demonstrated that keratins influence cell growth in an *in vivo* system free of compensation and aggregation artefacts. In the course of this paper (Vijayaraj et al., 2009), it was demonstrated that keratin IF proteins regulate embryo growth upstream of the mTOR pathway through GLUT receptor localization (Vijayaraj et al., 2009, Fig 5 E). Mislocalization of the GLUT-1 and -3 receptors to the cytoplasm resulted in low glucose levels within the cell (Vijayaraj et al., 2009, Fig 5 A-B). Limited nutrition repressed growth and protein biosynthesis, as early mouse embryos predominantly rely on glycolysis (Pantaleon and Kaye, 1998). This led to the activation of AMP kinase (AMPK), the cellular energy sensor of the cell, which is phosphorylated when AMP levels are elevated (Hardie, 2007). Phosphorylated AMPK inhibited the mTOR complex 1 (mTORC1) through the phosphorylation of Raptor (Vijayaraj et al., 2009, Fig 4 E-F). This resulted in the inactivation of the mTORC1 downstream targets p70 S6kinase and 4EBP1 (Vijayaraj et al., 2009, Fig 4 D). It was further noted that the stress protein eIF2α showed elevated phosphorylation levels in keratin depleted embryos, although the stress related Hsp70 could not be detected and 14-3-3 levels seemed unchanged as well (Vijayaraj et al.,

2009, Fig 4 A-B). The question remains, how embryonic keratins regulate GLUT localization and influence the mTOR pathway, which are the possible interacting proteins?

Previous reports demonstrated that keratins are involved in regulating vesicle transport and receptor localization. Along these lines, it was shown, that through an interaction of a mutated K5 head domain with the MT motor protein dynein, melanosome localization in keratinocytes of EBS patients with mottled pigmentation was altered (Betz et al., 2006; Uttam et al., 1996).

Furthermore, absence of K8 in the intestine results in the mislocalization of apical TM proteins like ion transporters, cystic fibrosis transmembrane receptors (CFTR) and also soluble *N*-ethylmaleimide-sensitive factor attachment protein receptors (SNARE) proteins like Syntaxin 3 (Ameen et al., 2001; Oriolo et al., 2007; Toivola et al., 2004).

Possible interacting proteins of keratins which can modulate membrane protein transport and cell polarization are 14-3-3 adapter proteins (Mellman and Nelson, 2008; Mrowiec and Schwappach, 2006), which can interact with Ser phosphorylation sides in the keratin head domains as demonstrated for various keratins (Kim et al., 2006; Ku et al., 1998). The 14-3-3 proteins are phosphoserine/phospho-threonine binding proteins that interact with a diverse array of binding partners. They represent a seven member family of highly conserved adapter proteins that are involved in vital cellular processes, such as metabolism, signal transduction, apoptosis and cell-cycle regulation (Morrison, 2009), often in association with keratins (Magin et al., 2007). In this fashion, it was proposed that keratin filaments function as “phospho-sink” amongst others during mitosis by competing for 14-3-3σ with Cdc25, therefore allowing it to enter the nucleus to promote G2/M transition (Margolis et al., 2006; Omary et al., 2006). Similar results were obtained in hepatocytes where the K18 mutation Ser33Ala inhibited cell cycle progression in a 14-3-3 dependent manner (Ku et al., 2002). Such a feature is consistent with the increased size of suprabasal keratinocytes and elevated 14-3-3σ levels that were observed in $K10^{-/-}$ mice, which also points to an arrest of the cell cycle (Reichelt and Magin, 2002).

In line with the presented data, keratin and 14-3-3 interaction in signal transduction was reported in cell metabolism. Association of the K17 head domain with the epithelial-specific 14-3-3σ isoform was suggested to modulate Akt and mTOR signaling in keratinocytes. As a result K17 absence caused reduction of the overall protein synthesis and a corresponding smaller size of K17 KO skin keratinocytes (Kim and Coulombe, 2007). However, one has to remember, that due to a single K17 KO, other keratin genes as K16 and K14 were upregulated and could compensate or alter cell responses.

Of note, phosphorylation of Raptor mediates 14-3-3 binding and is required for TORC1 inactivation in vivo (Gwinn et al., 2008). In addition, 14-3-3 proteins sequester the TSC1/TSC2 protein complex that serves as a negative regulator of mTOR (Morrison, 2009).

This might provide additional levels of keratin actions in the regulation of protein biosynthesis through the interaction with 14-3-3 adapter proteins in keratin depleted embryos. However, this was not detected in relation to keratins in this context, as the small size of embryos prevented detailed analysis. The molecular mechanisms as how keratins control cell growth and transporter localization are not yet known, but it is well established that the correct localization of cytosolic proteins and cell adhesion proteins depends on keratins and vimentin (Godsel et al., 2005; Mashukova et al., 2009; Nieminen et al., 2006; Toivola et al., 2004). Possibly, keratins orchestrate the local interaction of 14-3-3 proteins with their multiple binding partners during organelle transport, cell polarity, and signaling. It can even be speculated that different keratins interact tissue restricted with specific members of the 14-3-3 family, which can be tested through replacement experiments in the cell culture model developed in this thesis.

Besides the simple epithelial tissues of the embryo the extraembryonic tissues, the yolk sac and the placenta are core tissues of keratin expression in the early embryo. Therefore, the next step was to determine the effects of keratin deletion in these highly specialized epithelia. In the placenta, as was demonstrated in the yolk sac, GLUT transporters were clearly mislocalized (data not shown) and drastic growth retardation could be reported (Kröger et al., Figure 1). This was due to a defective development of maternal-fetal vascularization caused by keratin absence. The results provide for the first time evidence that keratins contribute to vascular remodeling in the decidua as well as proper vascularization of the labyrinth in placental development. It was proposed that this was mainly caused by the mislocalization of the TGC (Kröger et al., Figure 2). The giant cells are the first extraembryonic epithelial cells to interact with the maternal tissue in the process of invagination and are rich in keratins; they are responsible for the implantation of the embryo (Bany and Cross, 2006). The mislocalization of the TGCs could be caused by keratin deletion, as K8 deleted hepatoma cells were shown to exhibit severe migration and attachment defects (Bordeleau et al., 2010). In addition, TGCs are required for initiating decidualisation and regulate decidual development by the secretion of paracrine hormones, which remodel maternal vasculature and regulate vascularization in the developing placenta (Jackson et al., 1994). They control premature maternal blood flow and maintain the implantation side under hypoxic conditions. This is essential for the stabilization of the hypoxia inducible factor Hif1α, a transcription factor that activates the expression of VEGF (Levy et al., 1995; Ramirez-Bergeron et al., 2006). The growth factor VEGF induces vascularization and haematopoiesis in the developing placenta. Keratin deletion results in TGC malfunction, entails decidual hyperoxia and impaired placental vasculature, due to reduced levels of Hif1α and VEGF (Kröger et al., Figure 3 and 4). An involvement of keratins in the secretion of hormones due to an

attachment defect and a resulting defective crosstalk between epithelial and mesodermal tissue were the main findings described in Vijayaraj et al., 2010. Here it was demonstrated that the deletion of keratins in the yolk sac, caused an attachment defect of endodermal and mesodermal tissue, resulting in decreased haematopoiesis and vasculogenesis through reduced Foxf1 signaling and its downstream targets BMP4 and P-p38 MAPK in the mesoderm (Vijayaraj et al., 2010).

The defects in vasculogenesis and haematopoiesis in both the yolk sac and the placenta, led to a disruption of nutrient and gas exchange and due to reduced oxygen uptake, severe hypoxia and growth retardation of the embryo itself (Kröger et al., Figure 5 A-B).

Hypoxia and a low glucose level have been shown to induce analogous cellular responses which were reported in the keratin deleted embryos, namely mTOR inhibition through Raptor and AMPK activation (Wouters and Koritzinsky, 2008). Previous reports suggest that hypoxia and glucose deprivation even have an accumulative effect on AMPK activation, linked to a negative feedback loop. As repressed protein translation through mTOR deactivation leads to reduced Hif1α expression (Zhou et al., 2007), this could, next to decidual hyperoxia, also account for the reduced Hif1α levels in the keratin deleted placenta (Figure 5.1).

If embryonic keratins exercise alterations of tissue architecture via attachment and migration defects or rather through the improper secretion of hormones possibly through above discussed adapter proteins, or a combination of both needs to be determined. This requires biochemical assays with a quantitative readout and exceeds the scope of the keratin type II cluster KO mice.

CK minus: An epithelial cell culture model completely devoid of keratins

To be able to overcome limitations presented by the *in vivo* model, a cell culture model of keratin depleted keratinocytes was developed to answer the questions beyond the limitations of the *in vivo* model system. One of the aspects that were analyzed in the first round of experiments was to assess the role of keratins in cell architecture and organelle distribution. Immunofluorescence images of the ER and the Golgi complex demonstrated a clear enlargement of both organelles (Figure 4.4.9). One possible explanation for this phenotype could be ER stress, for instance due to an overload of unfolded proteins; which results in an increase of ER membrane biogenesis (Ron and Walter, 2007). Possible causes for ER stress are amongst others hypoxia and low intracellular glucose levels, both phenotypes in the keratin type II cluster KO mice (Wouters and Koritzinsky, 2008). Direct implications of ER stress are targets of the unfolded protein response (UPR), for instance an elevated P-PERK level, which in turn leads to a direct inactivation of eIF2α through phosphorylation (Ron and Walter, 2007), another phenomenon that we reported in the *in vivo* model (Vijayaraj et al., 2009, Fig 4 B) (Figure 5.1).

Complementary to the UPR during ER stress is the ER-associated degradation (ERAD) pathway, which targets misfolded proteins via an interplay of heat shock proteins (for example immunoglobulin binding protein, BiP (grp78)) and ubiquitination for cytosolic proteasomal degradation (Vembar and Brodsky, 2008) (Figure 5.1). K8 was previously suggested to directly associate with grp78 under conditions which induce ER stress and subsequently, ERAD, namely glucose starvation and treatment with tunicamycin, a drug which blocks the synthesis of N-linked glycoproteins (Liao et al., 1997). The interaction of keratins and chaperones including subsequent ubiquitination was also described in misfolded keratin aggregates, as reported for EBS mutations and in keratin associated MDB in liver diseases (Loffek et al., 2010; Omary et al., 2009). When keratins are missing, more heat shock proteins are available and can act on other target proteins, which might stimulate an increased ERAD reaction and in a positive feedback loop with the UPR, ER volume (Vembar and Brodsky, 2008; Watson et al., 2007). Therefore, chaperones provide an additional family of keratin interacting proteins, which could participate in mechanisms of keratin action.

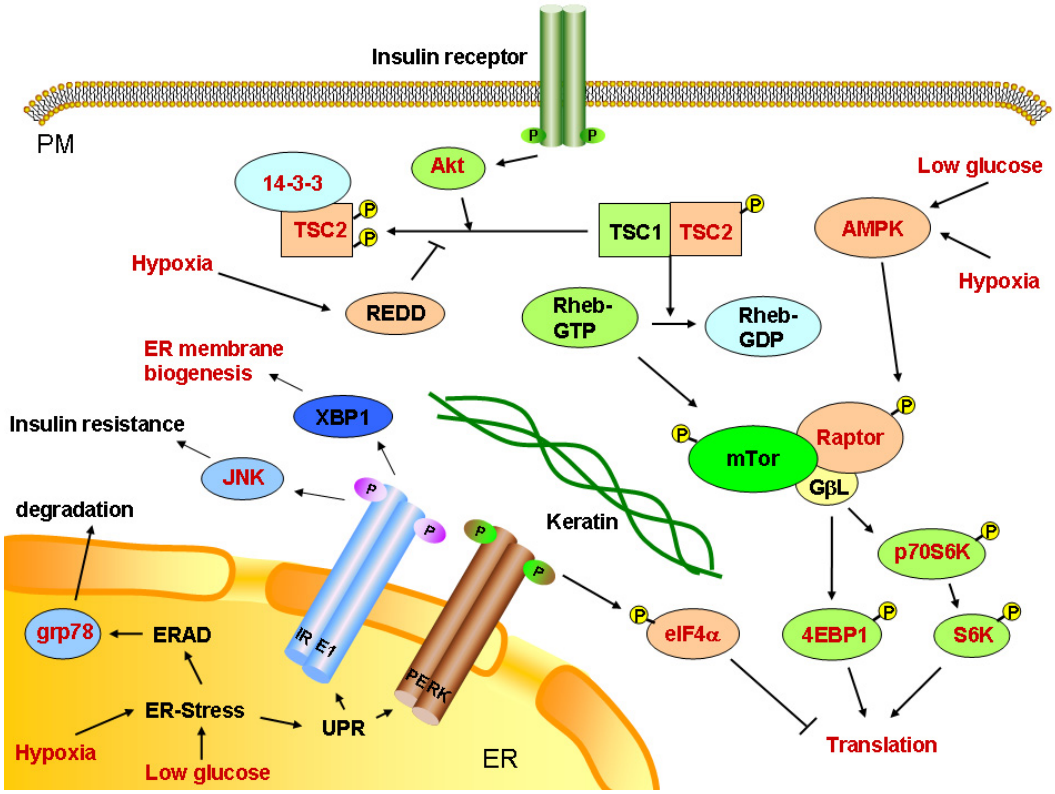

Figure 5.1 **Model for keratin affected signaling pathways.** As demonstrated in this model, keratin deletion has been demonstrated to influence translation from different angles, either regulating certain states of the cell, like low glucose levels through GLUT relocalization, or induction of hypoxia, or by influencing scaffolds and kinases of the translation signaling pathway around mTOR. The model further proposes ER-stress as an additional target of keratin regulation. The keratin associated signalling pathways are depicted in red, all translation inhibiting proteins in light red and the positive regulators in green.

Interdependence of function and organization between the Golgi and the other cytoskeletal networks of MTs and MFs were shown before (Brownhill et al., 2009; Dippold et al., 2009), the same holds true for the ER (Griffing, 2010). So far no association of keratin filaments with the ER was reported; recent reports describe an influence of keratins on Golgi complexes. Induction of keratin filament disassembly through transfections with the K18 mutant GFP-CK18 R89C resulted in a fragmentation of the Golgi-complex in hepatocellular carcinoma cell lines, however, not in HEK293 (Kumemura et al., 2004). The authors argued that this was not due to keratin aggregates induced by the mutation but rather the disassembly of the filament system. In this case HEK 293 cells were used as a model system, which supposedly did not express keratins and only vimentin which contradicts immunofluorescence data of our lab (data not shown). In contrast to those results, the CK minus cells, true keratin filaments free epithelia cells, displayed a drastically enlarged tubular network of the Golgi-complex, compared to WT keratinocytes (Figure 4.4.9 C-D). Recently, a direct association between the Golgi complex and vimentin was reported. Formiminotransferase cyclodeaminase (FTCD), a bifunctional enzyme involved in histidine metabolism, directly interacts with the vimentin filaments and Golgi membranes. Additional findings indicate that the Golgi protein FTCD is a potent modulator of the vimentin IF cytoskeleton, as FTCD overexpression led to bundling of the vimentin cytoskeleton and a fragmentation of the Golgi-complex. So far, molecular associations between keratins and the Golgi complex are lacking. The observation that the Golgi is reorganized in CK minus cells, suggests that either directly or through adapter proteins keratins interact with this organelle, similar to their IF family member vimentin (Gao and Sztul, 2001; Gao et al., 2002; Mao et al., 2004).

A possible candidate for an adapter protein linking keratins and the ER are calcium pumps. In the ER as well as in the Golgi, these were shown to regulate desmosome and actin organization upon calcium switch in keratinocytes. ATP2A2 encodes the sarco(endo)plasmic reticulum Ca^{2+}-ATPase isoform 2 (SERCA2) pump, while ATP2C1 encodes a secretory pathway Ca^{2+}/Mn^{2+}-ATPase (SPCA1) found in the Golgi apparatus (Dhitavat et al., 2004). SERCA2 was shown to bind DP and retain it at the ER during physiological calcium levels as a mode to regulate desmosome assembly (Dhitavat et al., 2003). This could provide the missing link between keratins and the ER, as DP is the linker protein that attaches keratins to desmosomes. Careful immunofluorescence and electron microscopy, followed by immunoprecipitation studies of CK minus cells should provide the answer, if this hypothesis is correct. Data analysing defective SPCA1 underlined that the right calcium concentration is essential for cell-cell adhesion and the associated actin reorganization as discussed further along. Since DP, as well as actin are rearranged in the CK minus cells (Figure 4.4.4 and 4.4.7), and since both are regulated by altered calcium concentrations, it would be sensible

to check cellular calcium concentrations in keratin KO cells, which can be done with various fluorescent dies (Grynkiewicz et al., 1985).

Furthermore, calcium release from the ER activates members from the PKC family (Ron and Walter, 2007; Wouters and Koritzinsky, 2008). Keratins have been shown to be targets for many kinases, amongst others for PKC (Omary et al., 2006). Conversely, simple keratins can act as modulators of kinase signaling pathways. In conjunction with chaperones, like Hsp70 they regulate rephosphorylation and localization of atypical PKC (Mashukova et al., 2009) and can also influence migration and cell adhesion in a PKC-mediated integrin/FAK dependent manner (Bordeleau et al., 2010; Osmanagic-Myers et al., 2006; Wallis et al., 2000). In addition, the assembly of desmosomes to the PM are also PKC-dependent. Knockdown of the α-isoform of PKC impairs calcium-dependent desmosome formation and results in retention of DP along keratins. The fact that PKCα also plays a positive role in desmosome assembly supports the idea that this kinase is important for rapid desmosome remodelling (either assembly or disassembly) in response to environmental cues (Green and Simpson, 2007; Wallis et al., 2000). Examining DP localization in the keratin deleted mouse model (Vijayaraj et al., 2009, Fig 2 A-B), as well as in the newly established cell culture model of CK minus cells (Figure 4.4.4), fluorescence images demonstrated that DP was clearly mislocalized and total protein levels, as determined by Western blotting were reduced by 30% (Figure 4.4.5). Both keratins and DP interact with PKC, as PKC is responsible for DP localization and keratin in turn controls PKC as well as DP localization. This suggests an interplay of all three proteins in the assembly of desmosomes.

Not only the IF-dependent intercellular contacts are regulated by PKC, also one class of cell-matrix interactions, the hemidesmosomes. Critical for the mechanical stability of hemidesomosmes is the interaction of cytokeratins to plectin and α6β4 integrins (Niessen et al., 1997; Rezniczek et al., 1998). This becomes destabilized by deleting the essential IF-linker component plectin (Andra et al., 1997). Deletion of β4 integrin on the other hand, did not have any obvious effects, besides faster migration rate of isolated keratinocytes (Raymond et al., 2005). When hemidesmosome disassembly is required in the cell, for instance, to allow keratinocyte migration during wound healing, PKCα is one of the kinases, which can trigger hemidesmosome disassembly by inducing phosphorylation of the β4 intracellular domain (Margadant et al., 2008). Plectin and to a certain degree, α6-integrin are mislocalized in CK minus cells and no colocalization of both proteins at hemidesmosomes could be observed (Figure 4.4.8). A possible explanation for the hemidesmosomal disassembly due to keratin deletion could either be the relocalization of plectin to the PM, but also a defective targeting of β4-integrin, for example through PKC, which upon phosphorylation induces the disassembly of hemidesmosomes (Margadant et al., 2008).

Plectin was further shown to control PKC activity by retaining an activating scaffold protein at the actin cytoskeleton (Osmanagic-Myers and Wiche, 2004) and mislocalization of plectin might therefore also influence PKC localization and activation. Along these lines, PKC might alter phosphorylation of desmosomes, as well as hemidesmosomes in CK minus cells due to the deletion of their associated cytoskeletal components and entailing mislocalization of their linker proteins. This could contribute to junctional re-/misassembly; one of the questions that can be targeted in CK minus cells with careful biochemical analysis of gain and loss of function studies.

DP KO studies in skin epithelia and DP depleted keratinocytes demonstrated that there is a crosstalk between desmosomes and adherens junctions. DP KO keratinocytes displayed dysfunctional adherens junctions, as demonstrated by E-cadherin staining, which influenced the attached microfilament system (Gumbiner et al., 1988; Vasioukhin et al., 2000; Vasioukhin et al., 2001; Wheelock and Jensen, 1992). Deleting keratins, no alterations in the adherens junctions nor in the focal adhesions could be detected per se, using VE-Cadherin and β1-integrin in the in vivo model (Vijayaraj et al., 2010, Figure 2 G-J) and using E-cadherin and vinculin staining in CK minus cells (data not shown). Although total protein amounts of vinculin were increased by 40%, which could possibly be a compensation mechanism for the defective IF-linked junctions.

Using careful immunofluorescence analysis, a mild misorganization in the actin cytoskeleton in CK minus cells could be detected (Figure 4.4.4 and 4.4.7), similar to the reported phenotype in the DP KO keratinocytes (Vasioukhin et al., 2001), but not as drastic and could be due to the misorganized and reduced amounts of DP in the CK minus cells (Figure 4.4.4 - 4.4.7). This correlates with the data that DP still incorporates into desmosomes, when DP-keratin binding is inhibited, but the timing is delayed due to altered particle trajectory and increasing particle pause times. On the other hand DP transport to the desmosomes is foremost actin dependent. Maturation and reorganization of adherens junction-associated cortical actin due to keratin deletion could therefore also alter DP localization (Godsel et al., 2005). Rescue experiments with K5 and DP mutants and on the other hand depletion experiments with actin depolymerising drugs, like cytochalasin should provide insight into this issue.

So which are the proteins, which could provide the link between the keratin and the actin cytoskeleton and in turn between desmosomes and adherens junctions?

Previous studies have suggested that the formation of adherens junctions is functionally linked to desmosome assembly through the armadillo protein, PG, which is the only known common component to both adherens junctions and desmosomes (Lewis et al., 1997).

Interestingly, PKPs also associate with actin, providing a potential link between the DP–IF network and actin-dependent DP/desmosome assembly (Godsel et al., 2005; Hatzfeld et al., 2000). Furthermore overexpression of the armadillo repeat domain of PKP1 induced a dominant negative phenotype with the formation of filopodia and long cellular protrusions, where PKP1 colocalized with actin filaments (Hatzfeld et al., 2000). This is similar to the phenotypes that were observed in the keratin deleted keratinocytes. Brightfield images of CK minus cells displayed increased protrusions and elongations, compared to WT cells (Figure 4.4.2 and 4.4.3) and filamentous actin images demonstrated an increased amount of filopodia-like structures in CK minus cells (Figure 4.4.4 B', Figure 4.4.7 B). If this is due to an increased soluble PKP pool, which is now free to interact with actin filaments, needs to be evaluated with further immunofluorescence and immunoprecipitation studies. Furthermore, recent studies showed an involvement of PKP1 in translational control, providing yet another link between keratins and protein biosynthesis regulations, which needs to be carefully evaluated through pathway analysis (Wolf et al., 2010).

The cytoskeletal linker plectin plays not only a central part in keratinocytes, linking keratins to cell junctions (Eger et al., 1997; Jefferson et al., 2004), but also connects keratins with other cytoskeletal filament systems, MF and MT. Furthermore, it is proposed to act as a signaling platform, providing the crucial link between cytoskeletal dynamics and signaling machineries (Osmanagic-Myers et al., 2006; Wiche, 1998). In CK minus cells a drastic relocalization of plectin from hemidesmosomes to the PM could be observed, as mentioned above (Figure 4.4.8), which could be a compensation for defective cell-cell junctions and which could in turn cause the misorganization of the MF system, this however needs to be further elucidated in additional experiments.

The regulation of the MF system is predominantely regulated by the family of Rho GTPases, they regulate actin organization into lamellipodia or filopodia and amongst others coordinate cell attachment (TJ and AJ) and migration (Heasman and Ridley, 2008; Popoff and Geny, 2009). Rac/Cdc42 mainly regulate the assembly–disassembly of AJ components, however the polarized actin cytoskeleton is dependent upon Rho and downstream Rock signaling. Along these lines, an actin dependent role of RhoA and Rock in higher order architecture was suggested, namely generating tension–based, polarized filamentous actin structures in the developing epidermal sheet (Vaezi et al., 2002). Misorganization of the actin cytoskeleton and defective cell junctions in CK minus cells, are signs for a defect in the Rho-GTPase signaling cascades, induced by keratin deletion. The roles of Rho GTPases have been extensively studied in different mammalian cell types using mainly dominant negative and constitutively active mutants. However, the recent availability of KO mice for several members of the Rho family revealed new information about their roles in signaling to the cytoskeleton. Furthermore, Rho/Ras-GTPases and the control of intercellular junctions are

the target of various bacterial toxins (Heasman and Ridley, 2008; Popoff and Geny, 2009). All of the above alternatives could be used to study an eventual regulation of keratins and their junctions by Rho/Ras-GTPases through molecular approaches using migration and attachment assays as a readout (Heasman and Ridley, 2008; Popoff and Geny, 2009).

In contrast to the MF system the MT system seems mostly unaltered in the CK minus cells (Figure 4.4.4 and 4.4.7). Although plectin was also shown to link MT and keratin filaments (Wiche, 1998), its reorganization did not seem to have an impact on MT organization. MTs also play an essential role in the formation of the intercellular junctions, which involves multiple phases of microtubule-dependent vesicular trafficking events that deliver the TM components (e.g., desmocollin, desmoglein, and plakoglobin) to the plasma membrane (Gloushankova et al., 2003; Pasdar and Nelson, 1989). Very recent data propose that this targeting is mediated by a subset of Sec3 containing exocyst complexes, which are conserved multisubunit complexes involved in the docking of post-Golgi transport vesicles to the PM (Andersen and Yeaman, 2010). On the other hand it was proposed that DP affects the organization of the microtubule cytoskeleton during epidermal differentiation. Microtubules were shown to shift away from a radially arrayed, centrosome associated organization in basal cells to accumulate in the cortical region near cell–cell junctions within suprabasal keratinocytes (Lechler and Fuchs, 2007; Wacker et al., 1992). Along with this, there is a redistribution of a centrosomal protein called ninein and the microtubule-associated protein, CLIP170 to desmosomes. This switch in ninein distribution and associated centrosomal γ-tubulin requires DP (Lechler and Fuchs, 2007). As CK minus cells displayed an altered DP localization it was to assume that the MT system was mislocalized as well. Surprisingly we did not see an overall disturbance in the MT system, compared to WT keratinocytes. During the induction of cell contacts, it was observed that the MT rearranged from a radial organization to a parallel one (Figure 4.4.4 and 4.4.7), however an accumulation of MTs to cell-cell junctions (Figure 4.4.4 and 4.4.7) or a dissociation of γ-tubulin from the centrosomes (data not shown) could not be detected in CK minus nor in CK plus cells. In contrast to the Lechler paper, no primary keratinocytes were used, but rather immortalized cell lines. Furthermore, the calcium switch was only performed for 2 days, for optimal junction expression, compared to 3 days for differentiation onset used in the Lechler paper. This might explain the rather normal MT phenotype in the CK minus cells. If prolonged differentiation conditions might have an effect on the MT and if this might be due to DP relocalization and reduction, needs to be tested in the future.

Although more than 30 years of research have been invested into the unraveling of the mechanisms of keratin functions, no definite results could be obtained so far. The fact, that

keratins belong to a multiprotein family of more than 50 highly insoluble proteins, which are prone to redundancy and compensation artifacts, makes them challenging to study.

Therefore, the essential questions are still unanswered. Do keratins have predominantly an architectural or rather scaffolding function, which indirectly regulates cell signaling? Or do keratins directly mediate signaling processes, which in turn determine their network architecture? And considering all the different keratin genes, what regulates filament pair specificity and do they have specific interacting proteins?

Candidates for interacting proteins are abundantly provided by the existing literature as discussed above, not only desmosomal proteins like desmoplakin and plakophilin and the cytoskeletal linker plectin, but also a myriad of kinases, for instance the PKC family and the family of 14-3-3 adapter proteins. The challenge however, is validating these candidates and demonstrating their mode of action in line with specific keratin isotype expression.

This thesis presents for the first time a cell culture model, the CK minus cells, which are completely depleted of keratin proteins. In combination with the *in vivo* model they provide a tool for loss of function studies, without compensation or redundancy issues. Furthermore, individual keratins can now be brought back into the filament system and their specific functions and their mechanism can be analyzed.

.

6. Perspectives

The establishment of a keratin-free cell culture model opens a variety of new possibilities to analyze keratin-dependent cellular functions and to address the fundamental question which of the many functions keratins perform, depend on their organization into polymeric filaments or into soluble oligomeric keratin species.

Ongoing to this thesis, transcriptome analysis was started comparing CK minus cells to CK plus cells to determine to which extent keratins affect the transcriptional state of keratinocytes. Preliminary data indicate the regulation of just two transcription factors and of several scaffold protein-coding genes. Furthermore, there are multiple phenotypes and alterations at the protein level detectable by immunofluorescence microscopy and Western blotting. These include altered organization and distribution of desmosomal and hemidesmosomal proteins. In addition, a significant reorganization of the actin cytoskeleton was observed. Unexpectedly, ER and the Golgi complex are profoundly altered. This indicated ER stress entailing reduced protein biosynthesis, in line with *in vivo* data showing that keratin-dependent mislocalization of glucose transporters resulted in translation inhibition and increased hypoxia in the embryo proper of the keratin type II cluster KO mice.

Which are the direct mechanisms and what immediate approaches could be taken to analyze these findings? The first step will be to demonstrate dependence of the phenotypes on keratins, by re-expression of individual keratin pairs. Next, dissection of signaling pathways would follow. Various assays are possible. DP and plectin relocalization are influenced by PKC levels, a kinase assay would be a plausible quantitative readout. Examining actin reorganization and associated Rho kinase signaling pathways, which directly influence cell attachment and migration, can be quantified using direct morphological and biochemical readouts. To address the role of keratins in organelle organization and transport, quantitative endocytosis and exocytosis assays, in combination with loss and gain of function experiments, will be performed.

The main questions, however are, weather keratins regulate cell architecture and influence signaling pathways as filamentous or soluble protein entities and which are the keratin interacting proteins that modulate cell morphology? Are they dependent on direct protein-protein interactions with regulated binding affinities, or are they a consequence of indirect signaling cascades? Along these lines, gain and loss of function experiments of interacting candidates, as well as re-expression approaches of individual keratins and of various keratin mutants which prevent keratin filament formation have to be conducted using biochemical readouts. This will answer the question which extent of assembly keratins have to undergo to

associate with their target proteins and to fulfill their functions in regulating cell architecture and signal transduction. To this end, the newly established keratin-free cells will for the first time help to clarify how keratin isotypes affect epithelial cell functions at the molecular level.

7. Summary

Keratin intermediate filament proteins form the major cytoskeleton in all epithelia. Increasing evidence suggests that keratins act as cytoskeletal scaffolds which locally regulate cell growth and survival. Many of these functions, however, are not understood in full, owing to keratin redundancy. Previous gene function studies have been impeded by gain of toxic function phenotypes. Therefore, transgenic mice lacking the entire keratin multiprotein family were analyzed and a corresponding keratinocyte cell line was generated.

The deletion of keratins resulted in prenatal death at E9.5 due to severe growth retardation. Within the scope of this thesis it was demonstrated that this was in part caused by repressed protein biosynthesis, due to mislocalized GLUTs mediated by the mTOR pathway. The analysis of extraembryonic tissue further revealed an influence of keratins on the adhesion between endodermal and mesodermal cell layers. As a consequence, keratin depleted embryos suffered from reduced yolk sac haematopoiesis and vasculogenesis, due to altered hormone and growth factor gradients. Similar effects were reported for mislocalized TGCs in the absence of keratins which altered signaling and hormone secretion leading to increased vascularization of the maternal decidua. Hyperoxia in the decidua entailed defective Hif1α and VEGF signaling, resulting in impaired placental vasculogenesis and concomitant impairment of maternal and embryonic gas and nutrient exchange.

To overcome the limitation of an *in vivo* model in determining functions at the molecular level, a cell culture model was generated, the CK minus keratinocytes. First data indicated drastic changes in morphology of the ER and the Golgi complex, possibly ER stress, a hypothesis emerging form the acquired *in vivo* data of decreased glucose levels and increased hypoxia. Furthermore, similar to the mouse model desmosomes were altered, as demonstrated by DP and plectin relocalization and a misorganization of the actin cytoskeleton was observed. This suggests that the amount of keratin and eventually specific isotypes regulate formation and turnover of other multiprotein complexes, as cell junctions and other cytoskeletal systems, influencing cell attachment and migration in the epithelial tissue environment.

Translational control, restructuring of the tissue environment and cell migration are implications for stem cell turnover during development and tissue repair, as well as tumorigenesis. This thesis provides for the first time the tools, the CK minus cells, to examine the influences of keratin free or keratin isotype specific cells on tumor development and tissue regeneration by reinjection. Furthermore, with this easily accessible cell culture system, isotype-specific functions can be examined by re-expression of individual keratin pairs. This will help to understand the function of keratins in vivo including their associated diseases and will have implications for therapy approaches.

8. References

Adams, D.J., P.J. Biggs, T. Cox, R. Davies, L. van der Weyden, J. Jonkers, J. Smith, B. Plumb, R. Taylor, I. Nishijima, Y. Yu, J. Rogers, and A. Bradley. 2004. Mutagenic insertion and chromosome engineering resource (MICER). *Nat Genet*. 36:867-71.

Adamson, S.L., Y. Lu, K.J. Whiteley, D. Holmyard, M. Hemberger, C. Pfarrer, and J.C. Cross. 2002. Interactions between trophoblast cells and the maternal and fetal circulation in the mouse placenta. *Dev Biol*. 250:358-73.

Adelman, D.M., M. Gertsenstein, A. Nagy, M.C. Simon, and E. Maltepe. 2000. Placental cell fates are regulated in vivo by HIF-mediated hypoxia responses. *Genes Dev*. 14:3191-203.

Ain, R., J.S. Tash, and M.J. Soares. 2003. Prolactin-like protein-A is a functional modulator of natural killer cells at the maternal-fetal interface. *Mol Cell Endocrinol*. 204:65-74.

Ameen, N.A., Y. Figueroa, and P.J. Salas. 2001. Anomalous apical plasma membrane phenotype in CK8-deficient mice indicates a novel role for intermediate filaments in the polarization of simple epithelia. *J Cell Sci*. 114:563-75.

Andersen, N.J., and C. Yeaman. 2010. Sec3-containing exocyst complex is required for desmosome assembly in mammalian epithelial cells. *Mol Biol Cell*. 21:152-64.

Andra, K., H. Lassmann, R. Bittner, S. Shorny, R. Fassler, F. Propst, and G. Wiche. 1997. Targeted inactivation of plectin reveals essential function in maintaining the integrity of skin, muscle, and heart cytoarchitecture. *Genes Dev*. 11:3143-56.

Andra, K., B. Nikolic, M. Stocher, D. Drenckhahn, and G. Wiche. 1998. Not just scaffolding: plectin regulates actin dynamics in cultured cells. *Genes Dev*. 12:3442-51.

Anson-Cartwright, L., K. Dawson, D. Holmyard, S.J. Fisher, R.A. Lazzarini, and J.C. Cross. 2000. The glial cells missing-1 protein is essential for branching morphogenesis in the chorioallantoic placenta. *Nat Genet*. 25:311-4.

Astorga, J., and P. Carlsson. 2007. Hedgehog induction of murine vasculogenesis is mediated by Foxf1 and Bmp4. *Development*. 134:3753-61.

Ausmees, N., J.R. Kuhn, and C. Jacobs-Wagner. 2003. The bacterial cytoskeleton: an intermediate filament-like function in cell shape. *Cell*. 115:705-13.

Bader, B.L., L. Jahn, and W.W. Franke. 1988. Low level expression of cytokeratins 8, 18 and 19 in vascular smooth muscle cells of human umbilical cord and in cultured cells derived therefrom, with an analysis of the chromosomal locus containing the cytokeratin 19 gene. *Eur J Cell Biol*. 47:300-19.

Bader, B.L., T.M. Magin, M. Freudenmann, S. Stumpp, and W.W. Franke. 1991. Intermediate filaments formed de novo from tail-less cytokeratins in the cytoplasm and in the nucleus. *J Cell Biol*. 115:1293-307.

Bader, B.L., H. Rayburn, D. Crowley, and R.O. Hynes. 1998. Extensive vasculogenesis, angiogenesis, and organogenesis precede lethality in mice lacking all alpha v integrins. *Cell*. 95:507-19.

Bagchi, S., H. Tomenius, L.M. Belova, and N. Ausmees. 2008. Intermediate filament-like proteins in bacteria and a cytoskeletal function in Streptomyces. *Mol Microbiol*. 70:1037-50.

Baldwin, H.S., H.M. Shen, H.C. Yan, H.M. DeLisser, A. Chung, C. Mickanin, T. Trask, N.E. Kirschbaum, P.J. Newman, S.M. Albelda, and et al. 1994. Platelet endothelial cell adhesion molecule-1 (PECAM-1/CD31): alternatively spliced, functionally distinct isoforms expressed during mammalian cardiovascular development. *Development*. 120:2539-53.

Bany, B.M., and J.C. Cross. 2006. Post-implantation mouse conceptuses produce paracrine signals that regulate the uterine endometrium undergoing decidualization. *Dev Biol*. 294:445-56.

Barak, Y., M.C. Nelson, E.S. Ong, Y.Z. Jones, P. Ruiz-Lozano, K.R. Chien, A. Koder, and R.M. Evans. 1999. PPAR gamma is required for placental, cardiac, and adipose tissue development. *Mol Cell*. 4:585-95.

Barak, Y., Y. Sadovsky, and T. Shalom-Barak. 2008. PPAR Signaling in Placental Development and Function. *PPAR Res*. 2008:142082.

Barbehenn, E.K., R.G. Wales, and O.H. Lowry. 1974. The explanation for the blockade of glycolysis in early mouse embryos. *Proc Natl Acad Sci U S A*. 71:1056-60.

Baribault, H., and R.G. Oshima. 1991. Polarized and functional epithelia can form after the targeted inactivation of both mouse keratin 8 alleles. *J Cell Biol*. 115:1675-84.

Baribault, H., J. Penner, R.V. Iozzo, and M. Wilson-Heiner. 1994. Colorectal hyperplasia and inflammation in keratin 8-deficient FVB/N mice. *Genes Dev*. 8:2964-73.

Baribault, H., J. Price, K. Miyai, and R.G. Oshima. 1993. Mid-gestational lethality in mice lacking keratin 8. *Genes Dev*. 7:1191-202.

Baron, M.H. 2005. Early patterning of the mouse embryo: implications for hematopoietic commitment and differentiation. *Exp Hematol*. 33:1015-20.

Bass-Zubek, A.E., R.P. Hobbs, E.V. Amargo, N.J. Garcia, S.N. Hsieh, X. Chen, J.K. Wahl, 3rd, M.F. Denning, and K.J. Green. 2008. Plakophilin 2: a critical scaffold for PKC alpha that regulates intercellular junction assembly. *J Cell Biol*. 181:605-13.

Basyuk, E., J.C. Cross, J. Corbin, H. Nakayama, P. Hunter, B. Nait-Oumesmar, and R.A. Lazzarini. 1999. Murine Gcm1 gene is expressed in a subset of placental trophoblast cells. *Dev Dyn*. 214:303-11.

Baumhueter, S., M.S. Singer, W. Henzel, S. Hemmerich, M. Renz, S.D. Rosen, and L.A. Lasky. 1993. Binding of L-selectin to the vascular sialomucin CD34. *Science*. 262:436-8.

Betz, R.C., L. Planko, S. Eigelshoven, S. Hanneken, S.M. Pasternack, H. Bussow, K. Van Den Bogaert, J. Wenzel, M. Braun-Falco, A. Rutten, M.A. Rogers, T. Ruzicka, M.M. Nothen, T.M. Magin, and R. Kruse. 2006. Loss-of-function mutations in the keratin 5 gene lead to Dowling-Degos disease. *Am J Hum Genet*. 78:510-9.

Bevilacqua, E.M., and P.A. Abrahamsohn. 1988. Ultrastructure of trophoblast giant cell transformation during the invasive stage of implantation of the mouse embryo. *J Morphol*. 198:341-51.

Blumenberg, M. 1988. Concerted gene duplications in the two keratin gene families. *J Mol Evol*. 27:203-11.

Bordeleau, F., L. Galarneau, S. Gilbert, A. Loranger, and N. Marceau. 2010. Keratin 8/18 modulation of protein kinase C-mediated integrin-dependent adhesion and migration of liver epithelial cells. *Mol Biol Cell*. 21:1698-713.

Bourget, P., C. Roulot, and H. Fernandez. 1995. Models for placental transfer studies of drugs. *Clin Pharmacokinet*. 28:161-80.

Bradford, M.M. 1976. A rapid and sensitive method for the quantitation of microgram quantities of protein utilizing the principle of protein-dye binding. *Anal Biochem*. 72:248-54.

Breier, G., M. Clauss, and W. Risau. 1995. Coordinate expression of vascular endothelial growth factor receptor-1 (flt-1) and its ligand suggests a paracrine regulation of murine vascular development. *Dev Dyn*. 204:228-39.

Brown, L.A., A.R. Rodaway, T.F. Schilling, T. Jowett, P.W. Ingham, R.K. Patient, and A.D. Sharrocks. 2000. Insights into early vasculogenesis revealed by expression of the ETS-domain transcription factor Fli-1 in wild-type and mutant zebrafish embryos. *Mech Dev*. 90:237-52.

Brownhill, K., L. Wood, and V. Allan. 2009. Molecular motors and the Golgi complex: staying put and moving through. *Semin Cell Dev Biol*. 20:784-92.

Brusselmans, K., F. Bono, D. Collen, J.M. Herbert, P. Carmeliet, and M. Dewerchin. 2005. A novel role for vascular endothelial growth factor as an autocrine survival factor for embryonic stem cells during hypoxia. *J Biol Chem*. 280:3493-9.

Bullock, W.E., and S.D. Wright. 1987. Role of the adherence-promoting receptors, CR3, LFA-1, and p150,95, in binding of Histoplasma capsulatum by human macrophages. *J Exp Med*. 165:195-210.

Byrd, N., S. Becker, P. Maye, R. Narasimhaiah, B. St-Jacques, X. Zhang, J. McMahon, A. McMahon, and L. Grabel. 2002. Hedgehog is required for murine yolk sac angiogenesis. *Development*. 129:361-72.

Byrne, C., M. Tainsky, and E. Fuchs. 1994. Programming gene expression in developing epidermis. *Development*. 120:2369-83.

Caniggia, I., H. Mostachfi, J. Winter, M. Gassmann, S.J. Lye, M. Kuliszewski, and M. Post. 2000. Hypoxia-inducible factor-1 mediates the biological effects of oxygen on human trophoblast differentiation through TGFbeta(3). *J Clin Invest*. 105:577-87.

Carberry, K., T. Wiesenfahrt, R. Windoffer, O. Bossinger, and R.E. Leube. 2009. Intermediate filaments in Caenorhabditis elegans. *Cell Motil Cytoskeleton*. 66:852-64.

Caulin, C., C.F. Ware, T.M. Magin, and R.G. Oshima. 2000. Keratin-dependent, epithelial resistance to tumor necrosis factor-induced apoptosis. *J Cell Biol*. 149:17-22.

Chang, H., D. Huylebroeck, K. Verschueren, Q. Guo, M.M. Matzuk, and A. Zwijsen. 1999. Smad5 knockout mice die at mid-gestation due to multiple embryonic and extraembryonic defects. *Development*. 126:1631-42.

Coan, P.M., A.C. Ferguson-Smith, and G.J. Burton. 2005. Ultrastructural changes in the interhaemal membrane and junctional zone of the murine chorioallantoic placenta across gestation. *J Anat*. 207:783-96.

Colosi, P., G. Thordarson, R. Hellmiss, K. Singh, I.A. Forsyth, P. Gluckman, and W.I. Wood. 1989. Cloning and expression of ovine placental lactogen. *Mol Endocrinol*. 3:1462-9.

Copp, A.J. 1979. Interaction between inner cell mass and trophectoderm of the mouse blastocyst. II. The fate of the polar trophectoderm. *J Embryol Exp Morphol*. 51:109-20.

Coulombe, P.A., M.L. Kerns, and E. Fuchs. 2009. Epidermolysis bullosa simplex: a paradigm for disorders of tissue fragility. *J Clin Invest*. 119:1784-93.

Coulombe, P.A., and M.B. Omary. 2002. 'Hard' and 'soft' principles defining the structure, function and regulation of keratin intermediate filaments. *Curr Opin Cell Biol*. 14:110-22.

Cowden Dahl, K.D., B.H. Fryer, F.A. Mack, V. Compernolle, E. Maltepe, D.M. Adelman, P. Carmeliet, and M.C. Simon. 2005. Hypoxia-inducible factors 1alpha and 2alpha regulate trophoblast differentiation. *Mol Cell Biol*. 25:10479-91.

Cross, J.C., L. Anson-Cartwright, and I.C. Scott. 2002. Transcription factors underlying the development and endocrine functions of the placenta. *Recent Prog Horm Res*. 57:221-34.

Cross, J.C., H. Nakano, D.R. Natale, D.G. Simmons, and E.D. Watson. 2006. Branching morphogenesis during development of placental villi. *Differentiation*. 74:393-401.

Das, S.K., S. Yano, J. Wang, D.R. Edwards, H. Nagase, and S.K. Dey. 1997. Expression of matrix metalloproteinases and tissue inhibitors of metalloproteinases in the mouse uterus during the peri-implantation period. *Dev Genet*. 21:44-54.

de Pereda, J.M., E. Ortega, N. Alonso-Garcia, M. Gomez-Hernandez, and A. Sonnenberg. 2009. Advances and perspectives of the architecture of hemidesmosomes: lessons from structural biology. *Cell Adh Migr*. 3:361-4.

Denk, H., E. Lackinger, P. Cowin, and W.W. Franke. 1985. Maintenance of desmosomes in mouse hepatocytes after drug-induced rearrangement of cytokeratin filament material. Demonstration of independence of desmosomes and intermediate-sized filaments. *Exp Cell Res*. 161:161-71.

Dhitavat, J., C. Cobbold, N. Leslie, S. Burge, and A. Hovnanian. 2003. Impaired trafficking of the desmoplakins in cultured Darier's disease keratinocytes. *J Invest Dermatol*. 121:1349-55.

Dhitavat, J., R.J. Fairclough, A. Hovnanian, and S.M. Burge. 2004. Calcium pumps and keratinocytes: lessons from Darier's disease and Hailey-Hailey disease. *Br J Dermatol*. 150:821-8.

Dickson, M.C., J.S. Martin, F.M. Cousins, A.B. Kulkarni, S. Karlsson, and R.J. Akhurst. 1995. Defective haematopoiesis and vasculogenesis in transforming growth factor-beta 1 knock out mice. *Development*. 121:1845-54.

Dippold, H.C., M.M. Ng, S.E. Farber-Katz, S.K. Lee, M.L. Kerr, M.C. Peterman, R. Sim, P.A. Wiharto, K.A. Galbraith, S. Madhavarapu, G.J. Fuchs, T. Meerloo, M.G. Farquhar, H. Zhou, and S.J. Field. 2009. GOLPH3 bridges phosphatidylinositol-4- phosphate and actomyosin to stretch and shape the Golgi to promote budding. *Cell*. 139:337-51.

Duarte, A., M. Hirashima, R. Benedito, A. Trindade, P. Diniz, E. Bekman, L. Costa, D. Henrique, and J. Rossant. 2004. Dosage-sensitive requirement for mouse Dll4 in artery development. *Genes Dev*. 18:2474-8.

Dumont, D.J., G. Gradwohl, G.H. Fong, M.C. Puri, M. Gertsenstein, A. Auerbach, and M.L. Breitman. 1994. Dominant-negative and targeted null mutations in the endothelial receptor tyrosine kinase, tek, reveal a critical role in vasculogenesis of the embryo. *Genes Dev*. 8:1897-909.

Dunwoodie, S.L. 2009. The role of hypoxia in development of the Mammalian embryo. *Dev Cell*. 17:755-73.

Dupressoir, A., C. Vernochet, O. Bawa, F. Harper, G. Pierron, P. Opolon, and T. Heidmann. 2009. Syncytin-A knockout mice demonstrate the critical role in placentation of a fusogenic, endogenous retrovirus-derived, envelope gene. *Proc Natl Acad Sci U S A*. 106:12127-32.

Eger, A., A. Stockinger, G. Wiche, and R. Foisner. 1997. Polarisation-dependent association of plectin with desmoplakin and the lateral submembrane skeleton in MDCK cells. *J Cell Sci*. 110 (Pt 11):1307-16.

El-Hashash, A.H., D. Warburton, and S.J. Kimber. 2010. Genes and signals regulating murine trophoblast cell development. *Mech Dev*. 127:1-20.

Erber, A., D. Riemer, M. Bovenschulte, and K. Weber. 1998. Molecular phylogeny of metazoan intermediate filament proteins. *J Mol Evol*. 47:751-62.

Fong, G.H., J. Rossant, M. Gertsenstein, and M.L. Breitman. 1995. Role of the Flt-1 receptor tyrosine kinase in regulating the assembly of vascular endothelium. *Nature*. 376:66-70.

Freeman, S.J., and J.B. Lloyd. 1983. Evidence that protein ingested by the rat visceral yolk sac yields amino acids for synthesis of embryonic protein. *J Embryol Exp Morphol*. 73:307-15.

Fuchs, E. 2007. Scratching the surface of skin development. *Nature*. 445:834-42.

Fuchs, E., and D.W. Cleveland. 1998. A structural scaffolding of intermediate filaments in health and disease. *Science*. 279:514-9.

Fuchs, E., and D. Marchuk. 1983. Type I and type II keratins have evolved from lower eukaryotes to form the epidermal intermediate filaments in mammalian skin. *Proc Natl Acad Sci U S A*. 80:5857-61.

Fuchs, E., and K. Weber. 1994. Intermediate filaments: structure, dynamics, function, and disease. *Annu Rev Biochem*. 63:345-82.

Gabriel, H.D., D. Jung, C. Butzler, A. Temme, O. Traub, E. Winterhager, and K. Willecke. 1998. Transplacental uptake of glucose is decreased in embryonic lethal connexin26-deficient mice. *J Cell Biol*. 140:1453-61.

Gale, N.W., M.G. Dominguez, I. Noguera, L. Pan, V. Hughes, D.M. Valenzuela, A.J. Murphy, N.C. Adams, H.C. Lin, J. Holash, G. Thurston, and G.D. Yancopoulos. 2004. Haploinsufficiency of delta-like 4 ligand results in embryonic lethality due to major defects in arterial and vascular development. *Proc Natl Acad Sci U S A*. 101:15949-54.

Ganguly, A., R.A. McKnight, S. Raychaudhuri, B.C. Shin, Z. Ma, K. Moley, and S.U. Devaskar. 2007. Glucose transporter isoform-3 mutations cause early pregnancy loss and fetal growth restriction. *Am J Physiol Endocrinol Metab*. 292:E1241-55.

Gao, Y., and E. Sztul. 2001. A novel interaction of the Golgi complex with the vimentin intermediate filament cytoskeleton. *J Cell Biol*. 152:877-94.

Gao, Y.S., A. Vrielink, R. MacKenzie, and E. Sztul. 2002. A novel type of regulation of the vimentin intermediate filament cytoskeleton by a Golgi protein. *Eur J Cell Biol*. 81:391-401.

Gerber, H.P., A.K. Malik, G.P. Solar, D. Sherman, X.H. Liang, G. Meng, K. Hong, J.C. Marsters, and N. Ferrara. 2002. VEGF regulates haematopoietic stem cell survival by an internal autocrine loop mechanism. *Nature*. 417:954-8.

Gilbert, S., A. Loranger, N. Daigle, and N. Marceau. 2001. Simple epithelium keratins 8 and 18 provide resistance to Fas-mediated apoptosis. The protection occurs through a receptor-targeting modulation. *J Cell Biol*. 154:763-73.

Gilbert, S., A. Loranger, and N. Marceau. 2004. Keratins modulate c-Flip/extracellular signal-regulated kinase 1 and 2 antiapoptotic signaling in simple epithelial cells. *Mol Cell Biol*. 24:7072-81.

Ginouves, A., K. Ilc, N. Macias, J. Pouyssegur, and E. Berra. 2008. PHDs overactivation during chronic hypoxia "desensitizes" HIFalpha and protects cells from necrosis. *Proc Natl Acad Sci U S A*. 105:4745-50.

Gloushankova, N.A., T. Wakatsuki, R.B. Troyanovsky, E. Elson, and S.M. Troyanovsky. 2003. Continual assembly of desmosomes within stable intercellular contacts of epithelial A-431 cells. *Cell Tissue Res*. 314:399-410.

Godsel, L.M., S.N. Hsieh, E.V. Amargo, A.E. Bass, L.T. Pascoe-McGillicuddy, A.C. Huen, M.E. Thorne, C.A. Gaudry, J.K. Park, K. Myung, R.D. Goldman, T.L. Chew, and K.J. Green. 2005. Desmoplakin assembly dynamics in four dimensions: multiple phases differentially regulated by intermediate filaments and actin. *J Cell Biol*. 171:1045-59.

Green, K.J., S. Getsios, S. Troyanovsky, and L.M. Godsel. 2010. Intercellular junction assembly, dynamics, and homeostasis. *Cold Spring Harb Perspect Biol*. 2:a000125.

Green, K.J., and J.C. Jones. 1996. Desmosomes and hemidesmosomes: structure and function of molecular components. *Faseb J*. 10:871-81.

Green, K.J., and C.L. Simpson. 2007. Desmosomes: new perspectives on a classic. *J Invest Dermatol*. 127:2499-515.

Griffing, L.R. 2010. Networking in the endoplasmic reticulum. *Biochem Soc Trans*. 38:747-53.

Grynkiewicz, G., M. Poenie, and R.Y. Tsien. 1985. A new generation of Ca2+ indicators with greatly improved fluorescence properties. *J Biol Chem*. 260:3440-50.

Gumbiner, B., B. Stevenson, and A. Grimaldi. 1988. The role of the cell adhesion molecule uvomorulin in the formation and maintenance of the epithelial junctional complex. *J Cell Biol*. 107:1575-87.

Gwinn, D.M., D.B. Shackelford, D.F. Egan, M.M. Mihaylova, A. Mery, D.S. Vasquez, B.E. Turk, and R.J. Shaw. 2008. AMPK phosphorylation of raptor mediates a metabolic checkpoint. *Mol Cell*. 30:214-26.

Hardie, D.G. 2007. AMP-activated/SNF1 protein kinases: conserved guardians of cellular energy. *Nat Rev Mol Cell Biol*. 8:774-85.

Hatzfeld, M., and W.W. Franke. 1985. Pair formation and promiscuity of cytokeratins: formation in vitro of heterotypic complexes and intermediate-sized filaments by homologous and heterologous recombinations of purified polypeptides. *J Cell Biol*. 101:1826-41.

Hatzfeld, M., C. Haffner, K. Schulze, and U. Vinzens. 2000. The function of plakophilin 1 in desmosome assembly and actin filament organization. *J Cell Biol*. 149:209-22.

Hatzfeld, M., and K. Weber. 1990. The coiled coil of in vitro assembled keratin filaments is a heterodimer of type I and II keratins: use of site-specific mutagenesis and recombinant protein expression. *J Cell Biol*. 110:1199-210.

Hatzfeld, M., and K. Weber. 1990. Tailless keratins assemble into regular intermediate filaments in vitro. *J Cell Sci*. 97 (Pt 2):317-24.

He, T., A. Stepulak, T.H. Holmstrom, M.B. Omary, and J.E. Eriksson. 2002. The intermediate filament protein keratin 8 is a novel cytoplasmic substrate for c-Jun N-terminal kinase. *J Biol Chem*. 277:10767-74.

Heasman, S.J., and A.J. Ridley. 2008. Mammalian Rho GTPases: new insights into their functions from in vivo studies. *Nat Rev Mol Cell Biol*. 9:690-701.

Henegariu, O., N.A. Heerema, L. Lowe Wright, P. Bray-Ward, D.C. Ward, and G.H. Vance. 2001. Improvements in cytogenetic slide preparation: controlled chromosome spreading, chemical aging and gradual denaturing. *Cytometry*. 43:101-9.

Hernandez-Verdun, D. 1974. Morphogenesis of the syncytium in the mouse placenta. Ultrastructural study. *Cell Tissue Res*. 148:381-96.

Herrmann, H., and U. Aebi. 1998. Intermediate filament assembly: fibrillogenesis is driven by decisive dimer-dimer interactions. *Curr Opin Struct Biol*. 8:177-85.

Herrmann, H., M. Hesse, M. Reichenzeller, U. Aebi, and T.M. Magin. 2003. Functional complexity of intermediate filament cytoskeletons: from structure to assembly to gene ablation. *Int Rev Cytol*. 223:83-175.

Herrmann, H., S.V. Strelkov, P. Burkhard, and U. Aebi. 2009. Intermediate filaments: primary determinants of cell architecture and plasticity. *J Clin Invest*. 119:1772-83.

Hesse, M., T. Franz, Y. Tamai, M.M. Taketo, and T.M. Magin. 2000. Targeted deletion of keratins 18 and 19 leads to trophoblast fragility and early embryonic lethality. *Embo J*. 19:5060-70.

Hesse, M., T.M. Magin, and K. Weber. 2001. Genes for intermediate filament proteins and the draft sequence of the human genome: novel keratin genes and a surprisingly high number of pseudogenes related to keratin genes 8 and 18. *J Cell Sci*. 114:2569-75.

Hesse, M., A. Zimek, K. Weber, and T.M. Magin. 2004. Comprehensive analysis of keratin gene clusters in humans and rodents. *Eur J Cell Biol*. 83:19-26.

Hu, D., and J.C. Cross. 2010. Development and function of trophoblast giant cells in the rodent placenta. *Int J Dev Biol*. 54:341-54.

Husken, K., T. Wiesenfahrt, C. Abraham, R. Windoffer, O. Bossinger, and R.E. Leube. 2008. Maintenance of the intestinal tube in Caenorhabditis elegans: the role of the intermediate filament protein IFC-2. *Differentiation*. 76:881-96.

Hustin, J., and J.P. Schaaps. 1987. Echographic [corrected] and anatomic studies of the maternotrophoblastic border during the first trimester of pregnancy. *Am J Obstet Gynecol*. 157:162-8.

Inui, M., G. Martello, and S. Piccolo. 2010. MicroRNA control of signal transduction. *Nat Rev Mol Cell Biol*. 11:252-63.

Irvine, A.D., and W.H. McLean. 1999. Human keratin diseases: the increasing spectrum of disease and subtlety of the phenotype-genotype correlation. *Br J Dermatol*. 140:815-28.

Ishikawa, T., Y. Tamai, A.M. Zorn, H. Yoshida, M.F. Seldin, S. Nishikawa, and M.M. Taketo. 2001. Mouse Wnt receptor gene Fzd5 is essential for yolk sac and placental angiogenesis. *Development*. 128:25-33.

Ivaska, J., K. Vuoriluoto, T. Huovinen, I. Izawa, M. Inagaki, and P.J. Parker. 2005. PKCepsilon-mediated phosphorylation of vimentin controls integrin recycling and motility. *Embo J*. 24:3834-45.

Jackson, B.W., C. Grund, E. Schmid, K. Burki, W.W. Franke, and K. Illmensee. 1980. Formation of cytoskeletal elements during mouse embryogenesis. Intermediate filaments of the cytokeratin type and desmosomes in preimplantation embryos. *Differentiation*. 17:161-79.

Jackson, D., O.V. Volpert, N. Bouck, and D.I. Linzer. 1994. Stimulation and inhibition of angiogenesis by placental proliferin and proliferin-related protein. *Science*. 266:1581-4.

Jahn, L., B. Fouquet, K. Rohe, and W.W. Franke. 1987. Cytokeratins in certain endothelial and smooth muscle cells of two taxonomically distant vertebrate species, Xenopus laevis and man. *Differentiation*. 36:234-54.

Jaquemar, D., S. Kupriyanov, M. Wankell, J. Avis, K. Benirschke, H. Baribault, and R.G. Oshima. 2003. Keratin 8 protection of placental barrier function. *J Cell Biol*. 161:749-56.

Jauniaux, E., J. Hempstock, N. Greenwold, and G.J. Burton. 2003. Trophoblastic oxidative stress in relation to temporal and regional differences in maternal placental blood flow in normal and abnormal early pregnancies. *Am J Pathol*. 162:115-25.

Jauniaux, E., A.L. Watson, J. Hempstock, Y.P. Bao, J.N. Skepper, and G.J. Burton. 2000. Onset of maternal arterial blood flow and placental oxidative stress. A possible factor in human early pregnancy failure. *Am J Pathol*. 157:2111-22.

Jefferson, J.J., C.L. Leung, and R.K. Liem. 2004. Plakins: goliaths that link cell junctions and the cytoskeleton. *Nat Rev Mol Cell Biol*. 5:542-53.

Jollie, W.P. 1990. Development, morphology, and function of the yolk-sac placenta of laboratory rodents. *Teratology*. 41:361-81.

Jones, C.M., K.M. Lyons, and B.L. Hogan. 1991. Involvement of Bone Morphogenetic Protein-4 (BMP-4) and Vgr-1 in morphogenesis and neurogenesis in the mouse. *Development*. 111:531-42.

Jonkman, M.F., A.M. Pasmooij, S.G. Pasmans, M.P. van den Berg, H.J. Ter Horst, A. Timmer, and H.H. Pas. 2005. Loss of desmoplakin tail causes lethal acantholytic epidermolysis bullosa. *Am J Hum Genet*. 77:653-60.

Kaminsky, R., C. Denison, U. Bening-Abu-Shach, A.D. Chisholm, S.P. Gygi, and L. Broday. 2009. SUMO regulates the assembly and function of a cytoplasmic intermediate filament protein in C. elegans. *Dev Cell*. 17:724-35.

Kanasaki, K., K. Palmsten, H. Sugimoto, S. Ahmad, Y. Hamano, L. Xie, S. Parry, H.G. Augustin, V.H. Gattone, J. Folkman, J.F. Strauss, and R. Kalluri. 2008. Deficiency in catechol-O-methyltransferase and 2-methoxyoestradiol is associated with pre-eclampsia. *Nature*. 453:1117-21.

Kao, W.W., C.Y. Liu, R.L. Converse, A. Shiraishi, C.W. Kao, M. Ishizaki, T. Doetschman, and J. Duffy. 1996. Keratin 12-deficient mice have fragile corneal epithelia. *Invest Ophthalmol Vis Sci*. 37:2572-84.

Katschinski, D.M., L. Le, S.G. Schindler, T. Thomas, A.K. Voss, and R.H. Wenger. 2004. Interaction of the PAS B domain with HSP90 accelerates hypoxia-inducible factor-1alpha stabilization. *Cell Physiol Biochem*. 14:351-60.

Katsuno, T., K. Umeda, T. Matsui, M. Hata, A. Tamura, M. Itoh, K. Takeuchi, T. Fujimori, Y. Nabeshima, T. Noda, S. Tsukita, and S. Tsukita. 2008. Deficiency of zonula occludens-1 causes embryonic lethal phenotype associated with defected yolk sac angiogenesis and apoptosis of embryonic cells. *Mol Biol Cell*. 19:2465-75.

Kerns, M.L., D. DePianto, A.T. Dinkova-Kostova, P. Talalay, and P.A. Coulombe. 2007. Reprogramming of keratin biosynthesis by sulforaphane restores skin integrity in epidermolysis bullosa simplex. *Proc Natl Acad Sci U S A*. 104:14460-5.

Kim, S., and P.A. Coulombe. 2007. Intermediate filament scaffolds fulfill mechanical, organizational, and signaling functions in the cytoplasm. *Genes Dev*. 21:1581-97.

Kim, S., P. Wong, and P.A. Coulombe. 2006. A keratin cytoskeletal protein regulates protein synthesis and epithelial cell growth. *Nature*. 441:362-5.

Kina, T., K. Ikuta, E. Takayama, K. Wada, A.S. Majumdar, I.L. Weissman, and Y. Katsura. 2000. The monoclonal antibody TER-119 recognizes a molecule associated with glycophorin A and specifically marks the late stages of murine erythroid lineage. *Br J Haematol*. 109:280-7.

King, B.F. 1982. A freeze-fracture study of the guinea pig yolk sac epithelium. *Anat Rec*. 202:221-30.

Kjenseth, A., T. Fykerud, E. Rivedal, and E. Leithe. 2010. Regulation of gap junction intercellular communication by the ubiquitin system. *Cell Signal*.

Kozak, W., S. Wrotek, and K. Walentynowicz. 2006. Hypoxia-induced sickness behaviour. *J Physiol Pharmacol*. 57 Suppl 8:35-50.

Kruger, O., A. Plum, J.S. Kim, E. Winterhager, S. Maxeiner, G. Hallas, S. Kirchhoff, O. Traub, W.H. Lamers, and K. Willecke. 2000. Defective vascular development in connexin 45-deficient mice. *Development*. 127:4179-93.

Ku, N.O., H. Fu, and M.B. Omary. 2004. Raf-1 activation disrupts its binding to keratins during cell stress. *J Cell Biol*. 166:479-85.

Ku, N.O., J. Liao, and M.B. Omary. 1998. Phosphorylation of human keratin 18 serine 33 regulates binding to 14-3-3 proteins. *Embo J*. 17:1892-906.

Ku, N.O., S. Michie, E.Z. Resurreccion, R.L. Broome, and M.B. Omary. 2002. Keratin binding to 14-3-3 proteins modulates keratin filaments and hepatocyte mitotic progression. *Proc Natl Acad Sci U S A*. 99:4373-8.

Ku, N.O., and M.B. Omary. 2000. Keratins turn over by ubiquitination in a phosphorylation-modulated fashion. *J Cell Biol*. 149:547-52.

Ku, N.O., and M.B. Omary. 2006. A disease- and phosphorylation-related nonmechanical function for keratin 8. *J Cell Biol*. 174:115-25.

Ku, N.O., R.M. Soetikno, and M.B. Omary. 2003. Keratin mutation in transgenic mice predisposes to Fas but not TNF-induced apoptosis and massive liver injury. *Hepatology*. 37:1006-14.

Ku, N.O., D.M. Toivola, P. Strnad, and M.B. Omary. 2010. Cytoskeletal keratin glycosylation protects epithelial tissue from injury. *Nat Cell Biol*.

Kumemura, H., M. Harada, M.B. Omary, S. Sakisaka, T. Suganuma, M. Namba, and M. Sata. 2004. Aggregation and loss of cytokeratin filament networks inhibit golgi organization in liver-derived epithelial cell lines. *Cell Motil Cytoskeleton*. 57:37-52.

Kuruc, N., and W.W. Franke. 1988. Transient coexpression of desmin and cytokeratins 8 and 18 in developing myocardial cells of some vertebrate species. *Differentiation*. 38:177-93.

Larkin, M.A., G. Blackshields, N.P. Brown, R. Chenna, P.A. McGettigan, H. McWilliam, F. Valentin, I.M. Wallace, A. Wilm, R. Lopez, J.D. Thompson, T.J. Gibson, and D.G. Higgins. 2007. Clustal W and Clustal X version 2.0. *Bioinformatics*. 23:2947-8.

Lazarides, E. 1980. Intermediate filaments as mechanical integrators of cellular space. *Nature*. 283:249-256.

Lechler, T., and E. Fuchs. 2007. Desmoplakin: an unexpected regulator of microtubule organization in the epidermis. *J Cell Biol*. 176:147-54.

Lescisin, K.R., S. Varmuza, and J. Rossant. 1988. Isolation and characterization of a novel trophoblast-specific cDNA in the mouse. *Genes Dev*. 2:1639-46.

Levy, A.P., N.S. Levy, S. Wegner, and M.A. Goldberg. 1995. Transcriptional regulation of the rat vascular endothelial growth factor gene by hypoxia. *J Biol Chem*. 270:13333-40.

Lewis, J.E., J.K. Wahl, 3rd, K.M. Sass, P.J. Jensen, K.R. Johnson, and M.J. Wheelock. 1997. Cross-talk between adherens junctions and desmosomes depends on plakoglobin. *J Cell Biol*. 136:919-34.

Liao, J., D. Price, and M.B. Omary. 1997. Association of glucose-regulated protein (grp78) with human keratin 8. *FEBS Lett*. 417:316-20.

Limbourg, F.P., K. Takeshita, F. Radtke, R.T. Bronson, M.T. Chin, and J.K. Liao. 2005. Essential role of endothelial Notch1 in angiogenesis. *Circulation*. 111:1826-32.

Lin, J., J. Poole, and D.I. Linzer. 1997. Three new members of the mouse prolactin/growth hormone family are homologous to proteins expressed in the rat. *Endocrinology*. 138:5541-9.

Linzer, D.I., and S.J. Fisher. 1999. The placenta and the prolactin family of hormones: regulation of the physiology of pregnancy. *Mol Endocrinol*. 13:837-40.

Lloyd, C., Q.C. Yu, J. Cheng, K. Turksen, L. Degenstein, E. Hutton, and E. Fuchs. 1995. The basal keratin network of stratified squamous epithelia: defining K15 function in the absence of K14. *J Cell Biol*. 129:1329-44.

Loffek, S., S. Woll, J. Hohfeld, R.E. Leube, C. Has, L. Bruckner-Tuderman, and T.M. Magin. 2010. The ubiquitin ligase CHIP/STUB1 targets mutant keratins for degradation. *Hum Mutat*. 31:466-76.

Long, H.A., V. Boczonadi, L. McInroy, M. Goldberg, and A. Maatta. 2006. Periplakin-dependent re-organisation of keratin cytoskeleton and loss of collective migration in keratin-8-downregulated epithelial sheets. *J Cell Sci*. 119:5147-59.

Loranger, A., S. Gilbert, J.S. Brouard, T.M. Magin, and N. Marceau. 2006. Keratin 8 modulation of desmoplakin deposition at desmosomes in hepatocytes. *Exp Cell Res*. 312:4108-19.

Lu, H., M. Hesse, B. Peters, and T.M. Magin. 2005. Type II keratins precede type I keratins during early embryonic development. *Eur J Cell Biol*. 84:709-18.

Ma, G.T., and D.I. Linzer. 2000. GATA-2 restricts prolactin-like protein A expression to secondary trophoblast giant cells in the mouse. *Biol Reprod*. 63:570-4.

Magin, T.M., J. Reichelt, and M. Hatzfeld. 2004. Emerging functions: diseases and animal models reshape our view of the cytoskeleton. *Exp Cell Res*. 301:91-102.

Magin, T.M., R. Schroder, S. Leitgeb, F. Wanninger, K. Zatloukal, C. Grund, and D.W. Melton. 1998. Lessons from keratin 18 knockout mice: formation of novel keratin filaments, secondary loss of keratin 7 and accumulation of liver-specific keratin 8-positive aggregates. *J Cell Biol*. 140:1441-51.

Magin, T.M., P. Vijayaraj, and R.E. Leube. 2007. Structural and regulatory functions of keratins. *Exp Cell Res*. 313:2021-32.

Mahlapuu, M., M. Ormestad, S. Enerback, and P. Carlsson. 2001. The forkhead transcription factor Foxf1 is required for differentiation of extra-embryonic and lateral plate mesoderm. *Development*. 128:155-66.

Maisonpierre, P.C., C. Suri, P.F. Jones, S. Bartunkova, S.J. Wiegand, C. Radziejewski, D. Compton, J. McClain, T.H. Aldrich, N. Papadopoulos, T.J. Daly, S. Davis, T.N. Sato, and G.D. Yancopoulos. 1997. Angiopoietin-2, a natural antagonist for Tie2 that disrupts in vivo angiogenesis. *Science*. 277:55-60.

Mao, Y., N.K. Vyas, M.N. Vyas, D.H. Chen, S.J. Ludtke, W. Chiu, and F.A. Quiocho. 2004. Structure of the bifunctional and Golgi-associated formiminotransferase cyclodeaminase octamer. *Embo J*. 23:2963-71.

Margadant, C., E. Frijns, K. Wilhelmsen, and A. Sonnenberg. 2008. Regulation of hemidesmosome disassembly by growth factor receptors. *Curr Opin Cell Biol*. 20:589-96.

Margolis, S.S., J.A. Perry, C.M. Forester, L.K. Nutt, Y. Guo, M.J. Jardim, M.J. Thomenius, C.D. Freel, R. Darbandi, J.H. Ahn, J.D. Arroyo, X.F. Wang, S. Shenolikar, A.C. Nairn, W.G. Dunphy, W.C. Hahn, D.M. Virshup, and S. Kornbluth. 2006. Role for the PP2A/B56delta phosphatase in regulating 14-3-3 release from Cdc25 to control mitosis. *Cell*. 127:759-73.

Mashukova, A., A.S. Oriolo, F.A. Wald, M.L. Casanova, C. Kroger, T.M. Magin, M.B. Omary, and P.J. Salas. 2009. Rescue of atypical protein kinase C in epithelia by the cytoskeleton and Hsp70 family chaperones. *J Cell Sci*. 122:2491-503.

Maynard, S.E., J.Y. Min, J. Merchan, K.H. Lim, J. Li, S. Mondal, T.A. Libermann, J.P. Morgan, F.W. Sellke, I.E. Stillman, F.H. Epstein, V.P. Sukhatme, and S.A. Karumanchi. 2003. Excess placental soluble fms-like tyrosine kinase 1 (sFlt1) may contribute to endothelial dysfunction, hypertension, and proteinuria in preeclampsia. *J Clin Invest*. 111:649-58.

Mc, M.J. 1948. Histological and histochemical uses of periodic acid. *Stain Technol*. 23:99-108.

McKeon, F.D., D.L. Tuffanelli, K. Fukuyama, and M.W. Kirschner. 1983. Autoimmune response directed against conserved determinants of nuclear envelope proteins in a patient with linear scleroderma. *Proc Natl Acad Sci U S A*. 80:4374-8.

Mellman, I., and W.J. Nelson. 2008. Coordinated protein sorting, targeting and distribution in polarized cells. *Nat Rev Mol Cell Biol*. 9:833-45.

Moll, R., W.W. Franke, D.L. Schiller, B. Geiger, and R. Krepler. 1982. The catalog of human cytokeratins: patterns of expression in normal epithelia, tumors and cultured cells. *Cell*. 31:11-24.

Morrison, D.K. 2009. The 14-3-3 proteins: integrators of diverse signaling cues that impact cell fate and cancer development. *Trends Cell Biol*. 19:16-23.

Mrowiec, T., and B. Schwappach. 2006. 14-3-3 proteins in membrane protein transport. *Biol Chem*. 387:1227-36.

Mudgett, J.S., J. Ding, L. Guh-Siesel, N.A. Chartrain, L. Yang, S. Gopal, and M.M. Shen. 2000. Essential role for p38alpha mitogen-activated protein kinase in placental angiogenesis. *Proc Natl Acad Sci U S A*. 97:10454-9.

Muller, H., B. Liu, B.A. Croy, J.R. Head, J.S. Hunt, G. Dai, and M.J. Soares. 1999. Uterine natural killer cells are targets for a trophoblast cell-specific cytokine, prolactin-like protein A. *Endocrinology*. 140:2711-20.

Nagamatsu, T., T. Fujii, M. Kusumi, L. Zou, T. Yamashita, Y. Osuga, M. Momoeda, S. Kozuma, and Y. Taketani. 2004. Cytotrophoblasts up-regulate soluble fms-like tyrosine kinase-1 expression under reduced oxygen: an implication for the placental vascular development and the pathophysiology of preeclampsia. *Endocrinology*. 145:4838-45.

Ness, S.L., W. Edelmann, T.D. Jenkins, W. Liedtke, A.K. Rustgi, and R. Kucherlapati. 1998. Mouse keratin 4 is necessary for internal epithelial integrity. *J Biol Chem*. 273:23904-11.

Neznanov, N., A. Umezawa, and R.G. Oshima. 1997. A regulatory element within a coding exon modulates keratin 18 gene expression in transgenic mice. *J Biol Chem*. 272:27549-57.

Nieminen, M., T. Henttinen, M. Merinen, F. Marttila-Ichihara, J.E. Eriksson, and S. Jalkanen. 2006. Vimentin function in lymphocyte adhesion and transcellular migration. *Nat Cell Biol*. 8:156-62.

Niessen, C.M., E.H. Hulsman, E.S. Rots, P. Sanchez-Aparicio, and A. Sonnenberg. 1997. Integrin alpha 6 beta 4 forms a complex with the cytoskeletal protein HD1 and induces its redistribution in transfected COS-7 cells. *Mol Biol Cell*. 8:555-66.

O'Neill, A., M.W. Williams, W.G. Resneck, D.J. Milner, Y. Capetanaki, and R.J. Bloch. 2002. Sarcolemmal organization in skeletal muscle lacking desmin: evidence for cytokeratins associated with the membrane skeleton at costameres. *Mol Biol Cell*. 13:2347-59.

Omary, M.B., P.A. Coulombe, and W.H. McLean. 2004. Intermediate filament proteins and their associated diseases. *N Engl J Med*. 351:2087-100.

Omary, M.B., N.O. Ku, P. Strnad, and S. Hanada. 2009. Toward unraveling the complexity of simple epithelial keratins in human disease. *J Clin Invest*. 119:1794-805.

Omary, M.B., N.O. Ku, G.Z. Tao, D.M. Toivola, and J. Liao. 2006. "Heads and tails" of intermediate filament phosphorylation: multiple sites and functional insights. *Trends Biochem Sci*. 31:383-94.

Oriolo, A.S., F.A. Wald, G. Canessa, and P.J. Salas. 2007. GCP6 binds to intermediate filaments: a novel function of keratins in the organization of microtubules in epithelial cells. *Mol Biol Cell*. 18:781-94.

Orkin, S.H., and L.I. Zon. 2008. Hematopoiesis: an evolving paradigm for stem cell biology. *Cell*. 132:631-44.

Oshima, M., H. Oshima, and M.M. Taketo. 1996. TGF-beta receptor type II deficiency results in defects of yolk sac hematopoiesis and vasculogenesis. *Dev Biol*. 179:297-302.

Oshima, R.G. 2002. Apoptosis and keratin intermediate filaments. *Cell Death Differ*. 9:486-92.